

**Characterization of the retinoic acid-induced
gene network responsible for pancreas
specification in *Xenopus laevis***

Dissertation for the award of the degree
“Doctor rerum naturalium (Dr.rer.nat)”

In the GGNB program “Genes and Development”
At the Georg August University of Göttingen
Faculty of Biology

submitted by
Maja B. Gere
born in Hoyerswerda, Germany

Göttingen, January 2016

Thesis committee member

Prof. Dr. Tomas Pieler (supervisor and reviewer)

Developmental Biochemistry, Georg August University of Göttingen

Prof. Dr. Herbert Jäckle (reviewer)

Molecular Developmental Biology, MPI for Biophysical Chemistry, Göttingen

Prof. Dr. Andreas Wodarz

Microscopic Anatomy and Molecular Cell Biology, University of Köln

Members of the extended examination board

Prof. Dr. Ahmed Mansouri

Molecular Cell Differentiation, MPI for Biophysical Chemistry, Göttingen

Prof. Dr. Ernst A. Wimmer

Developmental Biology, Georg August University of Göttingen

Prof. Dr. Matthias Dobbelstein

Molecular Oncology, Georg August University of Göttingen

Date of thesis submission: January 29, 2016

Date of oral examination: March 21, 2016

Affidavit

Herewith I declare that I prepared the Doctoral thesis “Characterization of the retinoic acid-induced gene network responsible for pancreas specification in *Xenopus laevis*” on my own and with no other sources and aids than quoted.

Date of submission:

January 29, 2016

Maja B. Gere

Table of contents

Abstract	11
1. Introduction	13
1.1 Pancreas morphology and morphogenesis.....	13
1.2 Endoderm formation and regional specification	16
1.3 Pancreas organogenesis.....	18
1.3.1 Pancreas specification.....	18
1.3.2 Pancreas differentiation.....	21
1.4 Role of RA-signaling in pancreas development	24
1.5 Role of Wnt-signaling in pancreas development.....	27
1.6 Potential of organoids in research and clinical applications	28
1.7 Aim of this study	31
2. Materials and Methods	33
2.1 Materials	33
2.1.1 Model Organism	33
2.1.2 Bacteria.....	33
2.1.3 Constructs.....	33
2.1.4 Oligonucleotides.....	37
2.2 Methods	41
2.2.1 DNA methods.....	41
2.2.2 RNA methods.....	46
2.2.3 <i>Xenopus laevis</i> embryo culture and micromanipulations	51
2.2.4 Whole mount <i>in situ</i> hybridization (WMISH).....	54
2.2.5 CRISPR/Cas system	58
2.2.6 Luciferase assay	59
3. Results	61
3.1 Formation of pancreatic organoids from <i>Xenopus</i> explants	61
3.1.1 RA-dependent induction of pancreatic marker genes in Vegf/Noggin-programmed ectodermal explants	61
3.1.2 Formation of pancreatic organoids that recapitulate the <i>in vivo</i> program of pancreas development	63
3.2 Identification, verification and expression characteristics of early RA-responsive genes.....	68
3.2.1 Induction of direct RA-target gene Cyp26a1 within one hour after RA-addition	68
3.2.2 Identification of early RA-target genes by RNA-sequencing	70

3.2.3	Verification of 22 RA-responsive genes	72
3.2.4	Expression characteristics of 22 verified RA-responsive genes.....	73
3.3	The direct RA-target gene Hnf1b is required for pancreas specification ..	75
3.3.1	Hnf1b is RA-responsively expressed in the dorsal endoderm during gastrulation	75
3.3.2	Hnf1b is directly induced by RA in pancreatic organoids	76
3.3.3	Hnf1b is required for pancreas specification <i>in vitro</i>	78
3.3.4	Hnf1b is required for pancreas specification <i>in vivo</i>	80
3.3.5	Hnf1b alone cannot substitute for RA-activity during pancreas specification	83
3.4	The direct target Fzd4/Fzd4s is required for pancreas specification	85
3.4.1	Fzd4 and the alternative splice variant Fzd4s are directly induced by RA ..	85
3.4.2	Fzd4/Fzd4s is enriched in the dorsal half of a gastrula embryo including the dorsal endoderm	86
3.4.3	Fzd4/Fzd4s is RA-responsively expressed during gastrulation.....	87
3.4.4	Fzd4/Fzd4s is required for pancreatic marker gene expression <i>in vitro</i> ...	88
3.4.5	Downregulation of Fzd4/Fzd4s leads to an increase in non-canonical Wnt-signaling activity <i>in vitro</i>	91
4.	Discussion.....	95
4.1	Pancreatic organoid formation and the requirement of retinoic acid	95
4.2	Identification of 22 RA-responsive genes	97
4.3	The direct RA-target Hnf1b is required for pancreas development	100
4.4	The direct RA-target Fzd4 is required for pancreas development.....	103
4.5	Wnt- and RA-signaling in pancreas development.....	105
4.6	Conclusions	108
5.	References	111
6.	Appendix	129
6.1	Formation of pancreatic organoids that recapitulate the <i>in vivo</i> program of pancreas development	129
6.2	Identification, verification and expression characteristics of early RA-responsive genes	131
6.3	Expression and functional analysis of the RA-target Hnf1b	136
6.4	Expression and functional analysis of RA-target Fzd4/Fzd4s	138
6.5	Nanostring analysis data for <i>in vitro</i> generation of pancreatic organoids	143
6.6	RNA-sequencing data for the identification of RA-target genes.....	145

6.7	Nanostring analysis data for the verification of RA-responsiveness of putative RA-target genes	155
6.8	Nanostring analysis data for expression characteristics of confirmed RA-responsive genes.....	171
6.9	Analysis of the Hnf1b-overexpression phenotype.....	177
6.10	Nanostring code sets.....	180
Abbreviations.....		189
List of figures.....		191
List of tables		193
Acknowledgements		195
Curriculum Vitae.....		197

Abstract

Retinoic acid (RA) is critically required for pancreas specification in *Xenopus* and other vertebrates. However, the gene network that is directly induced by RA-signaling in this context remains to be defined. We identified 22 RA-target genes through RNA-sequencing of *in vitro* generated pancreatic organoids. One of these is Hnf1b, which has been shown to be associated with a monogenic form of diabetes in humans and with pancreas hypoplasia in vertebrates. Functional analyses of Hnf1b in pancreatic organoids and whole *Xenopus* embryos revealed its early requirement for pancreatic progenitor formation. However, we also found that Hnf1b alone is not sufficient to substitute for RA in pancreas specification, indicating a requirement of one or more additional RA-responsive activities. Furthermore, we identified the Wnt-receptor Fzd4 as direct RA-target and novel regulator in pancreas development. Loss-of-function experiments in pancreatic organoids reveal a role of this Wnt-signaling component in pancreas development. Additional experimental data suggest that a modulation of non-canonical Wnt-signaling activity by RA, probably mediated through Fzd4, is required for a proper pancreas specification.

1. Introduction

The pancreas is an organ of the vertebrate digestive system that accomplishes two distinct functions based on its heterogeneous composition. It promotes a proper food digestion and maintains glucose homeostasis. The digestive enzyme producing exocrine tissue represents the major component, where clusters of hormone producing endocrine cells are embedded that control glucose homeostasis (Slack, 1995). Pancreas related diseases have encouraged the research on embryonic pancreas development for decades. Several studies showed that the early pancreas development in *Xenopus* is very similar to that of mice and that the same set of genes used in *Xenopus* is also involved in mammalian pancreas development (reviewed in Pearl et al., 2009). Lineage tracing experiments in *Xenopus* revealed that during gastrulation a pancreatic progenitor cell population is specified in the dorsal endoderm (Chalmers and Slack, 2000), considerably earlier than the expression of known pancreatic progenitor markers Ptf1a and Pdx1 (Afelik et al., 2006). It has been demonstrated that signals from the adjacent mesoderm, namely retinoic acid (RA), define a cell population in the dorsal endoderm during gastrulation. Later in development, these cells are capable to respond signals from the notochord which promotes pancreatic fate (Wells and Melton, 2000; Chen et al., 2004; Pan et al., 2007). An overview of the important aspects of pancreas development from endoderm formation over regional specification by mesodermal signals to budding and differentiation is given in the following sections, emphasizing the role of RA- and Wnt-signaling in pancreas development. Furthermore, the progress in research of *in vitro* organ formation and its relevance for clinical applications will be described.

1.1 Pancreas morphology and morphogenesis

The pancreas is 95% to 99% an exocrine gland, containing acinar cells that secrete a variety of digestive enzymes. Through a highly branched ductal epithelium, enzymes and bicarbonate ions are transported to the intestine (Slack, 1995). A small percentage of this gland consists of hormone secreting endocrine tissue. Five endocrine cell types, organized in clusters called the islets of Langerhans, are described for mammals, birds, reptiles and amphibians. The main part of the islets is formed by insulin-producing β -cells. Furthermore glucagon-producing α -cells, somatostatin-producing δ -cells, PP-cells that generate pancreatic polypeptide

(Maake et al., 1998) and ϵ -cells that secrete ghrelin (Rindi et al., 2004; Wierup et al., 2014) are included in the islets (reviewed in Brereton et al., 2015). Like other organs of the digestive tract, the pancreas originates from the endodermal germ layer. During embryogenesis, the endoderm forms the gut epithelium that is regionalized by various mesodermal signals into overlapping presumptive organ territories from anterior to posterior. The developing pancreas becomes evident as epithelial evaginations of the foregut endoderm.

In *Xenopus*, one dorsal bud can be detected at stage 35 and two ventral buds at the junction of the liver bud and duodenum at stage 37 (Kelly and Melton, 2000). The earliest known pancreatic markers Ptf1a and Pdx1 are detectable by WMISH before the budding starts at stage 32 (**Fig. 1.1 A**). Ptf1a expression in the endoderm is restricted to the regions of dorsal and ventral pancreatic tissue, whereas Pdx1 is more broadly expressed in the endoderm including the prospective duodenal and stomach tissue. It was shown that epithelium co-expressing these two transcription factors adopts a pancreatic fate (Afelik et al., 2006). During the evagination process, pancreatic progenitor proliferation and differentiation take place. Like in mouse and zebrafish, the Pdx1 expression gets restricted to β -cells, whereas Ptf1a expression remains only in the exocrine tissue (Krapp et al., 1998; Kawaguchi et al., 2002; Hesselson et al., 2011). In *Xenopus*, the first endocrine differentiation marker Insulin appears around stage 30 (**Fig. 1.1 C**) and is detectable only dorsally until stage 45 (Horb and Slack, 2002). Exocrine enzyme Pdia2 gene expression can be detected at stage 39 in both, dorsal and ventral pancreas (Afelik et al., 2004). Pdia2 staining by WMISH is used in **Fig. 1.1 B** to illustrate the fusion of the three pancreatic primordia at stage 40 caused by gut rotation. The fused pancreas is located predominantly in the left half of the embryo embedded between stomach and duodenum (**Fig. 1.1 B** panel 5). Transcripts of most of the exocrine marker genes (Amylase, Trypsinogen, Elastase) are first detectable at stage 41 exclusively in the ventral pancreas. Further endocrine markers and a second wave of Insulin expression are visible at stage 46 (reviewed in Pieler and Chen, 2006).

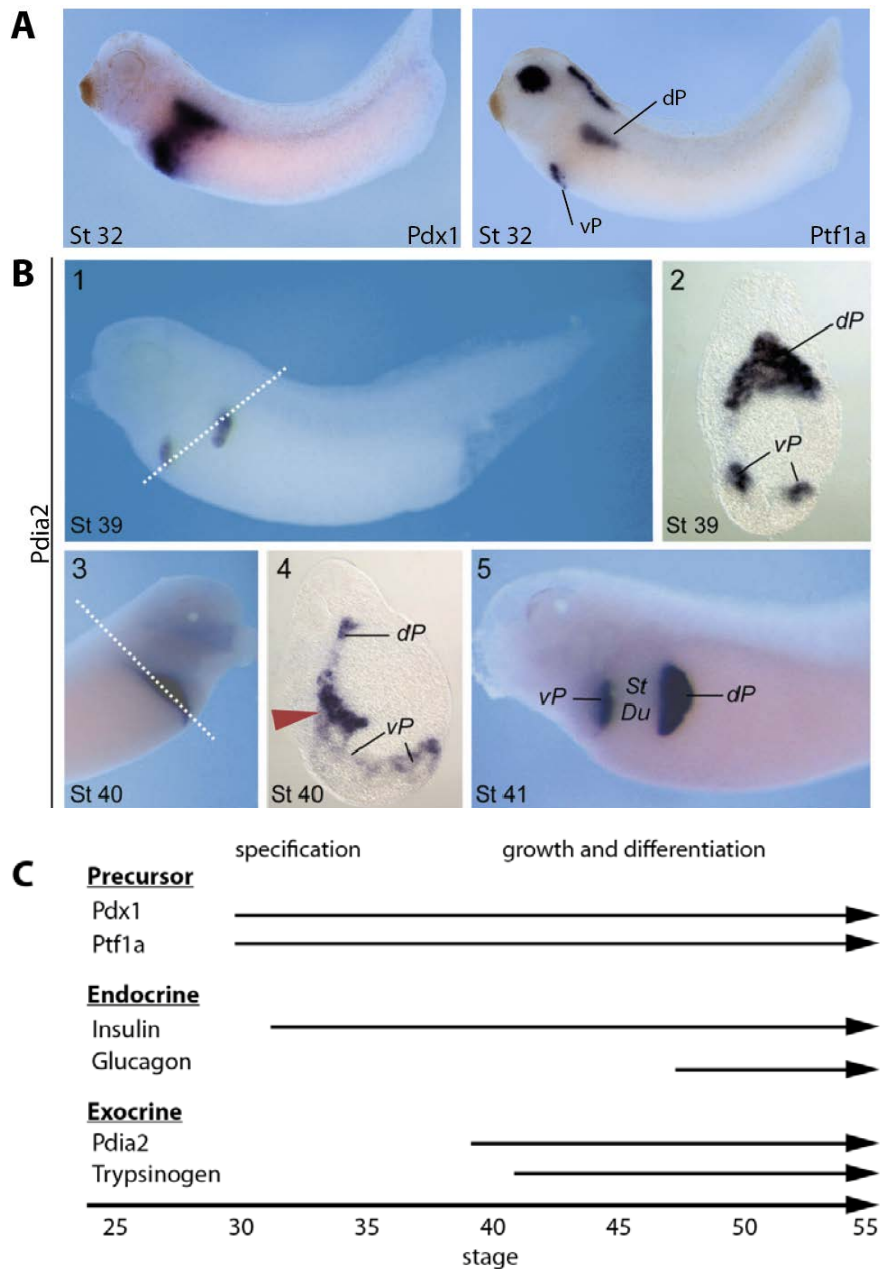


Fig. 1.1 Pancreas organogenesis in *Xenopus laevis*

(A) Expression of Pdx1 and Ptf1a at stage 32. (B) Pdia2 expression before (1,2) and after (3 to 5) fusion of the dorsal and two ventral pancreatic buds. Panels 2 and 4 show transversal sections across the white dotted line indicated in panels 1 and 3. (C) Temporal expression profile of pancreatic genes. dP = dorsal pancreatic bud; Du = duodenum; St = stomach, vP = ventral pancreatic buds. ((B) and (C) modified from Pieler and Chen, 2006)

1.2 Endoderm formation and regional specification

Although the process of endoderm, mesoderm and ectoderm segregation during gastrulation is different in mice, chicken, fish and frogs, the molecular pathway that directs endoderm formation is evolutionary conserved across these species (reviewed in Zorn and Wells, 2009). Maternal determinants initiate a gene network responsible for endoderm formation. However, these maternal factors differ between the species, while the induced network is conserved (reviewed in Grapin-Botton and Constam, 2007). In *Xenopus*, the pathway leading to endoderm formation is activated by the maternally provided transcription factor Vegt that is localized to the vegetal cortex of the egg (**Fig. 1.2 A**) (Hyde and Old, 2000; Xanthos et al., 2001). Vegt is a crucial regulator of endoderm formation in *Xenopus* as embryos developed from Vegt-depleted eggs lack the endodermal germ layer (Zhang et al., 1998). Vegt induces the expression of early endodermal genes like the transcription factors Sox7 (Zhang et al., 2005), Sox17a (Engleka et al., 2001), several Mix-type homeodomain factors (like Mix.1 and Mixer), GATA-factors (Xanthos et al., 2001) and Nodal-related genes (Xnrs) (Takahashi et al., 2000) (reviewed in Fukuda and Kikuchi, 2005; Heasman, 2006; Skirkanich et al., 2011).

Xnrs encode for secreted factors of the TGF β -family, which regulate the gene expression via transmembrane serine-threonine kinase receptors mediated by intracellular Smad proteins. In all vertebrates, the Nodal signaling pathway is essentially required for endoderm development as it induces additional endodermal genes and is capable of restoring the endodermal gene expression in Vegt-depleted embryos (Yasuo and Lemaire, 1999; Xanthos et al., 2001 and reviewed in reviewed in Grapin-Botton and Constam, 2007). Moreover, Nodal signaling also induces mesodermal genes depending on the level of signaling (Clements et al., 1999; Shen 2007). Vegt acts synergistically with dorsally stabilized β -Catenin for the activation of Xnr genes resulting in a gradient of high Nodal-signaling in the dorsal endoderm and lower levels in the ventral endoderm (**Fig. 1.2 B**, Agius et al., 2000). Furthermore, Nodal signaling cooperates with β -catenin/Tcf3-targets Siamois and Twin to induce mesodermal organizer genes like Noggin, Chordin and Follistatin (Brannon et al., 1997; Moon and Kimmelman, 1998; Bae et al., 2011). These secreted organizer molecules act as BMP-inhibitors and establish a dorso-ventral BMP-signaling gradient in all three germ layers (**Fig. 1.2 C**, Piccolo et al., 1996; Zimmerman et al., 1996). Thereby, dorsal endoderm, from which the pancreatic progenitors will arise, is characterized by low levels of BMP-signaling. In *Xenopus*, it

was shown that RA is sufficient to induce pancreatic gene expression in dorsal endodermal explants but not in ventral. Only when BMP-signaling was downregulated by Noggin, ventral endodermal explants expressed pancreas-specific genes in the presence of RA and mesoderm (Pan et al., 2007).

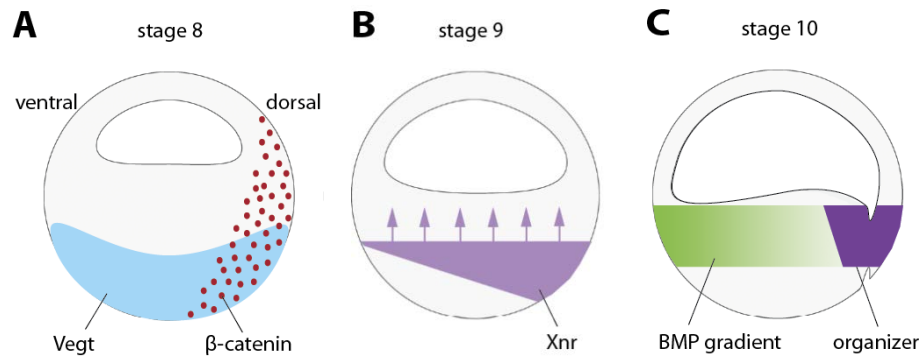


Fig. 1.2 Model for dorsal endoderm patterning, mesoderm induction and organizer formation in *Xenopus*

(A) At blastula stage, Vegt is localized at the vegetal hemisphere while β -catenin is stabilized dorsally. (B) At late blastula stage, a Xnr-gradient (Nodal-related) is generated by the synergistic activity of Vegt and β -catenin. (C) The mesoderm is specified by the Xnr-gradient and at early gastrula stage, the organizer is specified by synergistic activity of Xnr and β -catenin-targets Siamese and Twin. A BMP-gradient is generated by BMP-antagonists (for instance Noggin) secreted from the organizer (Adapted from Gilbert and Singer 8th edition 2006; after Agius et al., 2000).

During gastrulation all three germ layers become patterned along the anterior-posterior axis by the organizer. While endoderm and mesoderm involute, the dorsal anterior endoderm is positioned at the prospective ventral foregut whereas the more posterior dorsal endoderm becomes the future dorsal foregut (Fig. 1.3 A, light green and yellow, Keller, 1991). The initial anterior-posterior pattern of the endoderm is not committing as the endoderm remains able to respond to signals released from the overlying or subjacent mesoderm (Zeynali et al., 2000; Horb and Slack, 2001; McLin et al., 2007 and reviewed in McCracken and Wells, 2012). These include Wnt-, FGF-, BMP- and RA-signaling, which are associated with posteriorizing effects (Dessimoz et al., 2006; Rankin et al., 2011; Sherwood et al., 2011). The resulting gut tube is segmented into foregut, midgut and hindgut domains, whereby Pdx1 is expressed in the posterior foregut and anterior midgut (Wright et al., 1989). However, so far it is not known how FGF-, Wnt-, BMP- and RA-signaling co-operate during endoderm patterning.

1.3 Pancreas organogenesis

1.3.1 Pancreas specification

Through cell movements during foregut morphogenesis the dorsal and ventral foregut epithelium are placed into very different environments. This fact already indicates that the extrinsic signals and genetic programs that promote pancreas development in the dorsal and ventral foregut are different. A further difference is the derivation of several organs from the ventral foregut, whereas the dorsal foregut gives rise exclusively to the dorsal pancreas. This suggests that dorsal pancreas formation is a matter of induction, whereas ventral pancreas needs to be segregated from multiple organ lines (reviewed in McCracken and Wells, 2012). Several studies confirmed these assumptions. In chick, Kim and colleagues demonstrated in 1997 that presumptive dorsal pancreatic endoderm when cultivated in isolation showed no pancreatic gene expression, whereas ventral pre-pancreatic endoderm does (Kim et al., 1997). Extensive studies in ectodermal, mesodermal and endodermal explants from *Xenopus* embryos supplied the evidence that the dorsal pancreatic foregut endoderm initially receives inductive signals from the mesoderm at the onset of gastrulation. Retinoic acid (RA) could be identified as such an inductive signal and the involvement of one or more further signals is assumed (RA-source indicated in **Fig. 1.3 A** (red)) (Chen et al., 2004; Pan et al., 2007).

During foregut morphogenesis the dorsal foregut epithelium has initially contact with the notochord and subsequently with the dorsal aorta. Both tissues have been shown to be sources of permissive signals for pancreas formation (Kim et al., 1997; Lammert et al., 2001). In chicken, dorsal pancreas development could be prevented by the removal of the notochord at an early stage (Kim et al., 1997). However, the notochord is not able to induce pancreatic gene expression in early gastrula stage or non-pancreatic somite-stage endoderm (Wells and Melton, 2000), which is in accordance with the finding that pre-pancreatic foregut endoderm obtained the ability, at an earlier time, to react to permissive signals from the notochord. These permissive signals were identified as Activin- β B and FGF2 (**Fig. 1.3 B**). Hebrok and colleagues found them as secreted factors from the notochord that suppress the expression of Sonic hedgehog (Shh) in the pancreatic endoderm. Shh is broadly expressed in the endodermal epithelium but is excluded from pancreatic endoderm (Hebrok et al., 1998; Hebrok et al., 2000). The removal of the notochord leads to an ectopic Shh expression that inhibits dorsal pancreas development (Hebrok et al., 2000). It was shown that the repression of Shh in the dorsal endoderm induces

Pdx1 expression in a dose dependent manner (Hebrok et al., 1998). With continuing embryonal development, the notochord is displaced by fused dorsal aortae that further signals to the dorsal pre-pancreatic endoderm (Lammert et al., 2001). These signals are required for the maintenance of Pdx1 expression and for the induction of Ptf1a expression (Yoshitomi and Zaret, 2004). It is assumed that aortic endothelial signals in addition act indirectly on pancreatic endoderm as they promote the survival of dorsal mesenchyme (reviewed in Edlund, 2002). Dorsal mesenchyme secretes FGF10 that is required for the maintenance of Pdx1 and Ptf1a expression (Jacquemin et al., 2006).

The ventral foregut gets in proximity to two mesodermal derivatives, the cardiac mesoderm and *septum transversum* (**Fig. 1.3 B**). The posterior region of the ventral foregut was shown to give rise to the ventral pancreas and liver. Explant studies in zebrafish and mouse support the presumption of a common bi-potential cell population in the ventral foregut endoderm that differentiate into liver and ventral pancreas (Deutsch et al., 2001; Bort et al., 2006; Chung et al., 2008). In several studies, signaling pathways have been identified which are involved in the segregation of hepatic and pancreatic fate, most of them appear to repress pancreas formation and promote liver development. FGF-signaling from the cardiac mesoderm (Jung et al., 1999) and BMP-signaling from the *septum transversum* (Rossi et al., 2001) induce hepatic fate. Deutsch and colleagues found an expression of Pdx1 in cultures of isolated mouse ventral foregut endoderm, whereas the expression of liver marker Hhex required signals from the cardiac mesoderm (Deutsch et al., 2001). These findings suggest the pancreas as a default state of the ventral foregut. Furthermore, a BMP antagonist TGIF β -induced factor 2 (TGIF2) was found to be expressed in the posterior ventral foregut counteracting the expression of Hhex (Spagnoli and Brivanlou, 2008). Moreover, the assumption of pancreas as a default state is supported by the presence of a pre-existing chromatin modification pattern that promotes pancreas development in the ventral foregut endoderm (Xu et al., 2011; Arnes and Sussel, 2015).

Independent of the way of specification, both dorsal and ventral pancreatic progenitor cell populations are characterized by the co-expression of Pdx1 and Ptf1a (Afelik et al., 2006). During this early phase of pancreatic development, also referred to as primary transition, the pancreatic progenitors proliferate (Pictet et al., 1972). Thus, pancreatic foregut epithelium evaginates and forms the dorsal and two ventral buds. Furthermore, the first Insulin-expressing cells in *Xenopus* and Glucagon-expressing cells in mouse can be detected. In mouse, the primary transition occurs between E9.5 and E13.5 (Jorgensen et al., 2007). The

corresponding time period in *Xenopus* is from stage 28 to stage 38 (Horb and Slack, 2002).

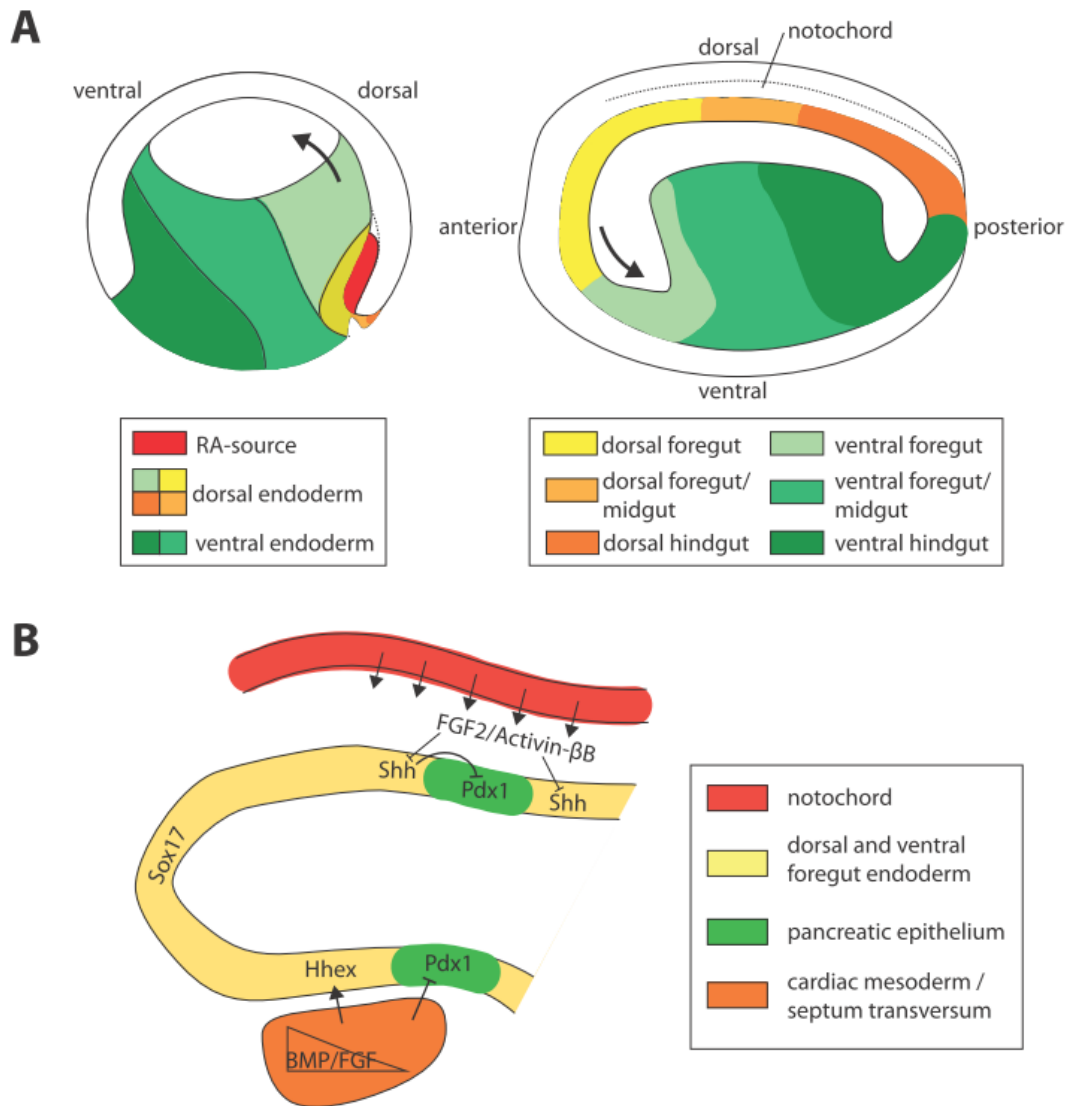


Fig. 1.3 Fate maps of *Xenopus* endoderm from gastrula to early somite stage and overview of signals involved in pancreas specification

(A) Gastrula stage (left) and early somite stage (right) *Xenopus* embryos with indicated colored domains that correspond to fate-map studies. The arrows indicate the migration/folding direction of the foregut. (modified after Zorn and Wells, 2009)

(B) Overview of signals involved in pancreas specification in an early somite stage embryo. In the dorsal foregut endoderm, permissive signals from the notochord (FGF2 and Activin- β B) repress Shh transcription in the pre-pancreatic epithelium and allow Pdx1 expression. FGF- and BMP-signaling from the cardiac mesoderm/*septum transversum* promote liver (Hhex) and inhibit pancreas fate (Pdx1) in the ventral foregut epithelium. (modified after McCracken and Wells, 2012)

Genetic lineage-tracing experiments in mice revealed that all pancreatic cell-subtypes arise from a common pool of multipotent progenitor cells co-expressing Pdx1 and Ptf1a (Gu et al., 2002; Kawaguchi et al., 2002; Burlison et al., 2008). In *Xenopus*, ectopic co-expression of Ptf1a and Pdx1 is sufficient to convert duodenal precursor cells into pancreatic tissue (Afelik et al., 2006). Furthermore, it was shown that constitutively active forms of Pdx1 or Ptf1a can push liver progenitors to a pancreatic fate (Horb et al., 2003; Jarikji et al., 2007). As soon as the ventral and dorsal pancreatic domains in the foregut epithelium are specified, a set of transcription factors becomes specifically expressed in these regions (**Fig. 1.4 A**). Beside Pdx1 and Ptf1a, the earliest transcription factor that marks pancreatic progenitor cells is Sox9 (Lioubinski et al., 2003; Lee and Saint-Jaennet, 2003). In mice, Sox9 was shown to be essential for proliferation and maintenance of pancreatic progenitors (Seymour et al., 2007; Seymour, 2014). Moreover, during the proliferation and expansion of the pancreatic progenitor field, Sox9 regulates a set of additional transcription factors in pancreatic progenitors including Hnf1b (Lynn et al., 2007). Genetic studies in mice revealed that Sox9 acts in cooperation with Pdx1 for the induction of pancreatic fate and the repression of the intestinal lineage differentiation (Shih et al., 2015).

1.3.2 Pancreas differentiation

At the end of the primary transition, pancreatic buds are still composed of undifferentiated multipotent progenitors expressing a set of transcription factors including Pdx1, Ptf1a, Sox9, Hnf1b, Nkx6.1 and Gata4 (**Fig. 1.4 A**) (reviewed in Shih et al., 2013; Seymour, 2014). The next phase of pancreas development, also referred to as secondary transition, is characterized by continuing proliferation and step-wise differentiation. This process starts with the segregation of a tip and trunk domain (Zhou et al., 2007; Villasenor et al., 2010). Lineage tracing experiments in mice showed that endocrine and ductal cells arise from bi-potential cells in the trunk domain whereas the tip regions are restricted to an acinar fate (reviewed in Pan and Wright, 2011). During the separation of tip and trunk, the expression of some transcription factors becomes restricted to only one of the two domains. Trunk specific expressed are Hnf1b, Sox9 and Nkx6.1, whereas Ptf1a and its target Cpa1 become restricted to the tips (**Fig. 1.4 B**, Zhou et al., 2007; Schaffer et al., 2010; Kopp et al., 2011b). The reciprocal repression between Nkx6.1 and Ptf1a is a critical mechanism through which the progenitors achieve distinct tip or trunk identity (Schaffer et al., 2010). Besides its early role in pancreas fate specification, Ptf1a

later regulates acinar cell differentiation (Kawaguchi et al., 2002; Masui et al., 2010). Ptf1a acts in a trimeric pancreas transcription factor complex (Ptf1) together with the bHLH-protein E2A and suppressor of hairless RBP-j or its paralog RBP-jl (Obata et al., 2001; Beres et al., 2006). Prior to acinar cell differentiation Ptf1a interacts with RBP-j, which is replaced by RBP-jl during the secondary transition (Masui et al., 2007; Miyatsuka et al., 2007). This complex, termed PTF1-L, directs the activation of acinar-specific genes (Rose et al., 2001; Masui et al., 2010). In *Xenopus*, the exocrine marker pancreatic protein disulfide isomerase (Pdia2) can be first observed at stage 39, whereas other exocrine markers are not detected before stage 41 (Afelik et al., 2004; Horb and Slack 2002). In the adult exocrine pancreas of mice, lineage-tracing experiments indicate the existence of a low number of Ptf1a-positive multipotent pancreatic cells that can be induced upon injury (Pan et al., 2013).

The trunk domain is bi-potential and gives rise to ductal and endocrine cells (Solar et al., 2009; Kopp et al., 2011a). A subset of progenitor cells within the trunk express the transcription factor Neurogenin 3 (Ngn3) which indicates the onset of endocrine cell differentiation (Gradwohl et al., 2000; Gu et al., 2002). Cells within the trunk that do not activate Ngn3 probably contribute to ductal tissue (Magenheim et al., 2011). Several studies suggest that the Notch-signaling target Hes1 plays an important role in repressing Ngn3 expression and preventing extensive Ngn3 activation (Apelqvist et al., 1999; Jensen et al., 2000; Lee et al., 2001; Shih et al., 2012) (**Fig. 1.4 C**). Once Ngn3 is expressed, progenitors exit the cell cycle and delaminate from the epithelium to form the islet structures (Gouzi et al., 2011). Ngn3 activates the endocrine differentiation program by inducing pro-endocrine transcription factors including NeuroD1 and further factors involved in the delamination process (Huang et al., 2000; Mellitzer et al., 2006; Rukstalis and Habener, 2007; Soyer et al., 2010). Johansson and colleagues have shown in mice that the competence of endocrine precursors to produce different endocrine cell types is temporally controlled (Johansson et al., 2007). In mice the progenitors first differentiate into α -cells, then β - and δ -cells, and finally PP-cells, each cell-type characterized by a distinct set of transcription factors caused by cross-regulation mechanisms between the single factors (reviewed in Pan and Wright, 2011; Beucher et al., 2012; Napolitano et al 2015). Despite the fact that in *Xenopus* endocrine progenitors first differentiate into β -cells (Kelly and Melton, 2000; Horb and Slack, 2002), the mechanism of subtype segregation may proceed in *Xenopus* similar to mice (**Fig. 1.4 D**). The formation of islets is completed in mice at E18.5 (Gittes, 2009) whereas in *Xenopus* a stable islet cell number is not observed before metamorphosis which is completed at stage 66

(Maake et al., 1998). Moreover, a complex ductal system in the frog pancreas is not observed before the end of metamorphosis (Mukhi et al., 2008).

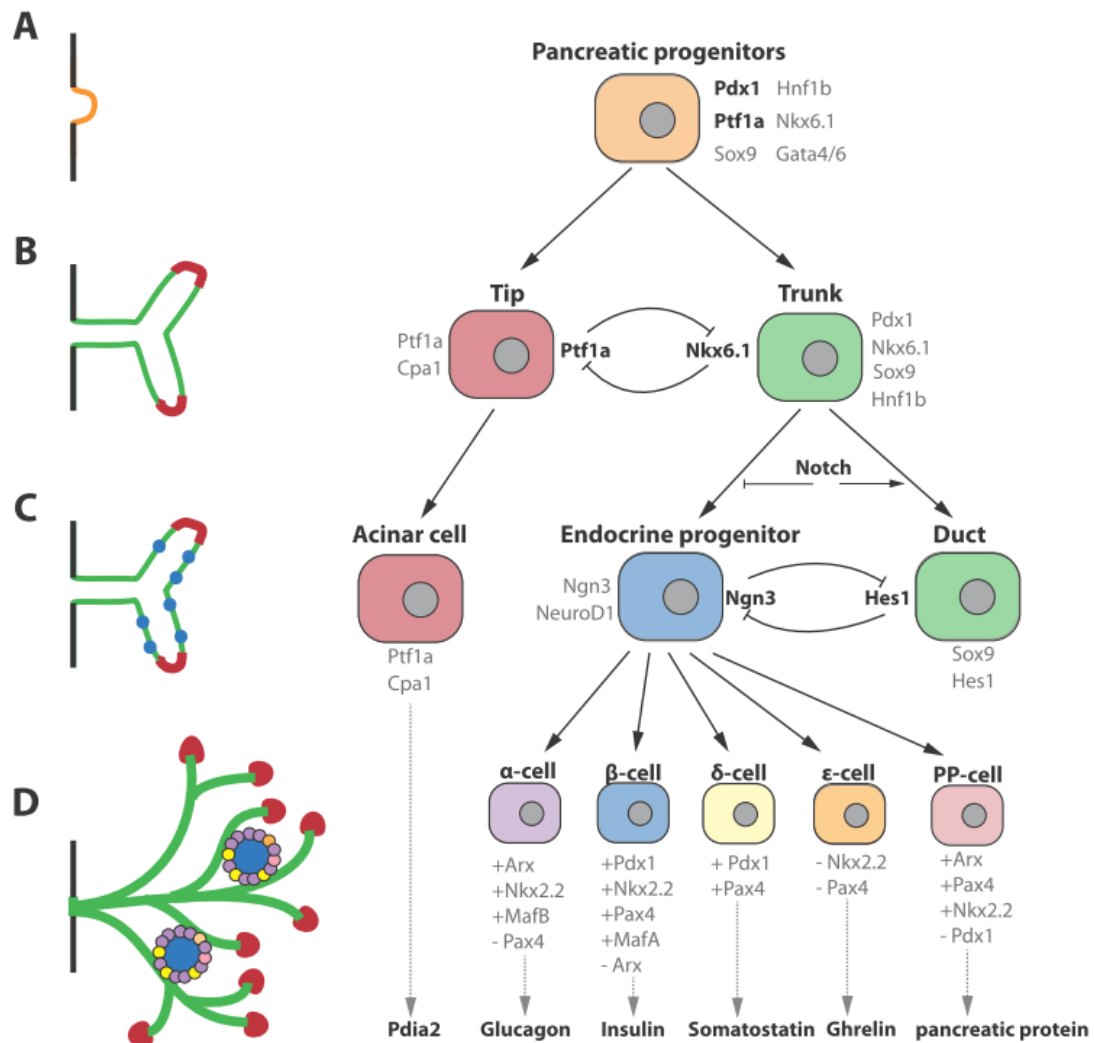


Fig. 1.4 Overview of pancreas organogenesis and lineage decisions

(A) During primary transition, pancreatic progenitors express transcription factors, including Pdx1, Ptf1a, Sox9, Hnf1b, Nkx6.1 and Gata4/6, which mediate proliferation and promote the maintenance of pancreatic identity. Thereby, pancreatic epithelium bulges out from the foregut epithelium to form a bud (orange). (B) At the onset of the secondary transition, the epithelial bud expands and branches. Pancreatic progenitors turn either into tip (red) or trunk (green) cells mediated by the cross-repression between Ptf1a and Nkx6.1. (C) Tip cells are restricted to an acinar fate (red) expressing Ptf1a and later enzymes like Pdia2. Bi-potential trunk cells adopt either ductal (green) or endocrine cell fate (blue). Ductal versus endocrine fate decision is regulated by Notch activity. High Notch signaling mediates ductal fate by the induction of the Ngn3-repressor Hes1. In endocrine progenitors, Ngn3 activates a set of transcription factors including NeuroD1 that regulate the endocrine differentiation.

(D) Endocrine progenitors subsequently delaminate from the trunk epithelium. Subsequently, they differentiate into five endocrine cell subtypes (marked by different colors) expressing distinct sets of transcription factors (+ present, - absent) and hormones. In mouse, at the end of embryogenesis, the pancreas consists of a highly branched ductal tree, connecting acinar cells with the intestine. Endocrine islets are scattered throughout the organ. In *Xenopus*, these histological structures are not observed before the end of metamorphosis (modified after Pan and Wright, 2011 and Shih, 2013).

1.4 Role of RA-signaling in pancreas development

Retinoic acid (RA) is essential for normal embryogenesis of all vertebrates (reviewed in Rhinn and Dolle, 2012). RA is a vitamin A-derived, small non-peptic, lipophilic molecule. This molecule differs strongly from other signaling factors as it does not need any cell-surface receptors for signal transduction. RA is able to enter the nucleus and binds to target genes through nuclear receptors that recognize RA-response elements (RAREs), thus switching from repressors to transcriptional activators (Germain et al., 2002). Vitamin A is absorbed from the food, stored in the liver and circulates as its alcohol form Retinol which is bound to a carrier protein, retinol-binding protein 4 (RBP4) (Quadro et al., 1999). During embryogenesis Retinol is maternally provided (Ismadi and Olson, 1982). Retinol-RBP4 enters cells, which is facilitated by the RA-inducible transmembrane protein STRA6 (stimulated by retinoic acid 6) (Kawaguchi et al., 2007) (**Fig. 1.5 A**). Within the cell, Retinol can be converted to RA in two enzymatic reactions. First, Retinol is reversibly oxidized by retinol dehydrogenases (ROLDH) to Retinal and subsequently irreversibly oxidized by retinal dehydrogenases (RALDH) to retinoic acid (RA) (reviewed in Duester, 2008). Therefore, Retinol is available to all cells of an embryo, but only cells which express one of the RALDHs can generate RA. In vertebrates, three isotypes of RALDH are described, whereby RALDH2 is earliest expressed (Niederreither et al., 1997). RA leaves the RA-generating cells and enters neighbouring cells where it has two main destinies. In cells which express one of the CYP26 genes (cytochrome P450 enzyme) at a high level, RA is converted into inactive metabolites (Ray et al., 1997; White et al., 1996; Hollemann et al., 1998). In cells without or low levels of CYP26, RA enters the nucleus and binds the heterodimeric receptors RAR/RXR (retinoic acid receptor/retinoid X receptor), thereby activating the transcription of genes containing RAREs (reviewed in Mark et al., 2006).

Several early studies in mice and quail using Vitamin A deficiency or RA-receptor mutations indicate the requirement of RA for the development of various organs (Dersch and Zile, 1993; Lohnes et al., 1994; Mendelsohn et al., 1994; Dickman et al., 1997; Clagett-Dame and DeLuca, 2002). Further studies revealed that the requirement of RA for pancreas development is conserved among the vertebrates. Two independent studies in mouse using RALDH2 mutants demonstrated the necessity of RA for dorsal pancreas development (Martin et al., 2005; Molotkov et al., 2005). In zebrafish, additionally to its requirement for dorsal pancreas development, RA is also indispensable for the ventral pancreas and liver (Stafford et

al., 2002). In *Xenopus*, studies using the synthetic RA-antagonist BMS453, which binds RA-receptors, show that like in mouse, RA is essential for dorsal pancreas development. Upon the inhibition of RA-signaling, expression of Shh was expanded into the prospective dorsal pancreatic endoderm, thereby repressing pancreatic fate. However, these effects of RA-inhibition were only observed when BMS453 was added before the end of gastrulation, indicating that RA acts at the onset of gastrulation in pancreas specification (Chen et al., 2004). Before that, in 2000 Asashima and colleagues already demonstrated the RA-dependent induction of pancreatic marker gene expression in dorsal lip explants from early gastrula stage *Xenopus* embryos (Moriya et al., 2000a). The assumption of a RA-gradient within the dorsal endoderm during gastrulation is supported by the expression pattern of RALDH2 and CYP26a1 during *Xenopus* gastrulation. These two enzyme-encoding genes show a non-overlapping expression in the dorsal mesoderm (**Fig. 1.5 B**). Thereby, RALDH2 is expressed in the internal involuting mesoderm, directly adjacent to the dorsal endoderm (Hollemann et al., 1998; Chen et al., 2001). Extensive combination experiments with endodermal and mesodermal explants revealed that RA acts directly on the dorsal endoderm as well as indirectly via the dorsal mesoderm (Pan et al., 2007). However, the RA-induced gene network that promotes pancreas fate has not yet been identified.

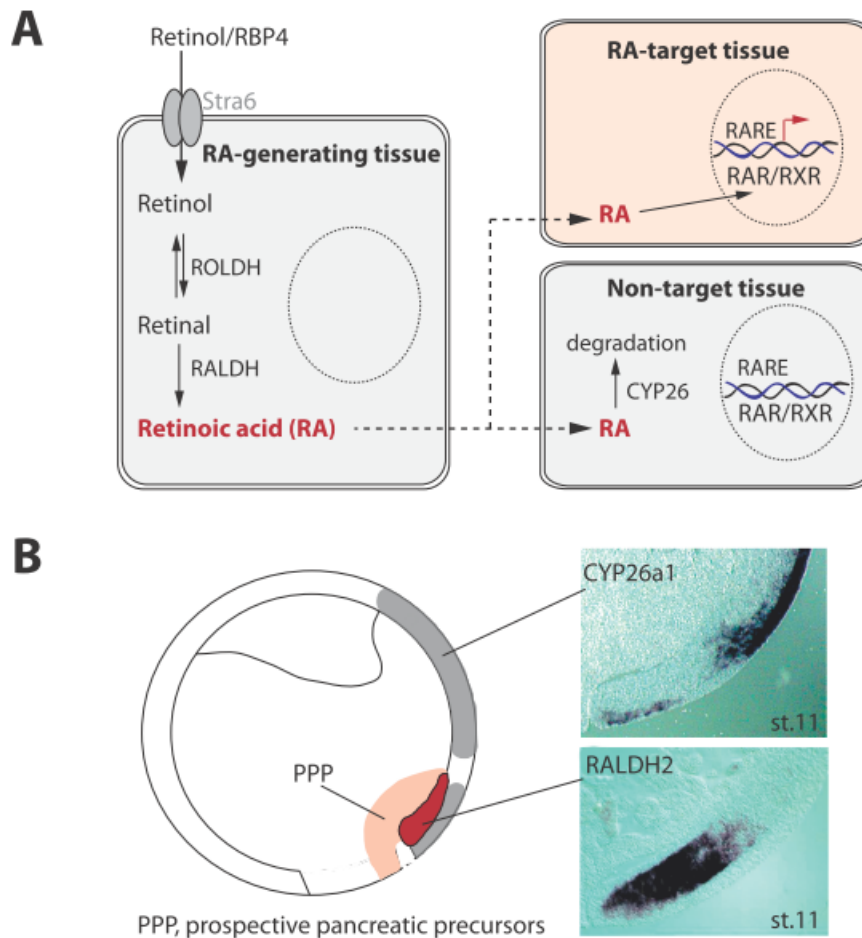


Fig. 1.5 Paracrine RA-signaling and expression of RA-metabolizing enzymes during *Xenopus* gastrulation

(A) Retinol is transported by the retinol-binding protein (RBP4) and enters the cells via the receptor Stra6 (Stimulated by retinoic acid 6). In RA-generating tissues, ROLDH (retinol dehydrogenases) is expressed which reversibly oxidize Retinol to Retinal. Retinal is further irreversibly oxidized to retinoic acid (RA) by RALDH (retinaldehyde dehydrogenases). RA is released and enters neighboring cells where it either gets oxidized by CYP26 (cytochrome P450) into inactive metabolites or it reaches the nucleus and binds to nuclear RA-receptor dimers RAR/RXR. RAR/RXR dimers are bound to RA-response elements (RARE) within the DNA and act as repressors until they form a complex with RA. The ternary RA-RAR/RXR complex acts as transcriptional activator recruiting further co-activators (modified from Duester, 2008). (B) Expression pattern of CYP26a1 and RALDH2 in a gastrula stage *Xenopus* embryo by WMISH. The pattern suggests the formation of a RA-gradient within the dorsal endoderm that specifies an area of putative dorsal pancreatic progenitors (modified after Hollemann et al., 1998; Chen et al., 2001).

1.5 Role of Wnt-signaling in pancreas development

During embryonal development in vertebrates, Wnt-signaling has diverse functions. These involve both Wnt-signaling pathways, canonical as well as non-canonical, both initiated by Wnt ligands and Frizzled receptors (Logan and Nusse, 2004). Early in development, maternal β -catenin is dorsally stabilized, thereby promoting organizer formation and anterior endoderm fate during gastrulation (Zorn et al., 1999; Schier and Talbot, 2005; Rankin et al., 2011). Shortly after gastrulation at early somite stage, zygotic Wnt-signaling has an opposite effect on anterior endoderm. Several studies in *Xenopus* demonstrated that Wnt-signaling must be inhibited to maintain foregut identity which is essentially required for pancreas development. McLin and colleagues found that foregut gene expression is repressed by Wnt8-overexpression, while in contrast the Pdx1 domain is expanded by over-expression of Wnt-antagonist Dkk1 (McLin et al., 2007). Furthermore, Li and colleagues identified the secreted Wnt-antagonist Sfrp5 (secreted frizzled-related protein 5) which is expressed in the early foregut epithelium. Embryos with downregulated Sfrp5 developed smaller foregut domains, while ectopic Sfrp5 expression leads to an expanded foregut domain at the expense of the hindgut (Li et al., 2008).

However, recent studies strongly indicate that the suggested model of a complete absence of Wnt-signaling for foregut development and high Wnt-signaling levels for hindgut development might be too simple. Two Wnt-signaling components, Wnt11 and Fzd7, were found to be expressed in the foregut endoderm, both mediating canonical as well as non-canonical Wnt-signaling (Wheeler and Hoppler, 1999; Djiane et al., 2000; Medina et al., 2000; Li et al., 2008). The depletion of Fzd7 in the foregut results in liver and pancreas agenesis. Therefore, low levels of Wnt/Fzd7 activity are found to be essential for foregut maintenance (Zhang et al., 2013a). Furthermore, Sfrps are shown to act biphasic on Wnt-signaling in a concentration dependent manner (Mii and Taira, 2009). A moderate dose of Sfrp5 was found to expand the foregut domain, whereas too low or too high concentrations lead to a reduction of foregut endoderm (Zhang et al., 2013a). Moreover, a comparative transcriptome analysis in mouse between liver and pancreas progenitors revealed a pancreas specific expression of Wnt-signaling components (Rodriguez-Seguel et al., 2013). These findings suggest the requirement of low Wnt-signaling activity for foregut maintenance and thereby pancreas development. Later in pancreas development, Wnt-signaling is essential for the expansion of pancreatic epithelium (Wells and Melton, 2000; Murtaugh et al., 2005; Dessimoz et al., 2005). However,

how Wnt-signaling is regulated during pancreas specification and how it promotes the pancreatic fate remains unclear.

1.6 Potential of organoids in research and clinical applications

Organoids are defined as multicellular structures containing multiple organ-characteristic cell types. Moreover, organoids recapitulate the *in vivo* organogenesis including the temporal program of lineage specification and the expression of cell-type specific marker genes (reviewed in Lancaster and Knoblich, 2014; Rookmaaker et al., 2015). Since decades, Amphibians and especially *Xenopus* were used as model system for *in vitro* organ formation as they provide a source of pluripotent cells. Already in the 1960s, Nieuwkoop and colleagues demonstrated the pluripotent state of blastocoel roof cells (Nieuwkoop, 1963). Blastocoel roof cells can be cultivated for weeks in a simple salt solution and without any further treatment they form an “atypical epidermis” (Jones, 1985). Thus, they are also named ectodermal explants. These pluripotent cells can be programmed by RNA-injections or chemical treatments to differentiate into the derivatives of all three germ layers. In several studies, Asashima and colleagues demonstrated the *in vitro* formation of various organoids and tissues from Activin A-treated dissociated and re-aggregated ectodermal explants (reviewed in Okabayashi and Asashima, 2006; Asashima et al., 2009). Activin A is a TGF β -family member which mimics nodal signaling in mouse (Conlon et al., 1994; Kubo et al., 2004). Asashima and colleagues found Activin A as concentration-dependent inducer of endodermal and mesodermal tissue (Ariizumi et al., 1991). Thereby, a high Activin A concentration induced the formation of head structures (Ariizumi and Asashima, 1995), whereas a moderate concentration leads to notochord structures and a low concentration to muscle tissue formation (Tamai et al., 1999). They further demonstrated that the additional treatment with RA induces pronephric or pancreatic gene expression (Chan et al., 1999; Moriya et al., 2000b; reviewed in Kurisaki et al., 2010). A later study in our lab applied a refined protocol for the *in vitro* generation of pancreatic structures from pluripotent ectodermal explants using Vegt and β -catenin as dorsal endoderm inducers and the BMP-inhibitor Noggin in addition to RA (Chen et al., 2004). A further notable study by Asashima and colleagues is the formation of ectopic beating hearts. Explants were treated with a high concentration of Activin A and started to beat after a few days. These beating structures were transplanted into neurula-stage embryos where they developed into ectopic beating hearts consisting of at least two chambers (Ariizumi et al., 2003; Kurisaki et al., 2010).

As vertebrate organogenesis is highly conserved between *Xenopus* and mammals at the molecular level, the knowledge about factors required for the formation of *Xenopus*-derived organoids were applied to protocols for the *in vitro* generation of mouse- and human-derived organoids. For the formation of mouse- and human-derived organoids the use of a matrigel was shown to promote organoid formation. The matrigel is an extracellular matrix containing collagen and lamins and it allows the use of the self-organization potential of stem cells. This was first demonstrated for epithelial intestine stem cells (Lgr5 positive) (Li et al., 1987). Cultures of these cells in a three-dimensional matrigel-system lead to the formation of structures comparable to intestinal crypts comprising of cell subtypes found in the intestine *in vivo* (Sato et al., 2009). This system has been adapted to form other organs including stomach (Barker et al., 2010) as well as organs with low self-renewal potential like prostate (Karthaus et al., 2014). The addition of distinct factors to the culture medium drives lineage determination and differentiation. For example, mouse pancreatic organoids could be generated from pancreatic ductal cells expressing Lgr5 induced by injury and treated with EGF, RSPO1, Noggin, FGF10 and Nicotinamide. These organoids differentiate into duct and endocrine cells upon transplantation (Huch et al., 2013a). The 3D matrigel-system was also applied to form organoids from human cells. Several human adult and embryonic stem-cell derived organoids have been generated including stomach (McCracken et al., 2014), small intestine (Sato et al., 2011), lung (Rock et al., 2009), liver (Huch et al., 2013b) and pancreas (Boj et al., 2015). However, most of the organoids are not “perfect” as they miss characteristic cell types or recapitulate only the earliest stages of organogenesis (reviewed in Willyard, 2015).

As the availability of human adult stem cells is limited and the use of human embryonic stem cells is associated with ethical concerns, several studies used induced pluripotent stem cells (iPSCs) as additional source for the generation of organoids. Human iPSCs have been used to generate kidney- (Takasato et al., 2015) and intestine-organoids (Finkbeiner et al., 2015). The remarkable discovery of *in vitro* generated "mini brains" was made by Lancaster and colleagues. They found that iPSCs treated with growth factors self-organize into cerebral organoids with distinct forebrain, midbrain and hindbrain regions, cell layers that resemble the cortical layers of a brain and rudiments of eye tissue. These cerebral organoids could be maintained for several months under supply of nutrients (Lancaster et al., 2013).

The ability of *in vitro* generated organoids to recapitulate the normal organogenesis leads to manifold application possibilities (**Fig. 1.6**). For clinical applications, biopsy

material can be cultivated in matrigel to form organoids. These can be used for studies of molecular pathogenesis in cancer-derived organoids as it was done for prostate cancer (Gao et al., 2014). Moreover, patient-derived organoids can serve for drug screens for high efficiency and low toxicity to allow a personalized medication. Furthermore, a recent study with organoids derived from patients with cystic fibrosis demonstrated the potential for gene therapy applications. Schwank and colleagues could repair the CFTR-mutation in patient-derived organoids by the use of CRISPR/Cas system (Schwank et al., 2013). This procedure is a promising method to provide patients with functional tissue. Further applications for research purposes are also conceivable. Some gene knockouts are lethal for mice and could be done in mice-derived organoids to allow functional analysis of these genes. Furthermore, the use of organoids could reduce the number of animals sacrificed for experiments. For instance, conditions can be tested in organoids first and the identified optimal conditions can then be applied to the animal model.

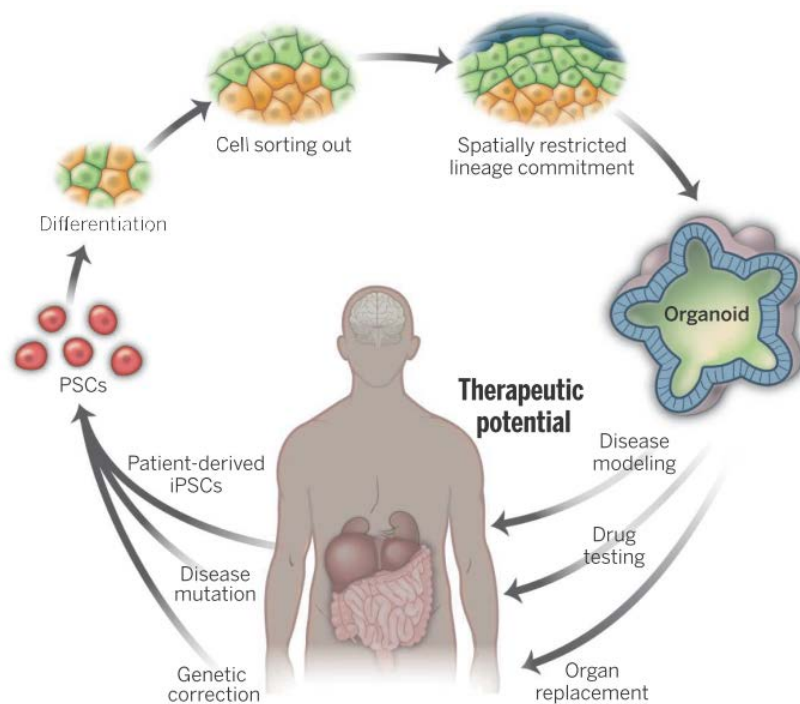


Fig. 1.6 Therapeutic potential of *in vitro* generated organoids

Biopsy material or patient-derived iPSCs can be used for *in vitro* organogenesis. The self-organizing potential through cell sorting and spatial restricted lineage determination promotes to the formation of organoids. These organoids can be used as model system for studies of molecular pathogenesis, drug testing or gene therapeutic applications. The image is adapted from Lancaster and Knoblich, 2014.

1.7 Aim of this study

As described in the previous sections, various studies in *Xenopus*, zebrafish and mouse revealed that the requirement of RA for pancreas specification is conserved among these species. However, the gene network that is induced by RA and promotes pancreas fate is unknown so far. Therefore, the main goal of this study was the identification of early direct RA-target genes in the endoderm. To reach this aim, pancreatic organoids, *in vitro* generated from ectodermal explants, were used. For this, pancreatic organoids were first verified for their potential to recapitulate pancreas development. The second goal was the validation of identified RA-target genes for their requirement in pancreas development.

2. Materials and Methods

2.1 Materials

2.1.1 Model Organism

For experimental studies, the African clawed frog *Xenopus laevis* was used. The frogs were purchased from Nasco (Ft. Atkinson, USA). The embryonic staging was based on the descriptions of Nieuwkoop and Faber (Nieuwkoop and Faber, 1967).

2.1.2 Bacteria

The following E.coli bacteria received from Stratagene GmbH (Heidelberg, Germany) were used for molecular biology standard methods: XL1-Blue recA1, endA1, gyrA96, thi-1, hsdR17, supE44, relA1, lac[F⁺proAB, lacI^qΔM15, Tn10(Tet^r)]^c (Stratagene).

2.1.3 Constructs

2.1.3.1 Constructs for sense and anti-sense RNA

2.1.3.1.1 *Constructs prepared during this study*

Hnf1b-pCS2+

The open reading frame of Hnf1b was amplified from XHnf1b-pGEM7Z(-) (Vignali et al., 2000) using oligonucleotides MG102 and MG103 and cloned into the ClaI and XbaI sites of pCS2+ vector (Rupp et al., 1994; Turner and Weintraub, 1994). This construct served as template for Hnf1b antisense RNA preparation and was linearized with BamHI and transcribed with T7-polymerase.

HNF1b-GRpCS2+

For the generation of a hormone-inducible Hnf1b for the purpose of gain of function experiments, the open reading frame of Hnf1b was amplified from XHnf1b-pGEM7Z(-) (Vignali et al., 2000) without the stop-codon using the oligonucleotides MG102 and MG156. The PCR-product was then cloned into the ClaI and XhoI sites of GRpCS2+, a pCS2+ derivate (Gammill and Sive, 1997), containing the sequence of the human glucocorticoid receptor (GR). For sense RNA preparation the construct was linearized with NotI and Hnf1b-GR transcribed with Sp6-polymerase.

Fzd4s-pCS2+

For Fzd4-knockdown rescue experiments, the Fzd4s sequence was amplified from cDNA of stage 13 embryos using oligonucleotides MG169 and MG170 and cloned into the pGem[®]-T Easy vector (Promega). The amplified sequence contained the ATG and 920 nucleotides downstream reaching the stop codon within the intron. From this construct the Fzd4s sequence was amplified with oligonucleotides MG173 and MG174 and cloned into the ClaI and XbaI sites of pCS2+. For sense RNA preparation, the construct was linearized with NotI and transcribed with Sp6-polymerase.

Fzd4_intron-pGEMTeasy

For specific Fzd4s-RNA detection in WMISH, a 600 nucleotide sequence of the Fzd4-intron was amplified from cDNA of stage 13 embryos using oligonucleotides MG165 and MG170 and cloned into pGem[®]-T Easy vector. Antisense RNA was prepared by Sall linearization and transcription with T7-polymerase.

2.1.3.1.2 Provided constructs for sense and antisense RNA**Tab. 2.1 Provided constructs for sense RNA**

Designation	Vector	Acession	reference	sense RNA	
				Cut	Pol.
Beta-Gal	pCS2+	NC_000913.3	Chitnis et al., 1995	NotI	Sp6
Cyp26a1	pBK-CMV	O93323	Hollemann et al., 1998	MluI	T3
Fzd4-3'MT	MT/pCS2+	NM_001090453	Swain et al., 2005	NotI	Sp6
GFP	MTpCS2+	NC_011521.1	Rubenstein et al., 1997	NotI	SP6
Noggin	pGEM5ZF	M98807	Smith et al., 1993	NotI	SP6
Vegt	pCS2+	AAB93301	Zhang and King, 1996	NotI	SP6
Wnt5a	MTpCS2+	M55056.1	Damianitsch et al., 2009	NotI	Sp6
Wnt8a	pSP64T	CAA40510	Smith and Harland, 1991	BamHI	Sp6

Tab. 2.2 Provided constructs for anti-sense RNA

Designation	Vector	Accession	reference/source	anti-sense RNA	
				Cut	Pol.
Cebpd	pCMV-Sport6	BC093576	(Ikuzawa et al., 2005) <i>Thermo Scientific</i> (7007767) cloned with shortened 3'UTR	EcoRI	T7
Cyp26a1	pBK-CMV	O93323	(Holleman et al., 1998)	Clal	T7
Dhrs3- 3'FLag	pCDNA3.1- Flag	NM_001092373	(Kam et al., 2010)	EcoRI	SP6
Foxh1	MT/pCS2+	NM_001088351 (missing first 183 bp from ATG)	(Kofron et al., 2004)	EcoRI	T7
Fst	pCMV-Sport6	BC068649	(Tashiro et al., 1991) <i>Thermo Scientific</i> (4406472)	Sall	T7
Fzd4	pCS2+	NM_001090453	(Swain et al., 2005)	BamHI	T7
Gbx2	pGem-Teasy	AF395825	(Maczkowiak et al., 2010)	Apal	SP6
Hnf1b	pCS2+	NM_001089811	(Vignali et al., 2000)	BamHI	T7
Hoxa1-b	pCMV-Sport6	CF28664	(Sive and Cheng, 1991) <i>BioScience</i> (IRBHp998F2212170Q)	Sall	T7
Hoxb1	pGEM-3ZF(-)	FJ422584	(Nieto et al., 1992)	EcoRI	SP6
Hoxd1	MT/pCS2+	Q08820	(Sive and Cheng, 1991)	EcoRI	T7
Hoxd4	pExpress	BC110765	(Klein et al., 2002) <i>BioScience</i> (IRBHp990G0190D)	EcoRI	T7
Igf3	pCMV-Sport6	AAL06242	(Richard-Parpaillon et al., 2002)	Sall	T7
Ins	pGem-Teasy	P12706	(Shuldiner et al., 1989)	Not	T7
Lhx1	pBluescript	NM_001090659	(Taira et al., 1994)	XhoI	T7
Meis3a	pSP64T	AF072895	(Salzberg et al., 1999)	Clal	T3
Nkx6.2	pBluescript	NM_001096886 +270 to +990	(Dichmann and Harland, 2011)	XhoI	T7
Pdia2	pBK-CMV	AY351916	(Sogame et al., 2003)	BamHI	T7
Pdx1	pGem-Teasy	NM_001172211	(Wright et al., 1989)	Apal	SP6
Prph	pCMV-Sport6	BC056020	(Sharpe et al., 1989) <i>ATTC®</i> (10167281)	Sall	T7
Ptf1a	pGem-Teasy	DQ007931	(Afelik et al., 2006)	Not	T7
XI.45046	pCMV-Sport6	CF286593	Source BioScience (IMAGp998J07121170Q)	Sall	T7
XI.47239	pCMV-Sport6	IRAK288Co6	Source BioScience (IRBHp990G0486)	Smal	T7
XI.51509	pCMV-Sport6	DY570900	Source BioScience (IMAGp998L119296Q)	Sall	T7
XI.57926	pCS111	C0387168	Source BioScience (IMAGp998C1718900Q)	Clal	T7

Designation	Vector	Accession	reference/source	anti-sense RNA	
				Cut	Pol.
Znf703-b	pExpress	DR726975	(Hufton et al., 2006) <i>BioScience</i> (IRBHp990A1190D)	Smal	T7

2.1.3.2 Constructs for Luciferase reporter assay

Tab. 2.3 Luciferase assay constructs

Designation	Vector	Reference
Atf2-firefly	pGL3B	(van der Sanden et al., 2004)
Renilla	pRL-TK	(Promega)
Siamois-firefly	pGL3B	(Brannon et al, 1997)

2.1.3.3 Constructs for CRISPR/Cas system

Tab. 2.4 CRISPR/Cas system constructs

Designation	Vector	Reference	Sense RNA	
			Cut	Pol.
Cas9	pCasX	(Blitz et al., 2013)	Acc651	T7
Fzd4-gRNA	pDR274	section 2.2.5.1	Dral	T7

2.1.3.4 Constructs for real-time RT-PCR standard curves

Tab. 2.5 Real-time PCR constructs

Designation	Vector	Reference
Insulin	pGem-T	(Shuldiner et al., 1989)
Odc	pGem-T	(Klisch, 2006 PhD)
Pdx1	pGem-T	(Wright et al., 1989)
Ptf1a	pGem-T	(Afelik et al., 2006)

2.1.4 Oligonucleotides

The oligonucleotides for cloning, sequencing and RT-PCR were purchased from SIGMA and dissolved in dH₂O to 100 µM stock solution. The antisense morpholino oligonucleotides were purchased from Gene Tools, LLC (Philomath, USA) and dissolved in RNase-free water to a concentration of 1 µM or 2 µM.

2.1.4.1 Cloning oligonucleotides

Tab. 2.6 Cloning oligonucleotides

(the digestion enzyme target site is underlined)

Label	oligonucleotide	Sequence 5' → 3'
MG102	XHNF1b_ClaI_fw	cc <u>ATCGAT</u> ggATGGTGTCCAAGCTATCGCC
MG103	XHNF1b_stXba1_rev	Gg <u>TCTAGAG</u> CTCACCATGCTTGCAAAGGACACTG
MG156	xHNF1b_Xho_rev	gcg <u>CTCGAG</u> cggCCATGCTTGCAAAGGACACTG
MG165	fz4_intron1_fw	GTTACGCGCAGCAAGTCATT
MG169	fz4S_sense_fw	ATGGGGGCAAGATCGCTGACC
MG170	fz4S_sense_rev	CACAGTCACTTTTTGTGGACG
MG173	fz4S_senseCla_fw	cc <u>ATCGAT</u> ggATGGGGGCAAGATCGCTGACC
MG174	fz4S_senseXba_rev	gc <u>TCTAGAG</u> gcCACAGTCACTTTTTGTGGACG
MG171	fz4_5UTRfl_fw	GATTGTCCGGGAGTGTGCTA
MG248	Fzd4s_P2_rev	GAAAGTAAACCCCTGTGCTGAG
MG273	fzd7_fw	GTTACGTGGGCATCAACAGC
MG274	fzd7_rev	TTGTAGTTGGGACAGGGCAC
MG275	kremen2_fw	TCACGGTGAATGGGAGAGAC
MG294	kremen2_rev3	ACAGTTTATTCATAGTGAAGCTCA
MG297	impad1_fw4	ATGACCTGAAATGGCTGCCT
MG298	impad1_rev2	CATGGTCTGCAGTTCGTGATG

2.1.4.2 Sequencing nucleotides

Tab. 2.7 Sequencing oligonucleotides

Designation	Sequence 5' → 3'
HNF1b_seq1	GTTCTGCTGCAAAGGCGATA
HNF1b_seq2	GTGGTGTATCTCCATCTAAAG
HNF1b_seq3	GGGCGTTCCATTGACGTAAATG
pCS2_seq	GGGCGTTCCATTGACGTAAATG
SP6	TTAGGTGACACTATAGAATAC
T3	AATTAACCCTCACTAAAGGG
T7 (pCS2+)	TCTACGTAATACGACTCACTATAG
T7 (pGem-T)	TAATACGACTCACTATAGGGCGA

2.1.4.3 Reverse transcriptase (RT) – PCR oligonucleotides

Tab. 2.8 RT-oligonucleotides and working conditions

Oligonucleotide	Label	Sequence	T _{Annealing} [°C]	Cycles
Amylase_fw	LP1	CAAGCTCTGCACTCGTTCTG	55	34
Amylase_rev	LP1	GTTTTCTATTTGCGCCATCGC		
Bmp4-F	338	GCATGTACGGATAAGTTCGATC	58	32
Bmp4-R	339	GATCTCAGACTCAACGGCAC		
Cer1-F	009	TGCCCATGGAAACAAAAGTGC	57	28
Cer1-R	010	AGCGTCAGGTGGTTCAGGGTAA		
CYP26_2C8_link_F	MG039	GTCGACCTGTGGATCCAAAGA	60	28
CYP26_2C8_link_R	MG040	GATGCGTCTTGTAGATGCGAC		
CYP26_3'UTR_F	MG025	CCCGGAGATTCTCGAGGTT	56	30
CYP26_3'UTR_R	MG026	GACACCACGACCAAGACCCG		
Darmin_RT_fw	MG005	GGTACCATTACTTGGAGG	60	33
Darmin_RT_rev	MG006	AGCATCATCTGGTCCACCAA		
Fzd4s_fw	MG247	CATCAGGATCACCATGTGCCAG	60	28
Fzd4s_rev	MG248	GAAAGTAAACCCCTGTGCTGAG		
Glucagon_RT_F	LP1	AGAATTTATTGAGTGGTTGA	56	35
Glucagon_RT_R	LP1	ATCGGCATGTCTTCTGTCC		
H4_RT_fw	35	CGGGATAACATTCAGGGTATCACT	56	26
H4_RT_rev	36	ATCCATGGCGGTAAGTGTCTTCT		

Oligonucleotide	Label	Sequence	T _{Annealing} [°C]	Cycles
HNF1b_E1_fw	MG138	GGACAGGTGCTCTGGGACAAG	58/56	28/31
HNF1b_E2_rev	MG139	CCCTTTGTTTCCTCACATACC	58	28
HNF1b_E3_rev	MG141	GTCCTTGAAGTTGATTTTGCT	56	31
HNF1b_inj_R	MG149	CGGGGACATGTGCAAGTTCT	54	30
HNF1b_RT_F	MG075	AAAGGGCAGAAGTGGACAGG	58	32
HNF1b_RT_R	MG076	ATGCAGCACGTTTTTGGGTC		
Hnf4a_RT_fw	MG157	AGACTCCCCAACCATCTCCA	60	33
Hnf4a_RT_rev	MG158	CGCTTTCCCAAAGAGGCAAC		
Insulin_RT_F	LP1	ATGGCTCTATGGATGCAGTG	56	33
Insulin_RT_F	LP1	AGAGAACATGTGCTGTGGCA		33
ODC_RT_F	324	GCCATTGTGAAGACTCTCTCCATTC	56	24
ODC_RT_R	325	TTCGGGTGATTCCCTTGCCAC		
pCS2_RT_F	PB	CAAGCTACTTGTCTTTTTGC	54	30
Pdx1_RT_fw	MG256	GTCCTCCAGACATCTCACCG	60	33
Pdx1_RT_rev	MG257	AGCATGACTGCCAGCTCTAC		
Pia2_RT_F	LP1	GGAGGAAAGAGGGACCAA	60	33
Pia2_RT_R	LP1	GCGCCAGGGCAAAAGTG		
Ptf1a_UTR_F	348	GTTGTCAGAACGGCCAAAGT	60	33
Ptf1a_UTR_R	349	GGTACCGAGTGGAACCAAAG		
Sox17a_RT_F	MG063	CAAGAGACTGGCACAGCAGA	60	33
Sox17a_RT_R	MG064	CTGCTTGGGGTTCCCTGTAG		
Sox2_fw	266	GAGGATGGACACTTATGCCAC	58	29
Sox2_rev	267	GGACATGCTGTAGGTAGGCCGA		
Xfz4_RTE1_fw	MG163	CCAAAATGCCCAACCTGGTG	64	26
Xfz4_RTE2_rev	MG164	TTGTGGTCATTCTGGGGTGG		
Xfz4S_RT_fw	MG161	TTGTTGTACCTCCTGTGCTGCCTC	60	29
Xfz4S_RT_rev	MG162	TGGTAGAGTGAAATGCGCAGCAGC		

2.1.4.4 Real-time PCR oligonucleotides

Tab. 2.9 Real-time PCR oligonucleotides

Oligonucleotide	Label	Sequence	target region (bp)
ODC_RT_F	324	GCCATTGTGAAGACTCTCTCCATTC	+222 to +441
ODC_RT_R	325	TTCGGGTGATTCCCTTGCCAC	
Insulin_RT_F	LP1	ATGGCTCTATGGATGCAGTG	+1 to +291
Insulin_RT_F	LP1	AGAGAACATGTGCTGTGGCA	
Pdx1_fw	MG256	GTCCTCCAGACATCTCACCG	+170 to +551
Pdx1_rev	MG257	AGCATGACTGCCAGCTCTAC	
Ptf1a_fw	MG271	GGTACAGTCCGATCTGCCGC	+522 to +732
Ptf1a_rev	MG272	GGAGTCCACACTTTGGCCGT	

2.1.4.5 sgRNA oligonucleotides

Target site in the Fzd4 gene	GGCACATG[GTGATCCTGATG]
Forward (5' Phos)	TAGGCACATGGTGATCCTGATG
Reverse (5' Phos)	AAACCATCAGGATCACCATGTG

2.1.4.6 Morpholino oligonucleotides

Tab. 2.10 Morpholino oligonucleotides

Designation	Target RNA	Sequence 5' → 3'
HNF1b-MO	<i>Xenopus laevis</i> HNF1 β intron 1/exon2 boundary	ATCCTCGCTGTGAACAAAACACAAA
Fzd4-MO	<i>Xenopus laevis</i> Fzd4 ATG region (Gorny et al., 2013)	ATTATTCTTCTTCTGTTGCCGCTGA
Fzd4-mmMO	mutated Fzd4-MO, which does not bind target	ATTATTaTTaTTCTaTTGCaGCTaA
ctr-MO	no target	CCTCTTACCTCAGTTACAATTTATA

2.2 Methods

2.2.1 DNA methods

2.2.1.1 Chemical transformation and cultivation of bacterial cells

LB-medium:	Bacto Trypton 10g (1 %); Bacto Yeast Extract 5g (0.5 %); NaCl 10g (17.1 mM); dH ₂ O to 1 l; pH to 7.5
LB-agar:	Agar 15g (1.5 %) to 1 l LB-medium
Ampicillin:	stock solution 100 mg/ml in dH ₂ O; stored at -20 °C; working solution 100 µg/ml
Kanamycin:	stock solution 100 mg/ml in dH ₂ O; stored at -20 °C; working solution 50 µg/ml

In order to increase the amount of DNA for analytical and preparative methods, chemically competent *E.coli* XL1blue were used. 200 µl of bacterial cell suspension were thawed on ice, mixed with 100 ng of plasmid DNA or 5 µl of ligation mix, incubated for 30 min on ice and heat-shocked for 90 sec at 42 °C and 1 min on ice. 800 µl LB-medium was added and the solution was incubated with mild shaking for 1h at 37 °C. The bacterial cells were then pelleted by 30 sec centrifugation at 10,000 rpm, re-suspended in 100 µl LB-medium and seeded on LB-agar plates supplemented with ampicillin or kanamycin. Colonies were grown over night at 37 °C. Single colonies were picked and cultivated in LB-medium containing the appropriate antibiotic (Sambrook and Russel, 2001).

2.2.1.2 Plasmid DNA preparations

For the plasmid preparation in analytical amounts, the “GeneJET™ Plasmid Miniprep” kit (Thermo Scientific) was used. For the isolation of plasmid DNA in preparative amounts the “NucleoBond®Xtra Mid” kit (Machery-Nagel) was used according to the manufacturer’s instructions. The DNA concentration was measured with the NanoDrop-2000c spectrometer (Thermo Scientific).

2.2.1.3 DNA restriction digestion

Restriction digests for the purpose of cloning or linearization were carried out with restriction enzymes from Thermo Scientific according to the manufacturer's protocol. The digestions were performed with 2 to 5 U of the appropriate enzyme per μg DNA and incubated at 37°C for at least 1 h.

2.2.1.4 Agarose gel electrophoresis

TAE (Tris/Acetate/EDTA): 40 mM Tris Acetate; 2 mM EDTA; pH 8.5

6x DNA loading dye: 10 mM Tris-HCL (pH 7.6); 0,03 % Bromophenol Blue; 0,03 % Xylene Cyanol FF; 60 % Glycerol; 60 mM EDTA

2x RNA loading dye: 95% Formamide; 18 mM EDTA; 0.025% of each SDS, Xylene Cyanol and Bromophenol Blue (Ambion)

The agarose gel electrophoresis was used for the analysis of DNA-restriction or PCR products as well as for the quality control of sense and antisense RNA (Sharp et al., 1973). Agarose was boiled in 1x TAE buffer to prepare a 0.7 % to 2% (w/v) gel, depending on the size of the DNA/RNA fragments. Standard DNA ladders were used to define the size of DNA fragments (Fermentas High, Middle or Low Range). DNA loading dye was added to DNA samples and RNA-samples were mixed with RNA loading dye prior to loading. To visualize the DNA/RNA, ethidium bromide (0.5 $\mu\text{g}/\text{ml}$) was added. For the documentation the ChemiDoc video documentation system (EASY view) was used.

2.2.1.5 Purification of DNA fragments from agarose gel or digestions

For the purification of DNA fragments from agarose gels or restriction digestions, the "Invisorb Fragment Cleanup" kit (Invitex) was used according to the manufacturer's instructions.

2.2.1.6 Polymerase chain reaction (PCR)

The amplification of DNA- or cDNA-fragments was done by PCR (Saiki et al., 1985; Mullis et al., 1986). The reaction needs oligonucleotides complementary to the ends of the sequence that is to be amplified, nucleotides and a DNA-polymerase. The reaction proceeds in three steps that are repeated. Initially, the DNA template is heated to 95°C to render it single-stranded (Denaturation). Next, the oligonucleotides bind to the complementary sequence at a lower temperature specific for their size and composition (Annealing). Finally, the bound oligonucleotides are extended by the DNA-polymerase at 72 °C (Elongation). The DNA-Polymerase as well as the length and composition of the oligonucleotides varied depending on the purpose of amplification.

2.2.1.6.1 Cloning PCR

For the purpose of molecular cloning, DNA fragments were amplified by the use of the High Fidelity PCR enzyme Mix (Thermo Scientific). This Mix contains *Taq* DNA Polymerase and an additional thermostable DNA polymerase that possesses 3'→5' exonuclease "proof-reading" activity. This "proof-reading" activity reduces the occurrence of point mutations during the amplification process.

The PCR reaction mixture contained the following components:

<u>µl</u>	<u>final conc.</u>	<u>component</u>
1	100 ng	100 ng/µl template DNA
10	1x	5x High Fidelity Buffer with 15 mM MgCl ₂
1	0.2 mM (each)	10mM dNTP Mix (Thermo Scientific)
1	0.2 µM	10 µM oligonucleotide mix each
0.5	0.02 U	High Fidelity PCR enzyme Mix (Thermo Scientific)
Add water to 50 µl		

The following cycling conditions were used for the amplification:

<u>Initial denaturation</u>	95 °C	5 min	} 35 cycles
Denaturation	95 °C	45 sec	
Annealing	x °C	45 sec	
<u>Elongation</u>	72 °C	1 min / 1 kb	
Final elongation	72 °C	5min	

2.2.1.6.2 Semi-quantitative PCR

For the semi-quantitative PCR, cDNA was used (preparation described in chapter 2.2.2.4). Thus, the semi-quantitative PCR was used to analyze temporal gene expression patterns or alterations of gene expression upon microinjections or chemical treatments. The following components and conditions were used.

<u>μl</u>	<u>final conc.</u>	<u>component</u>
2.5	~ 125ng	~ 50 ng/μl cDNA
2.5	1x	5x Flexi GoTaq buffer with 25 mM MgCl ₂
0.625	0.5 μM	10 μM gene specific oligonucleotide mix
0.1	0.5 U	GoTaq polymerase (Promega)

Add water to 12.5 μl

<u>Initial denaturation</u>	95 °C	5 min	x** cycles
Denaturation	95 °C	45 sec	
Annealing	x* °C	45 sec	
<u>Elongation</u>	72 °C	45 sec	
Final elongation	72 °C	5min	

x* = oligonucleotide specific annealing temperature
x** = cycle number depends on the mRNA copy number

2.2.1.6.3 Quantitative real-time PCR

For the quantification of gene expression levels, cDNA was applied to the real-time PCR. To detect the amplified DNA the fluorescent dye SYBR Green was used that intercalates into double stranded DNA. The fluorescence is measured each cycle and increases in correlation with the increase in PCR-product. For this purpose, a PCR reaction mix containing SYBR Green was used (Biorad) and the detection took place in the IQ5 Biorad machine. All measurements were performed as duplicates and normalized to the values of *ornithine decarboxylase (odc)*.

μl	final conc.	component
2.5	~ 250ng	~100 ng/ μl cDNA
10	1x	2x SYBRGreen supermix (Biorad)
0.4	0.2 μM	10 μM gene specific oligonucleotide mix

Add water to 20 μl

<u>Initial denaturation</u>	95 °C	3 min	60 cycles
Denaturation	95 °C	10 sec	
Annealing	59 °C	15 sec	
<u>Elongation</u>	72 °C	30 sec	
Melting curve	56 – 95 °C	+ 1 °C/sec	39 cycles

2.2.1.7 DNA sequencing analysis

To confirm correct DNA sequences, the Dye-termination sequencing method, based on Sanger's chain-termination sequencing, was used (Sanger et al., 1977). The Sequencing was performed with the "Big Dye Terminator Cycle Sequencing" kit (Applied Biosystems). The following sequencing PCR reaction components and conditions were applied.

μl	final conc.	component
1	500 ng	500 ng/ μl DNA
1.5		seq mix
1.5	1x	seq buffer
0.625	0.625 μM	10 μM sequencing oligonucleotide

Add water to 10 μl

<u>Denaturation</u>	95 °C	2 min	25 cycles
Denaturation	95 °C	10 sec	
Annealing	x °C	15 sec	
<u>Elongation</u>	60 °C	4 min	

x = oligonucleotide specific annealing temperature

The DNA fragments, obtained from the sequencing reaction, were purified by the addition of the following components to the 10 μ l reaction mix.

1 μ l	125mM EDTA (pH 8.0)
1 μ l	3 M sodium acetate (pH 5.4)
50 μ l	100 % ethanol

The mixture was incubated for 5 min at room temperature following a centrifugation for 15 min at 14000 rpm. DNA pellets were washed with 70 μ l 70 % ethanol. The air-dried DNA pellets were dissolved in 15 μ l HiDi™ buffer (Applied Biosystems). The obtained sequencing PCR products were analyzed by the ABI 3100 Automated Capillary DNA Sequencer (Applied Biosystems).

2.2.2 RNA methods

2.2.2.1 *In vitro* synthesis of capped and uncapped sense mRNA

Capped sense mRNAs for the microinjection into *Xenopus* embryos were *in vitro* synthesized using the SP6, T7 or T3 mMessage mMachine Kits™ (Ambion). 1 μ g of linearized plasmid DNA template was used in 20 μ l reaction mixture. For uncapped sgRNA preparation, 2 μ g of linearized plasmid DNA were used in 25 μ l reaction mixture with components indicated in section 2.2.2.2 devoid of Dig-UTP. After an incubation of 3 hours at 37 °C the DNA template was removed by 5 U of Turbo DNase I (Ambion) for 30 min at 37 °C. The synthesized RNA was purified by the use of the Illustra™ RNAspin Mini RNA Isolation Kit (GE Healthcare). RNA concentration was measured by the NanoDrop and the quality was analyzed on a 1 % agarose gel. RNA aliquots were stored at -80 °C.

2.2.2.2 *In vitro* synthesis of labeled antisense RNA

Anti-sense RNA probes were used to detect endogenous transcripts by whole mount *in situ* hybridization (see chapter 2.2.4.). 1 µg of linearized plasmid DNA was used in 25 µl reaction. Following components were included in the reaction to generate Dig-labeled anti-sense RNA:

µl	component
5	5x transcription buffer (Fermentas)
4	ATP, GTP, CTP, UTP, Dig-UTP (10mM each) (Boehringer)
1	DTT (0.75 M)
1	Ribolock RNase inhibitor (40 U/µl) (Thermo Scientific)
1.5	RNA polymerase (20 U/µl Fermentas)

The reaction mixture was incubated for 3 h at 37 °C. The DNA template was removed using 2 U/µl Turbo DNaseI (Ambion) for 30 min at 37 °C. Anti-sense RNA was purified with the RNeasy® Mini Kit (Qiagen). The RNA was eluted in 100 µl RNase-free water at 80 °C for 2 min. The RNA quality was analyzed on a 1 % agarose gel. 1ml of hybridization mix was added to the prepared anti-sense RNA and stored at -20°C.

2.2.2.3 RNA isolation from whole embryos and ectodermal explants

Trizol: peqGOLD TriFast reagent (peQlab)

For total RNA extraction, two to five embryos and 20 to 50 ectodermal explants were fixated in liquid nitrogen and stored at -80 °C. Total RNA was isolated with trizol. Embryos and explants were macerated in 400 µl trizol using a sterile Omnican® 40 syringe (Braun). Samples were vortexed for 30 sec, 80 µl of Chloroform (Roth) were added and again vortexed for 30 sec. To separate the phases, the samples were centrifuged for 10 min at 4 °C with maximum speed. The upper phase was transferred into a new tube and mixed with 200 µl of Chloroform for 30 sec. After a second centrifugation step for 5 min the upper phase was transferred into a new tube and 180 µl of 2-propanol (Roth) were added to precipitate nucleic acids over night at -20 °C. The next day, the nucleic acids were pelleted by a centrifugation for 30 min. The pellet was washed with 75 % ethanol. The air-dried pellet was dissolved in 12.5 µl RNase-free water. To remove genomic DNA, the sample was incubated with 1 U/µl DNaseI (Thermo Scientific) for 1.5 h at 37 °C. The DNaseI activity was

inactivated by heating to 70 °C for 10 min. For the confirmation of complete removal of genomic DNA, a PCR was performed with 1 µl RNA sample (50 ng/µl) described in 2.2.1.6.2 Semi-quantitative PCR using oligonucleotides for housekeeping gene H4.

2.2.2.4 Reverse transcription and PCR

For cDNA synthesis, 50 to 100 ng total RNA was used for a reaction volume of 10 µl. The following additional components were contained in the reaction mix.

µl	final conc.	component
2	1x	5x Go Taq flexi buffer (Promega)
2	5 mM	25 mM MgCl ₂
0.5	2.5 ng	50 ng random hexamer oligonucleotides (Invitrogen)
1	1 mM	10 mM dNTP mix
0.2	0.8 U	Ribolock RNase inhibitor
0.4	20 U	MuLV reverse transcriptase (Roche)

cDNA synthesis was performed under the following conditions.

step	temperature (°C)	time (min)
1	20	20
2	42	60
3	95	5

From 10 µl cDNA reaction, 2.5 µl were used for semi-quantitative PCR (see chapter 2.2.1.6.2).

2.2.2.5 Quantitative Nanostring analysis

For the simultaneous quantification of different transcripts, the digital multiplexed expression analysis system Nanostring was used with 600 ng of total RNA. The analyzed genes as well as the target region are shown in the appendix (**Tab. 6.25** and **Tab. 6.26**). For data analysis, the counts were normalized in two steps using the nSolver software program provided by Nanostring. First, the counts were normalized with respect to the mean of positive control counts. Second, the counts were normalized to the geometric mean of the housekeeping gene *ornithine carboxylase (odc)*. Finally, to consider the background, the mean and two-fold of the standard deviation of the eight negative controls were subtracted. Negative values were set to 1. Data from two independent experiments (A and B) were used to

calculate a mean value. Error bars indicate the standard error of the mean (SEM) which results from the division of the standard deviation by square of two.

2.2.2.6 RNA-sequencing

2.2.2.6.1 RNA isolation

To isolate total RNA for RNA-sequencing, the trizol-based method, described in chapter 2.2.2.3 (p.47), was used with the following modifications. Ectodermal explants were lysated in 360 μ l trizol and incubated for 10 min at RT. Next, 72 μ l chloroform were added and incubated for additional 5 min at RT. After a centrifugation step of 20 min at 4 °C, the upper phase was transferred to a new tube, mixed with 1 volume of chloroform and centrifuged for 10 min. Again, the upper phase was transferred to a new tube, mixed with 1 volume of 2-propanol and incubated over night at -20 °C. Next day, the nucleic acids were pelleted by centrifugation for 30 min at 4 °C. The pellet was washed with 500 μ l 75 % ethanol, air dried and dissolved in 20 μ l RNase-free water. To remove the genomic DNA, 1 μ l DNaseI (Thermo Scientific), 0.5 μ l RNase inhibitor (Thermo Scientific) and 1x DNase reaction buffer were added to a total volume of 50 μ l and incubated for 1 h at 37 °C. To eliminate the DNaseI, 100 μ l RNase-free water and 200 μ l phenol-chloroform-isoamylalcohol were added. After a centrifugation of 20 min at 4 °C, the upper phase was transferred to a new tube. 1/10 vol. 5 M ammoniumacetate and 1 vol. 2-propanol were added and incubated over night at -20 °C. Next day, the RNA was pelleted by a centrifugation for 30 min at 4 °C. The pellet was washed twice with 75 % ethanol, air-dried and dissolved in 12.5 μ l RNase-free water. RNA quality was analyzed by use of the 2100 Bioanalyzer (Agilent). To confirmation the complete removal of genomic DNA, a PCR was performed with 1 μ l RNA sample (100 ng/ μ l) using oligonucleotides for housekeeping gene H4.

2.2.2.6.2 Sample preparation and sequencing

RNA-samples were prepared in two independent experiments. For sequencing the RNA-samples were handled with the “TruSeq RNA Sample Prep Kit v2” according to the manufacturer instructions. The samples were sequenced via HiSeq 2000 (Illumina). The sequence reads consist of 50 base pairs from the single-end mode and the quality of this reads was checked by FastQC (<http://www.bioinformatics.babraham.ac.uk/projects/fastqc/>).

2.2.2.6.3 Sequence alignment

The sequence images were transformed to bcl files by the use of the Illumina software BaseCaller and were de-multiplexed to fastq files with CASAVA (version 1.8.2). The obtained sequence reads were aligned to the transcript reference sequences of *Xenopus tropicalis* (kindly provided by Michael J. Gilchrist; Gilchrist et al., 2004). In addition, the reads were also aligned to selected *Xenopus laevis* transcriptome sequences (UniGene) for genes which were not found in the *Xenopus tropicalis* transcriptome. The alignment was performed using Bowtie2 (version 2.1.0) in local alignment mode allowing 6 mismatches within 50 bases (Langmead and Salzberg, 2012). The resulting SAM files (Sequence Alignment/Map) were converted to sorted BAM files (binary version of SAM files) and unique hits were filtered. That means reads mapped to more than two genes were removed to facilitate the analysis.

2.2.2.6.4 Statistical analysis

The counting of mapped reads was conducted with samtools (Li et al., 2009). The obtained data were pre-processed and analyzed in the R/Bioconductor environment (<http://www.bioconductor.org>), loading edgeR (Robinson et al., 2010) and biomaRt packages. The counts were normalized to trimmed mean of M-values and the dispersion was estimated. For the detection of differentially expressed genes, a test based on a generalized linear model likelihood ratio assuming negative binomial data distribution was performed via edgeR. Candidate genes were filtered to a minimum of two fold change difference to the control and a FDR-corrected p-value of <0.05. Gene annotation was enriched by data from Xenbase (<http://www.xenbase.org>), ensemble (mouse) (<http://www.ensembl.org>) and biomaRt (<http://biomart.org>).

2.2.3 *Xenopus laevis* embryo culture and micromanipulations

2.2.3.1 Preparation of *Xenopus laevis* testis

10x MBS: 880 mM NaCl; 10 mM KCl; 10 mM MgSO₄; 25 mM NaHCO₃; 50 mM HEPES (pH 7.8)

1x MBS: 1x MBS; 0.7 mM CaCl₂

Frog narcotic: 2.5 % Tricaine methanesulfonate in tap water; adjusted to a neutral pH by Na₂HPO₄; reviewed in (Guenette et al., 2013)

For *in vitro* fertilization of the eggs, a male frog was narcotized and sacrificed. The isolated testis was washed in 1x MBS and stored at 4 °C. A small part of the testis was minced and diluted in 1x MBS. This solution was stored on ice until it was needed.

2.2.3.2 Stimulation of eggs

HCG: 2000 U/ml human chorionic gonadotropin (HCG) (SIGMA)

In the evening, the female frogs were stimulated for the next day's egg deposition by the injection of 1000 U HCG subcutaneously close to the dorsal lymph sac. The frogs were kept at 16 °C over night so that ovulation started approximately 10 hours later. For a later egg deposition, the frogs were stimulated first with 500 U HCG in the evening and 1000 U HCG in the next morning.

2.2.3.3 Fertilization

Laid eggs were collected and *in vitro* fertilized with minced testis in 1x MBS. By the addition of water to dilute the testis-salt solution 1 to 10, the sperm movement was activated. 20 min after the fertilization the clutch of eggs was covered with 0.1x MBS.

2.2.3.4 Embryo culture and microinjections

Cysteine: 2 % L-cysteine hydrochloride in 0.1x MBS; pH 8.0

Injection buffer: 2 % Ficoll in 1x MBS

To remove the jelly coat, the fertilized eggs/ embryos were treated with 2 % cysteine hydrochloride, pH 8.0. After the removal of the jelly coat, the embryos were washed

three times with 0.1x MBS and cultivated at 12.5 °C until the microinjections. The injections were performed on a cooling plate at 12.5 °C. The developmental stage as well as the position of injection was dependent on the purpose of the approach. The solutions for the microinjections were loaded into glass needles prepared on a needle puller (PN-30, Science Products GmbH). The Microinjector 5242 (Eppendorf) was used to inject 4 nl of injection mixture per blastomere. Injected embryos were kept in injection buffer at 12.5 °C until the next morning. This allowed the healing of the injection opening. Afterwards, the embryos were transferred into 0.1x MBS and either prepared for ectodermal explants or further cultivated to the desired developmental stage. The developmental stages were defined according to Nieuwkoop and Faber Table of *Xenopus laevis* (Nieuwkoop and Faber, 1967).

2.2.3.5 *Xenopus laevis* ectodermal explants

5x MBS EE: 440 mM NaCl; 5 mM KCl; 4.1 mM MgSO₄; 12 mM NaHCO₃;
2.05 mM CaCl₂; 1.65 mM Ca(NO₃)₂; 50 mM HEPES; pH 7.8

Agarose dish: 0.7 % agarose in 0.8x MBS EE

First, the vitelline membrane of a micro-manipulated or un-manipulated stage 8 to 9 embryo was removed. Then, the centre of the pigmented animal hemisphere (=blastocoel roof tissue) was isolated by the use of the gastromaster system (Xenotek Engineering, Bellville, USA). The explants were washed in 0.8x MBS EE on a 0.7 % agarose-coated Petri-dish and cultivated over night at 12°C. The next day, at the equivalent of stage 11, the explants were treated with RA and/or CHX or DEX for a defined time span and were subsequently washed in 0,8x MBS EE. The explants were then cultivated in 0,8x MBS EE containing Ampicillin (100 µg/ml), Kanamycin (10µg/ml) and Gentamycin (10 µg/ml) at 12 to 14 °C and were daily provided with fresh buffer solution until the control embryos reached the desired developmental stage (Nieuwkoop, 1963; Fukui et al., 2003).

2.2.3.6 *Xenopus laevis* embryo and explant treatments

2.2.3.6.1 Dexamethasone (DEX) treatment

Dexamethasone: stock solution 4 mg/ml in 100 % ethanol
working solution 10 µM

To induce protein activity at a certain time point during embryonic development, hormone-inducible constructs were injected. Therefore, the ligand-binding domain of

the glucocorticoid receptor (GR) was fused to the coding regions (Gammill and Sive, 1997). In the absence of the hormone dexamethasone (DEX), the fusion protein is held in an inactive state. This inactive state is caused by complex formation with a chaperone protein (Hutchison et al., 1993). Upon the addition of DEX a conformational change is caused that dissociates the chaperone (Tsai and O'Malley, 1994). Injected embryos or ectodermal explants were cultivated in the dark in the presence of 10 μ M DEX until the desired stage was reached.

2.2.3.6.2 Retinoic acid (RA) treatment

Retinoic acid: stock solution 100 mM in DMSO (stored at -80 °C, SIGMA);
10 mM in 100% ethanol (stored at -20 °C in the dark)
Working solution 5 μ M in 0.1x MBS or 0.8x MBS EE

Ectodermal explants and whole embryos at stage 11 were incubated in 5 μ M RA (all-*trans*-RA) in the corresponding buffer for 1 h at 12 °C under light protection. After the treatment, embryos and explants were cultivated until the controls reached the desired developmental stage.

2.2.3.6.3 BMS453 treatment

BMS453: stock solution 10 mM in DMSO (stored at -20 °C, gift from Bristol Myers Squibb).
working solution 0.25 μ M in 0.1x MBS or 0.8x MBS EE

To inhibit endogenous RA-signaling, the synthetic retinoid BMS453 was used. BMS453 specifically binds the RA-receptor RAR β thereby blocking the binding of RA (Chen et al., 1995). Whole embryos were incubated with 0.25 μ M BMS453 in 0.1x MBS at stage 8/9 until stage 12. Afterwards, embryos were cultivated in 0.1x MBS until they reached the desired stage.

2.2.3.6.4 Cycloheximide (CHX) treatment

Cycloheximide: stock solution 100 mg/ml in DMSO (Sigma-Aldrich)
working solution 10 μ g/ml

To inhibit protein biosynthesis Cycloheximide (CHX) was used. CHX blocks the translocation step in elongation (Schneider-Poetsch et al., 2010). Ectodermal explants were treated with 10 μ g/ml CHX in 0.8x MBS EE 30 min prior to additional treatments (Perron et al., 1999).

2.2.4 Whole mount *in situ* hybridization (WMISH)

To visualize the spatial and temporal pattern of endogenous transcripts, a whole mount *in situ* hybridization (WMISH) was performed. The performance essentially based on (Harland, 1991; Hollemann and Pieler, 1999; Nieber et al., 2009). For the detection, a Digoxigenin-11-UTP (Dig) labeled anti-sense RNA probe was used. The visualization was done by the use of an alkaline phosphatase-coupled anti-Dig antibody. All steps were performed at ambient temperature with mild shaking.

2.2.4.1 Fixation and X-Gal staining

10x MEM: 1 M Mops; 20 mM EGTA; 10 mM MgSO₄; pH 7.4 (stored light protected)

10x PBS: 1.75 M NaCl; 1 M KCl; 65 mM Na₂HPO₄; 18 mM KH₂PO₄; pH 7.4

K₃FE(CN)₆: 0.5 M in H₂O (stored light protected)

K₄FE(CN)₆: 0.5 M in H₂O (stored light protected)

MEMFA: 4% (v/v) formaldehyde (37%) in 1x MEM

X-Gal: 40 mg/ml 5-Bromo-4-chloro-3-indolyl-b-D-galactopyranoside in formamide (stored -20 °C light protected)

X-Gal staining solution: 1 mg/ml X-Gal; 5 mM K₃FE(CN)₆; 5 mM K₄FE(CN)₆; 2 mM MgCl₂ in 1x PBS

Embryos were fixated with MEMFA in glas vials for 1 hr at RT following three washing steps with 100 % ethanol for 5 min. β -gal injected embryos were fixated in MEMFA for only 25 min following three washing steps with 1x PBS for 10 min. The co-injection of RNA encoding for β -galactosidase (*gfb1*) was used as a control for the purpose of knockdown and over-expression studies. To visualize the β -gal presence, X-Gal staining was performed (Bourguignon et al., 1998). Therefore, the embryos were incubated in X-Gal staining solution under light protection until the desired staining level was achieved. To stop the staining reaction, the embryos were washed three times for 10 min in 1x PBS and refixated for 25 min in MEMFA. Finally, the embryos were washed three times for 5 min in 100 % ethanol and stored at -20 °C.

2.2.4.2 Rehydration

PTw: 0.1 % Tween-20 in 1x PBS

Embryos were rehydrated with an ethanol series (75 %, 50 %, 25 %) to PTw and washed three times in PTw for 10 min each at RT.

2.2.4.3 Proteinase-K treatment

Proteinase-K: 10 µg/ml in PTw

To allow a better penetration of the anti-sense RNA probe, embryos were treated with Proteinase-K. The embryos were incubated in 2 ml of PTw/proteinase-K solution for a defined time period and temperature depending on the developmental stage.

stage	time [min]	temperature
explants	1	RT
10 to 12	4	RT
32 to 35	18	RT
39 to 41	15	37°C

2.2.4.4 Acetylation and refixation

Triethanolamine: 0.1 M (0.93 g in H₂O); pH 7.5 (SIGMA)

Acetic anhydride: (SIGMA)

PTw-FA: 4 % formaldehyde (v/v) in PTw

The proteinase-K treatment was stopped by two washing steps with triethanolamine for 5 min. To prevent an unspecific reaction of the Dig-labeled anti-sense RNA probe, free amino-acid ends were blocked by the treatment with 25 µl acetic anhydride in triethanolamine. Next, the embryos were washed two times with PTw for 5 min and refixed in PTw-FA for 20 min. Afterwards the embryos were washed 5 times with PTw for 5 min.

2.2.4.5 Hybridization

Hybridization Mix: 50 % (v/v) formamide; 1 mg/ml Torula RNA (SIGMA); 100 µg/ml Heparin, 1x Denhardt's; 0.1 % (v/v) Tween-20; 0.1 % (w/v) CHAPS; 10 mM EDTA in 5x SSC

100x Denhardt's: 2 % BSA; 2 % Polyvinylpyrrolidone (PVP); 2 % Ficoll 400 in H₂O (w/v)

20x SSC: 3 M NaCl; 0.3 M NaCitrate; pH 7.2-7.4

The Hybridization with the anti-sense RNA probe was preceded by a pre-hybridization with 1 ml hybridization mix for 5 min followed by incubation with fresh hybridization mix for at least 5 h at 65 °C. Afterwards the embryos were incubated in 1 ml Dig-labeled anti-sense RNA containing Hybridization mix over night at 65 °C.

2.2.4.6 Washing

20x SSC: 3 M NaCl; 0.3 M NaCitrate; pH 7.2-7.4

MAB: 100 mM maleic acid; 150 mM NaCl; pH 7.5

RNase solution: 20 µg/ml RNase A and 10 U/ml RNase T1 (Fermentas) in 2x SSC

The next day, the anti-sense RNA probe was collected and stored at -20°C for reuse. The embryos were washed in hybridization mix for 10 min at 65 °C and three times with 2x SSC for 15 min at 65 °C. To remove the non-hybridized RNA molecules, the embryos were incubated in RNase solution for 1 h at 37 °C. Afterwards the embryos were washed once in 2x SSC at 37 °C and twice in 0.2x SSC at 65 °C. Next, the buffer was exchanged to MAB.

2.2.4.7 Blocking and antibody incubation

MAB: 100 mM maleic acid; 150 mM NaCl; pH 7.5

MAB/BMB: 2 % BMB (Boehringer Mannheim blocking reagent) in 1x MAB

MAB/BMB/HS: 20 % heat-treated horse serum (HS) in MAB/BMB

MAB/BMB/HS/AK: 1:5000 sheep-anti-Dig antibody linked to alkaline phosphatase (AP) in MAB/BMB/HS (SIGMA)

To minimize unspecific binding of the AP-linked anti-Dig antibody, embryos were blocked in MAB/BMB for 20 min and in MAB/BMB/HS for 40 min. For the detection, the embryos were incubated with anti-Dig antibody containing MAB/BMB/HS/AK for 4h at RT. Next, the embryos were extensively washed with MAB, first three times for 10 min and then overnight at 4 °C.

2.2.4.8 Staining reaction

APB: 100 mM Tris-HCL; 50 mM MgCl₂; 100 mM NaCl; 0.1 % Tween-20; pH 9.0

NBT: 100 mg/ml in 70 % Dimethylformamide (light sensitive)

BCIP: 50 mg/ml in 100 % Dimethylformamide (light sensitive)

Staining solution: 0.8 µl NBT and 3.5 µl BCIP in 1 ml APB

MEMFA: 4% (v/v) formaldehyde (37%) in 1x MEM

The washing with MAB was continued by three times for 10 min with MAB. Then the caps of the glass vials were exchanged and three additional washing steps with MAB followed. Next, the embryos were two times washed in APB for 5 min at 4 °C and then the staining solution was added. This solution contained NBT and BCIP, substrates for the alkaline phosphatase that were converted to a colored product. The staining reaction was performed in the dark at 4 °C until the staining was sufficient. To stop the colour reaction and to remove background staining, the embryos were transferred to 100 % methanol. Then the embryos were rehydrated with a methanol series (75 %, 50 %, 25 %) to MEMFA and incubated for 30 min.

2.2.4.9 Bleaching

20x SSC: 3 M NaCl; 0.3 M NaCitrate; pH 7.2-7.4

MEMFA: 4% (v/v) formaldehyde (37%) in 1x MEM

Bleaching solution: 50 % formamide and 1 – 2 % H₂O₂ in 5x SSC

To remove the pigments for an easier documentation of the staining, the embryos were first washed twice in 5x SSC and then incubated with the bleaching solution. Afterwards, the embryos were washed again twice in 5x SSC and re-fixated with MEMFA.

2.2.5 CRISPR/Cas system

The CRISPR/Cas system (Clustered Regularly Interspaced Short Palindromic Repeats/CRISPR-associated) was first identified as part of the bacterial adaptive defense mechanism against virus and plasmid DNA (Fineran and Dy, 2014; Hsu et al., 2014; Terns and Terns, 2014). There, the RNA-guided DNA endonuclease Cas9 causes double-strand breaks at the DNA target site that were often imperfectly repaired by non-homologous end-joining (NHEJ). As a result, deletion or insertion mutations occur frequently (reviewed in Waters et al., 2014). Most recently, this system has been successfully applied for genome modification in numerous organisms (Blitz et al., 2013; Nakayama et al., 2013; Guo et al., 2014; Sander and Joung, 2014; Wang et al., 2015). In this study the CRISPR/Cas technology was used for *fzd4*-gene disruption. The Cas9 protein forms a complex with two short non-coding RNAs, a CRISPR RNA (crRNA) that has complementary sequence to the target DNA and a trans-activating CRISPR RNA (tracrRNA) that base pairs with the crRNA. For genome editing applications, a synthetic guide RNA (sgRNA) was designed by ZiFIT Targeter version 4.1 (Sander et al., 2007; Sander et al., 2010) where the minimal features of both RNAs were combined and the target sequence of 20 bp was added.

2.2.5.1 sgRNA preparation

1x annealing buffer: 40mM Tris, 20mM MgCl₂, 50mM NaCl, 10mM EDTA;
pH 8.0

For the generation of the sgRNA, the DR274 vector (Hwang et al., 2013) was used containing a T7 promotor for *in vitro* transcription. The pDR274 plasmid (Addgene) was digested with Bsal. Forward and reverse oligonucleotides, containing the sgRNA sequence with overhangs compatible to the Bsal-digestion sites, were annealed (see sequence in section 2.1.4.5, p.40). 100µM of each oligonucleotide were heated to 95 °C and cooled (-1 °C per 30 sec) to 4 °C in a volume of 50µl 1x annealing buffer. 15 µM of the annealed oligonucleotides were used for the cloning into the pDR274 vector. For the co-injection with *cas9* RNA the sgRNA was transcribed as uncapped RNA (described in section 2.2.2.1).

2.2.5.2 Target- and potential off- target-mutation analysis

For mutation analysis of CRISPR/Cas treated explants, the genomic DNA was isolated by the use of the "DNeasy Blood & Tissue Kit" (Qiagen). The region around the Fzd4-gRNA target site was amplified from genomic DNA using oligonucleotides MG171 and MG248. The Fzd4 amplicon was cloned into the pGem[®]-T Easy vector and ten to twelve clones were sequenced using the SP6 oligonucleotide. Obtained sequences were aligned to Fzd4 genomic sequence. The CRISPR/Cas target sequence is characterized by twenty nucleotides followed by a protospacer adjacent motif (PAM) (Hsu et al., 2013). Since a stretch of twenty nucleotides can occur multiple times in a genome and mismatches can be accepted by the CRISPR/Cas system depending on their position, it was necessary to predict potential off-targets. For this purpose, the CRISPR/Cas Target online predictor (CCTop) was used (<http://crispr.cos.uni-heidelberg.de>; Stemmer et al., 2015). The potential off-target sites of Impad1 (MG297/MG298), Kremen2 (MG275/294) and Fzd7 (MG273/MG274) were amplified with the indicated oligonucleotides, cloned and analyzed for mutations.

2.2.6 Luciferase assay

For the quantification of Wnt-signaling activities, embryos were either injected with 50 pg Simois-Luc (Firefly luciferase) (Brannon et al., 1997) or 100 pg att2-Luc (Firefly luciferase) (Ohkawara and Niehrs, 2011) and 10 pg pRL-TK (Renilla luciferase) (Promega) reporter DNA in combination with respective mRNAs animal at two-cell stage. Ectodermal explants were fixated in liquid nitrogen and stored at -20 °C. Duplicates for each sample were taken using 2x 30 explants. For the preparation of lysates and measurement of Firefly- and Renilla-luciferase activity, the Dual Luciferase Assay Kit (Promega) was used according to the manufacturer's instructions. Measurements were performed with the Centro LB 960 Luminometer (Berthold Technologies). The ratio of Firefly- to Renilla-light units was calculated and was adjusted to 1 for the sample with injected reporter RNA only. The resulting data were presented as relative luciferase activity. Thereby, either the highest activity is set to 100 % or the fold inductions are shown.

3. Results

3.1 Formation of pancreatic organoids from *Xenopus* explants

The aim of this study is the identification of the gene network responsible for pancreas specification. For this purpose, *Xenopus laevis* was used as model system as it provides a rich source of pluripotent cells which can be programmed to differentiate into endodermal, mesodermal and neuro-ectodermal derivatives (reviewed in Borchers and Pieler, 2010). Furthermore, known factors involved in pancreas organogenesis appear to be conserved between *Xenopus* and mammals (reviewed in Zaret and Grompe, 2008). For the identification of novel key players in pancreas specification, *in vitro* generated pancreatic organoids were used.

3.1.1 RA-dependent induction of pancreatic marker genes in Vegt/Noggin-programmed ectodermal explants

A previous study demonstrated that ectodermal explants from *Xenopus* embryos injected with *vegt* and β -*catenin* RNA express liver specific genes and that the addition of RA at the equivalent of gastrula stage further induces various pancreatic marker genes. Moreover, the co-injection of RNA coding for the BMP-inhibitor Noggin significantly increased the expression of these pancreatic markers at the expense of liver specific markers (Chen et al., 2004). In order to further optimize this procedure, we first asked if a combined Vegt/Noggin activity is able to induce pancreatic markers, so that β -catenin can be omitted. RNAs coding for *vegt* and *noggin* were injected into the animal pole of a two-cell stage embryo. Blastocoel roof tissue was explanted at the late blastula stage and treated with RA for one hour at the equivalent of gastrula stage. Explants were cultivated to the equivalent of stage 30. Total RNA was isolated and analyzed by RT-PCR (**Fig. 3.1 A**). Indeed, the co-injection of *vegt* and *noggin* is sufficient to drive pancreatic gene expression in ectodermal explants. The induction of the pancreatic progenitor markers Ptf1a and Pdx1, the endocrine marker Insulin and the endodermal markers Darmin and Sox17a is observed. Moreover, the addition of RA further increases the level of pancreatic gene expression (**Fig. 3.1 B**). For Noggin it was shown that it induces the expression of the RA-generating enzyme Raldh2 which leads to elevated RA-levels in this system (Pan et al., 2007). Thus, we next asked if endogenous RA-signaling can be blocked in this system in order to allow a temporally controlled activity of RA-signaling in the context of pancreas development. Therefore, we examined if the

induction of pancreatic genes can be blocked by the use of Cyp26a1, a RA-degrading enzyme (Hollemann et al., 1998). The co-injection of *cyp26a1* with *vegt* and *noggin* RNA almost completely blocks the expression of pancreatic genes. Importantly, this can be fully rescued by the addition of RA (**Fig. 3.1 B**). These data show that the used explant system allows a controlled activation of RA-signaling and represents a convenient system to identify RA-target genes.

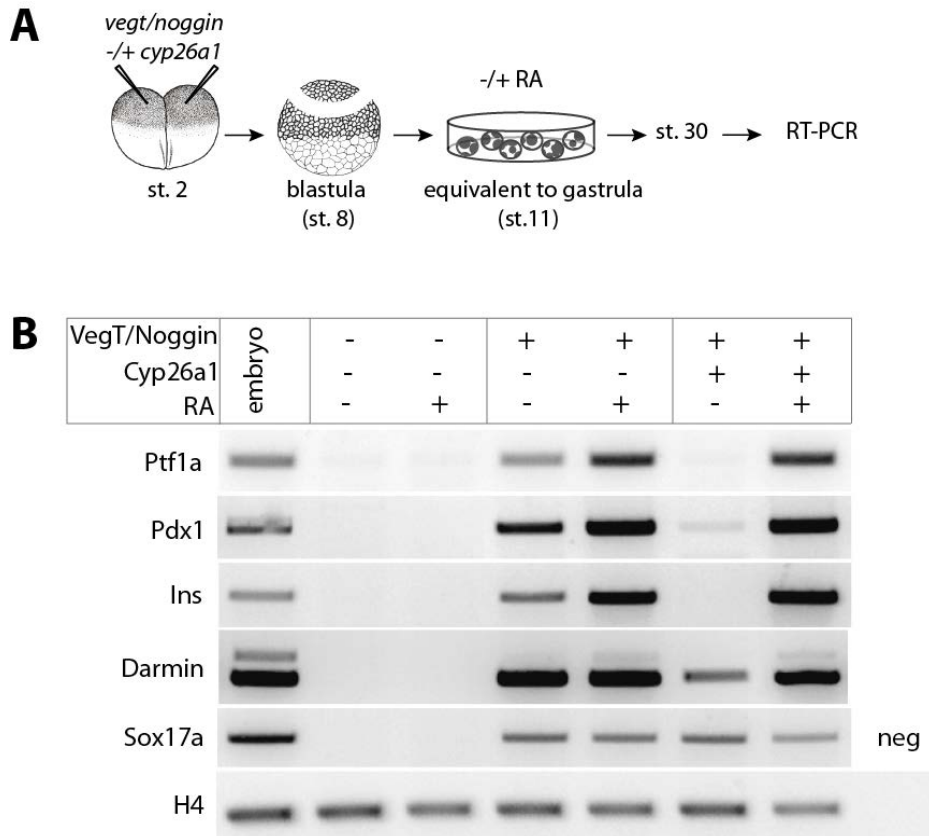


Fig. 3.1 RA-dependent induction of pancreatic marker genes in Vegt/Noggin-programmed explants

(A) Co-injection of *vegt* (500pg), *noggin* (500pg) and *cyp26a1* (2000pg) RNA into the animal pole of two-cell stage embryos. Tissue of the blastocoel roof was isolated at stage 8, cultivated and treated with 5µM RA at the equivalent of stage 11. Explants were cultivated until stage 30 and extracted RNA was analyzed by RT-PCR. (B) RT-PCR with indicated markers for endoderm (Darmin and Sox17a), pancreatic progenitors (Ptf1a and Pdx1) and endocrine tissue (Ins).

3.1.2 Formation of pancreatic organoids that recapitulate the *in vivo* program of pancreas development

We could show that ectodermal explants can be programmed to express pancreatic marker genes. In *Xenopus* embryos, the earliest known pancreatic progenitor marker genes can be detected at stage 29 by whole mount *in situ* hybridization (WMISH). The first endocrine marker is detected shortly after that at stage 32. Further endocrine and first exocrine differentiation marker genes were found at stage 39 and later (reviewed in Pieler and Chen, 2006). Therefore, we asked if our programmed explants show the same temporal expression profile of pancreatic progenitor and differentiation marker genes as observed *in vivo*. For this purpose, Vegt/Noggin/RA-programmed explants (pancreatic organoids/PO) were examined for pancreatic gene expression at different time points during development (**Fig. 3.2 A**). RT-PCR and the quantitative method of Nanostring analysis were used for the detection of selected transcripts. Transcript levels of tested marker genes in the pancreatic organoids were compared to whole embryos (embryo), Vegt/Noggin-programmed explants with blocked RA-signaling (\emptyset RA) and un-programmed explants (C) (**Fig. 3.2 B**). As observed in whole embryos, at the equivalent of stage 17, pancreatic organoids express endodermal marker genes Sox17a (**Fig. 3.2 B**), Sox17b and Darmin as well as mesodermal marker Xbra (**Fig. 6.1**). Unlike Sox17a and Sox17b, Darmin expression is RA-dependent enhanced in pancreatic organoids compared to explants with blocked RA-signaling. Transcripts of Gata4, a transcription factor involved in endoderm (Rehorn et al., 1996; Xanthos et al., 2001) and pancreas formation in mouse (Carrasco et al., 2012; Xuan et al., 2012), are detected at stage 17 (**Fig. 6.2**). Gata4 expression is RA-dependent maintained and further induced in pancreatic organoids at stage 24 together with the start of the expression of the pancreatic progenitor marker genes Ptf1a (**Fig. 6.2**) and Pdx1 (**Fig. 3.2 B**). The expression of the pancreatic endocrine progenitor marker Ngn3 (**Fig. 6.2**) is observed together with the start of Insulin expression (**Fig. 3.2 B**) at stage 24 in pancreatic organoids. The expression of Ngn3 appears to be transient and is detected only at low levels from stage 24 to 32. In contrast to pancreatic organoids, in whole embryos, Insulin expression is detected at stage 32 the earliest. Further differentiation marker genes for endocrine (Glucagon) and exocrine (Pdia2) tissue are detected at later stages (**Fig. 3.2 B** and **Fig. 6.2**). Moreover, the ventral pancreatic marker gene Tm4sf3, which is involved in the fusion of the ventral pancreatic buds with the dorsal bud, (Jarikji et al., 2009) is expressed together with the late exocrine marker Amylase (**Fig. 6.2**).

In summary, the temporal expression profile of analyzed markers in pancreatic organoids correlates with that in whole embryos (**Fig. 3.2 C**). Interestingly, the levels of endodermal and mesodermal markers detected in embryos and programmed explants with blocked RA-signaling are mostly higher than in pancreatic organoids. Furthermore, the pancreatic progenitor markers *Pdx1* and *Ptf1a* as well as the pancreatic differentiation markers *Amy2a* and *Pdia2* are more than 10 fold and Insulin more than 100 fold increased in pancreatic organoids as compared to control embryos. This observation argues for a very efficient conversion of the pluripotent blastocoel roof tissue into a pancreatic fate. Notably, the neuronal progenitor marker *Sox2* (Ellis et al., 2004) was also induced in pancreatic organoids (**Fig. 6.1**) which might reflect the innervation of pancreas by neurons as observed *in vivo* (Kirchgessner and Gershon, 1990). Detailed Nanostring data sets are shown in the appendix (**Tab. 6.1** and **Tab. 6.2**).

Fig. 3.2 Formation of pancreatic organoids that recapitulate the process of pancreas development

(A) RNAs coding for *Vegt* (500pg), *Noggin* (500pg) were co-injected into two-cell stage embryos. In order to block endogenous RA-signaling *cyp26a1* RNA (2000pg) was co-injected. Tissue from the blastocoel roof was explanted and cultivated. Explants were treated with 5 μ M RA at the equivalent of gastrula stage. Explants were fixated at the equivalent of stage 17 to 43 and total RNA was isolated and analyzed by RT-PCR and Nanostring.

(B) Diagrams show the number of counts detected by Nanostring nCounter for the indicated marker genes from two independent experiments. Figures on the right side show the results of the RT-PCR. (C) Summary of the temporal expression profile of indicated marker genes for embryos and pancreatic organoids. E = embryo; C = un-programed explants; PO = pancreatic organoid, ØRA = programed explants with blocked RA-signaling

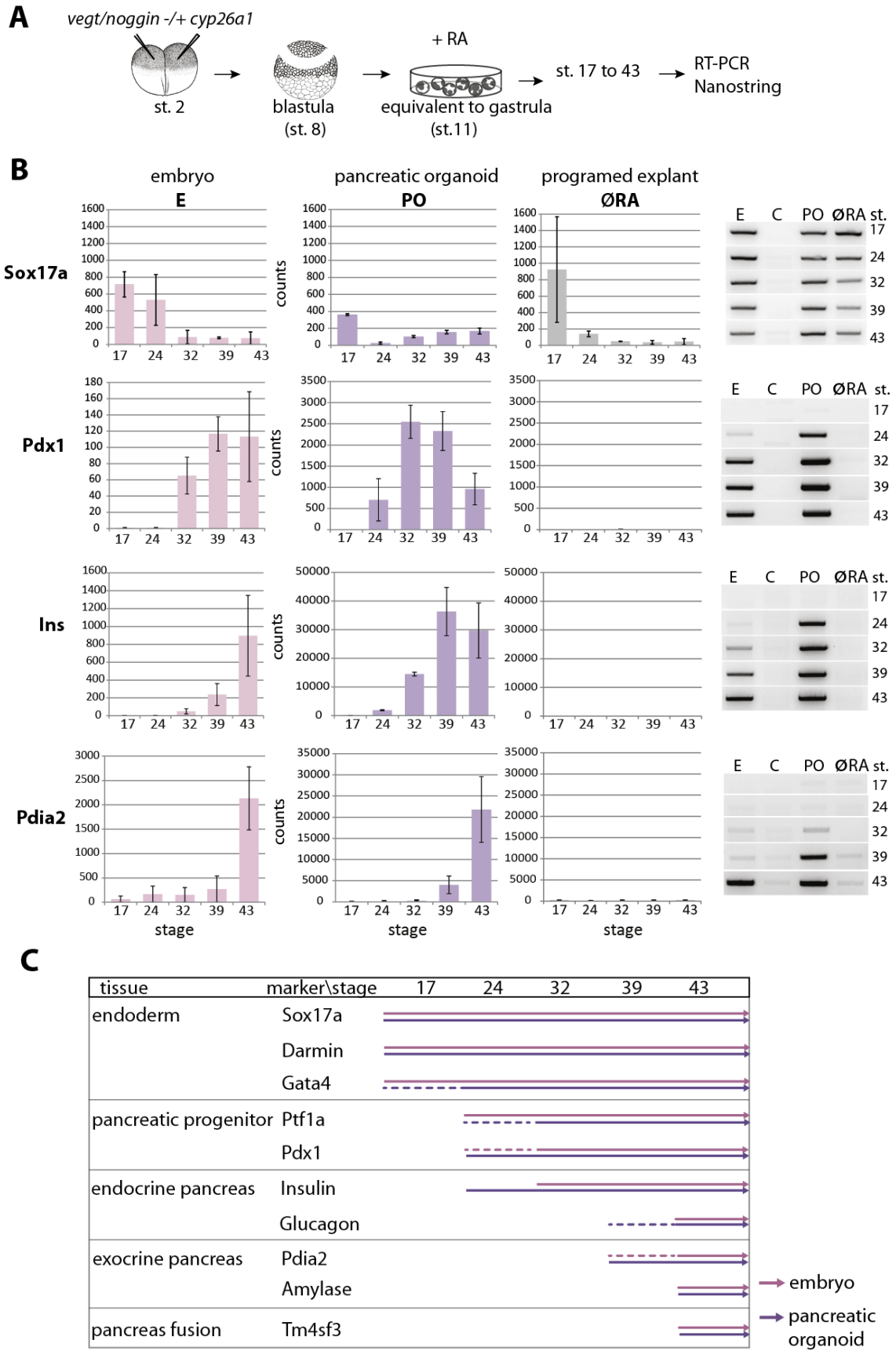


Fig. 3.2 Formation of pancreatic organoids that recapitulate the process of pancreas development

In order to detect how large the proportion of pancreatic progenitor and endocrine tissue in the organoids is, a WMISH was performed on the programmed explants at the equivalent of stage 35. Vegt/Noggin-programmed explants were not only treated with 5 μ M RA but also with 15 μ M and 30 μ M RA in order to see if the amount of pancreatic tissue is RA-concentration dependent increased (**Fig. 3.3 A**). For each RA concentration, explants with a different strength and distribution of pancreatic marker gene expression are observed and were grouped into the three phenotypes, weak, moderate and strong. Transcripts of progenitor marker genes *ptf1a* and *pdx1* are detected in larger domains whereas *insulin* transcripts are detected in single cells scattered within the organoid (**Fig. 3.3 B**). Indeed, a distinct increase in Ptf1a-, Pdx1- and Insulin-positive cells and percentage of explants showing an expression is observed with 15 μ M but no further clear increase is detected using 30 μ M RA. However, already the usually used concentration of 5 μ M RA leads to positive staining signals of tested marker genes in approximately 30% to 50% of the explants (**Fig. 3.3 C**).

In summary, we could show that Vegt/Noggin-programmed ectodermal explants promote pancreatic development in an RA-dependent manner. Therefore, this *in vitro* system of pancreatic organoids was further used for the identification of RA-target genes involved in early pancreatic development.

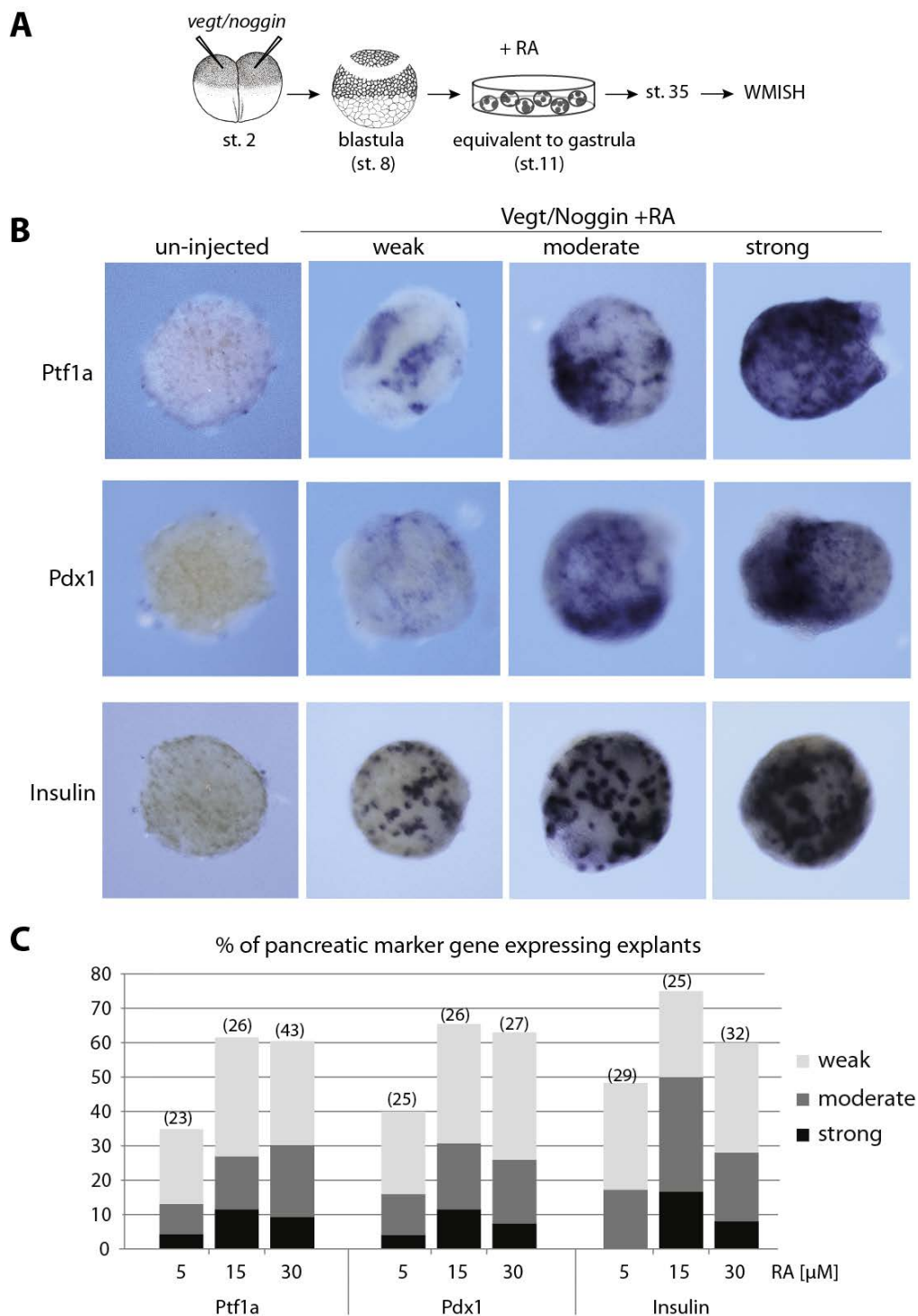


Fig. 3.3 Formation of pancreatic organoids from RA-programmed explants (WMISH)

(A) Co-injection of *vegt* (500pg) and *noggin* (500pg) RNA into the animal pole of two-cell stage embryos. Tissue of the blastocoel roof was isolated at stage 8, cultivated and treated with different concentrations of RA (5μM to 30μM) at the equivalent of stage 11. Explants were cultivated until the equivalent of stage 35 and used for WMISH against Ptf1a, Pdx1 and Insulin transcripts. Explants from un-injected embryos were used as negative control.

(B) Different phenotypes according to the intensity and distribution of pancreatic marker gene expression from weak to strong are presented. (C) The diagram shows the percentage of explants positive for pancreatic marker gene expression with the indicated phenotype. Total number of tested explants is indicated in brackets.

3.2 Identification, verification and expression characteristics of early RA-responsive genes

RA is known to be required at the onset of gastrulation for pancreas development in mice, zebrafish and *Xenopus* (Stafford and Prince, 2002; Stafford et al., 2004; Chen et al., 2004; Huang et al., 2014a). However, the gene network induced by RA that promotes pancreas development is still unknown. For the identification of RA-target genes in the context of pancreas development, the *in vitro* system of pancreatic organoids was used.

3.2.1 Induction of the direct RA-target gene Cyp26a1 within one hour after RA-addition

It has been shown that RA-activity at gastrula stage is required for pancreas specification *in vivo* (Chen et al., 2004). This observation correlates with the expression of the RA-generating enzyme Raldh2 in the dorsal involuting mesoderm during gastrulation (Hollemann et al., 1998; Chen et al., 2001). However, the first known pancreatic progenitor markers Pdx1 and Ptf1a are not detected before stage 24 (**Fig. 3.2**). In order to identify early direct RA-targets that mediate pancreas specification, it was essential to analyze the RA-response in a temporal manner. For this issue, we analyzed the temporal induction of the RA-hydroxylase Cyp26a1, a known direct RA-target gene (Ray et al., 1997; Abu-Abed et al., 1998). For this purpose, embryos were co-injected with RNA coding for Cyp26a1 that effectively blocks endogenous RA-signaling in pancreatic organoids (see above). Ectodermal explants were treated with RA at the equivalent of gastrula stage. In order to detect only direct targets, explants were further treated with the translational inhibitor cycloheximide (CHX) 30 min before RA-addition. Explants were fixated one and two hours after RA-addition. Endogenous *cyp26a1* transcripts were visualized using oligonucleotides targeting the 5'UTR of *cyp26a1* RNA. Endogenous *cyp26a1* was detected already one hour after RA-addition in the absence as well as in the presence of CHX. Levels of *cyp26a1* transcripts are further increased within two hours after RA addition (**Fig. 3.4**). In conclusion, the known direct RA-target Cyp26a1 is induced by RA within one hour in the *Xenopus* explant system used here.

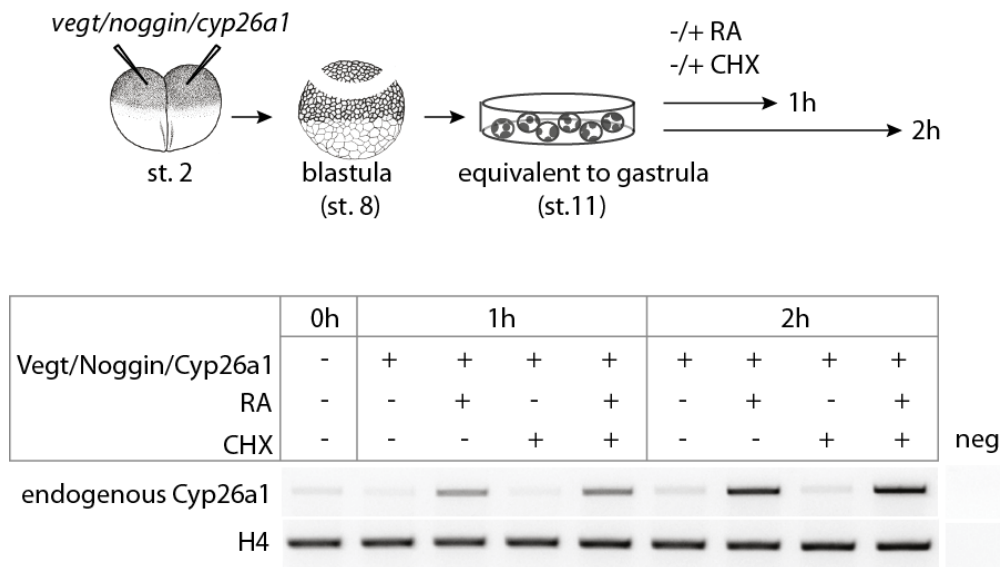


Fig. 3.4 Direct RA-target gene Cyp26a1 is induced within one hour

Vegt (500pg), *noggin* (500pg) and *cyp26a1* (2000pg) RNAs were co-injected into the animal pole of a two cell stage embryo. Blastocoel roof tissue was explanted at blastula stage. Explants were treated with RA and cycloheximide (CHX) at the equivalent of gastrula stage. One and two hours after RA addition, total RNA was isolated and analyzed by RT-PCR. Endogenous *cyp26a1* is detected one and two hours after RA-addition in the presence and absence of CHX.

3.2.2 Identification of early RA-target genes by RNA-sequencing

As the known direct RA-target Cyp26a1 was shown to be induced within one hour and further increased after two hours, these two time points were chosen for the identification of early RA-target genes in the context of pancreas specification. Pancreatic organoids were programmed by the co-injection of RNAs coding for Vegt, Noggin and Cyp26a1. RA and CHX were added at the equivalent of gastrula stage. Samples were taken one hour and two hours after RA-addition. For the identification of RA-target genes, total RNA was extracted and analyzed by RNA-sequencing for two independent experiments (**Fig. 3.5 A**). About 30.000 transcripts could be detected and at least 10 million sequence reads could be mapped to genomic sequences indicating a good quality of the RNA-sequencing (**Fig. 6.3 B**). Since the *X.laevis* genome was not completely sequenced, but is highly similar to that of the related species *X.tropicalis*, sequence reads were initially mapped to the *Xenopus tropicalis* genome and in second instance to the *Xenopus laevis* genome. Thereby, 102 genes are found to be differentially expressed in pancreatic organoids treated with RA versus untreated. Within one hour, 27 genes and within two hours after RA-addition 96 genes were recorded with an overlap of 21 genes (**Fig. 3.5 B, Tab. 6.3**). In the presence of the translational inhibitor CHX, 61 genes are differentially expressed (**Fig. 3.5 B, Tab. 6.4**). Most of the detected genes are up-regulated higher than two-fold and lower than five-fold. Only a few genes show an up-regulation higher than five-fold. And even less genes were found to be down-regulated (**Fig. 6.3 C**). Comparison of RA-regulated genes in the absence versus the presence of CHX was done to detect putative direct RA-targets. Almost half of the detected RA-targets are also differentially expressed during a block of translation (**Fig. 6.3 D, Tab. 6.5**). Hence, these 49 genes were referred to as candidates for putative direct RA-targets. However, since we want to identify the gene-network that leads to pancreas specification, all 102 detected genes were further analyzed. Detailed information of RNA-sequencing results are listed in the appendix (**Tab. 6.6 to Tab. 6.9**)

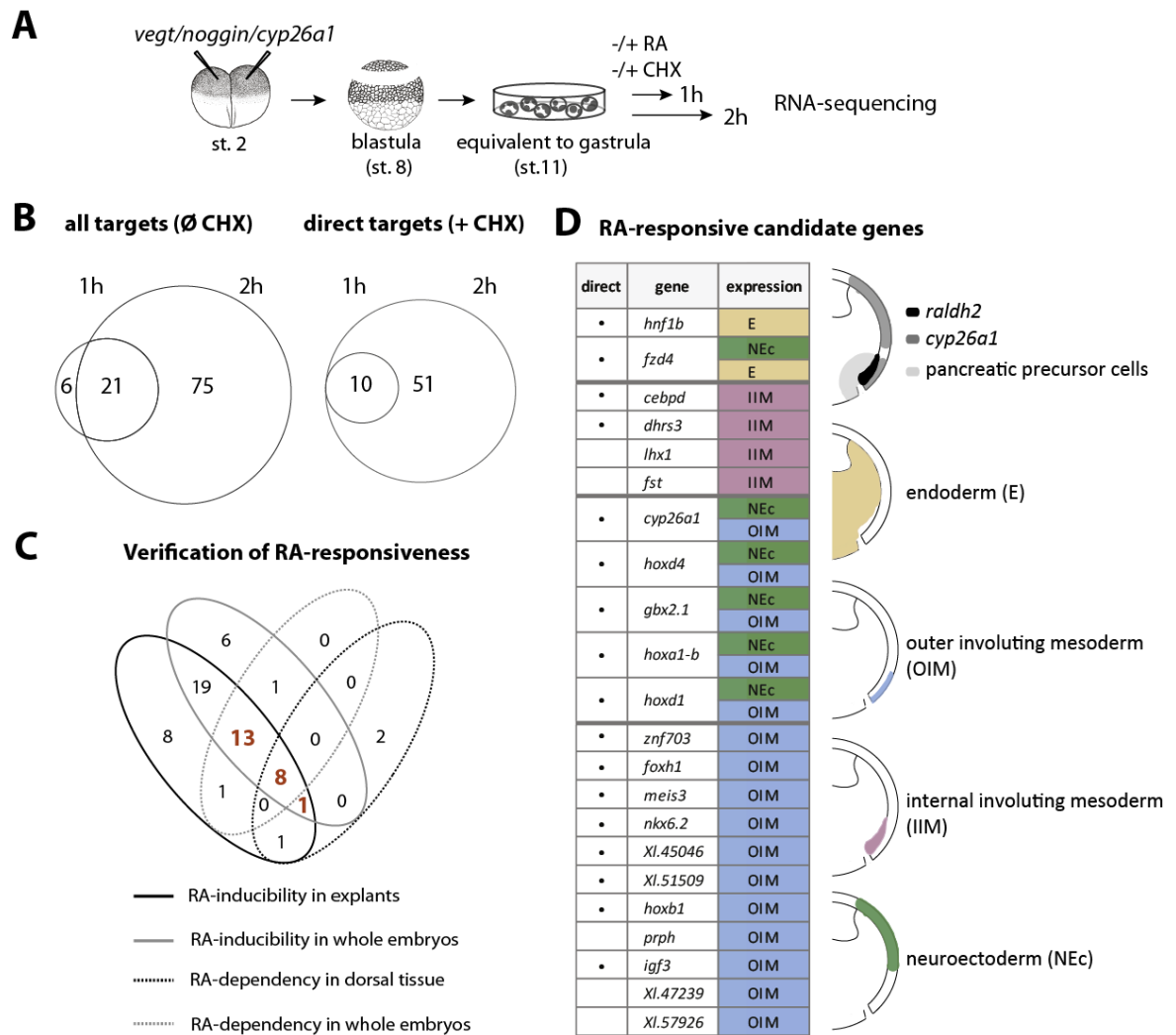


Fig. 3.5 Identification, verification and expression characteristics of early RA-responsive genes in the context of pancreas specification

(A) *Vegt* (500pg), *noggin* (500pg) and *cyp26a1* (2000pg) RNAs were co-injected into the animal pole of a two cell stage embryo. Blastocoel roof tissue was explanted at blastula stage. Explants were treated with RA and cycloheximide (CHX) at the equivalent of gastrula stage. One and two hours after RA addition samples were taken for RNA-sequencing.

(B) Venn diagrams show the number of differentially expressed genes within one and two hours after RA-addition in the presence or absence of CHX. Genes with less than 50 mapped reads were removed.

(C) Verification of RA-responsive genes. Indicated in red is the number of candidates confirmed for RA-inducibility in pancreatic organoids and/or whole embryos and RA-dependency in dorsal parts and/or whole embryos. 22 genes were confirmed for RA-responsiveness as they show both RA-inducibility and -dependency.

(D) 22 confirmed RA-responsive genes and their expression characteristics obtained by WMISH. Indicated with dots are the putative direct RA-target genes. The scheme on the upper right side indicates the expression domains of *Raldh2* (RA generating enzyme), *Cyp26a1* (RA-degrading enzyme) and the location of prospective pancreatic progenitors during gastrulation. The schemes below indicate the expression domains to which the candidates were assigned. E = endoderm, IIM = inner involuting mesoderm, NEc = prospective neuroectoderm, OIM = outer involuting mesoderm

3.2.3 Verification of 22 RA-responsive genes

Through RNA-sequencing, 102 putative RA-target genes could be identified. However, not all candidates could be used for further analysis. For 17 genes no sequence for *Xenopus laevis* was available at this phase of the study. For further three genes no Nanostring probe could be designed (**Tab. 6.3**). Thus, only 82 candidates were further examined.

In a first step, we re-examined the RA-responsiveness of these 82 presumptive RA-target genes. For this issue, RA-inducibility was quantitatively analyzed by Nanostring using the ectodermal explant system and whole embryos (**Fig. 6.4 A**). In the explant system, 51 of the 82 candidates were found to be more than 1.5 fold induced upon RA-addition. For the majority of these candidate genes, the expression is increased between 1.5 and 3 fold one hour after RA-addition compared to RA-negative programmed explants. After two hours, half of the induced genes are increased higher than 3 fold. In whole embryos, 48 of the 82 candidate genes were found to be induced more than 1.5 fold upon RA-treatment (**Fig. 6.4 A**). A comparative analysis revealed that 41 candidates could be confirmed for their RA-inducibility in both, the explant system and whole embryos (**Fig. 3.5 C**).

However, RA-inducibility does not necessarily mean that gene expression is dependent on RA-signaling activity. We further determined the RA-dependency of the 82 candidate genes by the inhibition of RA-signaling in embryos through the injection of *cyp26a1* RNA or through treatment with the RA-antagonist BMS453 (**Fig. 6.4 B**). We examined the gene expression by Nanostring analysis upon the inhibition of RA-signaling in whole embryos as well as in isolated dorsal tissue. We found the expression of 12 out of 82 candidate genes to be reduced more than 1.5 fold in RA-negative compared to untreated dorsal tissue. In whole embryos, 23 of the 82 candidates were found to be reduced more than 1.5 fold upon BMS453 treatment (**Fig. 6.4 B**).

The comparison of confirmed RA-inducible genes and verified RA-dependent candidates revealed a set of 22 candidate genes that are found to be RA-inducible as well as RA-dependent expressed (**Fig. 3.5 C and D**). The observed data are summarized in the appendix (**Tab. 6.10**) and shown in detail in **Tab. 6.11** to **Tab. 6.18**.

3.2.4 Expression characteristics of 22 verified RA-responsive genes

Identifying genes that control pancreatic specification in response to RA requires not only the determination of RA-responsiveness, but also the exclusion of those candidate genes that are not expressed at the right time and the right place during embryogenesis. RA-target genes involved in pancreas specification are expected to be expressed in the dorsal endoderm and/or the dorsal involuting mesoderm during gastrulation (Pan et al., 2007). Therefore, the expression patterns of the 22 RA-responsive candidate genes were analyzed at gastrula stage by WMISH. Thereby, candidates could be grouped according to their expression pattern (**Fig. 3.5 D**). We found that almost half of the candidates are expressed exclusively in the outer involuting mesoderm. A second group of five candidates display an additional expression domain in the prospective neuroectoderm and a third group of four candidates shows an expression in the inner involuting mesoderm (**Fig. 3.5 D, Fig. 6.5**). Two candidate genes, *Hnf1b* and *Fzd4*, exhibit an endodermal expression domain. *Hnf1b* is expressed in the entire endoderm with an enrichment in the dorsal area, whereas *Fzd4* expression domain is restricted in the endoderm at the dorsal side. Besides its endodermal expression domain, *Fzd4* shows a second expression domain in the prospective neuro-ectoderm (**Fig. 6.5**).

Pancreatic progenitor cells are known to derive from the dorsal endoderm under the control of RA that is synthesized in the dorsal involuting mesoderm (Pan et al., 2007.) Thus, it was important, especially for *Hnf1b*, to quantify transcript levels in the dorsal versus ventral endoderm and/or mesoderm. As by the use of the WMISH minor quantitative variations in gene expression cannot be determined, again Nanostring analysis was used for further analysis. Four-cell stage embryos were injected with RNA encoding GFP into the two dorsal blastomeres to facilitate the differentiation between GFP positive dorsal tissue and GFP negative ventral tissue. For the preparation of the endoderm, gastrula stage embryos were bisected from anterior to posterior along the dorso-ventral axis. From both, ectodermal and mesodermal tissue was removed to get pure dorsal and ventral endodermal tissue (**Fig. 6.6 A**). For the preparation of dorsal tissue surrounding the blastoporus lip, comprising cells of all three germ layers, also gastrula stage embryos were used. 10 preparations each were subjected to Nanostring analysis. Apart from the 22 RA-responsive candidate genes, the expression of marker genes for the three different germ layers was analyzed (**Fig. 6.6 B**). Candidate genes were grouped according to their expression characteristics into three groups: dorsally enriched, ventrally enriched and equally distributed (**Fig. 6.7**). *Fzd4* shows a clear dorsal enrichment in the endoderm. *Hnf1b* exhibits high pan-endodermal transcript numbers with a slight

dorsal enrichment (**Fig. 6.7 A**). Besides Hnf1b and Fzd4, six more candidates show a dorsal enrichment while eight candidates were found to be ventrally enriched and six candidates are equally distributed (**Fig. 6.7 B and C**). Data are shown in the appendix (**Tab. 6.19 to Tab. 6.21**).

As only Hnf1b and Fzd4 exhibit an endodermal expression, these two candidates were chosen for further functional analysis.

3.3 The direct RA-target gene Hnf1b is required for pancreas specification

In our screen, the homeodomain transcription factor Hnf1b was found as RA-responsive gene. We next examined the location of its RA-responsive expression domain during gastrulation. Furthermore, in order to determine the requirement of Hnf1b for pancreas specification, functional analyses were carried out *in vitro* and *in vivo*.

3.3.1 Hnf1b is RA-responsively expressed in the dorsal endoderm during gastrulation

During gastrulation, Hnf1b is expressed in the entire endoderm (**Fig. 6.8 A**) with a slight enrichment in the dorsal endoderm (**Fig. 6.8 B**). In a late neurula stage embryo (stage 18), Hnf1b transcripts are detected in the anterior endoderm that gives rise to foregut derivatives like liver and ventral pancreas. Furthermore, Hnf1b is expressed in the anterior archenteron roof that gives rise to the dorsal pancreatic anlage. An additional Hnf1b expression domain is observed in the neuroectoderm. At stage 23, Hnf1b is expressed in an anterior-posterior gradient within the endoderm including the ventral foregut that will later differentiate into liver and ventral pancreas. Additionally, Hnf1b is detected in the mesoderm derived pronephric anlage. At later stages, Hnf1b transcripts are found in the liver primordium, pronephros and proctodeum (**Fig. 6.8 A**).

The observed pan-endodermal expression of Hnf1b during gastrulation, with a slight enrichment in the dorsal endoderm, raises the question if differences in RA-responsiveness of endodermal Hnf1b expression domains exist. Therefore, Hnf1b expression in untreated, RA-treated and dorsally *cyp26a1*-injected gastrula stage embryos was examined by WMISH. We found that an excess of RA leads to a strong increase of Hnf1b expression in the dorsal endoderm, whereas the ventral endoderm remains unaffected (**Fig. 6.8 C**). Conversely, the degradation of endogenous RA by Cyp26a1 leads to a loss of Hnf1b expression in the dorsal endoderm. However, a strong decrease of Hnf1b in the ventral endoderm is observed as well (**Fig. 6.8 C**).

Additionally, RA-responsiveness of Hnf1b expression was quantified using Nanostring analysis. Embryos were either treated with RA or BMS453 at blastula stage (**Fig. 6.8 D**). Compared to untreated embryos, the excess of RA leads to a two-fold increase of Hnf1b transcript levels at stage 11 that is further increased at

stages 13 and 14. In contrast, the block of RA-signaling by BMS453 results in a two-fold decrease in Hnf1b expression compared to untreated embryos.

In summary, Hnf1b is expressed in the dorsal and ventral foregut and we found its endodermal expression to be RA-responsive.

3.3.2 Hnf1b is directly induced by RA in pancreatic organoids

Several previous studies in mouse identified RA-responsive elements within the genomic sequence of the *hnf1b* gene, including a DR1 element in the Hnf1b promoter (Power and Cereghini, 1995) and a second DR5 element within intron 4 (Pouilhe et al., 2007). These findings suggest that Hnf1b is a direct RA-target. However, a direct induction of Hnf1b expression in the endoderm by RA has not been shown so far. RNA-sequencing has revealed that Hnf1b is induced by RA within one hour and its expression is further increased within two hours after RA-addition. Hnf1b transcripts are upregulated upon RA-treatment in the absence as well as in the presence of the translational inhibitor CHX, indicating that Hnf1b is directly induced by RA (**Fig. 3.6 A**). These data were confirmed by RT-PCR and Hnf1b is found to behave in a similar fashion as the known direct RA-target Cyp26a1 (**Fig. 3.6 B**). However, in contrast to Cyp26a1, Hnf1b shows low but significant expression levels even in the absence of RA. In summary, Hnf1b is indeed a direct RA-target gene in *Xenopus*, but there must be an additional, RA-independent mechanism, regulating the pan-endodermal expression of Hnf1b.

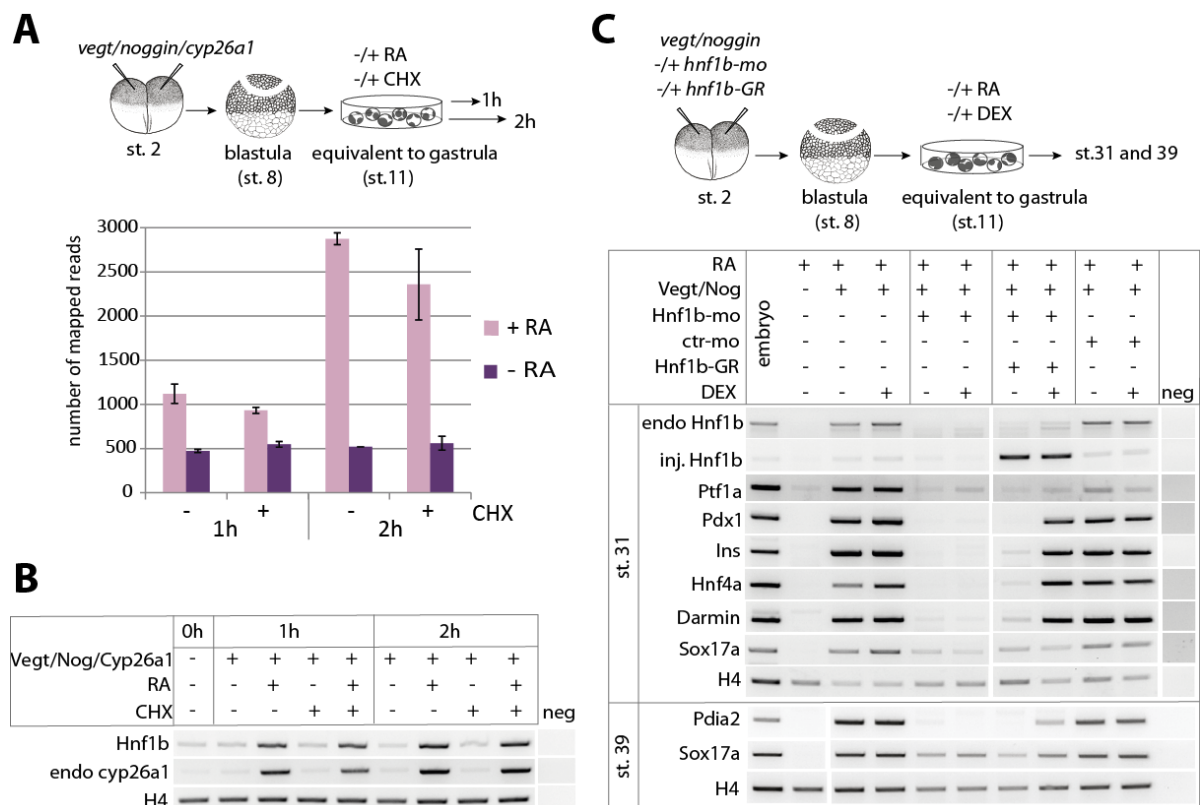


Fig. 3.6 Hnf1b is directly induced by RA and required for pancreas specification in pancreatic organoids

Direct induction of Hnf1b by RA (A) Two cell stage embryos were co-injected with *vegt* (500pg), *noggin* (500pg) and *cyp26a1* (2000pg) RNA. Blastocoele roof tissue was explanted, cultivated and treated with RA and CHX at the equivalent of gastrula stage. Samples for RNA-sequencing were taken one and two hours after RA-addition. Hnf1b expression levels are represented by the number of mapped reads. **(B)** RT-PCR analyzing Hnf1b, Cyp26a1 and the housekeeping gene H4 transcripts for samples of programmed explants before and one/two hours after RA addition.

Requirement of Hnf1b for pancreatic gene expression in pancreatic organoids

(C) 55 ng Hnf1b-morpholino (Hnf1b-mo) or 55 ng control-morpholino (ctr-mo) were co-injected with *vegt* (500pg) and *noggin* (500pg) RNA into two cell stage embryos. 800 pg of RNA for a hormone-inducible Hnf1b (Hnf1b-GR) was co-injected and explants were treated with dexamethasone (DEX) and RA at the equivalent of gastrula stage to rescue the morpholino-mediated phenotype. At the equivalent of stages 31 and 39, total RNA was isolated and subjected to RT-PCR. Detection of endogenous (endo) and injected Hnf1b (inj.), pancreatic progenitor markers Pdx1 and Ptf1a, early endocrine differentiation marker Insulin (Ins) and late differentiation marker Pdia2, direct Hnf1b target Hnf4a, endodermal markers Darmin and Sox17a, housekeeping gene H4.

3.3.3 Hnf1b is required for pancreas specification *in vitro*

In order to determine the requirement of Hnf1b for pancreas specification, Hnf1b protein expression was downregulated by the injection of a morpholino antisense oligonucleotide, targeting the intron1/exon2 boundary of the Hnf1b pre-mRNA (**Fig. 6.9 A**). Binding of the morpholino to the pre-mRNA should inhibit conventional splicing. In a first step, the functionality of the morpholino was tested in the explant system (**Fig. 6.9 B**). At the equivalent of neurula stage, the Hnf1b amplicon in Hnf1b-morpholino injected explants is shifted to a smaller size compared to the Hnf1b amplicon of control embryos and control-morpholino injected explants (**Fig. 6.9 C**). Sequencing of the amplicon revealed that indeed exon2 is lost in the presence of the Hnf1b-morpholino (data not shown). Thus, a frameshift occurs and a premature stop codon in exon3 is used that leads to a shortened open reading frame of Hnf1b. As a result, a shortened Hnf1b protein is translated that lacks the functional DNA-binding domains and the transactivation domain (**Fig. 6.9 A**).

First, we wanted to determine if Hnf1b is required for RA-mediated activation of pancreatic marker genes in pancreatic organoids. For this purpose, the morpholino was used to downregulate Hnf1b protein expression in pancreatic organoids (**Fig. 3.6 C**). At the equivalent of stage 31, endogenous Hnf1b is only detected in pancreatic organoids and control embryos (**Fig. 3.6 C** lanes 3 and 4) and is completely abolished upon co-injection of the Hnf1b-morpholino (**Fig. 3.6 C** lanes 5 and 6) suggesting that the smaller Hnf1b amplicon, observed at late neurula stage, is probably degraded at stage 31 due to nonsense-mediated mRNA decay (Chang et al., 2007). Pancreatic progenitor markers Pdx1 and Ptf1a as well as the early endocrine differentiation marker Insulin and the late exocrine marker Pdia2 are detected in control embryos (lane1) and pancreatic organoids (lanes 3 and 4) but not in un-programed explants (lane2) (**Fig. 3.6 C**). Furthermore, the direct Hnf1b target gene Hnf4a (Thomas et al., 2001) and endodermal marker genes Darmin and Sox17a are expressed in control embryos and pancreatic organoids. Upon co-injection of the Hnf1b-morpholino, Ptf1a expression is strongly decreased and the expression of Pdx1, Insulin, Pdia2 and Hnf4a are completely lost. In addition, the expression of Darmin is strongly decreased whereas the expression of the other endodermal marker Sox17a is only slightly affected. These effects were not observed in the presence of the control-morpholino (lanes 9 and 10) (**Fig. 3.6 C**). In order to demonstrate that the observed effects are specific for the loss of functional Hnf1b protein, a rescue experiment was performed. For this purpose, RNA encoding a hormone-inducible Hnf1b (Hnf1b-GR) was co-injected. Hnf1b protein function was activated at the equivalent of gastrula stage by dexamethasone (DEX) treatment.

Indeed, the activation of Hnf1b re-establishes the expression of the progenitor marker Pdx1, the direct Hnf1b target gene Hnf4a, the endodermal marker Darmin as well as the differentiation markers Insulin and Pdia2 (**Fig. 3.6 C**). However, results for Ptf1a expression under rescue conditions are inconsistent. In a few experiments Ptf1a expression could be fully rescued (not shown) and in other experiments it remained strongly decreased.

In summary, Hnf1b is required for RA-mediated expression of pancreatic marker genes in pancreatic organoids. Moreover, Darmin, which was found to be RA-inducible expressed in explants, appears to be downstream of Hnf1b.

3.3.4 Hnf1b is required for pancreas specification *in vivo*

As we could show that Hnf1b is required for pancreatic gene expression in *in vitro* generated pancreatic organoids, we next asked if Hnf1b is required for pancreas specification *in vivo*.

3.3.4.1 Hnf1b-overexpression leads to an expansion of the pancreatic progenitor field *in vivo*

In order to determine the role of Hnf1b for the development of pancreatic progenitor formation *in vivo*, a gain of function approach was done. RNAs encoding a hormone-inducible Hnf1b (Hnf1b-GR) and β -galactosidase (glb1) were injected vegetally into the two dorsal blastomeres of a four-cell stage embryo. Hnf1b activity was induced at gastrula stage through dexamethasone-treatment (DEX) until stage 32 and a WMISH was carried out to visualize Pdx1 and Ptf1a expression (**Fig. 3.7 A**). In control embryos, the progenitor marker Pdx1 is not exclusively expressed in the pancreas but is also detected in the adjacent duodenum. In Hnf1b-overexpressing embryos, the Pdx1 expression domain is expanded along the anterior-posterior axis. The second progenitor marker Ptf1a is expressed in the eye, the hindbrain and in the endoderm, where it is restricted to the dorsal and ventral pancreatic buds. Upon Hnf1b-overexpression, the dorsal as well as the ventral pancreatic Ptf1a expression domain is expanded whereas the expression in the eye and the hindbrain is unaffected (**Fig. 3.7 A**). The effects of Hnf1b-overexpression on Pdx1 and Ptf1a expression, observed by WMISH, were quantified for two independent experiments using ImageJ. At least 20 embryos per experiment were analyzed (**Tab. 6.22** and **Tab. 6.23**). In control embryos on average 9 % of the endodermal area is Pdx1-positive with a variation from 4 % to 17 %. Upon Hnf1b-overexpression, the average is significantly increased to 13 % Pdx1 domain in the endoderm with a variation from 8 % to 28 %. Ptf1a is expressed in 3% of the endoderm in control embryos. Hnf1b-overexpressing embryos show almost 5% of the endodermal area positive for Ptf1a with a variation of 2 % to 13 %. When dorsal and ventral pancreatic Ptf1a expression is examined individually, we find that the ventral pancreatic domain of Ptf1a is affected more dramatically than the dorsal domain (**Fig. 3.7 A**). In conclusion, Hnf1b-overexpression in the endoderm leads to the formation of an expanded pancreatic progenitor field.

3.3.4.2 Hnf1b-knockdown causes a decrease in or a complete loss of pancreatic progenitors *in vivo*

The observation that the morpholino-mediated knockdown of Hnf1b in pancreatic organoids results in a loss of Ptf1a and Pdx1 expression suggests that Hnf1b is required for pancreas specification. In order to verify this hypothesis, we carried out a morpholino-mediated Hnf1b loss-of-function analysis *in vivo*. Hnf1b-morpholino injected embryos were cultivated until stage 32 and the expression of Ptf1a and Pdx1 was determined by WMISH. Upon Hnf1b-knockdown, Pdx1 and the endodermal Ptf1a expression are completely lost. However, in control-morpholino injected embryos, Pdx1 and the endodermal Ptf1a expression are also affected as the WMISH signal is decreased (**Fig. 3.7 B**). Nevertheless, control-morpholino injected embryos do not show a phenotype as severe as caused by the injection of the Hnf1b-morpholino. In order to compare control- and Hnf1b-morpholino effects in more detail, a quantification of pancreatic marker gene expression using real-time PCR was done. The expression levels of Pdx1, Ptf1a and Insulin were calculated with respect to the levels of the housekeeping gene *ornithine decarboxylase (odc)*. In the presence of the Hnf1b-morpholino, the transcript levels of Pdx1, Ptf1a and Insulin are almost un-detectable. In contrast, in the presence of the control-morpholino, Pdx1 and Insulin transcript levels were decreased to 60% and 70 %, while Ptf1a levels were unaffected compared to control embryos. Hence, the downregulation of Hnf1b *in vivo* leads to strong decreased expression levels of pancreatic progenitor markers.

In summary, Hnf1b is required for pancreas specification in *Xenopus laevis* embryos.

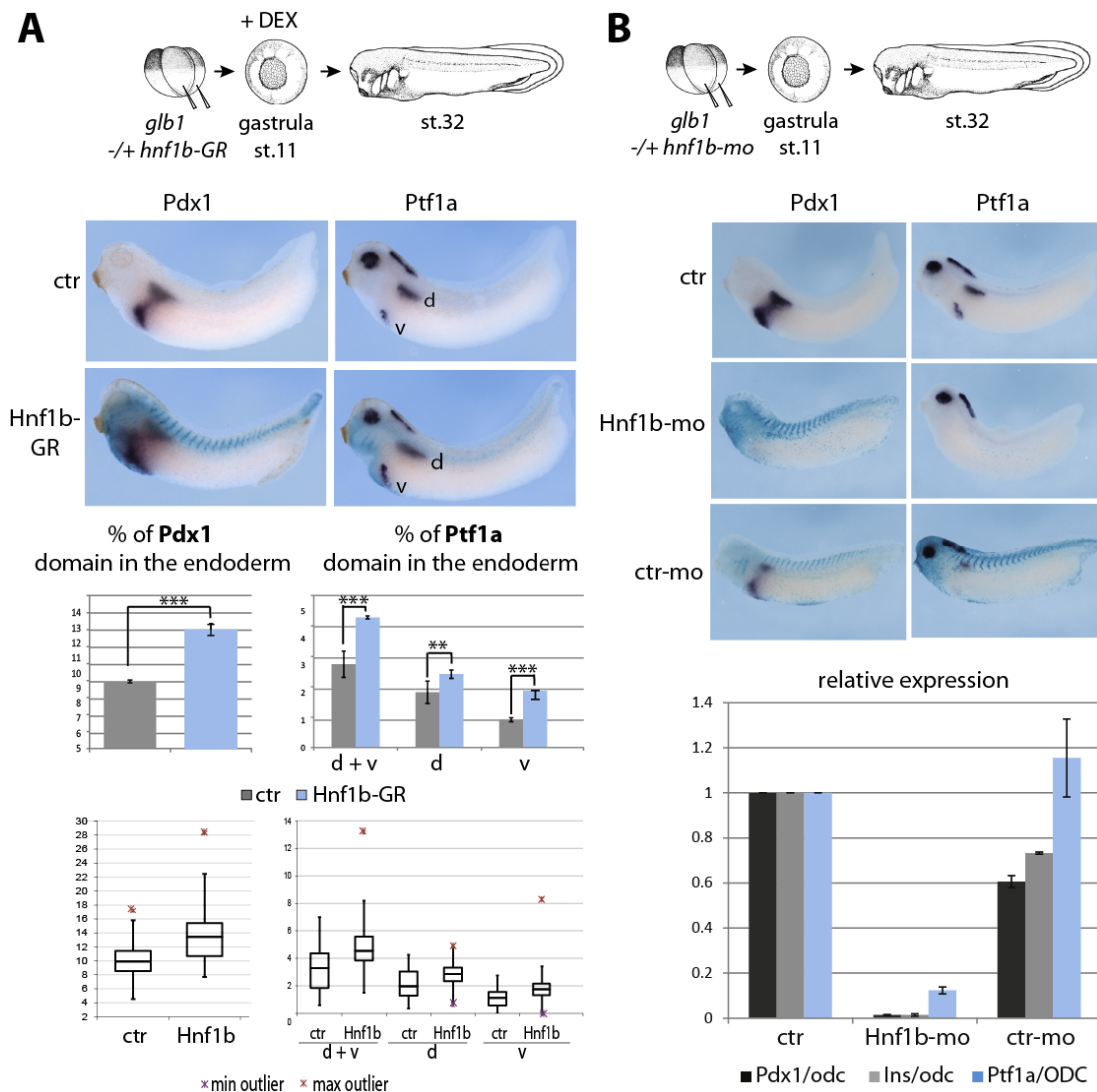


Fig. 3.7 Hnf1b is required for pancreas specification *in vivo*

Hnf1b-overexpression leads to expanded pancreatic progenitor field. (A) 200pg β -calactosidase (*glb1*) and 800pg Hnf1b-GR RNA were co-injected vegetally into the two dorsal blastomeres of a four-cell stage embryo. As control (ctr) served β -calactosidase RNA injected embryos. At gastrula stage, embryos were treated with dexamethasone (DEX) and cultivated until stage 32. WMISH against Pdx1 and Ptf1a in control and Hnf1b-overexpressing embryos is shown. Upper graphs show the percentage of Pdx1 and endodermal Ptf1a domains in the whole endoderm. Lower graphs are boxplots displaying the range of observed data and indicating outliers. P-values in a Student's *t*-test **<0.01, ***<0.001.

Hnf1b-downregulation leads to a strong decrease in pancreatic progenitor expression. (B) 200pg β -calactosidase (*glb1*) RNA and 25ng Hnf1b-morpholino or ctr-morpholino were co-injected vegetally into the two dorsal blastomeres of a four-cell stage embryo. Embryos at stage 32 were used for WMISH against Pdx1 and Ptf1a and real-time PCR analysis for Pdx1, Ptf1a and Insulin. Graph indicated the fold changes of tested markers in ratio to ODC. WMISH analysis was performed once and real-time PCR results emerge from two independent biological replicates.

3.3.5 Hnf1b alone cannot substitute for RA-activity during pancreas specification

As we could show that Hnf1b is required for pancreas specification *in vitro* as well as *in vivo*, we next asked if Hnf1b is the key factor that mediates RA-activity in the context of pancreas specification. The explant system was used to answer that question. RNA coding for the hormone-inducible Hnf1b-GR was co-injected with *vegt* and *noggin* RNA. Endogenous RA-signaling was blocked by the co-injection of *cyp26a1* RNA (**Fig. 3.8 A**). In control embryos and explants in the presence of RA, the pancreatic markers Pdx1, Ptf1a and Insulin, the direct Hnf1b target Hnf4a and the endodermal markers Darmin and Sox17a are expressed. If RA-signaling is blocked, only the endodermal marker Sox17a is detected. However, upon the induction of Hnf1b activity (+DEX), pancreatic marker gene expression is still not detectable (**Fig. 3.8 B**). Interestingly, the endodermal marker Darmin and the direct target Hnf4a are induced by Hnf1b, indicating the presence of functional Hnf1b protein. Taken together, Hnf1b is not sufficient to substitute for RA-activity in pancreas development. Hence, Hnf1b is not the only RA-responsive gene that is required for pancreas specification in *Xenopus*.

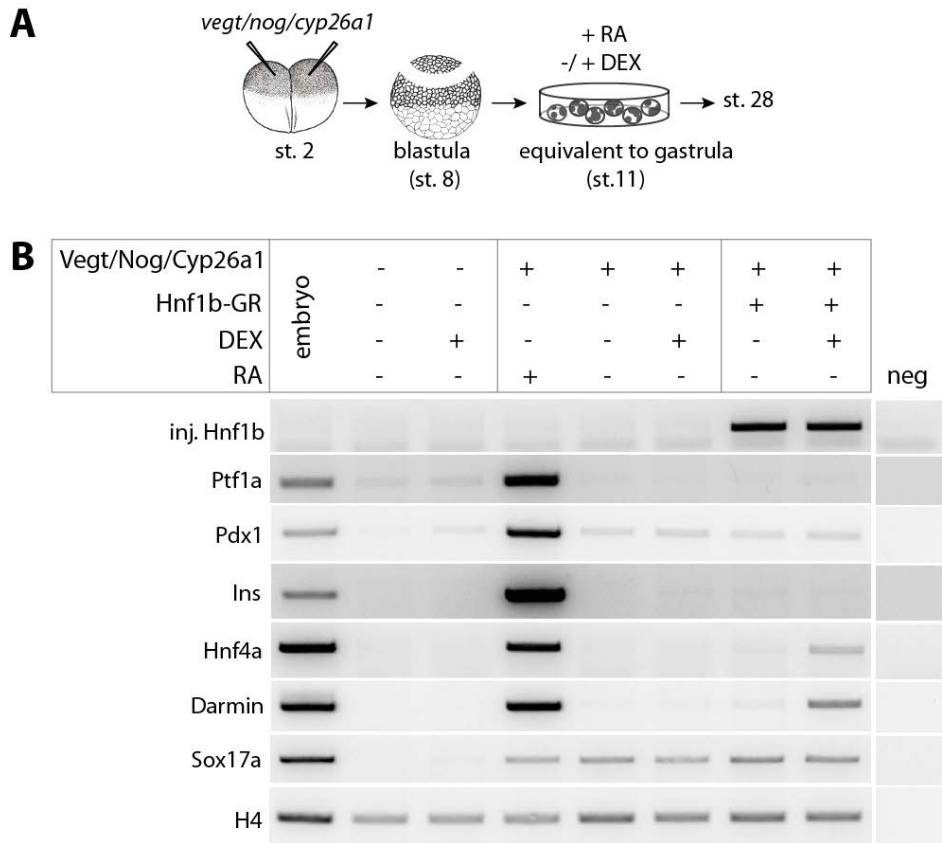


Fig. 3.8 Hnf1b is not sufficient to substitute for RA in pancreas specification in ectodermal explants

(A) Indicated RNAs were co-injected with 800 pg Hnf1b-GR RNA into a two-cell stage embryo. Ectodermal explants were prepared and cultivated. Treatments with dexamethasone (DEX) and RA were performed at the equivalent of gastrula stage. At the equivalent of stage 28, total RNA was isolated and analyzed by RT-PCR. (B) RT-PCR for pancreatic progenitor markers Pdx1 Ptf1a, differentiation marker Insulin (Ins), direct Hnf1b target Hnf4a, endodermal markers Darmin and Sox17a and housekeeping gene histone H4.

3.4 The direct target Fzd4/Fzd4s is required for pancreas specification

The second promising candidate, potentially involved in pancreas specification, is the Wnt-receptor Fzd4 as it was found to be induced by RA in the RNA sequencing experiment and is expressed in the dorsal endoderm during gastrulation.

3.4.1 Fzd4 and the alternative splice variant Fzd4s are directly induced by RA

RNA-sequencing data revealed that Fzd4 is induced by RA even in the presence of the translational inhibitor CHX (**Fig. 3.9 A**). Moreover, we found that Fzd4 is expressed in the dorsal endoderm during gastrulation, suggesting Fzd4 as a direct RA-target gene potentially involved in pancreas specification.

The Fzd4 gene includes two exons separated by a large intronic region. Through conventional splicing a Fzd4 protein is generated comprising a small extracellular cysteine-rich domain (CRD) for Wnt ligand interaction, a seven transmembrane domain (TM) and an intracellular domain (ICD) (**Fig. 6.10**). Additionally, an alternative splice variant for Fzd4 that retains the intron was discovered (Yam et al., 2005; Swain et al., 2005). This splice variant retains the Wnt-binding CRD domain, but is missing the transmembrane and the intracellular domain as a premature stop codon within the retained intron is used (**Fig. 6.10**). As this splice variant was assumed to be secreted it was named Fzd4s (Fzd4 secreted). Fzd4s can act as an activator as well as inhibitor of Wnt-signaling depending on the identity of the corresponding Wnt-ligand (Swain et al., 2005). The question arises if both Fzd4 variants are induced by RA. The RNA-sequencing data contain sequence reads mainly mapped to exon1 and exon2 of the Fzd4 gene locus, but a significant number of reads was mapped to intronic sequences as well (data not shown). Nanostring analysis, used for the verification process, does not give the information which variant is induced by RA as the Nanostring probe against Fzd4 targets the exon2 that is contained in both splice variants (**Fig. 6.11 C**). Therefore, oligonucleotides were designed either neighbouring the intronic sequence or targeting within the intron to distinguish between the different Fzd4 transcripts. As the intronic sequence is larger than 6 kb, amplicons generated by RT-PCR with oligonucleotides flanking the intron would give only a signal for Fzd4. With the oligonucleotides targeting the intronic region, only Fzd4s transcripts are detected. The RT-PCR results reveal that both variants of Fzd4 are directly induced by RA within two hours after RA-addition (**Fig. 3.9 B**).

3.4.2 Fzd4/Fzd4s is enriched in the dorsal half of a gastrula embryo including the dorsal endoderm

Fzd4/Fzd4s expression was examined during *Xenopus* development by WMISH in order to visualize expression domains (**Fig. 6.11 A/B**). An antisense probe was applied that was already used during the screen for the determination of Fzd4 expression characteristics. This antisense probe targets the complete open reading frame of the Fzd4 transcript. Theoretically, Fzd4s transcripts should also be targeted by this antisense probe as the major part of this probe binds to the sequence derived from exon2 (**Fig. 6.11 A**). Fzd4/Fzd4s transcripts are detected in the dorsal endoderm and the prospective neuroectoderm at gastrula stage. At neurula stage, Fzd4/Fzd4s transcripts are found in the prospective foregut, in the lateral plate mesoderm and in the forebrain region (**Fig. 6.11 A**). Later during development, Fzd4/Fzd4s is expressed in the head and the regions of pancreas, liver, duodenum and heart primordium. In order to specifically detect transcripts of the alternative splice variant Fzd4s, an antisense probe was designed targeting the intronic-derived sequence (**Fig. 6.11 B**). During gastrulation, WMISH signals are detected in the dorsal and ventral mesoderm, prospective neuroectoderm and in very low intensity in the entire endoderm. However, in contrast to the first antisense-probe, a clear dorsal enrichment was not observed. At neurula stage, Fzd4s is expressed in the notochord and in the prospective foregut region. Later during development, a moderate expression of Fzd4s is detected in the entire embryo with an enrichment in the head region (**Fig. 6.11 B**). As low levels of staining are found in the entire embryo for all tested developmental stages it cannot be excluded that the detected signals are unspecific. Thus, the expression of Fzd4 and Fzd4s during gastrulation was tested by RT-PCR using preparations of dorsal and ventral endoderm as well as of dorsal and ventral tissues as described in **Fig. 6.6 A**. Fzd4 and Fzd4s transcripts could not be detected in endodermal preparations (not shown). This might be due to the preparation technique by which a lot of endodermal tissue gets lost. Nevertheless, for preparations of the tissue surrounding the dorsal and ventral blastopore lip, Fzd4 as well as Fzd4s transcripts are found to be enriched in the dorsal half (**Fig. 6.11 C**). In order to quantify the level of dorsal enrichment, a Nanostring analysis was carried out, although a distinction between Fzd4 and Fzd4s transcripts is not possible as the Nanostring probe targets the region encoded by exon2. Fzd4/Fzd4s is 1.5-fold enriched in the dorsal compared to ventral endoderm (**Fig. 6.7 A**) and 4-fold enriched in the dorsal compared to the ventral part around the blastopore lip (**Fig. 6.11 C**).

However, neither the expression data from WMISH nor from RT-PCR allow a conclusion about which Fzd4 variant is expressed in the dorsal endoderm during gastrulation. Thus, further following designations concerning Fzd4 are termed as Fzd4/Fzd4s. In conclusion, Fzd4/Fzd4s is enriched in the dorsal tissue of a gastrula embryo including the dorsal endoderm. Later in development, Fzd4/Fzd4s expression is restricted to pancreas, liver, duodenum, heart primordium and head structures.

3.4.3 Fzd4/Fzd4s is RA-responsively expressed during gastrulation

In our screen, Fzd4/Fzd4s was identified as direct RA-responsive gene *in vitro*. In order to verify the RA-responsiveness of Fzd4/Fzd4s expression *in vivo* during gastrulation, WMISH and Nanostring analyses were performed (**Fig. 6.12**). Untreated, RA-treated and Cyp26a1-injected embryos were cultivated until gastrula stage and subjected to WMISH analysis using an antisense probe targeting both, Fzd4 and Fzd4s. Upon an excess of RA the expression of Fzd4/Fzd4s in the dorsal endoderm as well as that in the prospective neuro-ectoderm is strongly increased. Conversely, the degradation of endogenous RA by Cyp26a1 leads to a loss of endodermal Fzd4/Fzd4s expression whereas the prospective neuro-ectodermal expression is unaffected (**Fig. 6.12 A**). Thus, endodermal and neuro-ectodermal Fzd4/Fzd4s expression domains are RA-inducible but only the endodermal expression domain is RA-dependent.

Moreover, quantitative Nanostring analysis of stage 12 to 14 embryos reveals a clear increase of Fzd4/Fzd4s expression from 2 fold up to 2.5 fold in RA-treated embryos compared to untreated embryos. In contrast, upon the inhibition of RA-signaling by BMS453, a reduction in Fzd4/Fzd4s transcript levels up to 2 fold was observed (**Fig. 6.12 B**). In summary, during gastrulation the endodermal expression domain of Fzd4/Fzd4s is RA-responsive.

3.4.4 Fzd4/Fzd4s is required for pancreatic marker gene expression *in vitro*

In order to determine if Fzd4/Fzd4s is required for pancreas specification, we analyzed the function of Fzd4/Fzd4s in pancreatic organoids. For this issue, two loss-of-function approaches were done, interfere with the translation or impair the gene locus. First, a morpholino was used that targets the start-codon of the *fzd4* and *fzd4s* RNA and thereby blocks the translation of both Fzd4 variants (**Fig. 3.9 C**) (Gorny et al., 2013). The morpholino was co-injected with *vegt* and *noggin* RNA and pancreatic organoids were generated and cultivated until stage 28 and RNA was subjected to RT-PCR. Pancreatic progenitor markers Pdx1 and Ptf1a, the early differentiation marker Insulin as well as the endodermal marker Sox17a were strongly decreased upon Fzd4/Fzd4s-downregulation compared to control embryos or mismatch-morpholino-injected explants. In contrast, the endodermal marker Darmin was not affected (**Fig. 3.9 C**). These results indicate a requirement of Fzd4 for RA-mediated pancreatic marker gene induction. However, injection of various concentrations of *fzd4* and *fzd4s* RNA could not rescue the observed knockdown phenotype (not shown). We suppose that, for pancreatic gene expression, Fzd4/Fzd4s protein activity is required during gastrulation and that an earlier activity, caused by RNA injection at early cleavage stage and subsequent translation inhibits pancreatic gene expression. A temporally controlled activation of Fzd4/Fzd4s using the GR/DEX-system, as used for over-expression of Hnf1b, would not function for membrane bound or secreted factors. Due to this reasons, Fzd4 and Fzd4s encoding plasmid DNA was injected, which is not transcribed before MBT (mid blastula transition). However, the Fzd4/Fzd4s-knockdown phenotype of decreased pancreatic marker gene expression could not be restored (not shown). This might be due to an inadequate Fzd4/Fzd4s concentration as the appropriate level of active Fzd4/Fzd4s protein for proper pancreas specification remains to be determined.

In order to confirm the phenotype observed upon morpholino-mediated knockdown of Fzd4/Fzd4s, we went for a second type of loss-of-function approach. The CRISPR/Cas (Clustered Regularly Interspaced Short Palindromic Repeats/CRISPR-associated) is based on the RNA-guided DNA endonuclease Cas9 that can be targeted against a specific genomic region. A guide RNA (Fzd4-gRNA) was designed targeting a twenty nucleotide sequence within exon1 of the *fzd4* gene (**Fig. 3.9 D**). This guide RNA was co-injected with RNAs encoding for Cas9, Vegt and Noggin at one-cell stage. At blastula stage, ectodermal explants were prepared and cultivated as previously described. RA was not added as endogenous RA levels, indirectly induced by Noggin, are sufficient to induce pancreatic marker gene

expression (**Fig. 3.1**). Furthermore, a mosaicism of cells carrying wildtype or mutated *fzd4* gene in the explants is expected. Therefore, the system was not saturated with exogenous RA in order to detect an effect on pancreatic marker genes upon *Fzd4* gene disruption. RT-PCR analysis and genomic DNA extraction for mutation analysis were done using extracts from 50 explants each. Mutation analysis revealed a 100% mutation rate in total and 66% effective mutations which result in impaired protein function (**Fig. 3.9 D**; **Fig. 6.13**). Upon *Fzd4*-gRNA co-injection, transcript levels of *Ptf1a*, *Pdx1* and *Insulin* were strongly reduced as compared to Cas9 over-expressing pancreatic organoids. Furthermore, *Darmin* transcript levels are decreased whereas *Sox17a* levels are not affected (**Fig. 3.9 D**). Since a stretch of twenty nucleotides can be found multiple times in the genome and the CRISPR/Cas system can accept mismatches depending on their position, potential off-targets were predicted using the online tool CCTop (Stemmer et al., 2015). In doing so, eight potential off-target sequences within exonic regions of the *X. laevis* genome were predicted (**Tab. 6.24**). Three of them were analyzed for mutations in the presence of *Fzd4*-gRNA. The potential off-target sequence within genomic sequences of *Impad1*, *Kremen2* and *Fzd7* contain in total 5 mismatches. However, for *Kremen2* and *Impad1* only one mismatch is located within protospacer sequence proximal to the PAM (protospacer adjacent motif). A gRNA/Cas9 efficiency study in *Xenopus tropicalis* revealed that single mismatches within the protospacer completely abolish targeting activity of this RNA/endonuclease complex (Guo et al., 2014). Indeed, mutation analysis of the three potential off-targets revealed that no mutations were introduced into the gene loci. Data for *Kremen2* are shown in the appendix (**Fig. 6.13**).

Taken together, both loss-of-function approaches revealed that *Fzd4*/*Fzd4s* is indeed required for pancreatic gene induction in pancreatic organoids, suggesting a role for *Fzd4*/*Fzd4s* during pancreas specification.

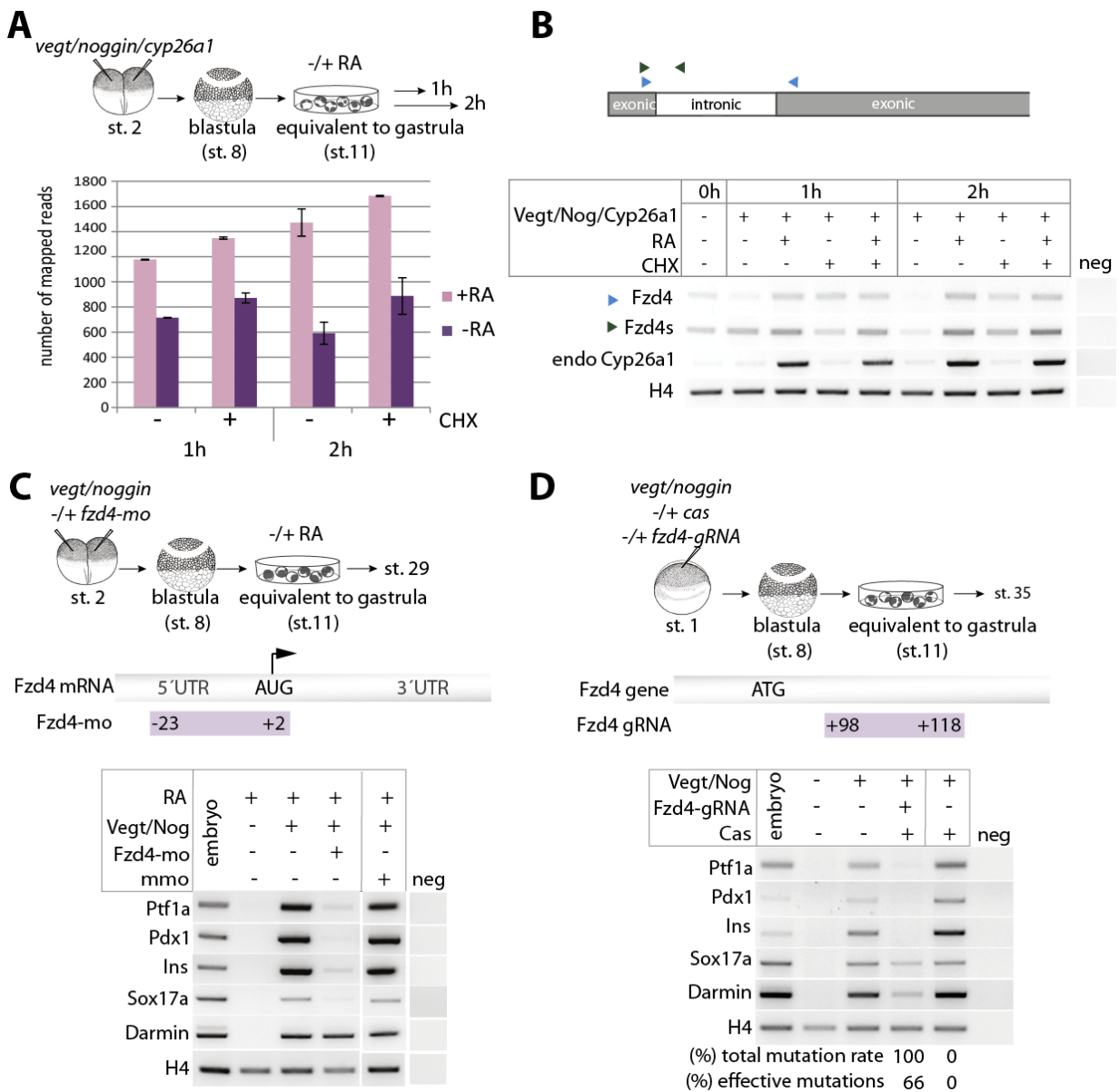


Fig. 3.9 Fzd4 and Fzd4s are directly induced by RA and required for pancreas specification in pancreatic organoids

Direct induction of Fzd4/Fzd4s by RA

(A) Two cell stage embryos were co-injected with *vegt*, *noggin* and *cyp26a1* RNA. Blastocoel roof tissue was explanted, cultivated and treated with RA and CHX at the equivalent of gastrula stage. One and two hours after RA-addition, total RNA was isolated and subjected to RNA-sequencing. Fzd4 expression levels are indicated as number of mapped reads. (B) RT-PCR for splice variants Fzd4 and Fzd4s, for Cyp26a1 as well as the housekeeping gene H4 in samples of programed explants before and one/two hours after RA addition.

Requirement of Fzd4/Fzd4s for pancreatic gene expression in pancreatic organoids

(C) Fzd4/Fzd4s-knockdown through translational blocking Fzd4-morpholino (Fzd4-mo). 45 ng Fzd4-mo or the corresponding mismatch-morpholino (mmo) were co-injected with *vegt* and *noggin* RNA and explants for pancreatic organoid formation were prepared. At the equivalent of stage 28, total RNA was isolated and subjected to RT-PCR. Amplification of pancreatic progenitor markers Pdx1 and Ptf1a, differentiation marker Insulin (Ins), endodermal markers Sox17a and Darmin. (D) Fzd4/Fzd4s knockdown through CRISPR/Cas-technique. Fzd4-gRNA was co-injected with RNAs encoding Cas9, Vegt and Noggin into one-cell stage embryos. Explants were cultivated until the equivalent of stage 35. RT-PCR for pancreatic and endodermal markers was done. Mutation rates are indicated for Cas9 only or Cas9 with Fzd4-gRNA.

3.4.5 Downregulation of Fzd4/Fzd4s leads to an increase in non-canonical Wnt-signaling activity *in vitro*

Fzd4/Fzd4s loss-of-function experiments in pancreatic organoids showed that the direct RA-target gene Fzd4/Fzd4s is required for pancreatic marker gene expression. Both variants, Fzd4 and Fzd4s, act as Wnt-interacting molecules (Xu et al., 2004; Swain et al., 2005; Mikels and Nusse, 2006). For this reason, we asked if the requirement of Fzd4/Fzd4s for pancreas specification is dependent on its function in Wnt-signaling. We first tested if Wnt-signaling is active in explants programmed with Vegt/Noggin and how RA-activity affects this level of Wnt-signaling activity. For this purpose, luciferase reporter assays were carried out using reporter constructs for both Wnt-signaling pathways, canonical as well as non-canonical (**Fig. 3.10 A**). RNAs coding for Vegt, Noggin and Cyp26a1 were co-injected with plasmids coding for either firefly-luciferase reporters under the control of the Siamois promotor (canonical Wnt-signaling target) or the Atf2 response element (non-canonical Wnt-signaling target). In addition, a plasmid coding for reporter Renilla-luciferase was co-injected in order to normalize the levels of Siamois- and Atf2-reporter activity. *Wnt8a* (canonical) and *wnt5a* (non-canonical) RNA co-injections served as positive controls (**Fig. 3.10**). Both, canonical as well as non-canonical Wnt-signaling reporter activity is detected in Vegt/Nog-programmed explants in the absence of RA-signaling. These activities were set to 100%. Upon RA-treatment, the level of canonical reporter is decreased to 70% and the level of the non-canonical reporter below 60% (**Fig. 3.10 B**). In conclusion, programmed explants exhibit a canonical and non-canonical Wnt-signaling activity that is decreased in the presence of RA-signaling, in which non-canonical Wnt-signaling is slightly stronger affected than canonical Wnt-signaling.

Next, we asked how a knockdown of Fzd4/Fzd4s in these explants would influence the Wnt-signaling activity. For this issue, the Fzd4-morpholino was co-injected. As Noggin indirectly activates endogenous RA-signaling, RA was not applied to the explants. The levels of luciferase activity in the samples injected with the reporters only were set to one (**Fig. 3.10 C**). Upon Fzd4/Fzd4s-downregulation, the level of canonical reporter activity increases from 10-fold in morpholino-un-injected explants and mismatch-morpholino-injected explants up to 16-fold. However, the high standard deviation between the data of four experiments indicates that the effect on canonical Wnt-signaling is not significant. In contrast, non-canonical reporter activity is significantly increased from two-fold in morpholino-un-injected explants to six-fold

upon Fzd4/Fzd4s downregulation (**Fig. 3.10 C**). Taken together, the downregulation of Fzd4/Fzd4s leads to an increase in non-canonical reporter activity.

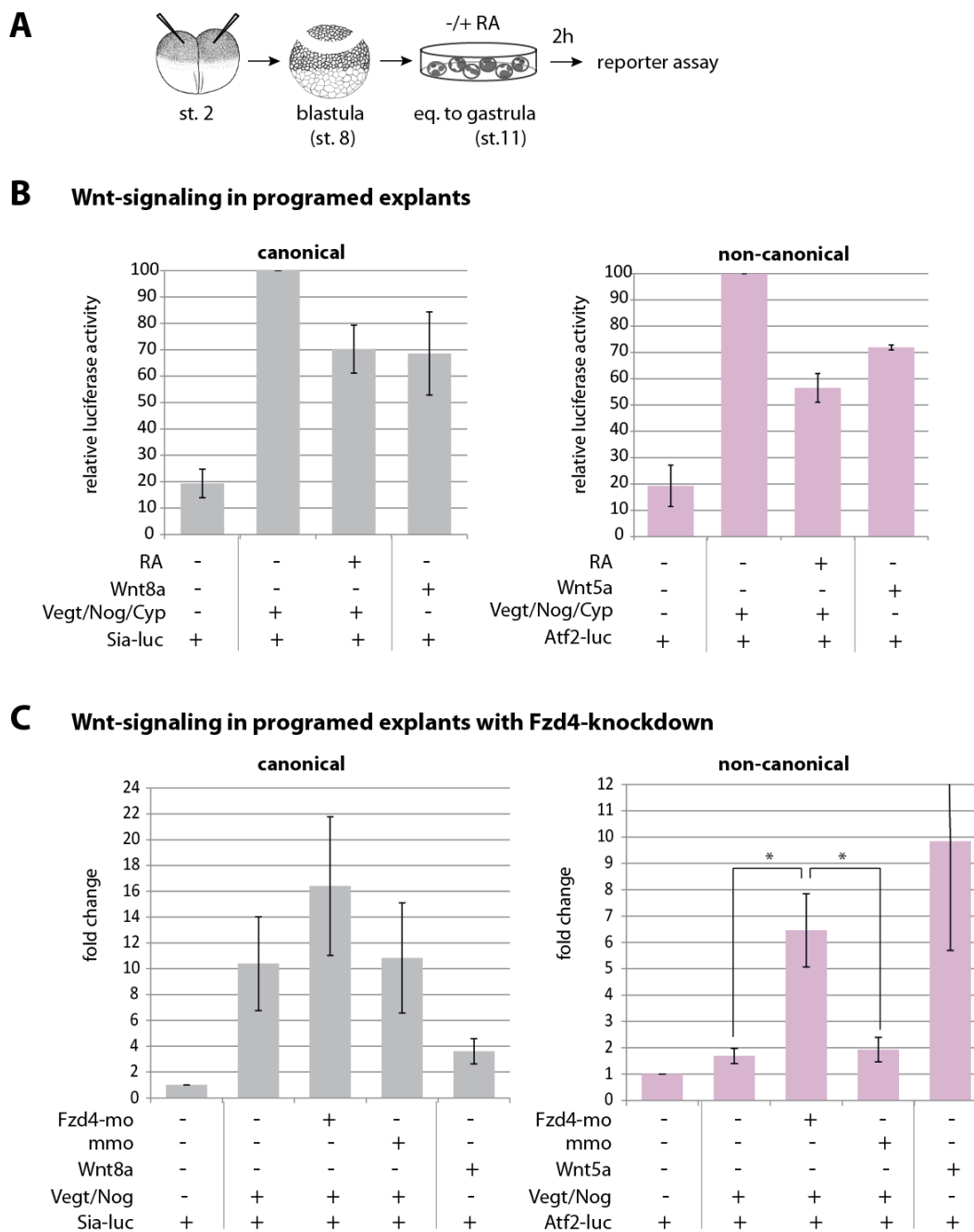


Fig. 3.10 Wnt-signaling in progamed explants

(A) RNAs coding for Vegt (500pg), Noggin (500pg) were co-injected with RNAs encoding Cyp26a1 (2000pg), Wnt8a (400 pg) or Wnt5a (500pg). DNAs coding for the canonical reporter Siamois-luciferase (50 pg), non-canonical reporter Atf2-luciferase (100 pg) and Renilla-luciferase (10 pg) were also co-injected. Blastocoel-roof tissue was explanted and treated with RA or kept untreated. Samples for reporter assay were taken as duplicates two hours after RA-addition or at the equivalent of stage 12. (B) Relative luciferase activities of canonical and non-canonical Wnt-reporters in progamed explants in the absence or presence of RA-signaling. (C) Fold changes of luciferase activities from canonical and non-canonical Wnt-reporters in Vegt/Noggin-progamed explants with downregulated Fzd4/Fzd4s. * P-values in a Student's *t*-test <0.05.

4. Discussion

4.1 Pancreatic organoid formation and the requirement of retinoic acid

We could demonstrate that pancreatic organoids can be generated *in vitro* from ectodermal explants of blastula stage *Xenopus* embryos. In a previous study, it was already shown that ectodermal explants can be programmed by Vegt, β -catenin, Noggin and RA-treatment to form pancreatic tissue (Chen et al., 2004). In comparison to that study, we found that β -catenin is not essential for the induction of pancreatic marker gene expression. Moreover, we provide clear evidences that our *in vitro* generated pancreatic organoids recapitulate the *in vivo* pancreas organogenesis as we detect the same temporal expression profile of pancreatic marker genes as described *in vivo*.

The co-expression of the two transcription factors Ptf1a and Pdx1 is characteristic for pancreatic progenitor cells (Chiang and Melton, 2003; Afelik et al., 2006). Both transcription factors could be detected starting the expression at stage 24 in our pancreatic organoids, indicating the presence of a pancreatic progenitor population. However, it remains to be evidenced that Ptf1a and Pdx1 are co-expressed in these organoids, what would reflect pancreatic progenitors. Single cell analysis through RNA-sequencing or Nanostring technique would be applicable to show a co-expression of Pdx1 and Ptf1a. Nevertheless, we could detect further genes described to be expressed in pancreatic progenitors. Gata4, which is not exclusively required for pre-pancreatic endoderm formation, but also for the general endoderm formation (Holtzinger and Evans, 2005) was detected in pancreatic organoids and embryos at all tested stages. We further found Gata4 transcript levels increased in pancreatic organoids at the same stage when Ptf1a and Pdx1 were detected. Gata4 was previously shown to be induced by the key endoderm regulator Vegt (Xanthos et al., 2001) what explains the early expression at stage 17. In mouse, Gata4 is further known to be expressed in the early pancreatic epithelium (Decker et al., 2006; Watt et al., 2007) and to be required for early pancreas development (Carrasco et al., 2012; Xuan et al., 2012; Rodriguez-Segui et al. 2012). The endocrine progenitor marker Ngn3 was only slightly and transiently expressed in pancreatic organoids at stages 24 to 32. This observation is consistent with the described findings in mouse, where Ngn3 was shown to act upstream of endocrine differentiation factors and its expression is turned off prior to final differentiation (Gradwohl et al., 2000; Jensen et al., 2000; Schwitzgebel et al., 2000; Maestro et

al., 2003). Moreover, in *Xenopus*, *ngn3* transcripts could not be detected in the pancreas at later stages (Nieber et al., 2009).

The earliest endocrine differentiation marker Insulin is detected already at stage 24 together with Ptf1a and Pdx1 in pancreatic organoids which indicates the first wave of Insulin expression during the primary transition phase of pancreas development (Kelly and Melton, 2000; Horb and Slack, 2002; Afelik et al., 2004). Insulin expression was further increased at stage 39, indicating the formation of β -cells. However the detection of Insulin expression does not necessarily mean that functional mature β -cells are formed. In several studies, iPSCs- or hESCs-derived *in vitro* generated β -cells have been frequently observed to express additional endocrine hormones together with Insulin. These poly-hormonal Insulin-positive cells were shown to be functional immature as they lack the capacity for Glucose-stimulated Insulin release (D'Amour et al., 2006; Basford et al., 2012; Schiesser et al., 2014). So far, we have not tested whether the Insulin-positive cells, found in pancreatic organoids, exclusively express Insulin and no additional hormones. A single cell analysis should bring clarification. Moreover, it remains to be tested if the presence of *insulin* transcripts reflects the availability of secreted functional Insulin peptide.

Further endocrine and exocrine differentiation markers were detected at later stages. The exocrine differentiation marker Pdia2 is detected at stage 39 and Amylase is expressed at stage 43 in pancreatic organoids comparable with the expression observed *in vivo* (Horb and Slack 2002; Afelik et al., 2004). The endocrine differentiation marker Glucagon is earlier detected in the organoids than in the embryos (Horb and Slack, 2002). This might be due to the generally observed higher levels of pancreatic marker gene expression in pancreatic organoids compared to embryos. An further evidence that the generated pancreatic organoids recapitulate the *in vivo* pancreas organogenesis is the detection of Tm4sf3 at stage 43. Tm4sf3 is a transmembrane protein which is described as ventral specific pancreatic marker in *Xenopus* with a function in the fusion of the two ventral buds with the dorsal bud at stage 40 (Jarikji et al., 2009).

WMISH against the pancreatic marker genes Ptf1a and Pdx1 further revealed that the generated pancreatic organoids exhibit broad expression domains of these markers. Moreover, Insulin-positive cells were detected throughout the organoid indicating that a large portion of the explant turned into pancreatic tissue. Therefore, we used this *in vitro* system of pancreatic organoids for the identification of RA-target genes involved in pancreas specification.

The identification of such RA-dependent regulators of pancreas development could bring us one step closer to the major aim of pancreas research which is the *in vitro* generation of functional β -cells for a replacement therapy in order to treat diabetes type 1. Several studies used hESCs (Kroon et al., 2008; Rezanian et al., 2012; Schulz et al., 2012; Pagliuca et al., 2014) or iPSCs (Zhang et al., 2009; Schiesser et al., 2014; Shaer et al., 2015) for a successful *in vitro* generation of β -cells. All studies applied stepwise differentiation protocols including the application of Activin A, a TGF β -family member that mimics nodal signaling required for endoderm formation (reviewed in Tam and Loebel, 2007), Noggin and RA. Our identified RA-induced pancreatic regulators could help to optimize these protocols and to increase the amount of generated β -cells. Moreover, our findings could help to find strategies for the trans-differentiation of patient-derived somatic cells into endocrine pancreatic cells. The trans-differentiation of somatic cells into pancreatic cells would be a promising alternative for ESC-derived pancreatic cells as the potential tumorigenicity of such cells is still a major concern and long-term studies are missing.

4.2 Identification of 22 RA-responsive genes

Unlike other signaling molecules, RA enters the cell independent of cell-surface receptors and binds directly to nuclear receptors (Rochette-Egly and Germain, 2009; Huang et al., 2014b). However, no studies are available dealing with the question in which time scale nuclear receptors are activated to induce target gene expression. We could show that the known direct RA-target Cyp26a1 (Loudig et al., 2000) is induced within one hour after RA-addition. Thus, for the identification of early RA-targets, the transcriptome of programmed explants was analyzed one and two hours after RA-addition. 102 genes were found to be differentially expressed in the presence of RA-signaling. Almost half of these genes were affected by RA in the presence of CHX, indicating them as putative direct RA-targets. Twelve genes were found to be differentially expressed upon CHX-treatments but not affected by RA-signaling. This might be due to the translational inhibition of transcriptional repressors. Under these conditions, genes are possibly transcribed that are usually repressed. The list of 102 differentially expressed genes arise from the alignment of 50 nucleotide short sequence reads to the genome of two *Xenopus* species, *tropicalis* and *laevis*. The inclusion of the *tropicalis* genome was necessary as the *laevis* genome is not fully sequenced. Thus, six mismatches were allowed during the process of alignment to target also the *tropicalis* genome. Beside the frequently occurring errors using small sequence reads, this further increased the risk of false

positive candidates (González and Joly, 2013). Thus, several approaches were used to validate the RA-responsiveness of the candidates.

By this, the list of RA-responsive genes was diminished to 22 candidates. This list contains nine homeobox transcription factors (Hnf1b, Lhx1, Gbx2.1, Meis3, Nkx6.2, Hoxd1, Hoxd4, Hoxa1, Hoxb1), three other transcription factors (Znf703, Foxh1, Cebp), two enzymes (Dhrs3 and Cyp26a1), two signaling components (Fzd4, Igf3), an intermediate filament protein (Prph), an autocrine glycoprotein (Fst) and four candidates with unknown identity. A review by Balmer and Blomhoff in 2002 evaluated published data from in total 1,191 papers covering 532 described RA-target genes and classified them into categories according to the probability of RA-regulation (Balmer and Blomhoff, 2002). However, most of these data were obtained in cell cultures without any developmental aspect. Nevertheless, 13 of the listed 22 RA-responsive genes in our study were already described as RA-regulated genes in the review of Balmer and Blomhoff or in following studies.

The homeobox-containing transcription factor Hnf1b was initially described as RA-inducible in a mouse stem cell line (De Simone et al., 1991). Furthermore, Hnf1b was found to be RA-induced in the mouse and zebrafish hindbrain (Hernandez et al., 2004; Pouilhe et al., 2007). It is described in several studies using zebrafish, mouse and *Xenopus* embryos that an RA-gradient during neural development contributes to the anterior-posterior expression pattern of homeobox-containing genes in the hindbrain (reviewed in Glover et al., 2006). Thus, the RA-inducibility of most of the Hox-genes in our list was previously described including Hoxd4 (Nolte et al., 2003), Hoxa1 (Boylan et al., 1993; Frasch et al., 1995), Hoxb1 (Huang et al., 2002; Ishioka et al., 2012), Hoxd1 (Kolm and Sive, 1994), Gbx2.1 (Bouillet et al., 1995) and Lhx1 (Strate et al., 2009). Furthermore, Fzd4 and Fst were previously shown to be up-regulated by RA in mouse embryonal tumor cells (Hashimoto et al., 1992; Katoh, 2002). For the RA-metabolic enzymes Cyp26a1 (Abu-Abed et al., 1998) and Dhrs3 (Kam et al., 2013), the zinc-finger transcription factor Znf-703 (Mitchell et al., 2015) and the intermediate filament Prph (De Genaro et al., 2013) the RA-inducibility was also shown previously. Beside these known RA-regulated genes detected in our screen, 9 additional candidates are identified as novel RA-target genes.

Based on the CHX-treatment data, we can distinguish between putative direct and indirect targets. However, the presence of retinoic acid response elements (RARE), as additional indicators for direct RA-regulation, remains to be proven. For *Xenopus laevis* genes this is a challenging venture as intronic and enhancer sequences are

not fully sequenced. RAREs are characterized by two direct repeats of the hexameric motif RGKTS_A (R=A/G, K=G/T, S=C/G) separated by either one, two or five nucleotide spacers. RAREs were found to be located between 10 kb upstream and downstream from the gene locus and were bound by RXR/RAR heterodimers that display distinct motif affinities. Both classes of RA-receptors exist as α -, β -, γ -isoforms and further numerous isoforms by differential promotor usage or alternative splicing exist, varying in RARE recognition (reviewed in Germain et al., 2006; Lalevee et al., 2011). Several studies in mouse and zebrafish detect RAREs within the gene loci of RA-responsive homeodomain-containing transcription factors. These include Hnf1b (Pouilhe et al., 2007), Hoxd4 (Nolte et al., 2003), Hoxa1 (Langston et al., 1997) and Hoxb1 (Huang et al., 2002).

The expression characteristics of the identified 22 RA-responsive genes during gastrulation gave us further indications about their possible function in pancreas development. Based on their RA-responsive endodermal expression domains, Hnf1b and Fzd4 were selected for functional analysis. Through loss and gain of function approaches, the requirement of Hnf1b for pancreas development could be confirmed and for Fzd4 a function in pancreatic fate determination is strongly suggested. These findings will be discussed in detail in the next sections. However, it remains to be urgently examined if the combined activity of Hnf1b and Fzd4 is sufficient to substitute for RA in pancreas specification.

If this is not the case, the list of RA-responsive genes from our screen contains some further interesting candidates. The results of a previous study, using different combinations of dorsal and ventral endodermal and mesodermal explants, suggests that RA-signaling acts simultaneously in both, dorsal endoderm and mesoderm, to promote pancreatic fate (Pan et al., 2007). In our list, four genes were found to be expressed in the dorsal internal involuting mesoderm which corresponds to the Raldh2 expression domain. Cebpd, a transcription factor of the C/EBP family, is linked to β -cell survival as it has an anti-apoptotic function in rat and human insulin-producing cells (Moore et al., 2012). The enzyme Dhcr3 exhibits a retinal reductase activity that converts retinal to retinol counteracting against RA-generation (Haeseleer et al., 1998). Fst (Follistatin), an autocrine glycoprotein, is an Activin inhibitor (Kogawa et al., 1991). In the context of pancreas development the inhibition of Activin was shown to expand pancreatic epithelium, but decrease the number of differentiated β -cells. Thus, it is suggested that Fst is required to regulate Activin activity to acquire the homeostasis of growth and differentiation in this context (Zhang et al., 2004). A further candidate, expressed in the dorsal involuting mesoderm, is the transcription factor Lhx1 for which no connection to pancreas

development is described. Not expressed in the internal involuting mesoderm but linked to pancreas development is Nkx6.2. In mouse, this transcription factor was found to be expressed in pancreatic progenitors regulating pancreatic subtype specification (Henseleit et al., 2005). Therefore, functional studies for the listed candidates appear to be important.

4.3 The direct RA-target Hnf1b is required for pancreas development

We identified the transcription factor Hnf1b as direct RA-target gene in the dorsal endoderm during gastrulation and could demonstrate that its function is required for pancreas development in *Xenopus*. In mouse, Hnf1b was found to be expressed in the endodermal germ layer and in endodermal derived structures including pancreas, liver, gallbladder and duodenum (Barbacci et al., 1999; Haumaitre et al., 2003). We could detect Hnf1b transcripts in the entire endoderm during gastrulation with a minor enrichment in the dorsal endoderm. At later stages, Hnf1b expression was observed in the foregut endoderm including the anterior archenteron roof that gives rise to the dorsal pancreatic anlagen. These observations are consistent with findings in mouse where Hnf1b expression was also detected in early proliferating pancreatic progenitor epithelium together with Pdx1 and Ptf1a (Haumaitre et al., 2005). Furthermore, Hnf1b was identified as pancreatic trunk marker in mouse and lineage tracing experiments showed that Hnf1b-positive cells of the pancreatic epithelium are precursors of acinar, duct and endocrine cells (Solar et al., 2009).

We could further show that the dorsal endodermal expression of Hnf1b during gastrulation is RA-responsive. So far, the induction of Hnf1b by RA was solely described for hindbrain tissue (reviewed in Glover et al., 2006) and the only evidence for endodermal RA-inducibility was found in gastric organoids derived from mouse embryonal stem cells (McCracken et al., 2014). We further identified Hnf1b as direct RA-target what is supported by the identification of two RAREs in the promotor sequence and within the fourth intron of the mouse Hnf1b gene locus (Power and Cereghini, 1995; Pouilhe et al., 2007). The RA-responsive expression in the dorsal endoderm strongly indicates a role for Hnf1b in the pre-arrangement of conditions promoting pancreatic fate. Indeed, upon the downregulation of functional Hnf1b in pancreatic organoids almost a complete loss of pancreatic markers was observed. Furthermore, the endodermal marker Darmin was also decreased whereas another endodermal marker Sox17a was only slightly affected. Darmin is described in *Xenopus* as an endodermal marker with unknown function (Pera et al.,

2003) and no indications for a regulation of *Darmin* by *Hnf1b* are found in the literature. Interestingly, *Hnf1b* and *Darmin* exhibit a similar expression in the entire endoderm in *Xenopus* blastula embryos and we find both genes to be RA-inducible expressed in programmed explants. As we found *Darmin* downstream of *Hnf1b*, *Darmin* could be identified as novel *Hnf1b* target genes with a possible role in pancreas development. The rescue of most pancreatic markers and *Darmin* by a hormone-inducible *Hnf1b* indicates that the observed knockdown-phenotype is specific due to the downregulation of functional *Hnf1b*. The data observed for the rescue of *Ptf1a* expression were inconsistent. Some rescue experiments showed a *Ptf1a* expression (not shown) and others not. The failed rescue of *Ptf1a* does not reflect a failed rescue of exocrine differentiation as *Pdia2* expression could be rescued. We have no convincing explanations for this observation, but we can provide some speculations. *Hnf1b* and *Ptf1a* are found to be co-expressed in pancreatic progenitors and later during the segregation of tip and trunk domains *Ptf1a* is expressed in acinar cells whereas *Hnf1b* expression is observed in bi-potential trunk cells where it promotes endocrine differentiation (reviewed in Pan and Wright, 2011; De Vas et al., 2015). The *Hnf1b*-GR fusion protein, used for rescue approaches, is probably more stable than endogenous protein and continuous DEX-treatment provides high levels of active *Hnf1b*. It is possible that high *Hnf1b* levels promote endocrine fate at the expense of exocrine fate. This would be supported by the low transcript levels of *Pdia2* in the rescue. However, we cannot provide evidences for this.

Nevertheless, our data indicate a function of *Hnf1b* in pancreas development and support and confirm previous studies. Mutations within the *Hnf1b* gene locus in humans cause a monogenetic form of diabetes, named MODY 5 (maturity onset diabetes of the young) and is further linked to kidney and genital malformations (reviewed in Ryffel, 2001; Wang et al., 2004; Haumaitre et al., 2006). Chimeric mutant mice with a specific loss of *Hnf1b* in the visceral endoderm exhibit a lack of the ventral pancreas and a hypoblastic dorsal pancreas (Haumaitre et al., 2005). Therefore, *Hnf1b* is considered as putative upstream regulator of pancreatic progenitor markers *Pdx1* and *Ptf1a*. Our findings in pancreatic organoids could be confirmed in whole embryos where the downregulation of *Hnf1b* leads to a decreased expression of *Pdx1*, *Ptf1a* and *Insulin*. Moreover, upon *Hnf1b* over-expression, endodermal *Ptf1a* and *Pdx1* expression domains were significantly expanded. This indicates an early function of *Hnf1b* in promoting pancreas progenitor formation. Further indications for an early function of *Hnf1b* in pancreas development were previously found by protein-DNA interaction analysis in mouse,

where Hnf1b was found to directly induce Hnf6 expression (Poll et al., 2006). Hnf6 precedes the expression of Pdx1 in the foregut-midgut region and is later restricted to the liver and the pancreas (Landry et al., 1997; Rausa et al., 1997). Hnf6 was shown to initiate Pdx1 expression in mouse and the inactivation of Hnf6 results in a delayed onset of Pdx1 expression leading to pancreatic hypoplasia (Jacquemin et al., 2003). Therefore, it is suggested that a sequential transcriptional cascade of Hnf1b, Hnf6 and Pdx1 directs endodermal cells into pancreatic progenitors (Poll et al., 2006). However, the fact that the Pdx1 expression in Hnf6 mutants is delayed and not completely missing indicates the requirement of additional factors, possibly further Hnf1b targets.

Besides the indicated early function of Hnf1b in progenitor formation, De Vas and colleagues demonstrated in a mouse system the requirement of Hnf1b for endocrine cell specification (De Vas et al., 2015). They inactivated Hnf1b specifically in pancreatic progenitors and observed the absence of Ngn3-positive endocrine precursor cells throughout embryogenesis. Another direct Hnf1b-target Hnf4a is also linked to MODY as β -cells in patients with Hnf4a mutations exhibit an impaired insulin secretory response to glucose (Yamagata et al., 1996; Hattersley, 1998; Lausen et al., 2000). Pancreatic organoids would be a suitable system for the identification of further direct Hnf1b targets that are possibly involved in pancreas development.

In summary, our data confirm several studies that found Hnf1b as direct RA-target and its requirement for pancreas development. We could provide further evidences for an early endodermal induction of Hnf1b by RA and its early function in pancreatic progenitor formation. However, the gene network induced by Hnf1b that is involved in pancreas development needs to be further investigated. Moreover, we show that Hnf1b is not sufficient to substitute for RA in pancreas development. Hence, Hnf1b is not the only RA-responsive gene that is required for pancreas development.

4.4 The direct RA-target Fzd4 is required for pancreas development

We identified the transmembrane Wnt-receptor Fzd4 and its secreted splice variant Fzd4s as direct RA-target genes required for pancreas development. Fzd4 was previously found to be upregulated together with other Wnt-receptors and Wnt-ligands by RA in human embryonal tumor cells (Katoh, 2002). Furthermore, evidences exist for an interplay of RA-signaling and Wnt-signaling in chondrocytes to regulate cartilage matrix homeostasis (Yasuhara et al., 2010). However, a connection of Fzd4 and RA-signaling in pancreas development is not described so far.

Two studies of Fzd4 in *Xenopus* describe an expression in the prospective neuroectoderm and later in the head region including the forebrain (Shi and Boucaut, 2000; Zhang et al., 2011). We found an additional Fzd4 RA-responsive expression domain in the dorsal endoderm of gastrula stage embryos. We initially observed this endodermal Fzd4 expression domain in RA-treated embryos only. A prolonged staining of un-treated embryos confirmed a weak endogenous endodermal expression of Fzd4 that have been missed by a too short staining. At later stages, Fzd4 expression was also detected in the foregut. For human and *Xenopus* Fzd4, an alternative splice variant through intron retention was identified (Sagara et al., 2001; Swain et al., 2005). This Fzd4 variant, named Fzd4s, encodes a small protein missing the transmembrane domain but still containing the Wnt-ligand binding cysteine rich domain (Swain et al., 2005). Therefore, the question appeared which variant is expressed in the dorsal endoderm. The endodermal expression domain was detected by the use of an antisense probe targeting the exonic sequence. This should theoretically detect both variants. Therefore, we additionally used an antisense probe targeting a part of the intronic region that should specifically detect Fzd4s. Steinbeisser and colleagues described an ubiquitous staining of Fzd4s transcripts during gastrulation and at tailbud stages in head region, not identical with Fzd4 but with overlaps in the eye (Swain et al., 2005). In contrast, beside a certain level of staining in the whole embryo, we could detect enriched regions in the mesoderm during gastrulation and later in the notochord and head region. The expression in the notochord was not observed with the probe that targets the exonic regions. Either the probe that targets the exons detects only Fzd4 and not Fzd4s or the probe targeting the intronic region results in an unspecific signal. Thus, we cannot conclude with certainty which variant exhibits the dorsal endodermal expression domain.

RNA-sequencing and RT-PCR data indicate that both variants of Fzd4 were induced by RA. However, compared to the other direct RA-target genes Hnf1b and Cyp26a1, the Fzd4 variants exhibit only a minor induction by RA. A certain level of Fzd4 and Fzd4s transcripts is detected also in the absence of RA. This probably corresponds to maternally provided transcripts in the case of Fzd4 (Shi and Boucaut, 2000) and for Fzd4s an additional RA-independent expression is conceivable.

The described loss-of-function studies through morpholino-oligonucleotide and CRISPR/Cas-system should affect both Fzd4 variants. Therefore, Fzd4 and Fzd4s were designated as Fzd4/Fzd4s in this context. We demonstrated that both, the knockdown of Fzd4/Fzd4s by morpholino-oligonucleotide and the knockout by RNA-guided Cas9 in pancreatic organoids showed a similar decrease of pancreatic marker gene expression. For the knockdown approach, several strategies failed to rescue the observed phenotype in order to demonstrate the specificity of the used morpholino-oligonucleotide. As mentioned in the results section, this might have several reasons. On the one hand, we were not able to provide active Fzd4 or Fzd4s specifically during gastrulation. On the other hand, we are not aware of the variant that is required and the appropriate level of active protein necessary for a proper pancreas development.

Both variants were not described to be involved in pancreas development so far. The transmembrane Fzd4 is described as mediator of both, canonical and non-canonical Wnt-signaling downstream of Wnt5a (Umbhauer et al., 2000; Chen et al., 2003; Mikels and Nusse, 2006; Xu et al., 2004). The activation of non-canonical/PCP pathway by Wnt5a/Fzd4-interaction was shown to be required for arterial network formation in mouse (Descamps et al., 2012). Furthermore, Fzd4 is the only known Wnt-receptor that binds Norrin and thereby activates canonical Wnt-signaling promoting retinal vascularization in mouse (Xu et al., 2004; reviewed in Ye et al., 2010). Fzd4s shows structural similarities to secreted frizzled-related proteins (sfrps) and is therefore considered to be secreted (Rattner et al., 1997). Fzd4s still contains the Wnt-ligand binding domain and was described in *Xenopus* as an activator or inhibitor of canonical Wnt-signaling dependent on its ligand. Steinbeisser and colleagues showed that dependent on the corresponding Wnt-ligand, the Wnt/Fzd4s complex is recognized by the LRP5/6-co-receptor and mediates Wnt-signaling or it is not recognized (Swain et al., 2005). Following studies revealed that the activatory or inhibitory function of Fzd4s is further dependent on its concentration. Low Fzd4s concentrations enhance and high concentrations repress Wnt-signaling in the presence of low Wnt-ligand levels (Gorny et al., 2013). This supports the assumption of the importance of appropriate Fzd4/Fzd4s levels

required to rescue the morpholino-mediated knockdown phenotype. Findings by the Fzd4/Fzd4s-knockout confirm the results of Fzd4/Fzd4s-knockdown in pancreatic organoids. We could demonstrate that the observed decrease of pancreatic marker gene expression is due to specific mutations within the Fzd4 gene locus as tested potential off-targets showed no mutations.

The next important question that needs to be answered is whether the function of Fzd4/Fzd4s in Wnt-signaling is required for pancreas development. For Fzd4 also a signaling function outside of the classical Wnt-signaling pathway was described. During Wnt-signaling, Fzd4 usually binds intracellular Disheveled via a PDZ-binding motif that mediates Wnt-signaling (Wong et al., 2003; reviewed in Niehrs, 2012). In a mouse neuronal cell culture, the intracellular PDZ-binding motif of Fzd4 was shown to interact with other PDZ-domain containing proteins than Dvl and thereby promoting dendrite outgrowth (Bian et al., 2015). Therefore, a function of Fzd4 in pancreas development independent from the Wnt-signaling pathway is possible. However, results from luciferase reporter assays showed an inhibitory effect of RA-treatment on canonical as well as non-canonical reporter activity in Vegf/Noggin-programmed explants. The activatory effect of the Fzd4-knockdown on non-canonical reporter activity in these explants suggests the involvement of Wnt-signaling in early pancreas development. This issue will be discussed in the next section. In summary, we identified Fzd4 and its splice variant Fzd4s as direct RA-target genes. Our results strongly suggest the requirement of Fzd4 and/or Fzd4s in pancreas development.

4.5 Wnt- and RA-signaling in pancreas development

We identified the Wnt-receptor Fzd4 and its secreted variant Fzd4s as direct RA-targets with a possible role in pancreas development. Therefore, we asked about the role of Wnt-signaling in pancreas development. Previous studies proposed that Wnt-signaling needs to be repressed for foregut maintenance and therefore to allow a proper pancreas development. In *Xenopus*, McLin and colleagues found several foregut markers repressed upon Wnt8 over-expression (McLin et al., 2007). Furthermore, Li and colleagues identified the secreted Wnt-inhibitor sfrp5 to be expressed in the early foregut epithelium of *Xenopus* embryos. A downregulation of functional sfrp5 leads to smaller foregut domains and in contrast the ectopic sfrp5 expression results in an expanded foregut domain at the expense of the hindgut (Li et al., 2008). However, a more recent study found evidences for the requirement of

low Wnt-signaling activity for foregut maintenance. It was shown that the depletion of Wnt-receptor Fzd7 in the foregut results in pancreas agenesis in *Xenopus* and that a low expression level of this Wnt-receptor is essential for foregut maintenance (Zhang et al., 2013a). Moreover, sfrps that were initially thought to be exclusively negative Wnt-signaling modulators emerged as biphasic regulators in a concentration dependent manner (Mii and Taira, 2009). These findings suggest a regulatory mechanism that ensures an appropriate Wnt-signaling activity in the foregut.

Our finding of Wnt-receptors Fzd4 and Fzd4s involved in pancreas development is further supported by transcriptome analysis of hepatic and pancreatic progenitors in mouse. The transcriptome of bi-potential hepato-pancreatic progenitors was compared to the transcriptome of developed dorsal and ventral pancreatic buds and the liver bud (Rodríguez-Seguel et al., 2013). They found intracellular Wnt-signaling transducers like Disheveled to be expressed equally in all samples whereas Wnt-ligands, receptors and co-receptors were strongly downregulated in liver progenitors. Among these differentially expressed Wnt-components, Fzd4 and its ligand Wnt5a were found. It was demonstrated that endodermal explants from *Xenopus* embryos treated with soluble Wnt5a exhibit an enhanced expression of Pdx1 and Ptf1a. Furthermore, liver cells treated with Wnt5a strongly induce Pdx1 expression (Rodríguez-Seguel et al., 2013). They suggest that non-canonical Wnt-signaling is a potential promotor of pancreatic fate. We found only Fzd4/Fzd4s expression regulated by RA and not Wnt5a expression. However, we observed an effect of RA-treatment on Wnt-signaling in our explant system. Two hours after RA-addition the activity of both, canonical and non-canonical Wnt-signaling reporter was decreased. Thereby, the non-canonical Wnt-reporter was slightly stronger affected. The described effect of RA-treatment on canonical Wnt-signaling is consistent with several other studies. Zhang and colleagues identified Ndr1 as RA-target and demonstrated that the inhibitory function of Ndr1 on canonical Wnt-signaling is required for foregut development (Zhang et al., 2013b). However, Ndr1 was not differentially expressed upon RA-treatment in our system. One explanation for this could be the late time point of Ndr1 induction by RA that was observed in stage 16 embryos earliest, but we searched for RA-targets that were induced within two hours after RA-addition. Another study using mouse ESCs also found the negative regulatory effect of RA on canonical Wnt-signaling (Osei-sarfo and Gudas, 2014). In addition, they found non-canonical Wnt-signaling activated by RA. This activatory effect of RA on non-canonical Wnt-signaling was also described by Harada and colleagues (Harada et al., 2007). There, RA-inducible G-protein-coupled receptors

were found to bind Wnt-receptors and thereby activating non-canonical Wnt-signaling. These findings seem to be contradictory to our observed negative regulation of non-canonical Wnt-reporter activity by RA-treatment. However, the term “non-canonical Wnt-signaling” comprises two different pathways. The planar cell polarity (PCP) pathway that involves Rho GTPase and JNK and on the other hand the calcium pathway that involves calcium-sensitive kinases and PKC (reviewed in Nusse, 2012). Our non-canonical Wnt-reporter system is based on an Atf2-response element that is activated by the PCP-pathway (Ohkawara and Niehrs, 2010). In contrast, both studies used a reporter that contains a binding site for the transcription factor NFAT. This transcription factor is activated by the Wnt/calcium pathway (Dejmek et al., 2006). Thus, the effect of RA on the NFAT-reporter needs to be tested in our system. It is possible that RA-signaling has a biphasic activity on different non-canonical Wnt-signaling pathways.

We further examined the effect of Fzd4-knockdown on Wnt-signaling reporter activity in the explant system. We found canonical Wnt-reporter activity only slightly and not significantly increased upon Fzd4-downregulation. In contrast, non-canonical Atf2-reporter activity was significantly increased. This finding complies with the observed decrease in non-canonical Wnt-reporter activity upon RA addition. Hence, these data suggest that the negative regulatory effect of RA on non-canonical Wnt-signaling is mediated by Fzd4 and/or Fzd4s. However, Fzd4 as well as Fzd4s were shown to positively regulate non-canonical Wnt/PCP-signaling (Descamps et al., 2012; Gorny et al., 2013). Therefore, the effect of Fzd4-downregulation on non-canonical Wnt-signaling needs to be further investigated. Moreover, it remains to be tested whether the downregulation of Wnt-signaling by RA is mediated by Fzd4 and if this Fzd4-function is required for pancreas specification.

A connection of Hnf1b and Wnt-signaling was shown in zebrafish. Lancman and colleagues demonstrated that Hnf1b and Wnt2b synergistically function in the specification of hepato-pancreatic progenitors (Lancman et al., 2013). Thus, it is necessary to examine if a combined activity of Hnf1b and Fzd4 and/or Fzd4s is sufficient to substitute for RA in pancreas specification.

4.6 Conclusions

In this study, a system of *in vitro* generated pancreatic organoids was used for the identification of RA-target genes involved in the early pancreas development. We could identify 22 RA-responsive genes, some of which have previously been described as RA-targets. For the transcription factor Hnf1b and the Wnt-receptor Fzd4, we found RA-responsive expression domains within the dorsal endoderm, the origin of pancreatic precursor cells, during gastrulation. Functional analysis for both factors revealed their requirement for pancreas development. We provide the evidence for an early function of Hnf1b in pancreatic progenitor formation. Moreover, we found non-canonical Wnt-signaling activity decreased upon RA-treatment, which is probably mediated by Fzd4. Based on our data we suggest the following model. During gastrulation, RA is secreted from the dorsal mesoderm and directly induces the expression of Hnf1b and Fzd4 in the dorsal endoderm. The overlapping activity of these two RA-target genes establishes a pre-pancreatic domain in the dorsal endoderm. Fzd4 activity down-regulates non-canonical Wnt-signaling which allows the specification of the pancreatic epithelium in the foregut endoderm characterized by the co-expression of Ptf1a and Pdx1. Hnf1b induces a transcriptional cascade via its direct target Hnf6 that leads to the expression of Pdx1. Finally, pancreatic progenitors proliferate and differentiate to endocrine and exocrine tissue constituting the pancreas (**Fig. 4.1**).

In order to extend and further confirm the suggested model, a few aspects remain to be investigated. It would be interesting to uncover which of the two Fzd4 splice variants is required for pancreas specification. Moreover, a further evidence is needed that the regulatory function of Fzd4 in respect to Wnt-signaling is involved in pancreas development. For the function of Hnf1b in pancreas development it would be interesting to search for additional direct targets in this context. Most importantly, it remains to be proven whether the combined activity of Hnf1b and Fzd4 is sufficient for pancreas development or if additional RA-regulated factors are required.

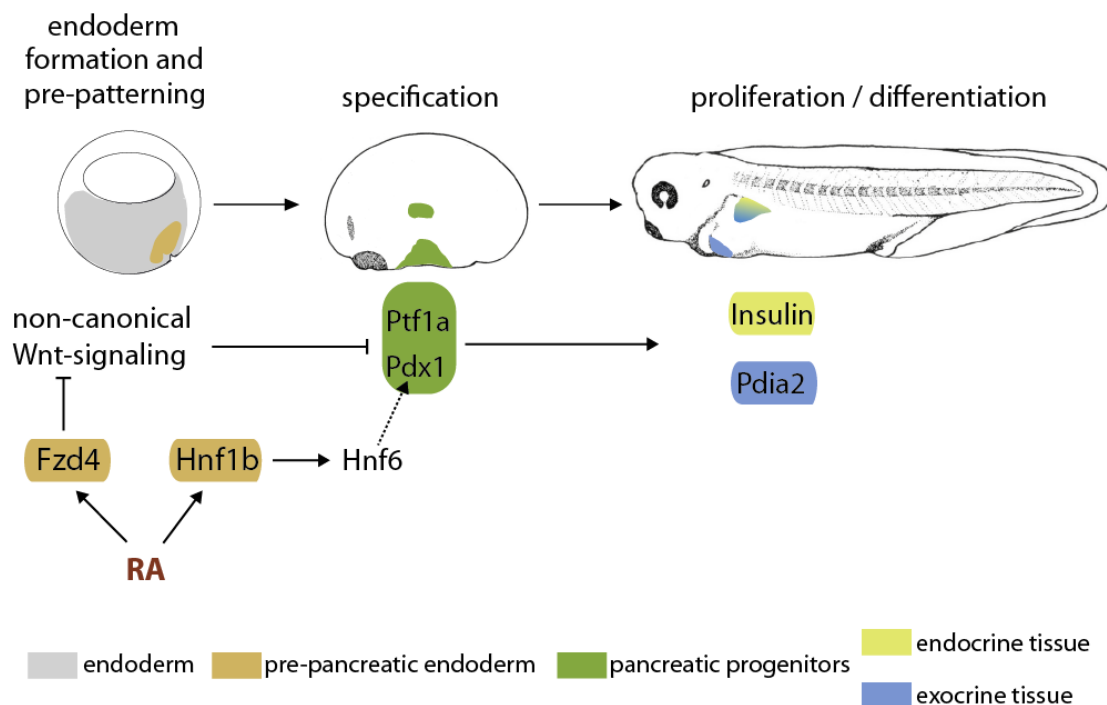


Fig. 4.1 Model of pancreas specification involving direct RA-targets, Fzd4 and Hnf1b, in *Xenopus* embryos.

During gastrulation, the expression of Fzd4 and Hnf1b is directly induced by RA. The overlapping activity of Fzd4 and Hnf1b establishes a pre-pancreatic domain within the dorsal endoderm. Fzd4 down-regulates non-canonical Wnt-signaling activity, which allows the specification of pancreatic progenitors characterized by the co-expression of Ptf1a and Pdx1. In addition, Hnf1b directs endodermal cells into pancreatic progenitors through a sequential transcriptional cascade including Hnf6 and Pdx1. Pancreatic progenitors subsequently proliferate and differentiate into endocrine and exocrine tissue.

5. References

- Abu-Abed, S.S., Beckett, B.R., Chiba, H., Chithalen, J.V., Jones, G., Metzger, D., Chambon, P. and Petkovich, M.** (1998) Mouse P450RAI (CYP26) expression and retinoic acid-inducible retinoic acid metabolism in F9 cells are regulated by retinoic acid receptor gamma and retinoid X receptor alpha. *J Biol Chem*, **273**, 2409-2415.
- Afelik, S., Chen, Y. and Pieler, T.** (2004) Pancreatic protein disulfide isomerase (XPDIp) is an early marker for the exocrine lineage of the developing pancreas in *Xenopus laevis* embryos. *Gene Expr Patterns*, **4**, 71-76.
- Afelik, S., Chen, Y. and Pieler, T.** (2006) Combined ectopic expression of Pdx1 and Ptf1a/p48 results in the stable conversion of posterior endoderm into endocrine and exocrine pancreatic tissue. *Genes Dev*, **20**, 1441-1446.
- Agius, E., Oelgeschlager, M., Wessely, O., Kemp, C. and De Robertis, E.M.** (2000) Endodermal Nodal-related signals and mesoderm induction in *Xenopus*. *Development*, **127**, 1173-1183.
- Apelqvist, A., Li, H., Sommer, L., Beatus, P., Anderson, D.J., Honjo, T., Hrabe de Angelis, M., Lendahl, U. and Edlund, H.** (1999) Notch signalling controls pancreatic cell differentiation. *Nature*, **400**, 877-881.
- Ariizumi, T. and Asashima, M.** (1995) Control of the embryonic body plan by activin during amphibian development. *Zoolog Sci*, **12**, 509-521.
- Ariizumi, T., Kinoshita, M., Yokota, C., Takano, K., Fukuda, K., Moriyama, N., Malacinski, G.M. and Asashima, M.** (2003) Amphibian in vitro heart induction: a simple and reliable model for the study of vertebrate cardiac development. *Int J Dev Biol*, **47**, 405-410.
- Ariizumi, T., Sawamura, K., Uchiyama, H. and Asashima, M.** (1991) Dose and time-dependent mesoderm induction and outgrowth formation by activin A in *Xenopus laevis*. *Int J Dev Biol*, **35**, 407-414.
- Arnes, L. and Sussel, L.** (2015) Epigenetic modifications and long noncoding RNAs influence pancreas development and function. *Trends Genet*, **31**, 290-299.
- Asashima, M., Ito, Y., Chan, T., Michiue, T., Nakanishi, M., Suzuki, K., Hitachi, K., Okabayashi, K., Kondow, A. and Ariizumi, T.** (2009) In vitro organogenesis from undifferentiated cells in *Xenopus*. *Dev Dyn*, **238**, 1309-1320.
- Bae, S., Reid, C.D. and Kessler, D.S.** (2011) Siamois and Twin are redundant and essential in formation of the Spemann organizer. *Dev Biol*, **352**, 367-381.
- Balmer, J.E. and Blomhoff, R.** (2002) Gene expression regulation by retinoic acid. *J Lipid Res*, **43**, 1773-1808.
- Barbacci, E., Reber, M., Ott, M.O., Breillat, C., Huetz, F. and Cereghini, S.** (1999) Variant hepatocyte nuclear factor 1 is required for visceral endoderm specification. *Development*, **126**, 4795-4805.
- Barker, N., Huch, M., Kujala, P., van de Wetering, M., Snippert, H.J., van Es, J.H., Sato, T., Stange, D.E., Begthel, H., van den Born, M., Danenberg, E., van den Brink, S., Korving, J., Abo, A., Peters, P.J., Wright, N., Poulsom, R. and Clevers, H.** (2010) Lgr5(+ve) stem cells drive self-renewal in the stomach and build long-lived gastric units in vitro. *Cell Stem Cell*, **6**, 25-36.
- Basford, C.L., Prentice, K.J., Hardy, A.B., Sarangi, F., Micallef, S.J., Li, X., Guo, Q., Elefanty, A.G., Stanley, E.G., Keller, G., Allister, E.M., Nostro, M.C. and Wheeler, M.B.** (2012) The functional and molecular characterisation of human embryonic stem cell-derived insulin-positive cells compared with adult pancreatic beta cells. *Diabetologia*, **55**, 358-371.
- Beres, T.M., Masui, T., Swift, G.H., Shi, L., Henke, R.M. and MacDonald, R.J.** (2006) PTF1 is an organ-specific and Notch-independent basic helix-loop-helix complex containing the mammalian Suppressor of Hairless (RBP-J) or its paralogue, RBP-L. *Mol Cell Biol*, **26**, 117-130.
- Beucher, A., Gjernes, E., Collin, C., Courtney, M., Meunier, A., Collombat, P. and Gradwohl, G.** (2012) The homeodomain-containing transcription factors Arx and Pax4 control enteroendocrine subtype specification in mice. *PLoS One*, **7**, e36449.
- Bian, W.J., Miao, W.Y., He, S.J., Wan, Z.F., Luo, Z.G. and Yu, X.** (2015) A novel Wnt5a-Frizzled4 signaling pathway mediates activity-independent dendrite morphogenesis via the distal PDZ motif of Frizzled 4. *Dev Neurobiol*, **75**, 805-822.
- Blitz, I.L., Biesinger, J., Xie, X. and Cho, K.W.** (2013) Biallelic genome modification in F(0)

- Xenopus tropicalis embryos using the CRISPR/Cas system. *Genesis*, **51**, 827-834.
- Boj, S.F., Hwang, C.I., Baker, L.A., Chio, I., Engle, D.D., Corbo, V., Jager, M., Ponz-Sarvisé, M., Tiriác, H., Spector, M.S., Gracanin, A., Oni, T., Yu, K.H., van Boxtel, R., Huch, M., Rivera, K.D., Wilson, J.P., Feigin, M.E., Ohlund, D., Handly-Santana, A., Ardito-Abraham, C.M., Ludwig, M., Elyada, E., Alagesan, B., Biffi, G., Yordanov, G.N., Delcuze, B., Creighton, B., Wright, K., Park, Y., Morsink, F.H., Molenaar, I.Q., Borel Rinkes, I.H., Cuppen, E., Hao, Y., Jin, Y., Nijman, I.J., Iacobuzio-Donahue, C., Leach, S.D., Pappin, D.J., Hammell, M., Klimstra, D.S., Basturk, O., Hruban, R.H., Offerhaus, G.J., Vries, R.G., Clevers, H. and Tuveson, D.A.** (2015) Organoid models of human and mouse ductal pancreatic cancer. *Cell*, **160**, 324-338.
- Borchers, A. and Pieler, T.** (2010) Programming pluripotent precursor cells derived from Xenopus embryos to generate specific tissues and organs. *Genes (Basel)*, **1**, 413-426.
- Bort, R., Signore, M., Tremblay, K., Martínez Barbera, J.P. and Zaret, K.S.** (2006) Hex homeobox gene controls the transition of the endoderm to a pseudostratified, cell emergent epithelium for liver bud development. *Dev Biol*, **290**, 44-56.
- Bouillet, P., Chazaud, C., Oulad-Abdelghani, M., Dolle, P. and Chambon, P.** (1995) Sequence and expression pattern of the Stra7 (Gbx-2) homeobox-containing gene induced by retinoic acid in P19 embryonal carcinoma cells. *Dev Dyn*, **204**, 372-382.
- Bourguignon, C., Li, J. and Papalopulu, N.** (1998) XBF-1, a winged helix transcription factor with dual activity, has a role in positioning neurogenesis in Xenopus competent ectoderm. *Development*, **125**, 4889-4900.
- Boylan, J.F., Lohnes, D., Taneja, R., Chambon, P. and Gudas, L.J.** (1993) Loss of retinoic acid receptor gamma function in F9 cells by gene disruption results in aberrant Hoxa-1 expression and differentiation upon retinoic acid treatment. *Proc Natl Acad Sci U S A*, **90**, 9601-9605.
- Brannon, M., Gomperts, M., Sumoy, L., Moon, R.T. and Kimelman, D.** (1997) A beta-catenin/XTcf-3 complex binds to the siamois promoter to regulate dorsal axis specification in Xenopus. *Genes Dev*, **11**, 2359-2370.
- Brannon, M. and Kimelman, D.** (1996) Activation of Siamois by the Wnt pathway. *Dev Biol*, **180**, 344-347.
- Brereton, M.F., Vergari, E., Zhang, Q. and Clark, A.** (2015) Alpha-, Delta- and PP-cells: Are They the Architectural Cornerstones of Islet Structure and Co-ordination? *J Histochem Cytochem*, **63**, 575-591.
- Burlison, J.S., Long, Q., Fujitani, Y., Wright, C.V. and Magnuson, M.A.** (2008) Pdx-1 and Ptf1a concurrently determine fate specification of pancreatic multipotent progenitor cells. *Dev Biol*, **316**, 74-86.
- Carrasco, M., Delgado, I., Soria, B., Martín, F. and Rojas, A.** (2012) GATA4 and GATA6 control mouse pancreas organogenesis. *J Clin Invest*, **122**, 3504-3515.
- Chalmers, A.D. and Slack, J.M.** (2000) The Xenopus tadpole gut: fate maps and morphogenetic movements. *Development*, **127**, 381-392.
- Chan, T.C., Ariizumi, T. and Asashima, M.** (1999) A model system for organ engineering: transplantation of in vitro induced embryonic kidney. *Naturwissenschaften*, **86**, 224-227.
- Chang, Y.F., Imam, J.S. and Wilkinson, M.F.** (2007) The nonsense-mediated decay RNA surveillance pathway. *Annual review of biochemistry*, **76**, 51-74.
- Chen, J.Y., Penco, S., Ostrowski, J., Balaguer, P., Pons, M., Starrett, J.E., Reczek, P., Chambon, P. and Gronemeyer, H.** (1995) RAR-specific agonist/antagonists which dissociate transactivation and AP1 transrepression inhibit anchorage-independent cell proliferation. *Embo j*, **14**, 1187-1197.
- Chen, W., ten Berge, D., Brown, J., Ahn, S., Hu, L.A., Miller, W.E., Caron, M.G., Barak, L.S., Nusse, R. and Lefkowitz, R.J.** (2003) Dishevelled 2 recruits beta-arrestin 2 to mediate Wnt5A-stimulated endocytosis of Frizzled 4. *Science*, **301**, 1391-1394.
- Chen, Y., Pan, F.C., Brandes, N., Afelik, S., Solter, M. and Pieler, T.** (2004) Retinoic acid signaling is essential for pancreas development and promotes endocrine at the expense of exocrine cell differentiation in Xenopus. *Dev Biol*, **271**, 144-160.
- Chen, Y., Pollet, N., Niehrs, C. and Pieler, T.** (2001) Increased XRALDH2 activity has a posteriorizing effect on the central nervous system of Xenopus embryos. *Mech Dev*, **101**, 91-103.
- Chiang, M.K. and Melton, D.A.** (2003) Single-cell transcript analysis of pancreas development. *Dev Cell*, **4**, 383-393.

- Chitnis, A., Henrique, D., Lewis, J., Ish-Horowicz, D. and Kintner, C.** (1995) Primary neurogenesis in *Xenopus* embryos regulated by a homologue of the *Drosophila* neurogenic gene Delta. *Nature*, **375**, 761-766.
- Chung, W.S., Shin, C.H. and Stainier, D.Y.** (2008) Bmp2 signaling regulates the hepatic versus pancreatic fate decision. *Dev Cell*, **15**, 738-748.
- Clagett-Dame, M. and DeLuca, H.F.** (2002) The role of vitamin A in mammalian reproduction and embryonic development. *Annu Rev Nutr*, **22**, 347-381.
- Clements, D., Friday, R.V. and Woodland, H.R.** (1999) Mode of action of VegT in mesoderm and endoderm formation. *Development*, **126**, 4903-4911.
- Cockell, M., Stevenson, B.J., Strubin, M., Hagenbuchle, O. and Wellauer, P.K.** (1989) Identification of a cell-specific DNA-binding activity that interacts with a transcriptional activator of genes expressed in the acinar pancreas. *Mol Cell Biol*, **9**, 2464-2476.
- Conlon, F.L., Lyons, K.M., Takaesu, N., Barth, K.S., Kispert, A., Herrmann, B. and Robertson, E.J.** (1994) A primary requirement for nodal in the formation and maintenance of the primitive streak in the mouse. *Development*, **120**, 1919-1928.
- Damianitsch, K., Melchert, J. and Pieler, T.** (2009) XsFRP5 modulates endodermal organogenesis in *Xenopus laevis*. *Dev Biol*, **329**, 327-337.
- D'Amour, K.A., Bang, A.G., Eliazar, S., Kelly, O.G., Agulnick, A.D., Smart, N.G., Moorman, M.A., Kroon, E., Carpenter, M.K. and Baetge, E.E.** (2006) Production of pancreatic hormone-expressing endocrine cells from human embryonic stem cells. *Nat Biotechnol*, **24**, 1392-1401.
- De Genaro, P., Simon, M.V., Rotstein, N.P. and Politi, L.E.** (2013) Retinoic acid promotes apoptosis and differentiation in photoreceptors by activating the P38 MAP kinase pathway. *Invest Ophthalmol Vis Sci*, **54**, 3143-3156.
- De Simone, V., De Magistris, L., Lazzaro, D., Gerstner, J., Monaci, P., Nicosia, A. and Cortese, R.** (1991) LFB3, a heterodimer-forming homeoprotein of the LFB1 family, is expressed in specialized epithelia. *Embo j*, **10**, 1435-1443.
- De Vas, M.G., Kopp, J.L., Heliot, C., Sander, M., Cereghini, S. and Haumaitre, C.** (2015) Hnf1b controls pancreas morphogenesis and the generation of Ngn3+ endocrine progenitors. *Development*, **142**, 871-882.
- Decker, K., Goldman, D.C., Grasch, C.L. and Sussel, L.** (2006) Gata6 is an important regulator of mouse pancreas development. *Dev Biol*, **298**, 415-429.
- Dejmek, J., Safholm, A., Kamp Nielsen, C., Andersson, T. and Leandersson, K.** (2006) Wnt-5a/Ca²⁺-induced NFAT activity is counteracted by Wnt-5a/Yes-Cdc42-casein kinase 1 α signaling in human mammary epithelial cells. *Molecular and cellular biology*, **26**, 6024-6036.
- Dersch, H. and Zile, M.H.** (1993) Induction of normal cardiovascular development in the vitamin A-deprived quail embryo by natural retinoids. *Dev Biol*, **160**, 424-433.
- Descamps, B., Sewduth, R., Ferreira Tojais, N., Jaspard, B., Reynaud, A., Sohet, F., Lacolley, P., Allieres, C., Lamaziere, J.M., Moreau, C., Dufourcq, P., Couffignal, T. and Duplaa, C.** (2012) Frizzled 4 regulates arterial network organization through noncanonical Wnt/planar cell polarity signaling. *Circ Res*, **110**, 47-58.
- Dessimoz, J., Bonnard, C., Huelsken, J. and Grapin-Botton, A.** (2005) Pancreas-specific deletion of beta-catenin reveals Wnt-dependent and Wnt-independent functions during development. *Curr Biol*, **15**, 1677-1683.
- Dessimoz, J., Opoka, R., Kordich, J.J., Grapin-Botton, A. and Wells, J.M.** (2006) FGF signaling is necessary for establishing gut tube domains along the anterior-posterior axis in vivo. *Mech Dev*, **123**, 42-55.
- Deutsch, G., Jung, J., Zheng, M., Lora, J. and Zaret, K.S.** (2001) A bipotential precursor population for pancreas and liver within the embryonic endoderm. *Development*, **128**, 871-881.
- Dichmann, D.S. and Harland, R.M.** (2011) Nkx6 genes pattern the frog neural plate and Nkx6.1 is necessary for motoneuron axon projection. *Dev Biol*, **349**, 378-386.
- Dickman, E.D., Thaller, C. and Smith, S.M.** (1997) Temporally-regulated retinoic acid depletion produces specific neural crest, ocular and nervous system defects. *Development*, **124**, 3111-3121.
- Djiane, A., Riou, J., Umbhauer, M., Boucaut, J. and Shi, D.** (2000) Role of frizzled 7 in the regulation of convergent extension movements during gastrulation in *Xenopus laevis*. *Development*, **127**, 3091-3100.
- Duester, G.** (2008) Retinoic acid synthesis and signaling during early organogenesis. *Cell*, **134**, 921-931.

- Edlund, H.** (2002) Pancreatic organogenesis--developmental mechanisms and implications for therapy. *Nat Rev Genet*, **3**, 524-532.
- Ellis, P., Fagan, B.M., Magness, S.T., Hutton, S., Taranova, O., Hayashi, S., McMahon, A., Rao, M. and Pevny, L.** (2004) SOX2, a persistent marker for multipotential neural stem cells derived from embryonic stem cells, the embryo or the adult. *Dev Neurosci*, **26**, 148-165.
- Engleka, M.J., Craig, E.J. and Kessler, D.S.** (2001) VegT activation of Sox17 at the midblastula transition alters the response to nodal signals in the vegetal endoderm domain. *Dev Biol*, **237**, 159-172.
- Fineran, P.C. and Dy, R.L.** (2014) Gene regulation by engineered CRISPR-Cas systems. *Curr Opin Microbiol*, **18**, 83-89.
- Finkbeiner, S.R., Freeman, J.J., Wieck, M.M., El-Nachef, W., Altheim, C.H., Tsai, Y.H., Huang, S., Dyal, R., White, E.S., Grikscheit, T.C., Teitelbaum, D.H. and Spence, J.R.** (2015) Generation of tissue-engineered small intestine using embryonic stem cell-derived human intestinal organoids. *Biol Open*, **4**, 1462-1472.
- Frasch, M., Chen, X. and Lufkin, T.** (1995) Evolutionary-conserved enhancers direct region-specific expression of the murine Hoxa-1 and Hoxa-2 loci in both mice and Drosophila. *Development*, **121**, 957-974.
- Fukuda, K. and Kikuchi, Y.** (2005) Endoderm development in vertebrates: fate mapping, induction and regional specification. *Dev Growth Differ*, **47**, 343-355.
- Fukui, Y., Furue, M., Myoishi, Y., Sato, J.D., Okamoto, T. and Asashima, M.** (2003) Long-term culture of Xenopus presumptive ectoderm in a nutrient-supplemented culture medium. *Dev Growth Differ*, **45**, 499-506.
- Gammill, L.S. and Sive, H.** (1997) Identification of otx2 target genes and restrictions in ectodermal competence during Xenopus cement gland formation. *Development*, **124**, 471-481.
- Gao, D., Vela, I., Sboner, A., laquinta, P.J., Karthaus, W.R., Gopalan, A., Dowling, C., Wanjala, J.N., Undvall, E.A., Arora, V.K., Wongvipat, J., Kossai, M., Ramazanoglu, S., Barboza, L.P., Di, W., Cao, Z., Zhang, Q.F., Sirota, I., Ran, L., MacDonald, T.Y., Beltran, H., Mosquera, J.M., Touijer, K.A., Scardino, P.T., Laudone, V.P., Curtis, K.R., Rathkopf, D.E., Morris, M.J., Danila, D.C., Slovin, S.F., Solomon, S.B., Eastham, J.A., Chi, P., Carver, B., Rubin, M.A., Scher, H.I., Clevers, H., Sawyers, C.L. and Chen, Y.** (2014) Organoid cultures derived from patients with advanced prostate cancer. *Cell*, **159**, 176-187.
- Germain, P., Chambon, P., Eichele, G., Evans, R.M., Lazar, M.A., Leid, M., De Lera, A.R., Lotan, R., Mangelsdorf, D.J. and Gronemeyer, H.** (2006) International Union of Pharmacology. LX. Retinoic acid receptors. *Pharmacol Rev*, **58**, 712-725.
- Germain, P., Iyer, J., Zechel, C. and Gronemeyer, H.** (2002) Co-regulator recruitment and the mechanism of retinoic acid receptor synergy. *Nature*, **415**, 187-192.
- Gilchrist, M.J., Zorn, A.M., Voigt, J., Smith, J.C., Papalopulu, N. and Amaya, E.** (2004) Defining a large set of full-length clones from a Xenopus tropicalis EST project. *Dev Biol*, **271**, 498-516.
- Gittes, G.K.** (2009) Developmental biology of the pancreas: a comprehensive review. *Dev Biol*, **326**, 4-35.
- Glover, J.C., Renaud, J.S. and Rijli, F.M.** (2006) Retinoic acid and hindbrain patterning. *J Neurobiol*, **66**, 705-725.
- Gonzalez, E. and Joly, S.** (2013) Impact of RNA-seq attributes on false positive rates in differential expression analysis of de novo assembled transcriptomes. *BMC Res Notes*, **6**, 503.
- Gorny, A.K., Kaufmann, L.T., Swain, R.K. and Steinbeisser, H.** (2013) A secreted splice variant of the Xenopus frizzled-4 receptor is a biphasic modulator of Wnt signalling. *Cell Commun Signal*, **11**, 89.
- Gouzi, M., Kim, Y.H., Katsumoto, K., Johansson, K. and Grapin-Botton, A.** (2011) Neurogenin3 initiates stepwise delamination of differentiating endocrine cells during pancreas development. *Dev Dyn*, **240**, 589-604.
- Gradwohl, G., Dierich, A., LeMeur, M. and Guillemot, F.** (2000) neurogenin3 is required for the development of the four endocrine cell lineages of the pancreas. *Proc Natl Acad Sci U S A*, **97**, 1607-1611.
- Grapin-Botton, A. and Constam, D.** (2007) Evolution of the mechanisms and molecular control of endoderm formation. *Mech Dev*, **124**, 253-278.
- Gu, G., Dubauskaite, J. and Melton, D.A.** (2002) Direct evidence for the pancreatic lineage: NGN3+ cells are islet progenitors and are distinct from duct progenitors.

- Development*, **129**, 2447-2457.
- Guenette, S.A., Giroux, M.C. and Vachon, P.** (2013) Pain perception and anaesthesia in research frogs. *Exp Anim*, **62**, 87-92.
- Guo, X., Zhang, T., Hu, Z., Zhang, Y., Shi, Z., Wang, Q., Cui, Y., Wang, F., Zhao, H. and Chen, Y.** (2014) Efficient RNA/Cas9-mediated genome editing in *Xenopus tropicalis*. *Development*, **141**, 707-714.
- Haeseleer, F., Huang, J., Lebioda, L., Saari, J.C. and Palczewski, K.** (1998) Molecular characterization of a novel short-chain dehydrogenase/reductase that reduces all-trans-retinal. *J Biol Chem*, **273**, 21790-21799.
- Harada, Y., Yokota, C., Habas, R., Slusarski, D.C. and He, X.** (2007) Retinoic acid-inducible G protein-coupled receptors bind to frizzled receptors and may activate non-canonical Wnt signaling. *Biochemical and biophysical research communications*, **358**, 968-975.
- Harland, R.M.** (1991) In situ hybridization: an improved whole-mount method for *Xenopus* embryos. *Methods Cell Biol*, **36**, 685-695.
- Hashimoto, M., Nakamura, T., Inoue, S., Kondo, T., Yamada, R., Eto, Y., Sugino, H. and Muramatsu, M.** (1992) Follistatin is a developmentally regulated cytokine in neural differentiation. *J Biol Chem*, **267**, 7203-7206.
- Hattersley, A.T.** (1998) Maturity-onset diabetes of the young: clinical heterogeneity explained by genetic heterogeneity. *Diabet Med*, **15**, 15-24.
- Haumaitre, C., Barbacci, E., Jenny, M., Ott, M.O., Gradwohl, G. and Cereghini, S.** (2005) Lack of TCF2/vHNF1 in mice leads to pancreas agenesis. *Proc Natl Acad Sci U S A*, **102**, 1490-1495.
- Haumaitre, C., Fabre, M., Cormier, S., Baumann, C., Delezoide, A.L. and Cereghini, S.** (2006) Severe pancreas hypoplasia and multicystic renal dysplasia in two human fetuses carrying novel HNF1beta/MODY5 mutations. *Hum Mol Genet*, **15**, 2363-2375.
- Haumaitre, C., Reber, M. and Cereghini, S.** (2003) Functions of HNF1 family members in differentiation of the visceral endoderm cell lineage. *J Biol Chem*, **278**, 40933-40942.
- Heasman, J.** (2006) Maternal determinants of embryonic cell fate. *Semin Cell Dev Biol*, **17**, 93-98.
- Hebrok, M., Kim, S.K. and Melton, D.A.** (1998) Notochord repression of endodermal Sonic hedgehog permits pancreas development. *Genes Dev*, **12**, 1705-1713.
- Hebrok, M., Kim, S.K., St Jacques, B., McMahon, A.P. and Melton, D.A.** (2000) Regulation of pancreas development by hedgehog signaling. *Development*, **127**, 4905-4913.
- Henry, G.L., Brivanlou, I.H., Kessler, D.S., Hemmati-Brivanlou, A. and Melton, D.A.** (1996) TGF-beta signals and a pattern in *Xenopus laevis* endodermal development. *Development*, **122**, 1007-1015.
- Henseleit, K.D., Nelson, S.B., Kuhlbrodt, K., Hennings, J.C., Ericson, J. and Sander, M.** (2005) NKX6 transcription factor activity is required for alpha- and beta-cell development in the pancreas. *Development*, **132**, 3139-3149.
- Hernandez, R.E., Rikhof, H.A., Bachmann, R. and Moens, C.B.** (2004) vhnf1 integrates global RA patterning and local FGF signals to direct posterior hindbrain development in zebrafish. *Development*, **131**, 4511-4520.
- Hesselson, D., Anderson, R.M. and Stainier, D.Y.** (2011) Suppression of Ptf1a activity induces acinar-to-endocrine conversion. *Curr Biol*, **21**, 712-717.
- Holleman, T., Chen, Y., Grunz, H. and Pieler, T.** (1998) Regionalized metabolic activity establishes boundaries of retinoic acid signalling. *Embo j*, **17**, 7361-7372.
- Holleman, T. and Pieler, T.** (1999) Xp1tx-1: a homeobox gene expressed during pituitary and cement gland formation of *Xenopus* embryos. *Mech Dev*, **88**, 249-252.
- Holtzinger, A. and Evans, T.** (2005) Gata4 regulates the formation of multiple organs. *Development*, **132**, 4005-4014.
- Horb, M.E., Shen, C.N., Tosh, D. and Slack, J.M.** (2003) Experimental conversion of liver to pancreas. *Curr Biol*, **13**, 105-115.
- Horb, M.E. and Slack, J.M.** (2001) Endoderm specification and differentiation in *Xenopus* embryos. *Dev Biol*, **236**, 330-343.
- Horb, M.E. and Slack, J.M.** (2002) Expression of amylase and other pancreatic genes in *Xenopus*. *Mech Dev*, **113**, 153-157.
- Hsu, P.D., Lander, E.S. and Zhang, F.** (2014) Development and applications of CRISPR-Cas9 for genome engineering. *Cell*, **157**, 1262-1278.
- Hsu, P.D., Scott, D.A., Weinstein, J.A., Ran, F.A., Konermann, S., Agarwala, V., Li, Y.,**

- Fine, E.J., Wu, X., Shalem, O., Cradick, T.J., Marraffini, L.A., Bao, G. and Zhang, F. (2013) DNA targeting specificity of RNA-guided Cas9 nucleases. *Nat Biotechnol*, **31**, 827-832.
- Huang, D., Chen, S.W. and Gudas, L.J. (2002) Analysis of two distinct retinoic acid response elements in the homeobox gene *Hoxb1* in transgenic mice. *Dev Dyn*, **223**, 353-370.
- Huang, H.P., Liu, M., El-Hodiri, H.M., Chu, K., Jamrich, M. and Tsai, M.J. (2000) Regulation of the pancreatic islet-specific gene *BETA2* (*neuroD*) by neurogenin 3. *Mol Cell Biol*, **20**, 3292-3307.
- Huang, P., Chandra, V. and Rastinejad, F. (2014b) Retinoic acid actions through mammalian nuclear receptors. *Chem Rev*, **114**, 233-254.
- Huang, W., Wang, G., Delaspre, F., Vitery Mdel, C., Beer, R.L. and Parsons, M.J. (2014a) Retinoic acid plays an evolutionarily conserved and biphasic role in pancreas development. *Dev Biol*, **394**, 83-93.
- Huch, M., Boj, S.F. and Clevers, H. (2013b) *Lgr5*(+) liver stem cells, hepatic organoids and regenerative medicine. *Regen Med*, **8**, 385-387.
- Huch, M., Bonfanti, P., Boj, S.F., Sato, T., Loomans, C.J., van de Wetering, M., Sojoodi, M., Li, V.S., Schuijers, J., Gracanin, A., Ringnalda, F., Begthel, H., Hamer, K., Mulder, J., van Es, J.H., de Koning, E., Vries, R.G., Heimberg, H. and Clevers, H. (2013a) Unlimited in vitro expansion of adult bi-potent pancreas progenitors through the *Lgr5*/*R-spondin* axis. *Embo j*, **32**, 2708-2721.
- Hufton, A.L., Vinayagam, A., Suhai, S. and Baker, J.C. (2006) Genomic analysis of *Xenopus* organizer function. *BMC Dev Biol*, **6**, 27.
- Hutchison, K.A., Scherrer, L.C., Czar, M.J., Stancato, L.F., Chow, Y.H., Jove, R. and Pratt, W.B. (1993) Regulation of glucocorticoid receptor function through assembly of a receptor-heat shock protein complex. *Ann N Y Acad Sci*, **684**, 35-48.
- Hwang, W.Y., Fu, Y., Reyon, D., Maeder, M.L., Tsai, S.Q., Sander, J.D., Peterson, R.T., Yeh, J.R. and Joung, J.K. (2013) Efficient genome editing in zebrafish using a CRISPR-Cas system. *Nat Biotechnol*, **31**, 227-229.
- Hyde, C.E. and Old, R.W. (2000) Regulation of the early expression of the *Xenopus* nodal-related 1 gene, *Xnr1*. *Development*, **127**, 1221-1229.
- Ikuzawa, M., Kobayashi, K., Yasumasu, S. and Iuchi, I. (2005) Expression of CCAAT/enhancer binding protein delta is closely associated with degeneration of surface mucous cells of larval stomach during the metamorphosis of *Xenopus laevis*. *Comp Biochem Physiol B Biochem Mol Biol*, **140**, 505-511.
- Ishioka, A., Jindo, T., Kawanabe, T., Hatta, K., Parvin, M.S., Nikaido, M., Kuroyanagi, Y., Takeda, H. and Yamasu, K. (2011) Retinoic acid-dependent establishment of positional information in the hindbrain was conserved during vertebrate evolution. *Dev Biol*, **350**, 154-168.
- Ismadi, S.D. and Olson, J.A. (1982) Dynamics of the fetal distribution and transfer of Vitamin A between rat fetuses and their mother. *Int J Vitam Nutr Res*, **52**, 112-119.
- Jacquemin, P., Lemaigre, F.P. and Rousseau, G.G. (2003) The *Onecut* transcription factor HNF-6 (*OC-1*) is required for timely specification of the pancreas and acts upstream of *Pdx-1* in the specification cascade. *Dev Biol*, **258**, 105-116.
- Jacquemin, P., Yoshitomi, H., Kashima, Y., Rousseau, G.G., Lemaigre, F.P. and Zaret, K.S. (2006) An endothelial-mesenchymal relay pathway regulates early phases of pancreas development. *Dev Biol*, **290**, 189-199.
- Jarikji, Z., Horb, L.D., Shariff, F., Mandato, C.A., Cho, K.W. and Horb, M.E. (2009) The tetraspanin *Tm4sf3* is localized to the ventral pancreas and regulates fusion of the dorsal and ventral pancreatic buds. *Development*, **136**, 1791-1800.
- Jarikji, Z.H., Vanamala, S., Beck, C.W., Wright, C.V., Leach, S.D. and Horb, M.E. (2007) Differential ability of *Ptf1a* and *Ptf1a-VP16* to convert stomach, duodenum and liver to pancreas. *Dev Biol*, **304**, 786-799.
- Jensen, J., Heller, R.S., Funder-Nielsen, T., Pedersen, E.E., Lindsell, C., Weinmaster, G., Madsen, O.D. and Serup, P. (2000) Independent development of pancreatic alpha- and beta-cells from neurogenin3-expressing precursors: a role for the notch pathway in repression of premature differentiation. *Diabetes*, **49**, 163-176.
- Johansson, K.A., Dursun, U., Jordan, N., Gu, G., Beermann, F., Gradwohl, G. and Grapin-Botton, A. (2007) Temporal control of neurogenin3 activity in pancreas progenitors reveals competence windows for the generation of different endocrine cell types. *Dev Cell*, **12**, 457-465.
- Jones, E.A. (1985) Epidermal development in *Xenopus laevis*: the definition of a monoclonal

- antibody to an epidermal marker. *J Embryol Exp Morphol*, **89 Suppl**, 155-166.
- Jorgensen, M.C., Ahnfelt-Ronne, J., Hald, J., Madsen, O.D., Serup, P. and Hecksher-Sorensen, J.** (2007) An illustrated review of early pancreas development in the mouse. *Endocr Rev*, **28**, 685-705.
- Jung, J., Zheng, M., Goldfarb, M. and Zaret, K.S.** (1999) Initiation of mammalian liver development from endoderm by fibroblast growth factors. *Science*, **284**, 1998-2003.
- Kam, R.K., Chen, Y., Chan, S.O., Chan, W.Y., Dawid, I.B. and Zhao, H.** (2010) Developmental expression of *Xenopus* short-chain dehydrogenase/reductase 3. *Int J Dev Biol*, **54**, 1355-1360.
- Kam, R.K., Shi, W., Chan, S.O., Chen, Y., Xu, G., Lau, C.B., Fung, K.P., Chan, W.Y. and Zhao, H.** (2013) Dhhrs3 protein attenuates retinoic acid signaling and is required for early embryonic patterning. *J Biol Chem*, **288**, 31477-31487.
- Karthaus, W.R., Iaquinta, P.J., Drost, J., Gracanin, A., van Boxtel, R., Wongvipat, J., Dowling, C.M., Gao, D., Begthel, H., Sachs, N., Vries, R.G., Cuppen, E., Chen, Y., Sawyers, C.L. and Clevers, H.C.** (2014) Identification of multipotent luminal progenitor cells in human prostate organoid cultures. *Cell*, **159**, 163-175.
- Katoh, M.** (2002) Regulation of WNT signaling molecules by retinoic acid during neuronal differentiation in NT2 cells: threshold model of WNT action (review). *Int J Mol Med*, **10**, 683-687.
- Kawaguchi, R., Yu, J., Honda, J., Hu, J., Whitelegge, J., Ping, P., Wiita, P., Bok, D. and Sun, H.** (2007) A membrane receptor for retinol binding protein mediates cellular uptake of vitamin A. *Science*, **315**, 820-825.
- Kawaguchi, Y., Cooper, B., Gannon, M., Ray, M., MacDonald, R.J. and Wright, C.V.** (2002) The role of the transcriptional regulator Ptf1a in converting intestinal to pancreatic progenitors. *Nat Genet*, **32**, 128-134.
- Keller, R.** (1991) Early embryonic development of *Xenopus laevis*. *Methods Cell Biol*, 61-113.
- Kelly, O.G. and Melton, D.A.** (2000) Development of the pancreas in *Xenopus laevis*. *Dev Dyn*, **218**, 615-627.
- Kim, S.K., Hebrok, M. and Melton, D.A.** (1997) Notochord to endoderm signaling is required for pancreas development. *Development*, **124**, 4243-4252.
- Kirchgessner, A.L. and Gershon, M.D.** (1990) Innervation of the pancreas by neurons in the gut. *J Neurosci*, **10**, 1626-1642.
- Klein, S.L., Strausberg, R.L., Wagner, L., Pontius, J., Clifton, S.W. and Richardson, P.** (2002) Genetic and genomic tools for *Xenopus* research: The NIH *Xenopus* initiative. *Dev Dyn*, **225**, 384-391.
- Klisch, T.** (2006) Transcriptional control in the context of primary neurogenesis *PhD thesis*.
- Kofron, M., Puck, H., Standley, H., Wylie, C., Old, R., Whitman, M. and Heasman, J.** (2004) New roles for FoxH1 in patterning the early embryo. *Development*, **131**, 5065-5078.
- Kogawa, K., Nakamura, T., Sugino, K., Takio, K., Titani, K. and Sugino, H.** (1991) Activin-binding protein is present in pituitary. *Endocrinology*, **128**, 1434-1440.
- Kolm, P.J. and Sive, H.L.** (1994) Complex regulation of *Xenopus* HoxA1 and HoxD1. *Biochem Soc Trans*, **22**, 579-584.
- Kopp, J.L., Dubois, C.L., Hao, E., Thorel, F., Herrera, P.L. and Sander, M.** (2011a) Progenitor cell domains in the developing and adult pancreas. *Cell Cycle*, **10**, 1921-1927.
- Kopp, J.L., Dubois, C.L., Schaffer, A.E., Hao, E., Shih, H.P., Seymour, P.A., Ma, J. and Sander, M.** (2011b) Sox9⁺ ductal cells are multipotent progenitors throughout development but do not produce new endocrine cells in the normal or injured adult pancreas. *Development*, **138**, 653-665.
- Krapp, A., Knofler, M., Ledermann, B., Burki, K., Berney, C., Zoerkler, N., Hagenbuchle, O. and Wellauer, P.K.** (1998) The bHLH protein PTF1-p48 is essential for the formation of the exocrine and the correct spatial organization of the endocrine pancreas. *Genes Dev*, **12**, 3752-3763.
- Kroon, E., Martinson, L.A., Kadoya, K., Bang, A.G., Kelly, O.G., Eliazar, S., Young, H., Richardson, M., Smart, N.G., Cunningham, J., Agulnick, A.D., D'Amour, K.A., Carpenter, M.K. and Baetge, E.E.** (2008) Pancreatic endoderm derived from human embryonic stem cells generates glucose-responsive insulin-secreting cells in vivo. *Nat Biotechnol*, **26**, 443-452.
- Kubo, A., Shinozaki, K., Shannon, J.M., Kouskoff, V., Kennedy, M., Woo, S., Fehling, H.J. and Keller, G.** (2004) Development of definitive endoderm from embryonic

- stem cells in culture. *Development*, **131**, 1651-1662.
- Kurisaki, A., Ito, Y., Onuma, Y., Intoh, A. and Asashima, M.** (2010) In vitro organogenesis using multipotent cells. *Hum Cell*, **23**, 1-14.
- Lalevee, S., Anno, Y.N., Chatagnon, A., Samarut, E., Poch, O., Laudet, V., Benoit, G., Lecompte, O. and Rochette-Egly, C.** (2011) Genome-wide in silico identification of new conserved and functional retinoic acid receptor response elements (direct repeats separated by 5 bp). *J Biol Chem*, **286**, 33322-33334.
- Lammert, E., Cleaver, O. and Melton, D.** (2001) Induction of pancreatic differentiation by signals from blood vessels. *Science*, **294**, 564-567.
- Lancaster, M.A. and Knoblich, J.A.** (2014) Organogenesis in a dish: modeling development and disease using organoid technologies. *Science*, **345**, 1247125.
- Lancaster, M.A., Renner, M., Martin, C.A., Wenzel, D., Bicknell, L.S., Hurles, M.E., Homfray, T., Penninger, J.M., Jackson, A.P. and Knoblich, J.A.** (2013) Cerebral organoids model human brain development and microcephaly. *Nature*, **501**, 373-379.
- Lancman, J.J., Zvenigorodsky, N., Gates, K.P., Zhang, D., Solomon, K., Humphrey, R.K., Kuo, T., Setiawan, L., Verkade, H., Chi, Y.I., Jhala, U.S., Wright, C.V., Stainier, D.Y. and Dong, P.D.** (2013) Specification of hepatopancreas progenitors in zebrafish by *hnf1ba* and *wnt2bb*. *Development*, **140**, 2669-2679.
- Landry, C., Clotman, F., Hioki, T., Oda, H., Picard, J.J., Lemaigre, F.P. and Rousseau, G.G.** (1997) HNF-6 is expressed in endoderm derivatives and nervous system of the mouse embryo and participates to the cross-regulatory network of liver-enriched transcription factors. *Dev Biol*, **192**, 247-257.
- Langmead, B. and Salzberg, S.L.** (2012) Fast gapped-read alignment with Bowtie 2. *Nat Methods*, **9**, 357-359.
- Langston, A.W., Thompson, J.R. and Gudas, L.J.** (1997) Retinoic acid-responsive enhancers located 3' of the Hox A and Hox B homeobox gene clusters. Functional analysis. *J Biol Chem*, **272**, 2167-2175.
- Lausen, J., Thomas, H., Lemm, I., Bulman, M., Borgschulze, M., Lingott, A., Hattersley, A.T. and Ryffel, G.U.** (2000) Naturally occurring mutations in the human HNF4alpha gene impair the function of the transcription factor to a varying degree. *Nucleic Acids Res*, **28**, 430-437.
- Lee, J.C., Smith, S.B., Watada, H., Lin, J., Scheel, D., Wang, J., Mirmira, R.G. and German, M.S.** (2001) Regulation of the pancreatic pro-endocrine gene neurogenin3. *Diabetes*, **50**, 928-936.
- Lee, Y.H. and Saint-Jeannet, J.P.** (2003) Sox9, a novel pancreatic marker in *Xenopus*. *Int J Dev Biol*, **47**, 459-462.
- Li, H., Handsaker, B., Wysoker, A., Fennell, T., Ruan, J., Homer, N., Marth, G., Abecasis, G. and Durbin, R.** (2009) The Sequence Alignment/Map format and SAMtools. *Bioinformatics*, **25**, 2078-2079.
- Li, M.L., Aggeler, J., Farson, D.A., Hatier, C., Hassell, J. and Bissell, M.J.** (1987) Influence of a reconstituted basement membrane and its components on casein gene expression and secretion in mouse mammary epithelial cells. *Proc Natl Acad Sci U S A*, **84**, 136-140.
- Li, Y., Rankin, S.A., Sinner, D., Kenny, A.P., Krieg, P.A. and Zorn, A.M.** (2008) *Sfrp5* coordinates foregut specification and morphogenesis by antagonizing both canonical and noncanonical Wnt11 signaling. *Genes Dev*, **22**, 3050-3063.
- Lioubinski, O., Muller, M., Wegner, M. and Sander, M.** (2003) Expression of Sox transcription factors in the developing mouse pancreas. *Dev Dyn*, **227**, 402-408.
- Logan, C.Y. and Nusse, R.** (2004) The Wnt signaling pathway in development and disease. *Annu Rev Cell Dev Biol*, **20**, 781-810.
- Lohnes, D., Mark, M., Mendelsohn, C., Dolle, P., Dierich, A., Gorry, P., Gansmuller, A. and Chambon, P.** (1994) Function of the retinoic acid receptors (RARs) during development (I). Craniofacial and skeletal abnormalities in RAR double mutants. *Development*, **120**, 2723-2748.
- Loudig, O., Babichuk, C., White, J., Abu-Abed, S., Mueller, C. and Petkovich, M.** (2000) Cytochrome P450RAI(CYP26) promoter: a distinct composite retinoic acid response element underlies the complex regulation of retinoic acid metabolism. *Molecular endocrinology* (Baltimore, Md.), **14**, 1483-1497.
- Loudig, O., Maclean, G.A., Dore, N.L., Luu, L. and Petkovich, M.** (2005) Transcriptional co-operativity between distant retinoic acid response elements in regulation of *Cyp26A1* inducibility. *Biochem J*, **392**, 241-248.

- Lynn, F.C., Smith, S.B., Wilson, M.E., Yang, K.Y., Nekrep, N. and German, M.S. (2007) Sox9 coordinates a transcriptional network in pancreatic progenitor cells. *Proc Natl Acad Sci U S A*, **104**, 10500-10505.
- Maake, C., Hanke, W. and Reinecke, M. (1998) An immunohistochemical and morphometric analysis of insulin, insulin-like growth factor I, glucagon, somatostatin, and PP in the development of the gastro-entero-pancreatic system of *Xenopus laevis*. *Gen Comp Endocrinol*, **110**, 182-195.
- Maczkowiak, F., Mateos, S., Wang, E., Roche, D., Harland, R. and Monsoro-Burq, A.H. (2010) The Pax3 and Pax7 paralogs cooperate in neural and neural crest patterning using distinct molecular mechanisms, in *Xenopus laevis* embryos. *Dev Biol*, **340**, 381-396.
- Maestro, M.A., Boj, S.F., Luco, R.F., Pierreux, C.E., Cabedo, J., Servitja, J.M., German, M.S., Rousseau, G.G., Lemaigre, F.P. and Ferrer, J. (2003) Hnf6 and Tcf2 (MODY5) are linked in a gene network operating in a precursor cell domain of the embryonic pancreas. *Hum Mol Genet*, **12**, 3307-3314.
- Magenheim, J., Klein, A.M., Stanger, B.Z., Ashery-Padan, R., Sosa-Pineda, B., Gu, G. and Dor, Y. (2011) Ngn3(+) endocrine progenitor cells control the fate and morphogenesis of pancreatic ductal epithelium. *Dev Biol*, **359**, 26-36.
- Mark, M., Ghyselinck, N.B. and Chambon, P. (2006) Function of retinoid nuclear receptors: lessons from genetic and pharmacological dissections of the retinoic acid signaling pathway during mouse embryogenesis. *Annu Rev Pharmacol Toxicol*, **46**, 451-480.
- Martin, M., Gallego-Llamas, J., Ribes, V., Keding, M., Niederreither, K., Chambon, P., Dolle, P. and Gradwohl, G. (2005) Dorsal pancreas agenesis in retinoic acid-deficient Raldh2 mutant mice. *Dev Biol*, **284**, 399-411.
- Masui, T., Long, Q., Beres, T.M., Magnuson, M.A. and MacDonald, R.J. (2007) Early pancreatic development requires the vertebrate Suppressor of Hairless (RBPJ) in the PTF1 bHLH complex. *Genes Dev*, **21**, 2629-2643.
- Masui, T., Swift, G.H., Deering, T., Shen, C., Coats, W.S., Long, Q., Elsasser, H.P., Magnuson, M.A. and MacDonald, R.J. (2010) Replacement of Rbpj with Rbpjl in the PTF1 complex controls the final maturation of pancreatic acinar cells. *Gastroenterology*, **139**, 270-280.
- Masui, T., Swift, G.H., Hale, M.A., Meredith, D.M., Johnson, J.E. and Macdonald, R.J. (2008) Transcriptional autoregulation controls pancreatic Ptf1a expression during development and adulthood. *Mol Cell Biol*, **28**, 5458-5468.
- McCracken, K.W., Cata, E.M., Crawford, C.M., Sinagoga, K.L., Schumacher, M., Rockich, B.E., Tsai, Y.H., Mayhew, C.N., Spence, J.R., Zavros, Y. and Wells, J.M. (2014) Modelling human development and disease in pluripotent stem-cell-derived gastric organoids. *Nature*, **516**, 400-404.
- McCracken, K.W. and Wells, J.M. (2012) Molecular pathways controlling pancreas induction. *Semin Cell Dev Biol*, **23**, 656-662.
- McLin, V.A., Rankin, S.A. and Zorn, A.M. (2007) Repression of Wnt/beta-catenin signaling in the anterior endoderm is essential for liver and pancreas development. *Development*, **134**, 2207-2217.
- Medina, A., Reintsch, W. and Steinbeisser, H. (2000) *Xenopus* frizzled 7 can act in canonical and non-canonical Wnt signaling pathways: implications on early patterning and morphogenesis. *Mech Dev*, **92**, 227-237.
- Mellitzer, G., Bonne, S., Luco, R.F., Van De Casteele, M., Lenne-Samuel, N., Collombat, P., Mansouri, A., Lee, J., Lan, M., Pipeleers, D., Nielsen, F.C., Ferrer, J., Gradwohl, G. and Heimberg, H. (2006) IA1 is NGN3-dependent and essential for differentiation of the endocrine pancreas. *Embo j*, **25**, 1344-1352.
- Mendelsohn, C., Lohnes, D., Decimo, D., Lufkin, T., LeMeur, M., Chambon, P. and Mark, M. (1994) Function of the retinoic acid receptors (RARs) during development (II). Multiple abnormalities at various stages of organogenesis in RAR double mutants. *Development*, **120**, 2749-2771.
- Mii, Y. and Taira, M. (2009) Secreted Frizzled-related proteins enhance the diffusion of Wnt ligands and expand their signalling range. *Development*, **136**, 4083-4088.
- Mikels, A.J. and Nusse, R. (2006) Purified Wnt5a protein activates or inhibits beta-catenin-TCF signaling depending on receptor context. *PLoS Biol*, **4**, e115.
- Mitchell, D.M., Stevens, C.B., Frey, R.A., Hunter, S.S., Ashino, R., Kawamura, S. and Stenkamp, D.L. (2015) Retinoic Acid Signaling Regulates Differential Expression of

- the Tandemly-Duplicated Long Wavelength-Sensitive Cone Opsin Genes in Zebrafish. *PLoS Genet*, **11**, e1005483.
- Miyatsuka, T., Matsuoka, T.A., Shiraiwa, T., Yamamoto, T., Kojima, I. and Kaneto, H.** (2007) Ptf1a and RBP-J cooperate in activating Pdx1 gene expression through binding to Area III. *Biochem Biophys Res Commun*, **362**, 905-909.
- Molotkov, A., Molotkova, N. and Duyster, G.** (2005) Retinoic acid generated by Raldh2 in mesoderm is required for mouse dorsal endodermal pancreas development. *Dev Dyn*, **232**, 950-957.
- Moon, R.T. and Kimelman, D.** (1998) From cortical rotation to organizer gene expression: toward a molecular explanation of axis specification in *Xenopus*. *Bioessays*, **20**, 536-545.
- Moore, F., Santin, I., Nogueira, T.C., Gurzov, E.N., Marselli, L., Marchetti, P. and Eizirik, D.L.** (2012) The transcription factor C/EBP delta has anti-apoptotic and anti-inflammatory roles in pancreatic beta cells. *PLoS One*, **7**, e31062.
- Moriya, N., Komazaki, S. and Asashima, M.** (2000a) In vitro organogenesis of pancreas in *Xenopus laevis* dorsal lips treated with retinoic acid. *Dev Growth Differ*, **42**, 175-185.
- Moriya, N., Komazaki, S., Takahashi, S., Yokota, C. and Asashima, M.** (2000b) In vitro pancreas formation from *Xenopus* ectoderm treated with activin and retinoic acid. *Dev Growth Differ*, **42**, 593-602.
- Mukhi, S., Mao, J. and Brown, D.D.** (2008) Remodeling the exocrine pancreas at metamorphosis in *Xenopus laevis*. *Proc Natl Acad Sci U S A*, **105**, 8962-8967.
- Mullis, K., Faloona, F., Scharf, S., Saiki, R., Horn, G. and Erlich, H.** (1986) Specific enzymatic amplification of DNA in vitro: the polymerase chain reaction. *Cold Spring Harb Symp Quant Biol*, **51 Pt 1**, 263-273.
- Murtaugh, L.C., Law, A.C., Dor, Y. and Melton, D.A.** (2005) Beta-catenin is essential for pancreatic acinar but not islet development. *Development*, **132**, 4663-4674.
- Nakayama, T., Fish, M.B., Fisher, M., Oomen-Hajagos, J., Thomsen, G.H. and Grainger, R.M.** (2013) Simple and efficient CRISPR/Cas9-mediated targeted mutagenesis in *Xenopus tropicalis*. *Genesis*, **51**, 835-843.
- Napolitano, T., Avolio, F., Courtney, M., Vieira, A., Druelle, N., Ben-Othman, N., Hadzic, B., Navarro, S. and Collombat, P.** (2015) Pax4 acts as a key player in pancreas development and plasticity. *Semin Cell Dev Biol*, **44**, 107-114.
- Nieber, F., Pieler, T. and Henningfeld, K.A.** (2009) Comparative expression analysis of the neurogenins in *Xenopus tropicalis* and *Xenopus laevis*. *Dev Dyn*, **238**, 451-458.
- Niederreither, K., McCaffery, P., Drager, U.C., Chambon, P. and Dolle, P.** (1997) Restricted expression and retinoic acid-induced downregulation of the retinaldehyde dehydrogenase type 2 (RALDH-2) gene during mouse development. *Mech Dev*, **62**, 67-78.
- Niehrs, C.** (2012) The complex world of WNT receptor signalling. *Nat Rev Mol Cell Biol*, **13**, 767-779.
- Nieto, M.A., Bradley, L.C., Hunt, P., Das Gupta, R., Krumlauf, R. and Wilkinson, D.G.** (1992) Molecular mechanisms of pattern formation in the vertebrate hindbrain. *Ciba Found Symp*, **165**, 92-102; discussion 102-107.
- Nieuwkoop, P.D.** (1963) Pattern formation in artificially activated ectoderm (*Rana pipiens* and *Ambystoma punctatum*). *Dev Biol*, **6**, 255-279.
- Nieuwkoop, P.D. and Faber, J.** (1967) Normal table of *Xenopus laevis*. (Daudin) *North Holland Publishing Co. Amsterdam*, 2nd ed.
- Nolte, C., Amores, A., Nagy Kovacs, E., Postlethwait, J. and Featherstone, M.** (2003) The role of a retinoic acid response element in establishing the anterior neural expression border of Hoxd4 transgenes. *Mech Dev*, **120**, 325-335.
- Nusse, R.** (2012) Wnt signaling. *Cold Spring Harbor perspectives in biology*, **4**.
- Obata, J., Yano, M., Mimura, H., Goto, T., Nakayama, R., Mibu, Y., Oka, C. and Kawaichi, M.** (2001) p48 subunit of mouse PTF1 binds to RBP-Jkappa/CBF-1, the intracellular mediator of Notch signalling, and is expressed in the neural tube of early stage embryos. *Genes Cells*, **6**, 345-360.
- Ohkawara, B. and Niehrs, C.** (2011) An ATF2-based luciferase reporter to monitor non-canonical Wnt signaling in *Xenopus* embryos. *Dev Dyn*, **240**, 188-194.
- Okabayashi, K. and Asashima, M.** (2006) In Vitro organogenesis using amphibian pluripotent cells. *Proc Jpn Acad Ser B Phys Biol Sci*, **82**, 197-207.
- Osei-Sarfo, K. and Gudas, L.J.** (2014) Retinoic acid suppresses the canonical Wnt signaling pathway in embryonic stem cells and activates the noncanonical Wnt signaling pathway. *Stem cells (Dayton, Ohio)*, **32**, 2061-2071.

- Oster, A., Jensen, J., Serup, P., Galante, P., Madsen, O.D. and Larsson, L.I. (1998) Rat endocrine pancreatic development in relation to two homeobox gene products (Pdx-1 and Nkx 6.1). *J Histochem Cytochem*, **46**, 707-715.
- Pagliuca, F.W., Millman, J.R., Gurtler, M., Segel, M., Van Dervort, A., Ryu, J.H., Peterson, Q.P., Greiner, D. and Melton, D.A. (2014) Generation of functional human pancreatic beta cells in vitro. *Cell*, **159**, 428-439.
- Pan, F.C., Bankaitis, E.D., Boyer, D., Xu, X., Van de Casteele, M., Magnuson, M.A., Heimberg, H. and Wright, C.V. (2013) Spatiotemporal patterns of multipotentiality in Ptf1a-expressing cells during pancreas organogenesis and injury-induced facultative restoration. *Development*, **140**, 751-764.
- Pan, F.C., Chen, Y., Bayha, E. and Pieler, T. (2007) Retinoic acid-mediated patterning of the pre-pancreatic endoderm in *Xenopus* operates via direct and indirect mechanisms. *Mech Dev*, **124**, 518-531.
- Pan, F.C. and Wright, C. (2011) Pancreas organogenesis: from bud to plexus to gland. *Dev Dyn*, **240**, 530-565.
- Pearl, E.J., Bilogan, C.K., Mukhi, S., Brown, D.D. and Horb, M.E. (2009) *Xenopus* pancreas development. *Dev Dyn*, **238**, 1271-1286.
- Pera, E.M., Martinez, S.L., Flanagan, J.J., Brechner, M., Wessely, O. and De Robertis, E.M. (2003) Darmin is a novel secreted protein expressed during endoderm development in *Xenopus*. *Gene Expr Patterns*, **3**, 147-152.
- Perron, M., Opdecamp, K., Butler, K., Harris, W.A. and Bellefroid, E.J. (1999) X-ngnr-1 and Xath3 promote ectopic expression of sensory neuron markers in the neurula ectoderm and have distinct inducing properties in the retina. *Proc Natl Acad Sci U S A*, **96**, 14996-15001.
- Piccolo, S., Sasai, Y., Lu, B. and De Robertis, E.M. (1996) Dorsoventral patterning in *Xenopus*: inhibition of ventral signals by direct binding of chordin to BMP-4. *Cell*, **86**, 589-598.
- Pictet, R.L., Clark, W.R., Williams, R.H. and Rutter, W.J. (1972) An ultrastructural analysis of the developing embryonic pancreas. *Dev Biol*, **29**, 436-467.
- Pieler, T. and Chen, Y. (2006) Forgotten and novel aspects in pancreas development. *Biol Cell*, **98**, 79-88.
- Poll, A.V., Pierreux, C.E., Lokmane, L., Haumaitre, C., Achouri, Y., Jacquemin, P., Rousseau, G.G., Cereghini, S. and Lemaigre, F.P. (2006) A vHNF1/TCF2-HNF6 cascade regulates the transcription factor network that controls generation of pancreatic precursor cells. *Diabetes*, **55**, 61-69.
- Pouilhe, M., Gilardi-Hebenstreit, P., Desmarquet-Trin Dinh, C. and Charnay, P. (2007) Direct regulation of vHnf1 by retinoic acid signaling and MAF-related factors in the neural tube. *Dev Biol*, **309**, 344-357.
- Power, S.C. and Cereghini, S. (1996) Positive regulation of the vHNF1 promoter by the orphan receptors COUP-TF1/Ear3 and COUP-TFII/Arp1. *Mol Cell Biol*, **16**, 778-791.
- Quadro, L., Blaner, W.S., Salchow, D.J., Vogel, S., Piantedosi, R., Gouras, P., Freeman, S., Cosma, M.P., Colantuoni, V. and Gottesman, M.E. (1999) Impaired retinal function and vitamin A availability in mice lacking retinol-binding protein. *Embo j*, **18**, 4633-4644.
- Rankin, S.A., Kormish, J., Kofron, M., Jegga, A. and Zorn, A.M. (2011) A gene regulatory network controlling hhex transcription in the anterior endoderm of the organizer. *Dev Biol*, **351**, 297-310.
- Rattner, A., Hsieh, J.C., Smallwood, P.M., Gilbert, D.J., Copeland, N.G., Jenkins, N.A. and Nathans, J. (1997) A family of secreted proteins contains homology to the cysteine-rich ligand-binding domain of frizzled receptors. *Proc Natl Acad Sci U S A*, **94**, 2859-2863.
- Rausa, F., Samadani, U., Ye, H., Lim, L., Fletcher, C.F., Jenkins, N.A., Copeland, N.G. and Costa, R.H. (1997) The cut-homeodomain transcriptional activator HNF-6 is coexpressed with its target gene HNF-3 beta in the developing murine liver and pancreas. *Dev Biol*, **192**, 228-246.
- Ray, W.J., Bain, G., Yao, M. and Gottlieb, D.I. (1997) CYP26, a novel mammalian cytochrome P450, is induced by retinoic acid and defines a new family. *J Biol Chem*, **272**, 18702-18708.
- Rehorn, K.P., Thelen, H., Michelson, A.M. and Reuter, R. (1996) A molecular aspect of hematopoiesis and endoderm development common to vertebrates and *Drosophila*. *Development*, **122**, 4023-4031.
- Rezania, A., Bruin, J.E., Riedel, M.J., Mojibian, M., Asadi, A., Xu, J., Gauvin, R.,

- Narayan, K., Karanu, F., O'Neil, J.J., Ao, Z., Warnock, G.L. and Kieffer, T.J.** (2012) Maturation of human embryonic stem cell-derived pancreatic progenitors into functional islets capable of treating pre-existing diabetes in mice. *Diabetes*, **61**, 2016-2029.
- Rhinn, M. and Dolle, P.** (2012) Retinoic acid signalling during development. *Development*, **139**, 843-858.
- Richard-Parpaillon, L., Heligon, C., Chesnel, F., Boujard, D. and Philpott, A.** (2002) The IGF pathway regulates head formation by inhibiting Wnt signaling in *Xenopus*. *Dev Biol*, **244**, 407-417.
- Rindi, G., Torsello, A., Locatelli, V. and Solcia, E.** (2004) Ghrelin expression and actions: a novel peptide for an old cell type of the diffuse endocrine system. *Exp Biol Med (Maywood)*, **229**, 1007-1016.
- Robinson, M.D., McCarthy, D.J. and Smyth, G.K.** (2010) edgeR: a Bioconductor package for differential expression analysis of digital gene expression data. *Bioinformatics*, **26**, 139-140.
- Rochette-Egly, C. and Germain, P.** (2009) Dynamic and combinatorial control of gene expression by nuclear retinoic acid receptors (RARs). *Nucl Recept Signal*, **7**, e005.
- Rock, J.R., Onaitis, M.W., Rawlins, E.L., Lu, Y., Clark, C.P., Xue, Y., Randell, S.H. and Hogan, B.L.** (2009) Basal cells as stem cells of the mouse trachea and human airway epithelium. *Proc Natl Acad Sci U S A*, **106**, 12771-12775.
- Rodriguez-Seguel, E., Mah, N., Naumann, H., Pongrac, I.M., Cerda-Esteban, N., Fontaine, J.F., Wang, Y., Chen, W., Andrade-Navarro, M.A. and Spagnoli, F.M.** (2013) Mutually exclusive signaling signatures define the hepatic and pancreatic progenitor cell lineage divergence. *Genes Dev*, **27**, 1932-1946.
- Rodriguez-Segui, S., Akerman, I. and Ferrer, J.** (2012) GATA believe it: new essential regulators of pancreas development. *J Clin Invest*, **122**, 3469-3471.
- Rookmaaker, M.B., Schutgens, F., Verhaar, M.C. and Clevers, H.** (2015) Development and application of human adult stem or progenitor cell organoids. *Nat Rev Nephrol*, **11**, 546-554.
- Rose, S.D., Swift, G.H., Peyton, M.J., Hammer, R.E. and MacDonald, R.J.** (2001) The role of PTF1-P48 in pancreatic acinar gene expression. *J Biol Chem*, **276**, 44018-44026.
- Rossi, J.M., Dunn, N.R., Hogan, B.L. and Zaret, K.S.** (2001) Distinct mesodermal signals, including BMPs from the septum transversum mesenchyme, are required in combination for hepatogenesis from the endoderm. *Genes Dev*, **15**, 1998-2009.
- Rubenstein, A., Merriam, J. and Klymkowsky, M.W.** (1997) Localizing the adhesive and signaling functions of plakoglobin. *Dev Genet*, **20**, 91-102.
- Rukstalis, J.M. and Habener, J.F.** (2007) Snail2, a mediator of epithelial-mesenchymal transitions, expressed in progenitor cells of the developing endocrine pancreas. *Gene Expr Patterns*, **7**, 471-479.
- Rupp, R.A., Snider, L. and Weintraub, H.** (1994) *Xenopus* embryos regulate the nuclear localization of XMyoD. *Genes Dev*, **8**, 1311-1323.
- Ryffel, G.U.** (2001) Mutations in the human genes encoding the transcription factors of the hepatocyte nuclear factor (HNF)1 and HNF4 families: functional and pathological consequences. *J Mol Endocrinol*, **27**, 11-29.
- Sagara, N., Kirikoshi, H., Terasaki, H., Yasuhiko, Y., Toda, G., Shiokawa, K. and Katoh, M.** (2001) FZD4S, a splicing variant of frizzled-4, encodes a soluble-type positive regulator of the WNT signaling pathway. *Biochem Biophys Res Commun*, **282**, 750-756.
- Saiki, R.K., Scharf, S., Faloona, F., Mullis, K.B., Horn, G.T., Erlich, H.A. and Arnheim, N.** (1985) Enzymatic amplification of beta-globin genomic sequences and restriction site analysis for diagnosis of sickle cell anemia. *Science*, **230**, 1350-1354.
- Salzberg, A., Elias, S., Nachaliel, N., Bonstein, L., Henig, C. and Frank, D.** (1999) A Meis family protein caudalizes neural cell fates in *Xenopus*. *Mech Dev*, **80**, 3-13.
- Sambrook, J. and Russel, D.W.** (2001) Molecular Cloning: a laboratory manual. *Cold Spring Harbour Laboratory Press, Cold Spring Harbour, New York.*, **3rd edition**.
- Sander, J.D. and Joung, J.K.** (2014) CRISPR-Cas systems for editing, regulating and targeting genomes. *Nat Biotechnol*, **32**, 347-355.
- Sander, J.D., Maeder, M.L., Reyon, D., Voytas, D.F., Joung, J.K. and Dobbs, D.** (2010) ZIFIT (Zinc Finger Targeter): an updated zinc finger engineering tool. *Nucleic Acids Res*, **38**, W462-468.
- Sander, J.D., Zaback, P., Joung, J.K., Voytas, D.F. and Dobbs, D.** (2007) Zinc Finger

- Targeter (ZiFiT): an engineered zinc finger/target site design tool. *Nucleic Acids Res*, **35**, W599-605.
- Sanger, F., Nicklen, S. and Coulson, A.R.** (1977) DNA sequencing with chain-terminating inhibitors. *Proc Natl Acad Sci U S A*, **74**, 5463-5467.
- Sato, T., van Es, J.H., Snippert, H.J., Stange, D.E., Vries, R.G., van den Born, M., Barker, N., Shroyer, N.F., van de Wetering, M. and Clevers, H.** (2011) Paneth cells constitute the niche for Lgr5 stem cells in intestinal crypts. *Nature*, **469**, 415-418.
- Sato, T., Vries, R.G., Snippert, H.J., van de Wetering, M., Barker, N., Stange, D.E., van Es, J.H., Abo, A., Kujala, P., Peters, P.J. and Clevers, H.** (2009) Single Lgr5 stem cells build crypt-villus structures in vitro without a mesenchymal niche. *Nature*, **459**, 262-265.
- Schaffer, A.E., Freude, K.K., Nelson, S.B. and Sander, M.** (2010) Nkx6 transcription factors and Ptf1a function as antagonistic lineage determinants in multipotent pancreatic progenitors. *Dev Cell*, **18**, 1022-1029.
- Schier, A.F. and Talbot, W.S.** (2005) Molecular genetics of axis formation in zebrafish. *Annu Rev Genet*, **39**, 561-613.
- Schiesser, J.V., Micallef, S.J., Hawes, S., Elefanty, A.G. and Stanley, E.G.** (2014) Derivation of insulin-producing beta-cells from human pluripotent stem cells. *Rev Diabet Stud*, **11**, 6-18.
- Schneider-Poetsch, T., Ju, J., Eyler, D.E., Dang, Y., Bhat, S., Merrick, W.C., Green, R., Shen, B. and Liu, J.O.** (2010) Inhibition of eukaryotic translation elongation by cycloheximide and lactimidomycin. *Nature chemical biology*, **6**, 209-217.
- Schulz, T.C., Young, H.Y., Agulnick, A.D., Babin, M.J., Baetge, E.E., Bang, A.G., Bhoumik, A., Cepa, I., Cesario, R.M., Haakmeester, C., Kadoya, K., Kelly, J.R., Kerr, J., Martinson, L.A., McLean, A.B., Moorman, M.A., Payne, J.K., Richardson, M., Ross, K.G., Sherrer, E.S., Song, X., Wilson, A.Z., Brandon, E.P., Green, C.E., Kroon, E.J., Kelly, O.G., D'Amour, K.A. and Robins, A.J.** (2012) A scalable system for production of functional pancreatic progenitors from human embryonic stem cells. *PLoS One*, **7**, e37004.
- Schwank, G., Koo, B.K., Sasselli, V., Dekkers, J.F., Heo, I., Demircan, T., Sasaki, N., Boymans, S., Cuppen, E., van der Ent, C.K., Nieuwenhuis, E.E., Beekman, J.M. and Clevers, H.** (2013) Functional repair of CFTR by CRISPR/Cas9 in intestinal stem cell organoids of cystic fibrosis patients. *Cell Stem Cell*, **13**, 653-658.
- Schwitzgebel, V.M., Scheel, D.W., Conners, J.R., Kalamaras, J., Lee, J.E., Anderson, D.J., Sussel, L., Johnson, J.D. and German, M.S.** (2000) Expression of neurogenin3 reveals an islet cell precursor population in the pancreas. *Development*, **127**, 3533-3542.
- Seymour, P.A.** (2014) Sox9: a master regulator of the pancreatic program. *Rev Diabet Stud*, **11**, 51-83.
- Seymour, P.A., Freude, K.K., Tran, M.N., Mayes, E.E., Jensen, J., Kist, R., Scherer, G. and Sander, M.** (2007) SOX9 is required for maintenance of the pancreatic progenitor cell pool. *Proc Natl Acad Sci U S A*, **104**, 1865-1870.
- Shaer, A., Azarpira, N., Vahdati, A., Karimi, M.H. and Shariati, M.** (2015) Differentiation of human-induced pluripotent stem cells into insulin-producing clusters. *Exp Clin Transplant*, **13**, 68-75.
- Sharp, P.A., Sugden, B. and Sambrook, J.** (1973) Detection of two restriction endonuclease activities in *Haemophilus parainfluenzae* using analytical agarose-ethidium bromide electrophoresis. *Biochemistry*, **12**, 3055-3063.
- Sharpe, C.R., Pluck, A. and Gurdon, J.B.** (1989) XIF3, a *Xenopus* peripherin gene, requires an inductive signal for enhanced expression in anterior neural tissue. *Development*, **107**, 701-714.
- Shen, M.M.** (2007) Nodal signaling: developmental roles and regulation. *Development*, **134**, 1023-1034.
- Sherwood, R.I., Maehr, R., Mazzoni, E.O. and Melton, D.A.** (2011) Wnt signaling specifies and patterns intestinal endoderm. *Mech Dev*, **128**, 387-400.
- Shi, D.L. and Boucaut, J.C.** (2000) *Xenopus* frizzled 4 is a maternal mRNA and its zygotic expression is localized to the neuroectoderm and trunk lateral plate mesoderm. *Mech Dev*, **94**, 243-245.
- Shih, H.P., Kopp, J.L., Sandhu, M., Dubois, C.L., Seymour, P.A., Grapin-Botton, A. and Sander, M.** (2012) A Notch-dependent molecular circuitry initiates pancreatic endocrine and ductal cell differentiation. *Development*, **139**, 2488-2499.

- Shih, H.P., Seymour, P.A., Patel, N.A., Xie, R., Wang, A., Liu, P.P., Yeo, G.W., Magnuson, M.A. and Sander, M. (2015) A Gene Regulatory Network Cooperatively Controlled by Pdx1 and Sox9 Governs Lineage Allocation of Foregut Progenitor Cells. *Cell Rep*, **13**, 326-336.
- Shih, H.P., Wang, A. and Sander, M. (2013) Pancreas organogenesis: from lineage determination to morphogenesis. *Annu Rev Cell Dev Biol*, **29**, 81-105.
- Shuldiner, A.R., Phillips, S., Roberts, C.T., Jr., LeRoith, D. and Roth, J. (1989) Xenopus laevis contains two nonallelic preproinsulin genes. cDNA cloning and evolutionary perspective. *J Biol Chem*, **264**, 9428-9432.
- Singer, G.a. (2006) Developmental Biology. *Sinauer Associates Inc.*, **8th edition**.
- Sive, H.L. and Cheng, P.F. (1991) Retinoic acid perturbs the expression of Xhox.lab genes and alters mesodermal determination in Xenopus laevis. *Genes Dev*, **5**, 1321-1332.
- Skirkanich, J., Luxardi, G., Yang, J., Kodjabachian, L. and Klein, P.S. (2011) An essential role for transcription before the MBT in Xenopus laevis. *Dev Biol*, **357**, 478-491.
- Slack, J.M. (1995) Developmental biology of the pancreas. *Development*, **121**, 1569-1580.
- Smith, W.C. and Harland, R.M. (1991) Injected Xwnt-8 RNA acts early in Xenopus embryos to promote formation of a vegetal dorsalizing center. *Cell*, **67**, 753-765.
- Smith, W.C., Knecht, A.K., Wu, M. and Harland, R.M. (1993) Secreted noggin protein mimics the Spemann organizer in dorsalizing Xenopus mesoderm. *Nature*, **361**, 547-549.
- Sogame, A., Hayata, T. and Asashima, M. (2003) Screening for novel pancreatic genes from in vitro-induced pancreas in Xenopus. *Dev Growth Differ*, **45**, 143-152.
- Solar, M., Cardalda, C., Houbracken, I., Martin, M., Maestro, M.A., De Medts, N., Xu, X., Grau, V., Heimberg, H., Bouwens, L. and Ferrer, J. (2009) Pancreatic exocrine duct cells give rise to insulin-producing beta cells during embryogenesis but not after birth. *Dev Cell*, **17**, 849-860.
- Soyer, J., Flasse, L., Raffelsberger, W., Beucher, A., Orvain, C., Peers, B., Ravassard, P., Vermot, J., Voz, M.L., Mellitzer, G. and Gradwohl, G. (2010) Rfx6 is an Ngn3-dependent winged helix transcription factor required for pancreatic islet cell development. *Development*, **137**, 203-212.
- Spagnoli, F.M. and Brivanlou, A.H. (2008) The Gata5 target, TGIF2, defines the pancreatic region by modulating BMP signals within the endoderm. *Development*, **135**, 451-461.
- Stafford, D., Hornbruch, A., Mueller, P.R. and Prince, V.E. (2004) A conserved role for retinoid signaling in vertebrate pancreas development. *Dev Genes Evol*, **214**, 432-441.
- Stafford, D. and Prince, V.E. (2002) Retinoic acid signaling is required for a critical early step in zebrafish pancreatic development. *Curr Biol*, **12**, 1215-1220.
- Stemmer, M., Thumberger, T., Del Sol Keyer, M., Wittbrodt, J. and Mateo, J.L. (2015) CCTop: An Intuitive, Flexible and Reliable CRISPR/Cas9 Target Prediction Tool. *PLoS One*, **10**, e0124633.
- Strate, I., Min, T.H., Iliev, D. and Pera, E.M. (2009) Retinol dehydrogenase 10 is a feedback regulator of retinoic acid signalling during axis formation and patterning of the central nervous system. *Development*, **136**, 461-472.
- Swain, R.K., Katoh, M., Medina, A. and Steinbeisser, H. (2005) Xenopus frizzled-4S, a splicing variant of Xfz4 is a context-dependent activator and inhibitor of Wnt/beta-catenin signaling. *Cell Commun Signal*, **3**, 12.
- Taira, M., Otani, H., Jamrich, M. and Dawid, I.B. (1994) Expression of the LIM class homeobox gene Xlim-1 in pronephros and CNS cell lineages of Xenopus embryos is affected by retinoic acid and exogastrulation. *Development*, **120**, 1525-1536.
- Takahashi, S., Yokota, C., Takano, K., Tanegashima, K., Onuma, Y., Goto, J. and Asashima, M. (2000) Two novel nodal-related genes initiate early inductive events in Xenopus Nieuwkoop center. *Development*, **127**, 5319-5329.
- Takasato, M., Er, P.X., Chiu, H.S., Maier, B., Baillie, G.J., Ferguson, C., Parton, R.G., Wolvetang, E.J., Roost, M.S., Chuva de Sousa Lopes, S.M. and Little, M.H. (2015) Kidney organoids from human iPS cells contain multiple lineages and model human nephrogenesis. *Nature*, **526**, 564-568.
- Tam, P.P. and Loebel, D.A. (2007) Gene function in mouse embryogenesis: get set for gastrulation. *Nat Rev Genet*, **8**, 368-381.
- Tamai, K., Yokota, C., Ariizumi, T. and Asashima, M. (1999) Cytochalasin B inhibits morphogenetic movement and muscle differentiation of activin-treated ectoderm in

- Xenopus. *Dev Growth Differ*, **41**, 41-49.
- Tashiro, K., Yamada, R., Asano, M., Hashimoto, M., Muramatsu, M. and Shiokawa, K.** (1991) Expression of mRNA for activin-binding protein (follistatin) during early embryonic development of *Xenopus laevis*. *Biochem Biophys Res Commun*, **174**, 1022-1027.
- Terns, R.M. and Terns, M.P.** (2014) CRISPR-based technologies: prokaryotic defense weapons repurposed. *Trends Genet*, **30**, 111-118.
- Thomas, H., Jaschowitz, K., Bulman, M., Frayling, T.M., Mitchell, S.M., Roosen, S., Lingott-Frieg, A., Tack, C.J., Ellard, S., Ryffel, G.U. and Hattersley, A.T.** (2001) A distant upstream promoter of the HNF-4alpha gene connects the transcription factors involved in maturity-onset diabetes of the young. *Hum Mol Genet*, **10**, 2089-2097.
- Tsai, M.J. and O'Malley, B.W.** (1994) Molecular mechanisms of action of steroid/thyroid receptor superfamily members. *Annual review of biochemistry*, **63**, 451-486.
- Turner, D.L. and Weintraub, H.** (1994) Expression of achaete-scute homolog 3 in *Xenopus* embryos converts ectodermal cells to a neural fate. *Genes Dev*, **8**, 1434-1447.
- Umbhauer, M., Djiane, A., Goisset, C., Penzo-Mendez, A., Riou, J.F., Boucaut, J.C. and Shi, D.L.** (2000) The C-terminal cytoplasmic Lys-thr-X-X-X-Trp motif in frizzled receptors mediates Wnt/beta-catenin signalling. *Embo j*, **19**, 4944-4954.
- van der Sanden, M.H., Meems, H., Houweling, M., Helms, J.B. and Vaandrager, A.B.** (2004) Induction of CCAAT/enhancer-binding protein (C/EBP)-homologous protein/growth arrest and DNA damage-inducible protein 153 expression during inhibition of phosphatidylcholine synthesis is mediated via activation of a C/EBP-activating transcription factor-responsive element. *J Biol Chem*, **279**, 52007-52015.
- Vignali, R., Poggi, L., Madeddu, F. and Barsacchi, G.** (2000) HNF1(beta) is required for mesoderm induction in the *Xenopus* embryo. *Development*, **127**, 1455-1465.
- Villasenor, A., Chong, D.C., Henkemeyer, M. and Cleaver, O.** (2010) Epithelial dynamics of pancreatic branching morphogenesis. *Development*, **137**, 4295-4305.
- Wang, F., Shi, Z., Cui, Y., Guo, X., Shi, Y.B. and Chen, Y.** (2015) Targeted gene disruption in *Xenopus laevis* using CRISPR/Cas9. *Cell Biosci*, **5**, 15.
- Wang, L., Coffinier, C., Thomas, M.K., Gresh, L., Eddu, G., Manor, T., Levitsky, L.L., Yaniv, M. and Rhoads, D.B.** (2004) Selective deletion of the Hnf1beta (MODY5) gene in beta-cells leads to altered gene expression and defective insulin release. *Endocrinology*, **145**, 3941-3949.
- Waters, C.A., Strande, N.T., Wyatt, D.W., Pryor, J.M. and Ramsden, D.A.** (2014) Nonhomologous end joining: a good solution for bad ends. *DNA Repair (Amst)*, **17**, 39-51.
- Watt, A.J., Zhao, R., Li, J. and Duncan, S.A.** (2007) Development of the mammalian liver and ventral pancreas is dependent on GATA4. *BMC Dev Biol*, **7**, 37.
- Wells, J.M. and Melton, D.A.** (2000) Early mouse endoderm is patterned by soluble factors from adjacent germ layers. *Development*, **127**, 1563-1572.
- Wheeler, G.N. and Hoppler, S.** (1999) Two novel *Xenopus* frizzled genes expressed in developing heart and brain. *Mech Dev*, **86**, 203-207.
- White, J.A., Guo, Y.D., Baetz, K., Beckett-Jones, B., Bonasoro, J., Hsu, K.E., Dilworth, F.J., Jones, G. and Petkovich, M.** (1996) Identification of the retinoic acid-inducible all-trans-retinoic acid 4-hydroxylase. *J Biol Chem*, **271**, 29922-29927.
- Wierup, N., Sundler, F. and Heller, R.S.** (2014) The islet ghrelin cell. *J Mol Endocrinol*, **52**, R35-49.
- Willyard, C.** (2015) The boom in mini stomachs, brains, breasts, kidneys and more. *Nature*, **523**, 520-522.
- Wong, H.C., Bourdelas, A., Krauss, A., Lee, H.J., Shao, Y., Wu, D., Mlodzik, M., Shi, D.L. and Zheng, J.** (2003) Direct binding of the PDZ domain of Dishevelled to a conserved internal sequence in the C-terminal region of Frizzled. *Mol Cell*, **12**, 1251-1260.
- Wright, C.V., Schnegelsberg, P. and De Robertis, E.M.** (1989) XIHbox 8: a novel *Xenopus* homeo protein restricted to a narrow band of endoderm. *Development*, **105**, 787-794.
- Xanthos, J.B., Kofron, M., Wylie, C. and Heasman, J.** (2001) Maternal VegT is the initiator of a molecular network specifying endoderm in *Xenopus laevis*. *Development*, **128**, 167-180.
- Xu, C.R., Cole, P.A., Meyers, D.J., Kormish, J., Dent, S. and Zaret, K.S.** (2011) Chromatin "prepattern" and histone modifiers in a fate choice for liver and pancreas. *Science*,

- 332, 963-966.
- Xu, Q., Wang, Y., Dabdoub, A., Smallwood, P.M., Williams, J., Woods, C., Kelley, M.W., Jiang, L., Tasman, W., Zhang, K. and Nathans, J. (2004) Vascular development in the retina and inner ear: control by Norrin and Frizzled-4, a high-affinity ligand-receptor pair. *Cell*, **116**, 883-895.
- Xuan, S., Borok, M.J., Decker, K.J., Battle, M.A., Duncan, S.A., Hale, M.A., Macdonald, R.J. and Sussel, L. (2012) Pancreas-specific deletion of mouse Gata4 and Gata6 causes pancreatic agenesis. *J Clin Invest*, **122**, 3516-3528.
- Yam, J.W., Chan, K.W., Ngan, E.S. and Hsiao, W.L. (2005) Genomic structure, alternative splicing and tissue expression of rFrp/sFRP-4, the rat frizzled related protein gene. *Gene*, **357**, 55-62.
- Yamagata, K., Furuta, H., Oda, N., Kaisaki, P.J., Menzel, S., Cox, N.J., Fajans, S.S., Signorini, S., Stoffel, M. and Bell, G.I. (1996) Mutations in the hepatocyte nuclear factor-4alpha gene in maturity-onset diabetes of the young (MODY1). *Nature*, **384**, 458-460.
- Yasuhara, R., Yuasa, T., Williams, J.A., Byers, S.W., Shah, S., Pacifici, M., Iwamoto, M. and Enomoto-Iwamoto, M. (2010) Wnt/beta-catenin and retinoic acid receptor signaling pathways interact to regulate chondrocyte function and matrix turnover. *J Biol Chem*, **285**, 317-327.
- Yasuo, H. and Lemaire, P. (1999) A two-step model for the fate determination of presumptive endodermal blastomeres in *Xenopus* embryos. *Curr Biol*, **9**, 869-879.
- Ye, X., Wang, Y. and Nathans, J. (2010) The Norrin/Frizzled4 signaling pathway in retinal vascular development and disease. *Trends Mol Med*, **16**, 417-425.
- Yoshitomi, H. and Zaret, K.S. (2004) Endothelial cell interactions initiate dorsal pancreas development by selectively inducing the transcription factor Ptf1a. *Development*, **131**, 807-817.
- Zaret, K.S. and Grompe, M. (2008) Generation and regeneration of cells of the liver and pancreas. *Science*, **322**, 1490-1494.
- Zeynali, B., Kalionis, B. and Dixon, K.E. (2000) Determination of anterior endoderm in *Xenopus* embryos. *Dev Dyn*, **218**, 531-536.
- Zhang, C., Basta, T., Fawcett, S.R. and Klymkowsky, M.W. (2005) SOX7 is an immediate-early target of VegT and regulates Nodal-related gene expression in *Xenopus*. *Dev Biol*, **278**, 526-541.
- Zhang, D., Jiang, W., Liu, M., Sui, X., Yin, X., Chen, S., Shi, Y. and Deng, H. (2009) Highly efficient differentiation of human ES cells and iPS cells into mature pancreatic insulin-producing cells. *Cell Res*, **19**, 429-438.
- Zhang, J., Houston, D.W., King, M.L., Payne, C., Wylie, C. and Heasman, J. (1998) The role of maternal VegT in establishing the primary germ layers in *Xenopus* embryos. *Cell*, **94**, 515-524.
- Zhang, J. and King, M.L. (1996) *Xenopus* VegT RNA is localized to the vegetal cortex during oogenesis and encodes a novel T-box transcription factor involved in mesodermal patterning. *Development*, **122**, 4119-4129.
- Zhang, K., Harada, Y., Wei, X., Shukla, D., Rajendran, A., Tawansy, K., Bedell, M., Lim, S., Shaw, P.X., He, X. and Yang, Z. (2011) An essential role of the cysteine-rich domain of FZD4 in Norrin/Wnt signaling and familial exudative vitreoretinopathy. *J Biol Chem*, **286**, 10210-10215.
- Zhang, T., Guo, X. and Chen, Y. (2013b) Retinoic acid-activated Ndr1a represses Wnt/beta-catenin signaling to allow *Xenopus* pancreas, oesophagus, stomach, and duodenum specification. *PLoS One*, **8**, e65058.
- Zhang, Y.Q., Cleary, M.M., Si, Y., Liu, G., Eto, Y., Kritzik, M., Dabernat, S., Kayali, A.G. and Sarvetnick, N. (2004) Inhibition of activin signaling induces pancreatic epithelial cell expansion and diminishes terminal differentiation of pancreatic beta-cells. *Diabetes*, **53**, 2024-2033.
- Zhang, Z., Rankin, S.A. and Zorn, A.M. (2013a) Different thresholds of Wnt-Frizzled 7 signaling coordinate proliferation, morphogenesis and fate of endoderm progenitor cells. *Dev Biol*, **378**, 1-12.
- Zhou, Q., Law, A.C., Rajagopal, J., Anderson, W.J., Gray, P.A. and Melton, D.A. (2007) A multipotent progenitor domain guides pancreatic organogenesis. *Dev Cell*, **13**, 103-114.
- Zimmerman, L.B., De Jesus-Escobar, J.M. and Harland, R.M. (1996) The Spemann organizer signal noggin binds and inactivates bone morphogenetic protein 4. *Cell*, **86**, 599-606.

- Zorn, A.M., Butler, K. and Gurdon, J.B.** (1999) Anterior endomesoderm specification in *Xenopus* by Wnt/beta-catenin and TGF-beta signalling pathways. *Dev Biol*, **209**, 282-297.
- Zorn, A.M. and Wells, J.M.** (2009) Vertebrate endoderm development and organ formation. *Annu Rev Cell Dev Biol*, **25**, 221-251.

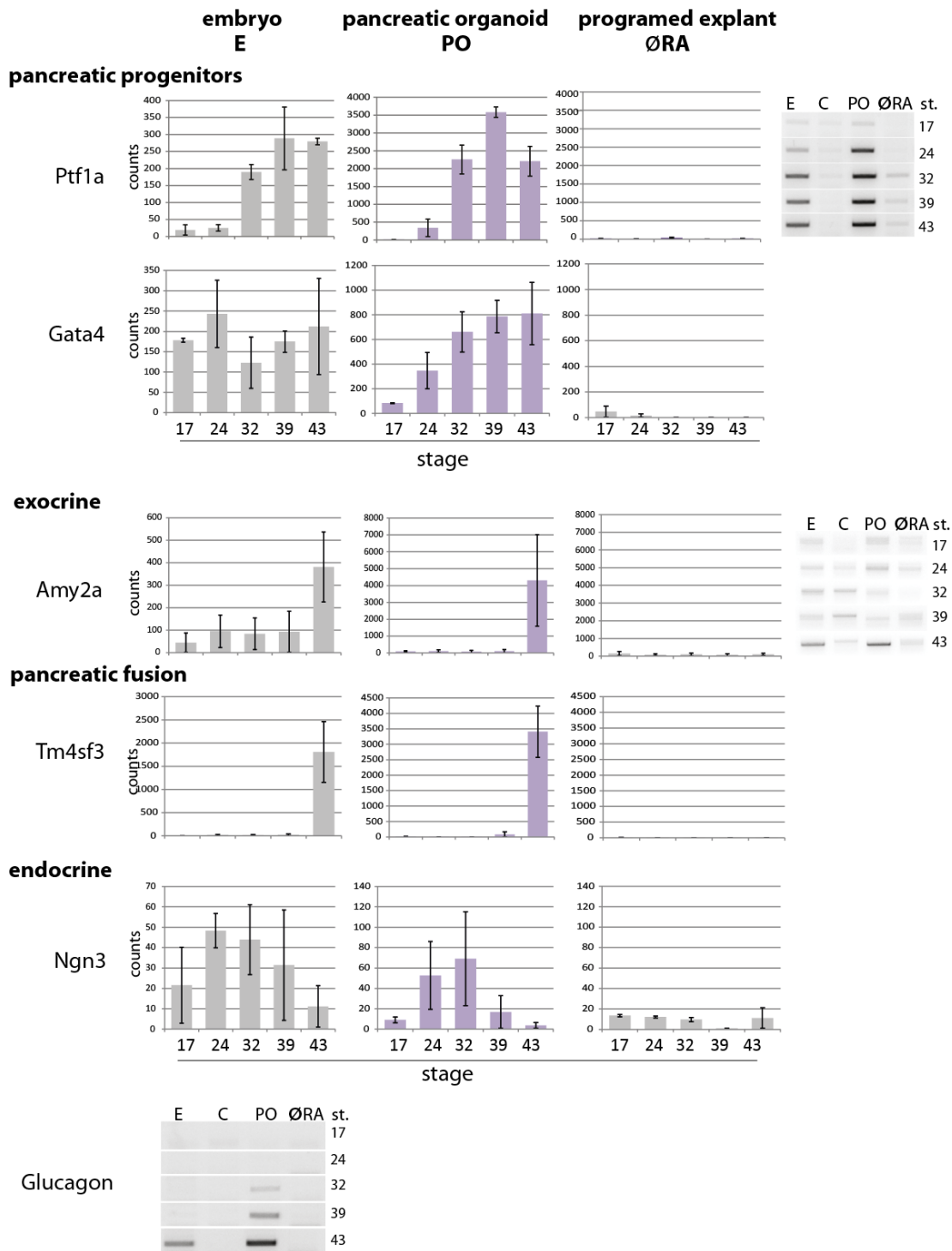


Fig. 6.2 Detection of marker genes for pancreatic structures

Nanostring analysis and RT-PCR results for whole embryos (embryo, E), Vegt/Noggin/RA-programed explants (pancreatic organoids, PO), Vegt/Noggin/Cyp26a1-programed explants (ØRA) and un-programed explants (C) are shown. Diagrams indicate the mean of normalized Nanostring counts from two independent experiments. Figures on the right and at the bottom show RT-PCR results for indicated marker genes.

6.2 Identification, verification and expression characteristics of early RA-responsive genes

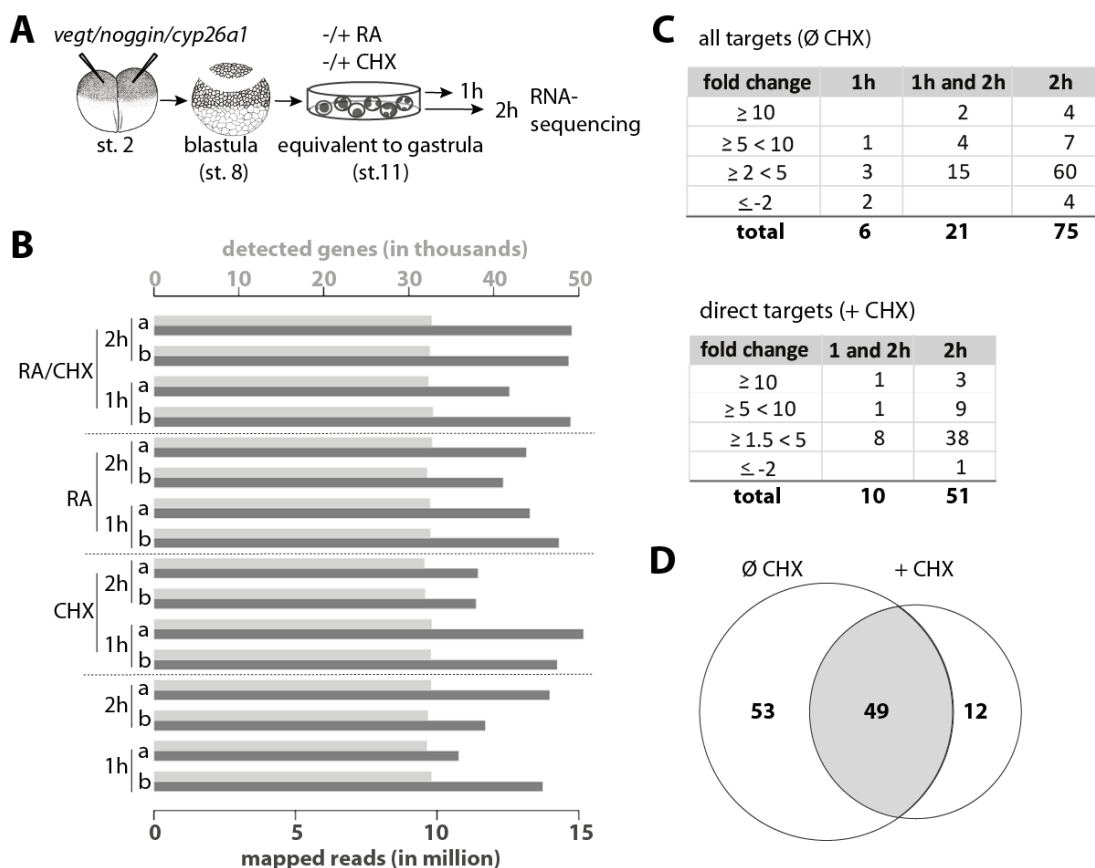
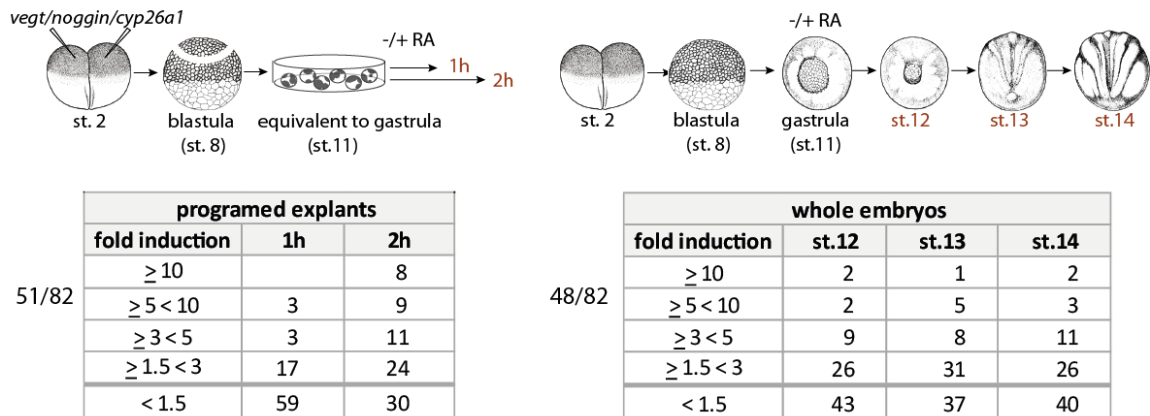


Fig. 6.3 Detection of early direct and indirect RA-target genes by RNA-sequencing

(A) *Vegt* (500pg), *noggin* (500pg) and *cyp26a1* (2000pg) RNAs were co-injected into the animal pole of a two-cell stage embryo. Blastocoel roof tissue was explanted at blastula stage. Explants were treated with 5µM RA and cycloheximide (CHX) at the equivalent of gastrula stage. One and two hours after RA addition, total RNA was isolated and analyzed by RNA-sequencing. (B) Number of detected genes and mapped reads for each sample (a and b indicate two independent experiments) are shown. (C) Fold changes are shown for differentially expressed genes in RA-treated versus untreated pancreatic organoids. Tables are shown indicating all targets (absence of CHX) and putative direct targets (presence of CHX). (D) Comparison of differentially expressed genes in the presence versus absence of CHX. The overlap indicates the number of putative direct RA-targets.

A RA-inducibility



B RA-dependency

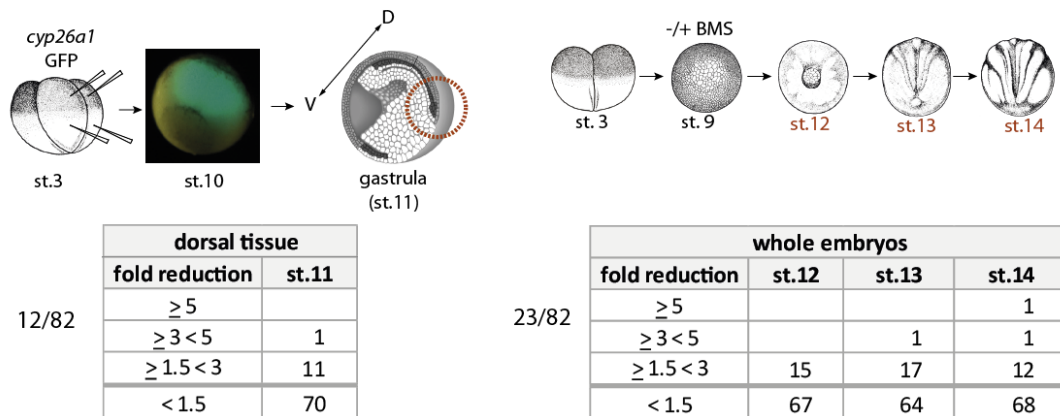


Fig. 6.4 Confirmation of RA-responsiveness

(A) RA-inducibility was analyzed using two different experimental approaches. Ectodermal explants from *vegt/nog/cyp26a1*-injected embryos or whole embryos were treated with RA for one hour or left untreated. Candidate gene expression was analyzed by the use of quantitative Nanostring analysis for the time points indicated in red.

(B) RA-dependency was determined by the use of two different concepts. Embryos were injected with RNAs encoding Cyp26a1 (2000 pg) and GFP (200 pg) into the two dorsal blastomeres of a four-cell stage embryo. At stage 10, dorsal GFP-positive embryos were selected. At stage 11 the tissue surrounding the dorsal blastopore lip (red dotted line = dorsal part) was resected and again verified for a GFP signal. In total, 10 dorsal tissues from injected and un-injected embryos were analyzed. Additionally, embryos were treated with the RA-antagonist BMS453 at stage 9. Five embryos of stages 12 to 14 were analyzed. Numbers in front of the tables indicate confirmed candidates. The tables show number of genes and their level of induction or reduction for the individual approaches analyzed by Nanostring.

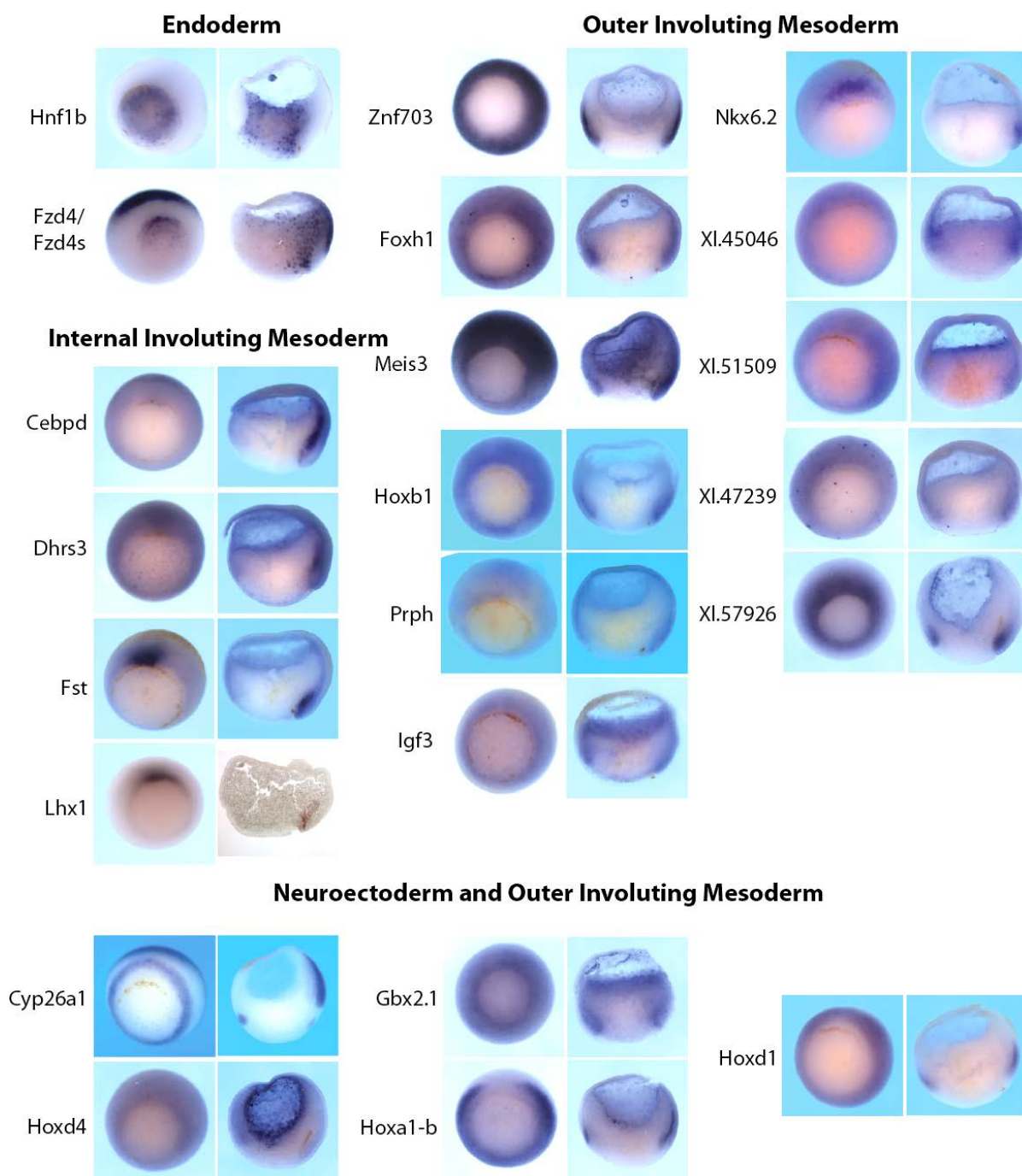


Fig. 6.5 Expression of RA-responsive genes at gastrula stage by WMISH

Expression pattern of the 22 confirmed RA-responsive genes at gastrula stage 11 by WMISH. On the left side, whole embryos (dorsal side up) and on right side bisected embryos (dorsal side right) are shown. Candidates were grouped according to their expression domains in four groups. Hnf1b and Fzd4 exhibit an endodermal expression. Cebpd, Dhrs3, Fst and Lhx1 are expressed in the dorsal internal involuting mesoderm. Znf703, Foxh1, Meis3, Hoxb1, Prph, Igf3, Nkx6.2, XI.45046, XI.51509, XI.47239 and XI.57926 are expressed in the outer involuting mesoderm. Cyp26a1, Hoxd4, Gbx2.1, Hoxa1-b and Hoxd1 are expressed in both, prospective neuro-ectoderm and outer involuting mesoderm.

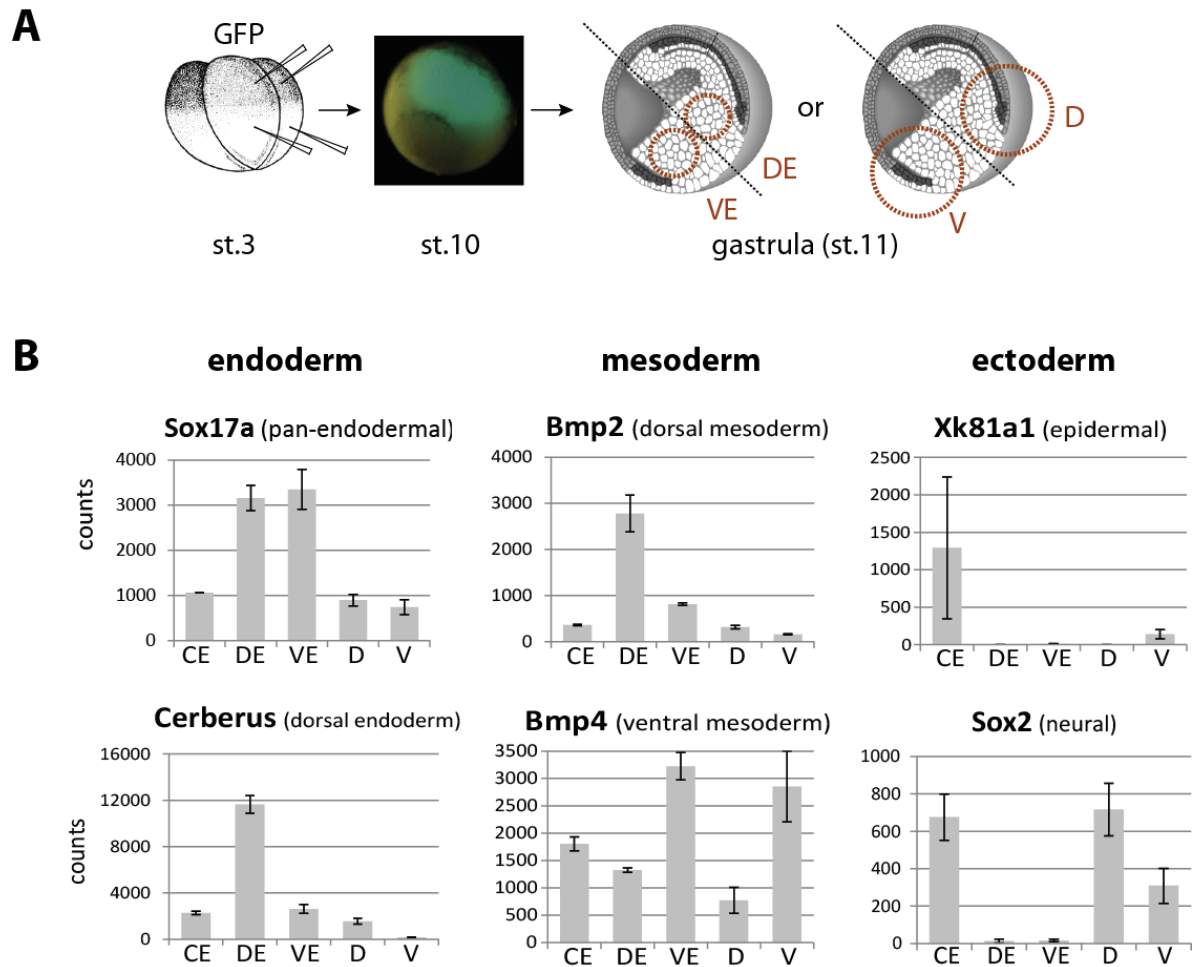


Fig. 6.6 Expression characteristics of endodermal, mesodermal and ectodermal markers at gastrula stage by Nanostring analysis

(A) Four-cell stage embryos were injected with RNA coding for GFP into the two dorsal blastomeres. At stage 10, embryos with a GFP signal at the dorsal site were selected for further cultivation. At stage 11, either dorsal and ventral endoderm was isolated or the whole tissue surrounding the dorsal blastoporus lip and the corresponding ventral tissue were isolated. (B) Graphs show Nanostring counts for endodermal, mesodermal and ectodermal marker genes for the different preparations of two independent experiments. CE = control embryo, DE = dorsal endoderm, VE = ventral endoderm, D = dorsal part, V = ventral part

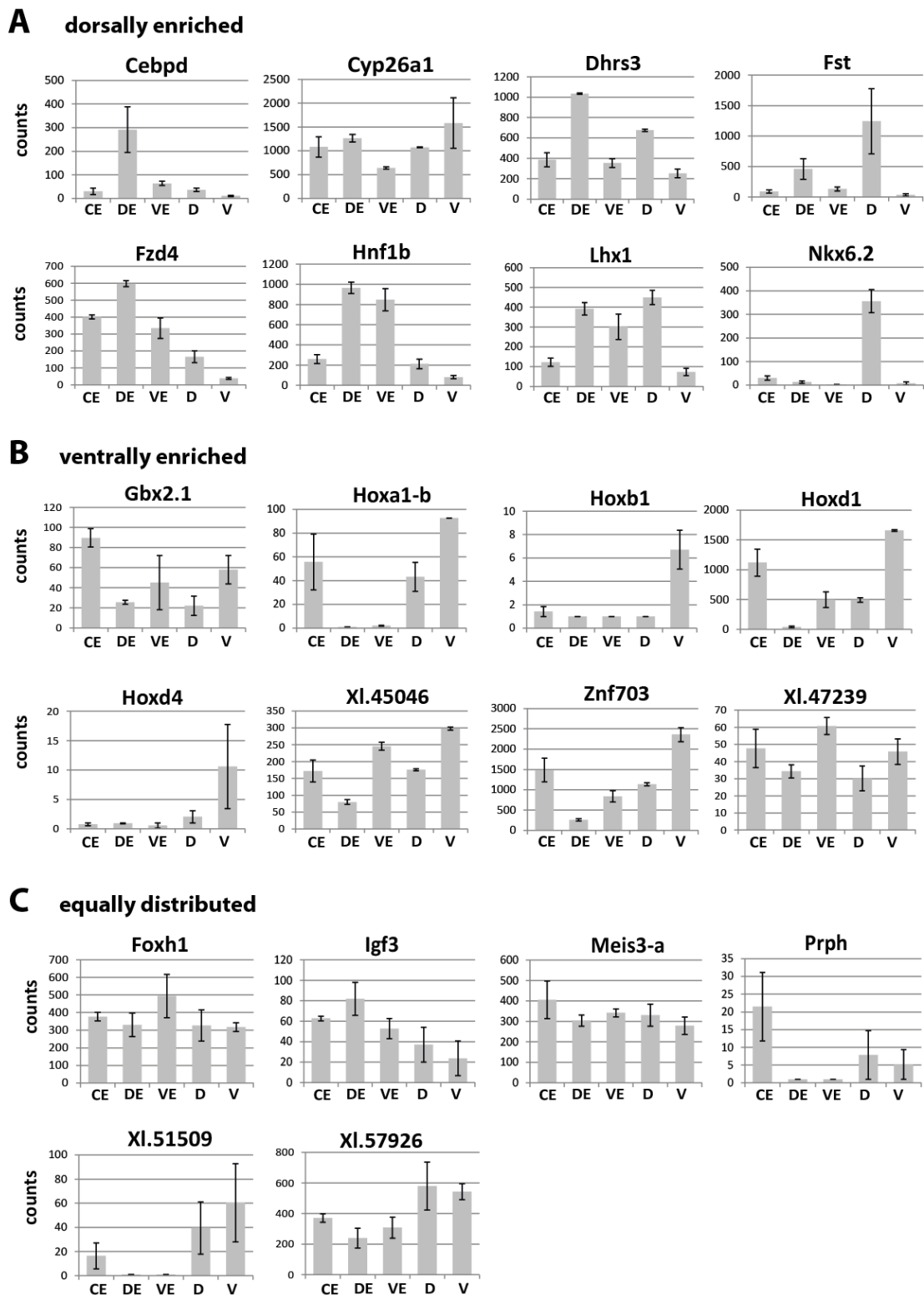
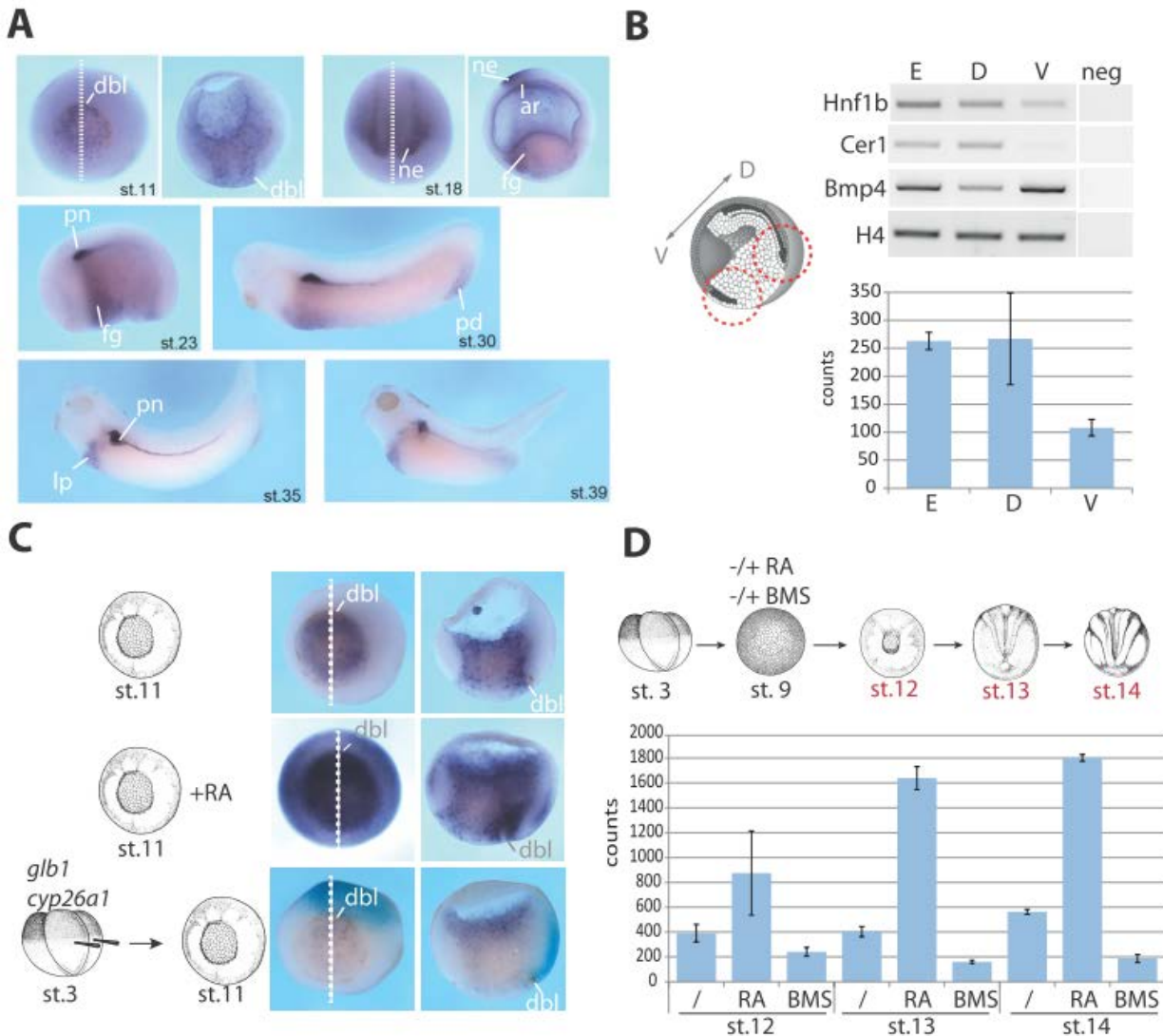


Fig. 6.7 Expression characteristics of RA-responsive genes at gastrula stage by Nanostring analysis

Samples were prepared like described in **Fig. 6.6**. The 22 RA-responsive genes were grouped according to a dorsal (**A**) or ventral enrichment (**B**) in the different preparations or for their equal distribution (**C**). Graphs indicate Nanostring counts for two independent experiments. Error bars indicate the SEM. DE=dorsal endoderm; VE= ventral endoderm; D=dorsal blastopore; V= ventral blastopore

6.3 Expression and functional analysis of the RA-target Hnf1b



6.4 Expression and functional analysis of RA-target Fzd4/Fzd4s

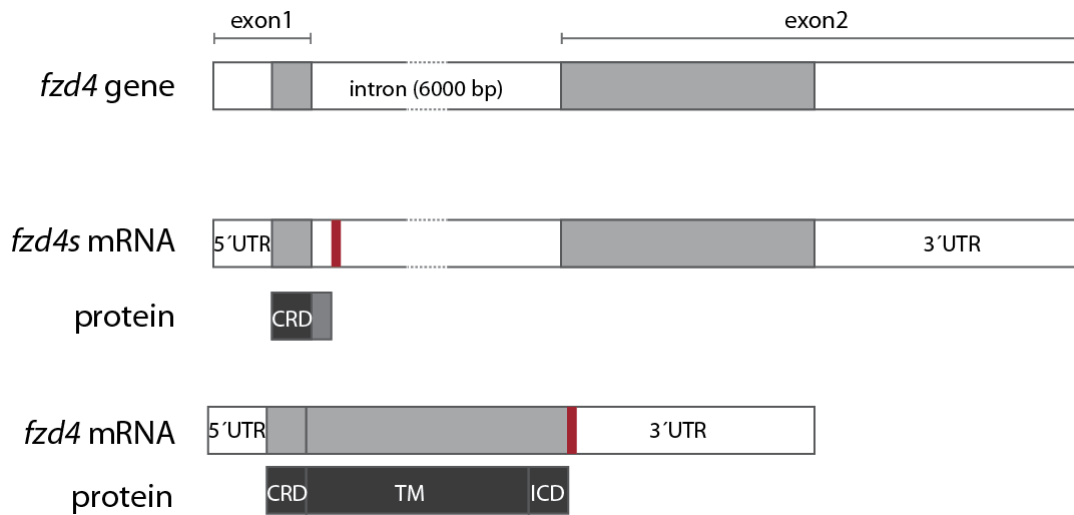


Fig. 6.10 Fzd4 has an alternative splice variant Fzd4s

The Fzd4 gene consists of two exons and one large intronic region. Conventional splicing results in the loss of the intron and a protein is generated containing a small extracellular cysteine-rich domain (CRD), a seven transmembrane domain (TM) and an intracellular domain (ICD) (Shi and Boucaut, 2000). Through alternative splicing, the intron sequence is retained. Thereby, a premature stop codon in the intron is used resulting in a shortened open reading frame. The alternative splice variant Fzd4s gives rise to a secreted protein containing the Wnt-ligand binding cysteine-rich domain (Swain et al., 2005).

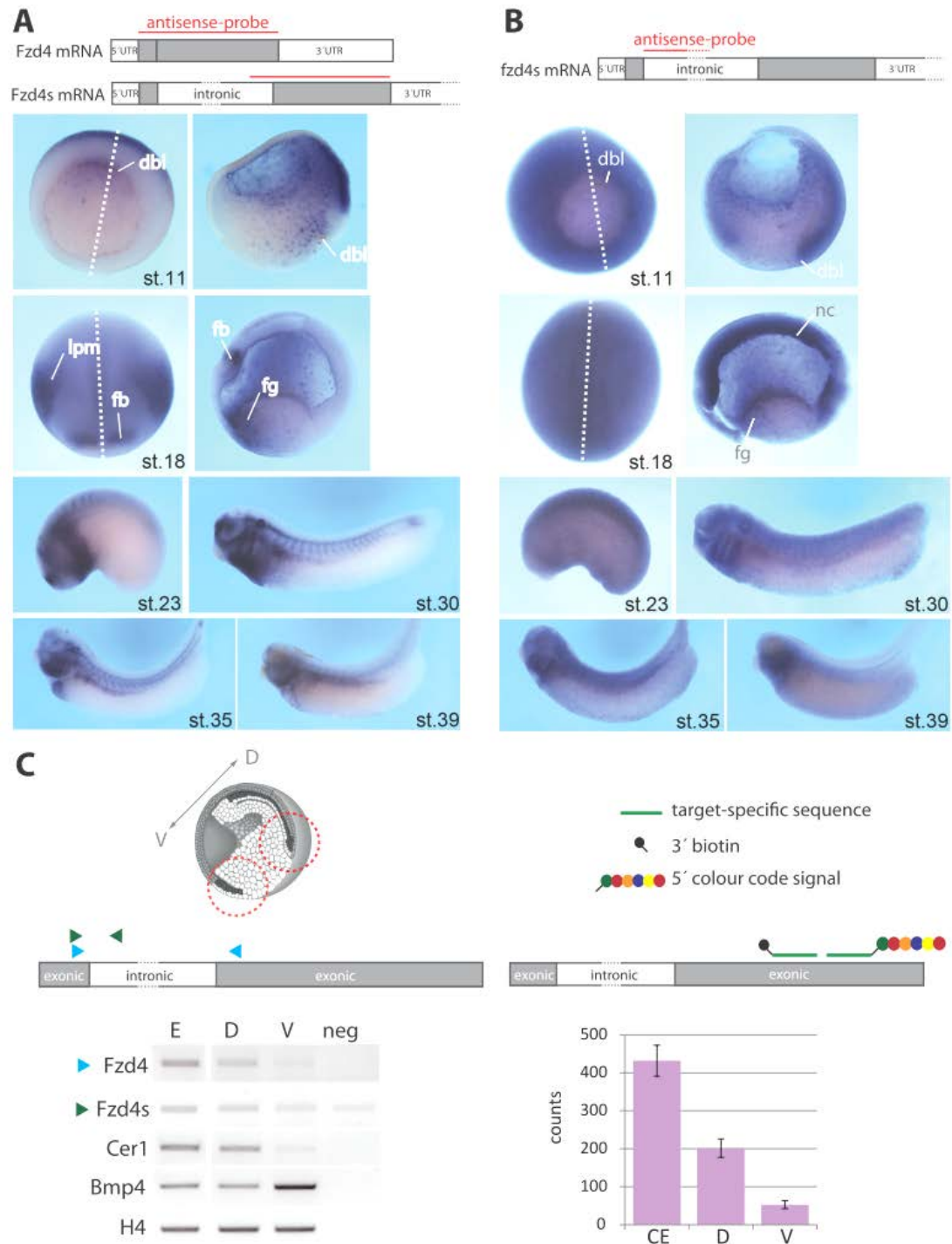
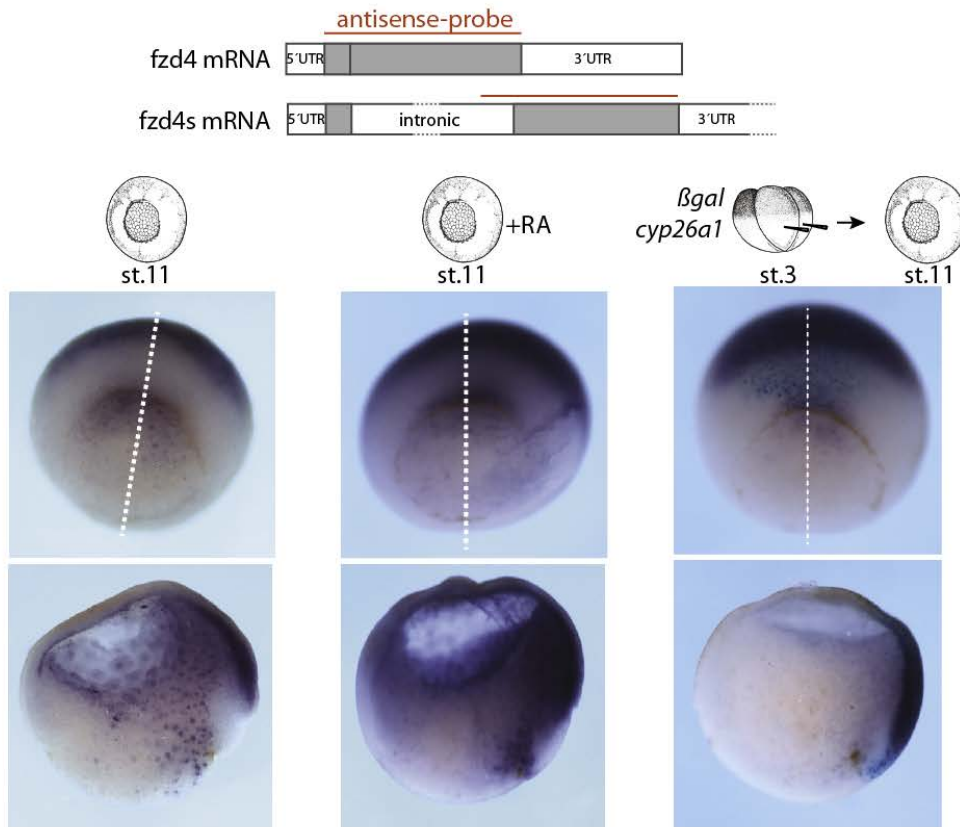


Fig. 6.11 Fzd4/Fzd4s expression analysis

(A) WMISH using an antisense probe that targets transcripts of both splice variants, Fzd4 and Fzd4s. (B) WMISH with an antisense probe that specifically targets the alternative splice variant Fzd4s. Embryos at indicated developmental stages were used. (C) Gastrula stage embryos were used for preparations of the tissue surrounding the dorsal blastopore lip and the corresponding ventral part. RT-PCR for Fzd4 and Fzd4s using the indicated oligonucleotides is shown. Cerberus (Cer1) was used as dorsal anterior marker and *bmp4* as ventral marker. Nanostring analysis was done to quantify the dorsal enrichment of Fzd4/Fzd4s.

E = whole embryo, D = dorsal tissue, V = ventral tissue, dorsal blastopore lip = dbi, lateral plate mesoderm = lpm, forebrain = fb, foregut = fg, notochord = nc

A



B

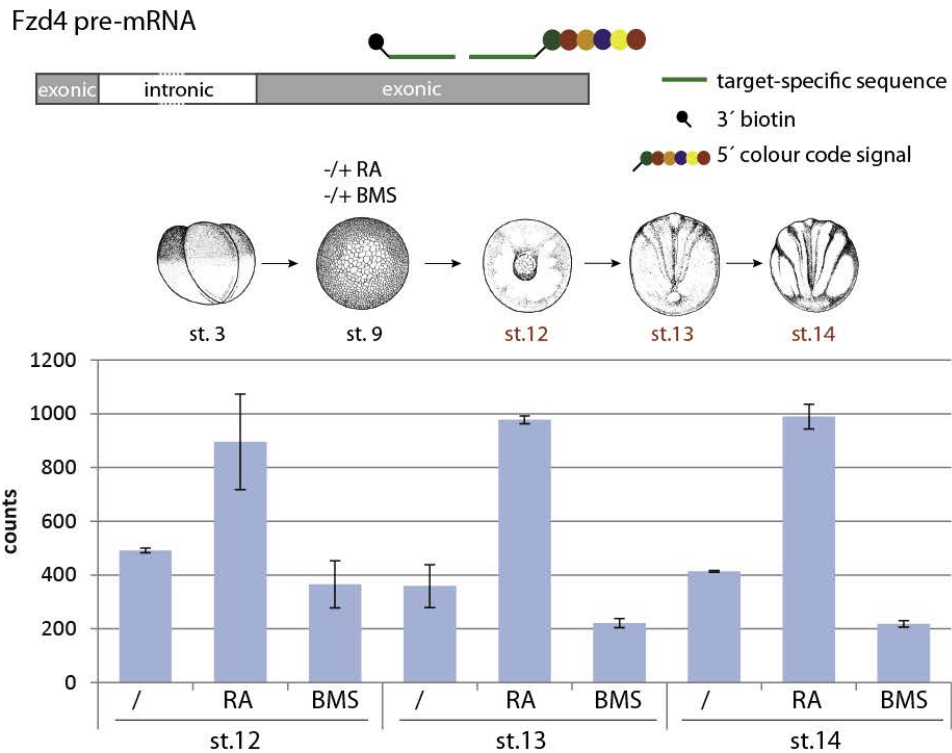


Fig. 6.12 RA-responsive expression of Fzd4/Fzd4s

(A) WMISH against Fzd4/Fzd4s during gastrulation in untreated, RA-treated and *cyp26a1*-injected embryos. Upper images show whole embryos (dorsal side up) and lower images show bisected embryos (dorsal side right). (B) Nanostring analysis of untreated, RA- and BMS-treated embryos. Indicated is the number of counts for Fzd4/Fzd4s transcripts in embryos at stages 12, 13 and 14.

A Cas9

WT	AGCGGCGCTG	CGACCCCATC	AGGATCACCA	TGTGCCAGAA	CCTCGGCTAC	AATGTCACCA
1	AGCGGCGCTG	CGACCCCATC	AGGATCACCA	TGTGCCAGAA	CCTCGGCTAC	AATGTCACCA
2	AGCGGCGCTG	CGACCCCATC	AGGATCACCA	TGTGCCAGAA	CCTCGGCTAC	AATGTCACCA
3	AGCGGCGCTG	CGACCCCATC	AGGATCACCA	TGTGCCAGAA	CCTCGGCTAC	AATGTCACCA
4	AGCGGCGCTG	CGACCCCATC	AGGATCACCA	TGTGCCAGAA	CCTCGGCTAC	AATGTCACCA
5	AGCGGCGCTG	CGACCCCATC	AGGATCACCA	TGTGCCAGAA	CCTCGGCTAC	AATGTCACCA
6	AGCGGCGCTG	CGACCCCATC	AGGATCACCA	TGTGCCAGAA	CCTCGGCTAC	AATGTCACCA
7	AGCGGCGCTG	CGACCCCATC	AGGATCACCA	TGTGCCAGAA	CCTCGGCTAC	AATGTCACCA
8	AGCGGCGCTG	CGACCCCATC	AGGATCACCA	TGTGCCAGAA	CCTCGGCTAC	AATGTCACCA
9	AGCGGCGCTG	CGACCCCATC	AGGATCACCA	TGTGCCAGAA	CCTCGGCTAC	AATGTCACCA
10	AGCGGCGCTG	CGACCCCATC	AGGATCACCA	TGTGCCAGAA	CCTCGGCTAC	AATGTCACCA
11	AGCGGCGCTG	CGACCCCATC	AGGATCACCA	TGTGCCAGAA	CCTCGGCTAC	AATGTCACCA

Cas9 + Fzd4-gRNA

WT	AGCGGCGCTG	CGACCCCATC	AGGATCACCA	TGTGCCAGAA	CCTCGGCTAC	AATGTCACCA	0
1	AGCGGCGCTG	CGACCCCA	-GGATCACCA	TGTGCCAGAA	CCTCGGCTAC	AATGTCACCA	-3
2	AGCGGCGCTG	CGACCCCA	-GGATCACCA	TGTGCCAGAA	CCTCGGCTAC	AATGTCACCA	-3
3	AGCGGCGCTG	CGACCCCAT	-GGATCACCA	TGTGCCAGAA	CCTCGGCTAC	AATGTCACCA	-2
4	AGNGGCGCTG	NGNCCCCA	TGTGCCAGAA	CCTCGGCTAC	AATGTCACCA	-12
5	AGCGGCGCTG	CGACCCCA	TGTGCCAGAA	CCTCGGCTAC	AATGTCACCA	-12
6	AGCGGCGCTG	CGACCCCGAA	CCTCGGCTAC	AATGTCACCA	-20
7	AGCGGCGCTG	CGACCCC	-ATGTCACCA	-34
8	AGCGGCGCTG	CGACCCCAN	-140
9	AGCGGCGCTG	CGASCCC	-140
10	AGCGGCGCTG	CGACYCM	-142
11	AGCGGCGCTG	CGACMCN	-140
12	AGCGGCGCTG	CGACCCC	-140

B Cas9

WT	ACCACACAGC	ACTTGTACAA	TGCTCAGTCT	GATCCTGATG	GGGAGCTAGG	GCTGGGCAAC
1	ACCACACAGC	ACTTGTACAA	TGCTCAGTCT	GATCCTGATG	GGGAGCTAGG	GCTGGGCAAC
2	ACCACACAGC	ACTTGTACAA	TGCTCAGTCT	GATCCTGATG	GGGAGCTAGG	GCTGGGCAAC
3	ACCACACAGC	ACTTGTACAA	TGCTCAGTCT	GATCCTGATG	GGGAGCTAGG	GCTGGGCAAC
4	ACCACACAGC	ACTTGTACAA	TGCTCAGTCT	GATCCTGATG	GGGAGCTAGG	GCTGGGCAAC
5	ACCACACAGC	ACTTGTACAA	TGCTCAGTCT	GATCCTGATG	GGGAGCTAGG	GCTGGGCAAC
6	ACCACACAGC	ACTTGTACAA	TGCTCAGTCT	GATCCTGATG	GGGAGCTAGG	GCTGGGCAAC
7	ACCACACAGC	ACTTGTACAA	TGCTCAGTCT	GATCCTGATG	GGGAGCTAGG	GCTGGGCAAC
8	ACCACACAGC	ACTTGTACAA	TGCTCAGTCT	GATCCTGATG	GGGAGCTAGG	GCTGGGCAAC
9	ACCACACAGC	ACTTGTACAA	TGCTCAGTCT	GATCCTGATG	GGGAGCTAGG	GCTGGGCAAC

Cas9 + Fzd4-gRNA

WT	ACCACACAGC	ACTTGTACAA	TGCTCAGTCT	GATCCTGATG	GGGAGCTAGG	GCTGGGCAAC	0
1	ACCACACAGC	ACTTGTACAA	TGCTCAGTCT	GATCCTGATG	GGGAGCTAGG	GCTGGGCAAC	0
2	ACCACACAGC	ACTTGTACAA	TGCTCAGTCT	GATCCTGATG	GGGAGCTAGG	GCTGGGCAAC	0
3	ACCACACAGC	ACTTGTACAA	TGCTCAGTCT	GATCCTGATG	GGGAGCTAGG	GCTGGGCAAC	0
4	ACCACACAGC	ACTTGTACAA	TGCTCAGTCT	GATCCTGATG	GGGAGCTAGG	GCTGGGCAAC	0
5	ACCACACAGC	ACTTGTACAA	TGCTCAGTCT	GATCCTGATG	GGGAGCTAGG	GCTGGGCAAC	0
6	ACCACACAGC	ACTTGTACAA	TGCTCAGTCT	GATCCTGATG	GGGAGCTAGG	GCTGGGCAAC	0
7	ACCACACAGC	ACTTGTACAA	TGCTCAGTCT	GATCCTGATG	GGGAGCTAGG	GCTGGGCAAC	0
8	ACCACACAGC	ACTTGTACAA	TGCTCAGTCT	GATCCTGATG	GGGAGCTAGG	GCTGGGCAAC	0
9	ACCACACAGC	ACTTGTACAA	TGCTCAGTCT	GATCCTGATG	GGGAGCTAGG	GCTGGGCAAC	0
10	ACCACACAGC	ACTTGTACAA	TGCTCAGTCT	GATCCTGATG	GGGAGCTAGG	GCTGGGCAAC	0

Fig. 6.13 Mutation analysis of CRISPR/Cas-treated pancreatic organoids by DNA sequencing

The Fzd4-gRNA target sequence is yellow highlighted and number of deleted nucleotides is indicated.

(A) Cloned Fzd4 amplicons from Cas9 only or Cas9 with Fzd4-gRNA treated pancreatic organoids aligned to genomic Fzd4 *X.leavis* sequence. (B) Cloned Kremen2 amplicons from treated pancreatic organoids aligned to genomic Kremen2 *X.leavis* sequence.

6.5 Nanostring analysis data for *in vitro* generation of pancreatic organoids

Tab. 6.1 Normalized data of two independent experiments

(Indicated are the Nanostring counts from two independent experiments (A and B) which were normalized to the internal positive controls and Odc and with subtracted mean of the negative controls as described in the “Materials and Methods” section).

CE = control embryo; ctr = control explants; VNRA = Vegt/Noggin/RA-programed explants (pancreatic organoids); VNC = Vegt/Noggin/cyp26a1-programed explants

experiment	A																				B																				
	17				24				32				39				43				17				24				32				39				43				
	gene	CE	ctr	VNRA	VNC	CE	ctr	VNRA	VNC	CE	ctr	VNRA	VNC	CE	ctr	VNRA	VNC	CE	ctr	VNRA	VNC	CE	ctr	VNRA	VNC	CE	ctr	VNRA	VNC	CE	ctr	VNRA	VNC	CE	ctr	VNRA	VNC	CE	ctr	VNRA	VNC
<i>actb</i>	73963	230942	89328	92082	148889	618976	220253	150714	197130	1001126	202572	149700	196927	675288	125569	146916	256624	665176	188525	213177	82253	233126	85318	112599	157732	768182	148369	115666	178143	1114331	178001	135310	273991	660584	168013	113843	196069	633118	134282	154958	
<i>aldh1a2</i>	2272	7	281	335	905	1	62	97	603	14	548	120	768	25	217	126	3016	147	1221	1221	1904	18	258	1987	632	24	64	164	360	65	359	97	1196	54	1222	405	1190	115	835	1027	
<i>amy2a/b</i>	2	14	60	20	23	96	24	21	14	116	4	12	2	50	1	1	225	124	7008	96	88	292	135	260	168	897	198	190	154	1185	155	172	184	568	210	137	536	616	1592	162	
<i>chrd</i>	2843	1	13794	17524	1268	1	1995	2915	218	1	730	1466	96	1	306	564	4134	48	4858	27903	1234	42	1263	2050	303	64	525	549	226	70	192	163	47	40	23	133					
<i>crabp1</i>	1	1	1	1	60	1	8	1	139	1	2	1	236	1	1	14	930	30	1	1	32	6	1	2	5	11	20	1	19	26	12	2	320	23	317	1	430	43	25	4	
<i>crabp1</i>	4177	34	7193	14059	3355	183	2896	7820	2487	160	2406	3907	2506	95	2771	3622	1767	184	2703	4580	7020	38	2937	11951	3192	73	3040	7582	1821	113	3570	4871	2023	35	3356	6808	1136	430	1373	5548	
<i>cyp26a1</i>	1061	169	1806	928	983	372	544	980	1150	470	597	529	1026	78	256	250	873	265	76	157	908	149	4271	338	721	249	1121	505	761	204	1182	679	573	36	157	89	515	37	41	44	
<i>darmin</i>	4232	1	2398	1	22848	1	7406	176	33275	1	10557	259	29375	1	13914	132	518	1012	863	289	5339	1	9666	1	18550	1	26918	741	31328	2	18482	3235	13760	1	2186	398	1294	1	71	316	
<i>dkk1</i>	323	4	151	103	452	258	1115	163	418	538	1558	131	329	342	1699	163	8914	17873	29995	20473	310	61	259	135	298	373	1143	188	239	296	1278	250	362	440	1135	271	323	1747	725	609	
<i>foxe1</i>	1	13	0	1	67	1	1	54	75	1	1	233	90	1	1	296	437	2124	314	798	1	38	1	1	10	13	1	1	22	4	1	31	240	138	4	529	293	2233	39	888	
<i>foxe3/4</i>	9	1	1	1	63	1	1	213	28	1	1	22	25	1	1	5	15	1	1	181	9	13	1	1	122	4	1	1	125	15	1	17	46	20	7	1	1	1	1		
<i>gppd</i>	213	317	153	167	389	405	328	223	601	809	354	297	657	716	351	347	1826	3183	1592	1276	320	403	228	442	421	410	354	273	469	798	417	318	1077	1170	679	391	1276	3294	797	678	
<i>gapdh</i>	484	115	7400	3519	3287	378	11606	7115	8211	6139	25463	15990	8914	17873	29995	20473	13120	55968	26476	26065	486	224	4457	2706	1849	649	17404	9814	3622	3672	28323	19604	12545	26639	50004	32283	7120	26706	22295	18203	
<i>gata2</i>	1997	12664	444	1191	1003	2566	268	155	229	1588	126	131	168	616	64	126	165	64	32	87	1338	11828	67	1240	514	5133	145	56	187	1505	189	91	327	354	177	45	137	204	98	60	
<i>gata4-a/b</i>	183	1	80	4	326	33	200	1	186	35	498	1	149	1	654	1	330	0	1063	1	173	1	87	89	160	14	494	29	59	18	825	1	201	10	918	1	94	1	556	1	
<i>hes1-a</i>	1531	611	787	1069	2062	766	495	552	1025	1238	578	676	921	788	721	643	842	683	887	1036	922	901	446	954	918	1150	778	671	464	1811	1215	714	726	892	1617	714	515	519	1195	799	
<i>hhex</i>	49	507	0	41	281	84	24	87	141	1	95	1	108	1	58	1	181	1	65	31	33	343	1	1	90	131	90	13	8	174	218	27	104	91	135	1	16	60	134	9	
<i>hoxa1-b</i>	489	2517	1029	130	502	2509	608	224	134	379	469	232	105	288	207	205	62	1478	217	257	934	1781	1031	153	514	1705	920	243	247	604	791	500	138	396	410	193	19	1140	179	154	
<i>ins-a</i>	1	1	1	1	3	1	1986	1	80	1	13790	1	114	1	27894	1	444	1	39295	1	1	3	1	1	1	1	3	1786	1	22	6	15128	5	361	1	44745	1	1345	1	20108	1
<i>ins-b</i>	1	1	1	1	1	1	1226	1	44	1	10840	1	97	1	22683	1	420	1	29168	1	1	23	1	8	10	21	831	1	59	38	10045	8	274	17	36162	1	1417	35	15327	1	
<i>isl-1</i>	152	660	80	164	268	631	97	300	266	481	126	237	178	211	48	141	269	251	73	146	126	398	20	163	176	786	54	103	97	840	94	179	304	424	120	116	201	410	65	110	
<i>neurog3</i>	3	25	12	15	40	87	20	13	27	82	23	12	2	4	44	1	21	80	7	21	40	45	6	12	57	1	86	11	61	46	115	8	58	1	33	1	1	1	1	1	
<i>nkx2-1</i>	188	1	27	54	238	1	23	32	328	1	1	50	242	1	1	260	248	13	1	20	243	1	1	51	256	1	1	1	284	2	1	7	539	1	19	1	336	1	1	1	
<i>nkx2-2</i>	57	1	26	8	105	1	164	1	104	1	3	13	72	1	1	97	93	1	22	39	74	3	23	1	119	1	44	1	99	3	26	32	124	7	33	1	68	1	1	27	
<i>nkx6-1</i>	31	20	95	57	100	90	47	37	105	179	69	100	73	107	1	138	173	121	41	112	50	30	18	109	56	184	21	18	68	258	64	50	206	121	81	61	99	100	30	82	
<i>nog</i>	336	124	17428	19057	847	544	14286	18473	729	461	12818	10726	632	49	13341	10565	1065	104	7962	7707	2834	661	18990	20059	3461	5413	9138	6861	2865	3558	8739	8636	5200	773	8824	12187	3998	1325	4149	9596	
<i>odc1</i>	27375	27368	27383	27380	27377	27369	27372	27369	27369	27342	27359	27373	27364	27347	27328	27348	27370	27376	27360	27374	27368	27385	27368	27375	27353	27385	27369	27370	27338	27387	27363	27382	27363	27382	27371	27344	27313	27366	27372	27358	
<i>onecut</i>	213	4	254	73	405	1	117	69	339	1	388	423	354	1	7	539	277	1	58	144	290	78	1	2	472	14	174	31	518	19	236	157	439	8	443	192	222	9	118	164	
<i>pax6-b</i>	733	1	651	264	952	1	241	132	866	1	474	727	702	1	279	375	740	3	233	281	934	39	802	196	616	1	266	143	894	13	607	138	1337	14	516	93	744	22	110	72	
<i>pdia</i>	1	1	4	1	1	1	1	1	1	1	119	1	1	1	1934	1	1485	50	29570	1	128	387	130	283	333	1298	271	194	301	2018	427	253	541	1506	6101	239	2779	1464	14034	258	
<i>pdx1</i>	1	1	2	1	1	1	208	1	88	1	2156	1	138	1	2789	1	168	7	1336	1	1	1	1	1	1	1	1	1202	1	43	16	2943	9	96	1	1872	1	58	1	585	1
<i>ptf1a-a/b</i>	4	32	16	7	35	87	94	11	188	177	1856	57	196	90	3730	1	289	168	2628	21	34	33	12	22	16	47	585	1	212	77	2658	16	381	31	3432	1	270	51	1791	1	
<i>stfpc</i>	1	51	72	34	33	192	22	13	21	171	23	18	23	129	1	1	5789	198	46	66	6	1	21	1	1	1	51	1	1	1	30	1	1	176	46	7	1	6734	55	1	1
<i>sox1</i>	105	1	45	39	274	1	69	44	233	1	53	284	138	1	1	347	130	17	1	94	62	79	1	30	80	237	26	10	94	387	56	36	133	191	57	12	82	163	31	28	
<i>sox17a-a</i>	866	1	353	282	831	1	15	174	169	1	117	47	88	1	138	58	148	1	204	83	566	1	372	1569	227	15	40	108	6	10	90	52	70	1	178	15	1	0	136	9	
<i>sox17b</i>	437	1	26	27	170	1	1	1	5	1	1	1	1	1	1	1	1	1	1	1	312	1	15	2162	60																

Appendix

Tab. 6.2 Calculated mean and standard error of mean (SEM)

(Mean and SEM were calculated from the normalized Nanostring counts of two independent experiments)

CE = control embryo; ctr = control explants; VNRA = Vegt/Noggin/RA-programed explants (pancreatic organoids); VNC = Vegt/Noggin/cyp26a1-programed explants

		mean																				SEM																						
stage	17				24				32				39				43				stage	17				24				32				39				43						
gene	CE	ctr	VNRA	VNC	CE	ctr	VNRA	VNC	CE	ctr	VNRA	VNC	CE	ctr	VNRA	VNC	CE	ctr	VNRA	VNC	CE	ctr	VNRA	VNC	CE	ctr	VNRA	VNC	CE	ctr	VNRA	VNC	CE	ctr	VNRA	VNC	CE	ctr	VNRA	VNC	CE	ctr	VNRA	VNC
<i>actb</i>	78108	232034	87323	102341	153310	693579	184311	133190	187636	1057729	190286	142505	235459	667936	146791	130380	226347	649147	161404	184067	<i>actb</i>	4145	1092	2005	10259	4421	74603	35942	17524	9494	56603	12285	7195	38532	7352	21222	16536	30278	16029	27121	29109			
<i>aldh1a2</i>	2088	13	270	1161	769	12	63	131	482	40	454	108	982	39	719	265	2103	131	1028	1124	<i>aldh1a2</i>	184	5	11	826	136	11	1	33	121	26	94	12	214	15	503	139	913	16	193	97			
<i>amy2a/b</i>	45	153	98	140	95	496	111	76	84	650	80	92	93	309	106	69	381	370	4300	99	<i>amy2a/b</i>	43	139	37	120	72	401	87	54	70	534	76	80	91	259	105	68	155	246	2708	63			
<i>chrd</i>	3489	25	9326	22713	1251	21	1629	2483	260	33	627	1007	161	35	249	363	57	21	47	123	<i>chrd</i>	645	24	4468	5189	17	20	366	433	42	32	102	459	65	34	57	201	10	20	23	10			
<i>crabp1</i>	16	3	1	1	33	6	14	1	79	14	7	1	278	12	159	7	680	36	13	2	<i>crabp1</i>	15	2	0	0	27	5	6	0	60	13	5	0	42	11	158	6	250	6	12	1			
<i>crabp1</i>	5599	36	5065	13005	3273	128	2968	7701	2154	136	2988	4389	2264	65	3064	5215	1452	307	2038	5064	<i>crabp1</i>	1421	2	2128	1054	81	55	72	119	333	24	582	482	241	30	292	1593	315	123	665	484			
<i>cyp26a1</i>	985	159	3038	633	852	311	832	742	955	337	889	604	799	57	207	169	694	151	58	101	<i>cyp26a1</i>	76	10	1233	295	131	62	289	237	194	133	293	75	226	21	50	80	179	114	18	57			
<i>darmin</i>	4785	1	6032	1	20699	1	17162	459	32301	2	14519	1747	21567	1	8050	265	4205	2	307	230	<i>darmin</i>	553	0	3634	0	2149	0	9756	283	973	1	3962	1488	7808	0	5864	133	2911	1	236	86			
<i>dkk1</i>	316	33	205	119	375	316	1129	176	329	417	1418	190	346	391	1417	217	421	1380	794	449	<i>dkk1</i>	6	29	54	16	77	58	14	12	90	121	140	59	16	49	282	54	97	368	69	160			
<i>foxe1</i>	1	25	1	1	38	7	1	28	48	3	1	132	165	70	2	412	365	2179	177	843	<i>foxe1</i>	0	13	0	0	29	6	0	27	26	2	0	101	75	69	1	117	72	54	137	45			
<i>foxe3/4</i>	9	7	1	1	92	2	1	107	77	8	1	19	36	10	4	3	8	1	1	91	<i>foxe3/4</i>	0	6	0	0	29	1	0	106	48	7	0	3	11	9	3	2	7	0	0	90			
<i>gfpd</i>	266	360	190	305	405	408	341	248	535	803	385	307	867	943	515	369	1551	3238	1194	977	<i>gfpd</i>	54	43	37	138	16	2	13	25	66	6	31	11	210	227	164	22	275	55	398	299			
<i>gapdh</i>	485	169	5928	3112	2568	514	14505	8464	5916	4905	26893	17797	10729	22256	40000	26378	10120	41337	24386	22134	<i>gapdh</i>	1	54	1472	407	719	135	2899	1350	2295	1234	1430	1807	1816	4383	10004	5905	3000	14631	2091	3931			
<i>gata2</i>	1668	12246	255	1216	759	3850	206	106	208	1546	158	111	247	485	120	86	151	134	65	73	<i>gata2</i>	329	418	189	25	245	1284	62	49	21	41	31	20	79	131	57	41	14	70	33	14			
<i>gata4-a/b</i>	178	1	83	46	243	23	347	15	123	27	661	1	175	5	786	1	212	1	810	1	<i>gata4-a/b</i>	5	0	3	43	83	9	147	14	63	8	164	0	26	4	132	0	118	0	253	0			
<i>hes1-a</i>	1227	756	616	1012	1490	958	636	612	744	1524	896	695	824	840	1169	679	678	601	1041	918	<i>hes1-a</i>	304	145	170	58	572	192	141	60	280	287	318	19	98	52	448	36	163	82	154	118			
<i>hhex</i>	41	425	1	21	185	107	57	50	75	87	157	14	106	46	96	1	99	30	100	20	<i>hhex</i>	8	82	0	20	96	24	33	37	66	86	61	13	2	45	38	0	83	29	34	11			
<i>hoxa1-b</i>	711	2149	1030	141	508	2107	764	233	190	491	630	366	121	342	308	199	40	1309	198	206	<i>hoxa1-b</i>	223	368	1	11	6	402	156	9	57	113	161	134	16	54	102	6	21	169	19	51			
<i>ins-a</i>	1	2	1	1	2	2	1886	1	51	4	14459	3	238	1	36320	1	895	1	29702	1	<i>ins-a</i>	0	1	0	0	1	1	100	0	29	3	669	2	123	0	8426	0	450	0	9593	0			
<i>ins-b</i>	1	12	1	4	6	11	1028	1	52	20	10442	5	185	9	29422	1	918	18	22248	1	<i>ins-b</i>	0	11	0	3	5	10	197	0	7	19	397	4	89	8	6740	0	499	17	6920	0			
<i>isl-1</i>	139	529	50	164	222	709	76	202	182	660	110	208	241	317	84	128	235	331	69	128	<i>isl-1</i>	13	131	30	0	46	78	21	99	84	180	16	29	63	107	36	13	34	79	4	18			
<i>neurog3</i>	22	35	9	13	48	44	53	12	44	64	69	10	31	22	17	1	11	41	4	11	<i>neurog3</i>	19	10	3	1	8	43	33	1	17	18	46	2	27	21	16	0	10	40	3	10			
<i>nkx2-1</i>	215	1	14	53	247	1	12	16	306	2	1	29	390	1	10	130	292	7	1	10	<i>nkx2-1</i>	28	0	13	2	9	0	11	15	22	1	0	22	148	0	9	129	44	6	0	9			
<i>nkx2-2</i>	66	2	24	4	112	1	104	1	101	2	15	23	98	4	17	49	81	1	12	33	<i>nkx2-2</i>	9	1	1	3	7	0	60	0	2	1	11	10	26	3	16	48	13	0	11	6			
<i>nkx6-1</i>	40	25	57	83	78	137	34	27	86	219	66	75	139	114	41	100	136	110	35	97	<i>nkx6-1</i>	10	5	39	26	22	47	13	9	18	39	3	25	66	7	40	38	37	11	5	15			
<i>nog</i>	1585	392	18209	19558	2154	2978	11712	12667	1797	2010	10778	9681	2916	411	11083	11376	2532	714	6056	8651	<i>nog</i>	1249	268	781	501	1307	2435	2574	5806	1068	1548	2040	1045	2284	362	2258	811	1467	610	1907	945			
<i>odc1</i>	27372	27377	27375	27377	27365	27377	27371	27370	27353	27365	27361	27378	27364	27365	27350	27346	27342	27371	27366	27366	<i>odc1</i>	3	9	7	2	12	8	1	1	15	22	2	4	0	17	21	2	29	5	6	8			
<i>onecut</i>	252	41	128	38	438	8	145	50	429	10	312	290	396	4	225	366	250	5	88	154	<i>onecut</i>	39	37	127	36	33	7	29	19	89	9	76	133	43	3	218	173	27	4	30	10			
<i>pax6-b</i>	833	20	727	230	784	1	254	137	880	7	541	432	1019	8	398	234	742	13	171	177	<i>pax6-b</i>	100	19	75	34	168	0	13	5	14	6	66	295	317	7	118	141	2	9	62	104			
<i>pdia</i>	65	194	67	142	167	649	136	98	151	1010	273	127	217	753	4018	120	2132	757	21802	130	<i>pdia</i>	64	193	63	141	166	648	135	97	150	1009	154	126	270	752	2084	119	647	707	7768	129			
<i>pdx1</i>	1	1	2	1	1	1	705	1	65	8	2549	5	117	1	2331	1	113	4	960	1	<i>pdx1</i>	0	0	1	0	0	0	497	0	23	7	394	4	21	0	458	0	55	3	376	0			
<i>ptf1a-a/b</i>	19	32	14	14	25	67	340	6	190	127	2257	37	288	60	3581	1	279	109	2210	11	<i>ptf1a-a/b</i>	15	0	2	8	10	20	245	5	22	50	401	20	92	29	149	0	10	58	419	10			
<i>sftpc</i>	1	36	36	18	17	122	12	7	11	100	12	9	99	88	4	1	6262	126	23	34	<i>sftpc</i>	0	15	35	17	16	70	11	6	10	71	11	9	77	41	3	0	472	71	22	33			
<i>sox1</i>	84	40	23	35	177	119	48	27	163	194	54	160	135	96	29	180	106	90	16	61	<i>sox1</i>	22	39	22	5	97	118	22	17	70	193	2	124	3	95	28	168	24	73	15	33			
<i>sox17a-a</i>	716	1	362	925	529	8	28	141	88	6	104	50	79	1	158	37	75	1	170	46	<i>sox17a-a</i>	150	0	10	644	302	7	12	33	82	5	13	3	9	0	20	22	74	0	34	37			
<i>sox17b</i>	375	1	20	119	115	1	1	1	3	1	1	1	1	1	3</																													

6.6 RNA-sequencing data for the identification of RA-target genes

Tab. 6.3 Summary of 102 differentially expressed genes in the absence of CHX.

Fold changes of indicated genes in explants 1h and 2h after RA addition (-RA versus + RA; Ø CHX)

* no sequence known for *X.laevis*

† no nanostring probe designable

1h (6)		1 and 2h (21)		2h (75)			
gene	FC	gene	FC	gene	FC	gene	FC
<i>hoxb1</i>	6.79	<i>hoxa1</i>	16.62 / 26.39	<i>mesp2*</i>	27.90	<i>Xl.80298*</i>	2.60
<i>Xl.32109</i>	2.32	<i>hoxa2</i>	15.43 / 21.88	<i>Xl.8753</i>	16.22	<i>Xetrov72036339*</i>	2.57
<i>olig4*</i>	2.20	<i>duosp6</i>	5.75 / 8.51	<i>mespa</i>	15.57	<i>Xetrov72039973*</i>	2.55
<i>Xl.59256</i>	2.19	<i>Xl.9874</i>	5.04 / 7.31	<i>hoxa3</i>	13.07	<i>gadd45a†</i>	2.52
<i>Xl.9822</i>	-2.16	<i>Xl.67202</i>	4.85 / 5.63	<i>cebpd</i>	7.04	<i>stox1</i>	2.50
<i>sp9*</i>	-3.14	<i>dhrs3</i>	4.36 / 7.23	<i>s1pr5*</i>	6.74	<i>fzd4</i>	2.50
		<i>znf703</i>	3.94 / 7.73	<i>hoxb4</i>	6.51	<i>hoxa4*</i>	2.50
		<i>hoxa5</i>	3.85 / 7.26	<i>cyp26a1</i>	6.27	<i>Xl.68408</i>	2.48
		<i>bhlhe40</i>	3.77 / 4.97	<i>nodal1</i>	5.84	<i>duosp5</i>	2.40
		<i>hoxd1</i>	3.75 / 5.36	<i>sox9</i>	5.12	<i>Xl.80297</i>	2.40
		<i>neurog2</i>	3.46 / 4.13	<i>Xl.82687*</i>	5.11	<i>tril*</i>	2.39
		<i>cxcr7</i>	2.81 / 3.57	<i>prph</i>	4.70	<i>Xl.57926</i>	2.36
		<i>rgs2</i>	2.81 / 4.33	<i>nkx6-2</i>	4.39	<i>erf</i>	2.32
		<i>cdx4</i>	2.72 / 2.62	<i>Xl.45046</i>	4.38	<i>Xl.70850</i>	2.31
		<i>Xl.15091</i>	2.68 / 12.58	<i>mespb</i>	4.23	<i>lhx1</i>	2.27
		<i>Xl.71159</i>	2.42 / 2.72	<i>nr2f5</i>	4.20	<i>hoxd4</i>	2.25
		<i>hnf1b</i>	2.37 / 5.55	<i>trib1</i>	4.08	<i>fhdc1*</i>	2.25
		<i>Xl.58101</i>	2.35 / 3.69	<i>Xl.84363*</i>	3.84	<i>rgs14</i>	2.22
		<i>fgf16 †</i>	2.32 / 2.68	<i>fst</i>	3.83	<i>kirrel2</i>	2.16
		<i>txnip</i>	2.22 / 2.83	<i>c10orf140</i>	3.59	<i>pim1</i>	2.16
		<i>Xl.4906</i>	2.21 / 3.09	<i>Xetrov72011149†</i>	3.55	<i>dact1</i>	2.15
				<i>Xl.51509</i>	3.53	<i>Xl.47239</i>	2.14
				<i>Xl.6091</i>	3.47	<i>rara</i>	2.12
				<i>hunk</i>	3.06	<i>pkdcc.1</i>	2.10
				<i>tmem72</i>	3.00	<i>mx1</i>	2.07
				<i>Xl.16263</i>	2.85	<i>cass4</i>	2.06
				<i>nodal2</i>	2.81	<i>Xl.79790</i>	2.06
				<i>foxh1</i>	2.78	<i>Xl.82247*</i>	2.04
				<i>kiaa0182</i>	2.76	<i>fgfr4</i>	2.03
				<i>meis3</i>	2.74	<i>slc38a8*</i>	2.03
				<i>znf503*</i>	2.72	<i>hey1</i>	2.02
				<i>myc</i>	2.70	<i>hoxb3</i>	2.02
				<i>igf3</i>	2.70	<i>mn1*</i>	2.02
				<i>Xl.74263</i>	2.68	<i>spry2</i>	2.02
				<i>tdgf1p2</i>	2.66	<i>Xl.85251</i>	-2.08
				<i>gbx2.1</i>	2.65	<i>Xl.13572*</i>	-2.09
				<i>Xl.57027</i>	2.60	<i>twist1</i>	-2.26
						<i>pdgfb</i>	-3.02

Tab. 6.4 Summary of differentially expressed genes in the presence of CHX

Fold changes of indicated genes in explants 1h and 2h after RA addition (-RA versus + RA; + CHX)

1 and 2h (10)		2h (51)			
gene	FC	symbol	FC	symbol	FC
<i>hoxa1</i>	11.94 / 28.34	<i>hoxa3</i>	24.89	<i>Xl.29118</i>	3.26
<i>hoxa2</i>	6.47 / 14.11	<i>hoxb4</i>	12.79	<i>foxh1</i>	3.07
<i>Xl.9874</i>	4.62 / 4.61	<i>foxi4.2</i>	10.73	<i>Xl.58101</i>	3.02
<i>Xl.15091</i>	3.98 / 3.93	<i>hoxb1</i>	9.61	<i>Xl.6091</i>	2.93
<i>dusp6</i>	3.82 / 4.92	<i>Xl.78389</i>	9.49	<i>klb</i>	2.86
<i>nkx6-2</i>	3.20 / 3.26	<i>Xl.67202</i>	6.59	<i>hoxd4</i>	2.81
<i>dhrs3</i>	2.91 / 4.74	<i>cyp26c1</i>	6.58	<i>olig4</i>	2.75
<i>hoxa5</i>	2.89 / 8.13	<i>znf703</i>	6.53	<i>hoxb8</i>	2.68
<i>rgs2</i>	2.18 / 3.23	<i>cyp26a1</i>	5.64	<i>Xl.84363</i>	2.58
<i>bhlhe40</i>	2.05 / 4.24	<i>s1pr5</i>	5.59	<i>hoxb3</i>	2.55
		<i>Xl.82687</i>	5.54	<i>hoxa4</i>	2.45
		<i>sox9</i>	5.06	<i>Xl.13431</i>	2.43
		<i>Xl.45046</i>	4.76	<i>rara</i>	2.31
		<i>trib1</i>	4.69	<i>myc</i>	2.30
		<i>hoxd1</i>	4.66	<i>igf3</i>	2.30
		<i>cebpd</i>	4.48	<i>nr2f5</i>	2.28
		<i>hnf1b</i>	4.21	<i>edn1</i>	2.24
		<i>gbx2.2</i>	4.06	<i>hunk</i>	2.22
		<i>hoxc4</i>	3.93	<i>Xl.79790</i>	2.20
		<i>Xl.51509</i>	3.93	<i>Xl.41047</i>	2.15
		<i>tmem72</i>	3.90	<i>meis3</i>	2.14
		<i>gata3</i>	3.87	<i>kiaa0182</i>	2.12
		<i>neurog2</i>	3.56	<i>tril</i>	2.07
		<i>c10orf140</i>	3.52	<i>Xl.74263</i>	2.05
		<i>gbx2.1</i>	3.46	<i>fzd4</i>	1.90
				<i>twist1</i>	-2.14

Tab. 6.5 Comparison of differentially expressed genes absence versus presence of CHX (putative direct RA-targets).

- CHX only (53)	+ CHX only (12)	- CHX and + CHX (putative direct targets) (49)
<i>cass4</i>	<i>cyp26c1</i>	<i>bhlhe40</i>
<i>cdx4</i>	<i>edn1</i>	<i>c10orf140</i>
<i>cxcr7</i>	<i>foxi4.2</i>	<i>cebpd</i>
<i>dact1</i>	<i>gata3</i>	<i>cyp26a1</i>
<i>dusp5</i>	<i>gbx2.2</i>	<i>dhrs3</i>
<i>erf</i>	<i>hoxb8</i>	<i>dusp6</i>
<i>fgf16</i>	<i>hoxc4</i>	<i>fzd4</i>
<i>fgfr4</i>	<i>klb</i>	<i>foxh1</i>
<i>fhdc1</i>	<i>Xl.13431</i>	<i>gbx2.1</i>
<i>fst</i>	<i>Xl.29118</i>	<i>hnf1b</i>
<i>gadd45a</i>	<i>Xl.41047</i>	<i>hoxa1</i>
<i>hey1</i>	<i>Xl.78389</i>	<i>hoxa2</i>
<i>kirrel2</i>		<i>hoxa3</i>
<i>lhx1</i>		<i>hoxa4</i>
<i>mesp2</i>		<i>hoxa5</i>
<i>mespa</i>		<i>hoxb1</i>
<i>mespb</i>		<i>hoxb3</i>
<i>mn1</i>		<i>hoxb4</i>
<i>mxi1</i>		<i>hoxd1</i>
<i>nodal1</i>		<i>hoxd4</i>
<i>nodal2</i>		<i>hunk</i>
<i>pdgfb</i>		<i>igf3</i>
<i>pim1</i>		<i>kiaa0182</i>
<i>pkdccc.1</i>		<i>meis3</i>
<i>prph</i>		<i>myc</i>
<i>rgs14</i>		<i>neurog2</i>
<i>slc38a8</i>		<i>nkx6-2</i>
<i>sp9</i>		<i>nr2f5</i>
<i>spry2</i>		<i>olig4</i>
<i>stox1</i>		<i>rara</i>
<i>tdgf1p2</i>		<i>rgs2</i>
<i>txnip</i>		<i>s1pr5</i>
<i>Xetrov72011149</i>		<i>sox9</i>
<i>Xetrov72036339</i>		<i>tmem72</i>
<i>Xetrov72039973</i>		<i>trib1</i>
<i>Xl.13572</i>		<i>tril</i>
<i>Xl.16263</i>		<i>twist1</i>
<i>Xl.32109</i>		<i>Xl.15091</i>
<i>Xl.47239</i>		<i>Xl.45046</i>
<i>Xl.4906</i>		<i>Xl.51509</i>
<i>Xl.57027</i>		<i>Xl.58101</i>
<i>Xl.57926</i>		<i>Xl.6091</i>
<i>Xl.59256</i>		<i>Xl.67202</i>
<i>Xl.68408</i>		<i>Xl.74263</i>
<i>Xl.70850</i>		<i>Xl.79790</i>
<i>Xl.80297</i>		<i>Xl.82687</i>
<i>Xl.80298</i>		<i>Xl.84363</i>
<i>Xl.82120</i>		<i>Xl.9874</i>
<i>Xl.82247</i>		<i>znf703</i>
<i>Xl.85251</i>		
<i>Xl.8753</i>		
<i>Xl.9822</i>		
<i>znf503</i>		

Tab. 6.6 RNA-sequencing of explants 1h after RA addition in the absence of CHX. Normalized data (1h Ø CHX).

Genes with > 60 mapped reads in samples with RA.

no.	symbol	accession number	gene function	UnigeneID_XL	log2FC +RA/-RA	FDR	- RA		+ RA	
							A	B	A	B
1	<i>hoxa1</i>	BC080895,NM_001008016	homeodomain transcription factor	XI.23512,XI.283	4.05	0.00%	38	31	699	499
2	<i>hoxa2</i>	CU025162	homeodomain transcription factor	XI.12098,XI.751	3.95	0.00%	8	7	157	103
3	<i>hoxb1</i>	XM_002938017	homeodomain transcription factor	XI.85422	2.76	0.40%	10	11	105	48
4	<i>dusp6</i>	NM_001045578,CR848381,BC118778,	MAP kinase phosphatase	XI.31935,XI.49155,XI.52935,XI.8002	2.52	0.00%	669	562	4471	2737
5	<i>XI.9874</i>			XI.9874	2.33	0.00%	10	28	69	123
6	<i>XI.67202</i>			XI.67202	2.28	0.81%	29	34	210	87
7	<i>dhrs3</i>	NM_001008431,CR848157,BC080136,		XI.77868,XI.59231,XI.83090	2.13	0.00%	992	1367	4475	5786
8	<i>znf703</i>	NM_001030507,BC093467	Zn-finger	XI.1529,XI.23634,XI.69973	1.98	4.87%	950	500	4766	1416
9	<i>hoxa5</i>	BC088772,NM_001011405	homeodomain transcription factor	XI.58357	1.94	0.00%	32	28	131	103
10	<i>bhlhe40</i>	BC168818,BC169139,XM_002938312,B	basic helix-loop-helix (bHLH) transcription factor, circadian regulator	XI.19778,XI.26256	1.92	0.00%	75	48	270	200
11	<i>hoxd1</i>	CR760220,NM_001016678,BC170965,	homeodomain transcription factor	XI.53491,XI.11612,XI.76294	1.91	0.40%	813	398	2970	1553
12	<i>neurog2</i>	XM_002934243	basic helix-loop-helix transcription factor	XI.369,XI.370,XI.79613	1.79	1.80%	30	15	137	34
13	<i>cxcr7</i>	NM_001030434,BC091057	glycoprotein hormone receptor	XI.15037	1.49	2.16%	247	379	745	1004
14	<i>rgs2</i>	BC091089,NM_001030451		XI.49812,XI.76046,XI.85582	1.49	0.00%	97	42	281	117
15	<i>cdx4</i>	AF417199,CT030483,BC167866,NM_2	homeodomain transcription factor	XI.26888	1.44	0.05%	1728	866	5059	2168
16	<i>XI.15091</i>			XI.15091	1.42	0.53%	26	29	80	69
17	<i>XI.71159</i>			XI.71159	1.28	0.00%	175	147	454	330
18	<i>hnf1b</i>	CR760425,XM_002939634,XM_002939	homeodomain transcription factor	XI.65135,XI.12667	1.25	0.01%	454	490	1010	1230
19	<i>XI.58101</i>			XI.58101	1.23	0.13%	117	127	210	381
20	<i>XI.32109</i>			XI.32109	1.21	0.11%	86	74	200	174
21	<i>fgf16</i>	XM_002931813	heparin-binding growth factor		1.21	0.00%	245	219	547	532
22	<i>txnip</i>	XM_002938464,BC121658		XI.77253,XI.13359,XI.57371,XI.7636	1.15	2.96%	155	102	388	194
23	<i>XI.4906</i>			XI.4906	1.15	2.27%	351	460	933	803
24	<i>olig4</i>	BC161514,NM_001045715,CR848409	transcription factor	XI.72230	1.14	0.84%	33	42	73	95
25	<i>XI.59256</i>			XI.59256	1.13	1.45%	51	46	107	108
26	<i>XI.9822</i>			XI.9822	-1.11	1.45%	130	133	74	47
27	<i>sp9</i>	BC121268,NM_001078801			-1.65	0.14%	64	58	28	10

Tab. 6.7 RNA-sequencing of explants 2h after RA addition in the absence of CHX. Normalized data (2h Ø CHX).

Genes with > 60 mapped reads in samples with RA.

no.	symbol	accession	gene function	UnigeneID_XL	log2FC +RA/-RA	FDR	- RA		+ RA	
							A	B	A	B
1	<i>mesp2</i>				4.80	0.11%	1	1	138	10
2	<i>hoxa1</i>	BC080895,NM_001008016	homeodomain transcription factor	XI.23512,XI.283	4.72	0.00%	70	24	1295	1129
3	<i>hoxa2</i>	CU025162	homeodomain transcription factor	XI.12098,XI.751	4.45	0.00%	18	9	334	276
4	<i>Xl.8753</i>			XI.8753	4.02	0.00%	2	4	64	65
5	<i>mespa</i>	CR848619,NM_001045719,BC15731	transcription factor	XI.55,XI.54	3.96	0.17%	89	96	3066	248
6	<i>hoxa3</i>	NM_001127429,BC166398	homeodomain transcription factor	XI.9439	3.71	0.00%	18	6	153	173
7	<i>Xl.15091</i>			XI.15091	3.65	0.00%	11	16	224	157
8	<i>dusp6</i>	NM_001045578,CR848381,BC11877	MAP kinase phosphatase	XI.31935,XI.49155,XI.52935,XI.80026	3.09	0.00%	619	512	6084	3726
9	<i>znf703</i>	NM_001030507,BC093467	Zn-finger	XI.1529,XI.23634,XI.69973	2.95	0.00%	1013	263	4168	4062
10	<i>Xl.9874</i>			XI.9874	2.87	0.00%	18	35	160	240
11	<i>hoxa5</i>	BC088772,NM_001011405	homeodomain transcription factor	XI.58357	2.86	0.00%	29	35	226	252
12	<i>dhrs3</i>	NM_001008431,CR848157,BC08013		XI.77868,XI.59231,XI.83090	2.85	0.00%	1015	1453	8872	8548
13	<i>cebpd</i>	NM_001030414,CR942782,BC09102	basic-leucine zipper (bZIP) transcription	XI.29876,XI.25857,XI.81500	2.82	0.00%	38	24	158	238
14	<i>s1pr5</i>	BC161459,NM_001127068		XI.75787,XI.9971	2.75	0.03%	82	43	390	481
15	<i>hoxb4</i>	BC090114,BC161550,NM_00112301	Transcription factor zerknullt and related	XI.54392,XI.49715,XI.72333	2.70	0.00%	51	14	192	200
16	<i>cyp26a1</i>	NM_001016147,CR761993,BC17108	retinoic acid hydroxylase	XI.50113,XI.456	2.65	0.00%	3148	3665	18022	26048
17	<i>nodal1</i>	BC171037,CR761456,NM_00101632	transforming growth factor beta and bone	XI.1037,XI.85704	2.55	0.04%	21	35	240	75
18	<i>Xl.67202</i>			XI.67202	2.49	0.04%	37	22	154	193
19	<i>hnf1b</i>	CR760425,XM_002939634,XM_0029	homeodomain transcription factor	XI.65135,XI.12667	2.47	0.00%	518	518	2808	2942
20	<i>hoxd1</i>	CR760220,NM_001016678,BC17096	homeodomain transcription factor	XI.53491,XI.11612,XI.76294	2.42	0.00%	1020	306	3243	3015
21	<i>sox9</i>	NM_001016853,CR855424	HMG-box transcription factor	XI.28992,XI.1690,XI.82068	2.36	0.00%	51	29	157	270
22	<i>Xl.82687</i>			XI.82687	2.35	0.00%	12	13	39	103
23	<i>bhlhe40</i>	BC168818,BC169139,XM_002938312	basic helix-loop-helix (bHLH) transcription	XI.19778,XI.26256	2.31	0.00%	79	76	399	375
24	<i>prph</i>	NM_001001235,BC067967	intermediate filament	XI.27,XI.16232	2.23	4.01%	9	7	11	93
25	<i>nkx6-2</i>	CT010540,XM_002937790	homeodomain transcription factor	XI.55860,XI.49827	2.13	0.00%	111	203	419	1028
26	<i>Xl.45046</i>			XI.45046	2.13	0.00%	82	42	268	267
27	<i>rgs2</i>	BC091089,NM_001030451		XI.49812,XI.76046,XI.85582	2.11	0.00%	52	26	234	111
28	<i>mespb</i>	NM_001016653,CR760340	transcription factor	XI.51050,XI.81675	2.08	4.27%	583	240	4138	453
29	<i>nr2f5</i>	XM_002938463	hormone receptor	XI.1157,XI.13423,XI.81917,XI.83500	2.07	0.00%	28	28	149	97
30	<i>neurog2</i>	XM_002934243	basic helix-loop-helix transcription factor	XI.369,XI.370,XI.79613	2.05	0.04%	35	8	102	62
31	<i>trib1</i>	XM_002938661		XI.75411,XI.81850	2.03	0.88%	13	16	46	83

Appendix

no.	symbol	accession	gene function	UnigeneID_XL	log2FC +RA/-RA	FDR	- RA		+ RA	
							A	B	A	B
32	<i>Xl.84363</i>			Xl.84363	1.94	0.00%	37	38	158	137
33	<i>fst</i>	NM_001008056,B C080943	activin and bmp7 antagonist, also	Xl.1094,Xl.75880,Xl. .79342,Xl.83742	1.94	3.02%	131	974	1323	1718
34	<i>Xl.58101</i>			Xl.58101	1.88	0.00%	98	170	508	462
35	<i>c10orf140</i>	NM_001126649,B C159015,BC15904		Xl.52870,Xl.80054	1.84	0.00%	119	59	294	340
36	<i>cxc7</i>	NM_001030434,B C091057	glycoprotein hormone receptor	Xl.15037	1.84	0.01%	216	466	1409	817
37	<i>Xetrov72 011149</i>				1.83	0.00%	28	29	94	111
38	<i>Xl.51509</i>			Xl.51509	1.82	0.11%	35	17	90	87
39	<i>Xl.6091</i>			Xl.6091	1.80	0.00%	32	21	109	81
40	<i>Xl.4906</i>			Xl.4906	1.63	0.00%	289	329	891	1022
41	<i>hunk</i>	NM_001127077,B C161479		Xl.24322,Xl.12483, Xl.83064	1.61	0.00%	449	355	1193	1254
42	<i>tmem72</i>	BC158380,XM_00 2939555		Xl.17444	1.59	0.10%	38	24	97	87
43	<i>Xl.16263</i>			Xl.16263	1.51	0.00%	146	92	403	274
44	<i>txnip</i>	XM_002938464,B C121658		Xl.77253,Xl.13359, Xl.57371,Xl.76363,	1.50	0.00%	123	111	470	224
45	<i>nodal2</i>	XM_002932721	transforming growth factor beta and bone	Xl.1038	1.49	0.33%	88	279	506	412
46	<i>foxb1</i>	CR761447,NM_00 1017084	winged helix transcription factor	Xl.381	1.47	0.68%	70	66	183	200
47	<i>kiaa0182</i>	XM_002936097,B C125792		Xl.78028,Xl.1433,Xl. .78276	1.47	0.00%	290	169	553	706
48	<i>meis3</i>	CR760178,BC0755 89,NM_00100678	homeodomain transcription factor	Xl.23066,Xl.452,Xl. 80020,Xl.82977	1.46	0.00%	2458	1457	5909	4590
49	<i>Xl.71159</i>			Xl.71159	1.45	0.00%	160	153	556	316
50	<i>znf503</i>	BC124040,NM_00 1079230	zinc finger, C2H2 type	Xl.60819,Xl.80579	1.44	0.00%	437	380	926	1324
51	<i>myc</i>	BC064880,NM_20 4059,CR761143		Xl.826,Xl.1155	1.43	0.00%	1447	527	2915	1943
52	<i>igf3</i>	BC161167,CR8483 77,NM_00112694		Xl.12078,Xl.78527	1.43	0.00%	49	35	122	107
53	<i>fgf16</i>	XM_002931813	heparin-binding growth factor		1.42	0.00%	289	322	893	746
54	<i>Xl.74263</i>			Xl.74263	1.42	0.01%	153	82	262	339
55	<i>tdgf1p2</i>	XM_002940604	EGF-like growth factor	Xl.15503,Xl.51406	1.41	0.10%	32	42	112	88
56	<i>gbx2.1</i>	XM_002932000,X M_002932001	homeodomain transcription factor	Xl.77345	1.41	0.08%	74	53	169	166
57	<i>cdx4</i>	AF417199,CT0304 83,BC167866,NM	homeodomain transcription factor	Xl.26888	1.39	0.03%	2515	1094	6302	3014
58	<i>Xl.57027</i>			Xl.57027	1.38	0.10%	29	34	78	88
59	<i>Xl.80298</i>			Xl.80298	1.38	0.21%	47	32	106	99
60	<i>Xetrov72 036339</i>				1.36	0.00%	108	135	213	440
61	<i>Xetrov72 039973</i>				1.35	3.33%	27	31	63	88
62	<i>gadd45a</i>	NM_001016151,B C167898,BC12153	40S ribosomal protein S12	Xl.79095,Xl.71159, Xl.81981	1.33	0.22%	1216	1180	4394	1907

no.	symbol	accession	gene function	UnigeneID_XL	log2FC +RA/-RA	FDR	- RA		+ RA	
							A	B	A	B
63	<i>stox1</i>	XM_002936869	Conserved protein Knockout	,XI.15086	1.32	0.02%	1164	668	1955	2459
64	<i>fzd4</i>	XM_002936543	transmembrane receptor in the wnt	XI.460,XI.53888	1.32	0.00%	681	503	1365	1581
65	<i>hoxa4</i>		homeodomain transcription factor		1.32	0.72%	163	85	318	286
66	<i>XI.68408</i>			XI.68408	1.31	1.33%	35	45	59	151
67	<i>dusp5</i>	BC090366,NM_001015856	MAP kinase phosphatase	XI.79939,XI.15374	1.26	0.11%	799	620	1677	1690
68	<i>XI.80297</i>			XI.80297	1.26	0.45%	213	316	813	440
69	<i>tril</i>	XM_002933390		XI.73400,XI.78580	1.26	0.00%	821	401	1596	1160
70	<i>XI.57926</i>			XI.57926	1.24	0.03%	867	751	2007	1811
71	<i>erf</i>	NM_001015821,BC090103	transcription factor	XI.41820,XI.47734,XI.78801	1.22	2.07%	691	307	961	1174
72	<i>XI.70850</i>			XI.70850	1.21	0.00%	81	121	176	298
73	<i>lhx1</i>	NM_001100228,BC135731	LIM and homeodomain	XI.32655,XI.79655,XI.81258,XI.82262	1.19	0.18%	2515	4358	8329	6707
74	<i>hoxd4</i>	XM_002935672,XM_002935673	homeodomain transcription factor	XI.34346,XI.85858	1.17	4.14%	60	65	91	207
75	<i>fhdc1</i>	CR942785,XM_002933493			1.17	0.07%	897	632	1490	1885
76	<i>rgs14</i>	XM_002938062		XI.14836	1.15	0.64%	48	54	88	142
77	<i>kirrel2</i>	NM_001142126,BC168130	Immunoglobulin C-2 Type/fibronectin type	XI.76492,XI.60720,XI.76486,XI.81573	1.11	1.50%	541	706	1333	1350
78	<i>pim1</i>	NM_001008131,BC081340,CR76042		XI.48564,XI.68517,XI.78542	1.11	0.30%	1575	1405	4311	2312
79	<i>dact1</i>	BC080457,CR761983,NM_00100794	antagonist of beta-catenin and c-jun N-	XI.7602,XI.19185	1.11	0.05%	3586	2838	8553	5424
80	<i>XI.47239</i>			XI.47239	1.10	0.07%	126	96	264	211
81	<i>rara</i>	NM_001171194,CT025407	transcription factor, steroid receptor class	XI.158,XI.57139	1.09	1.03%	250	162	387	472
82	<i>pkdccc.1</i>	BC168090,NM_001142110		XI.80884,XI.55752,XI.59589	1.07	0.98%	774	1264	2368	1864
83	<i>mx1</i>	NM_001008128,CR942348,BC08133	transcription factor	XI.50498	1.05	1.27%	286	218	398	635
84	<i>cass4</i>	XM_002942273	p53-interacting protein 53BP/ASPP,	XI.22909	1.04	0.51%	258	324	507	700
85	<i>XI.79790</i>			XI.79790	1.04	2.54%	29	38	41	103
86	<i>XI.82247</i>			XI.82247	1.03	0.62%	213	190	459	371
87	<i>fgfr4</i>	CR761450,NM_001016323,BC17095	receptor tyrosine kinase	XI.1008,XI.1016	1.02	0.00%	2621	2113	5280	4345
88	<i>slc38a8</i>	CR760593,NM_001044435		XI.70342,XI.78242	1.02	1.11%	550	803	1420	1269
89	<i>hey1</i>	CR760684,NM_001007910,BC08034	helix-loop-helix transcription	XI.469,XI.7544,XI.76323	1.02	0.02%	185	162	396	311
90	<i>hoxb3</i>	CR848404,BC135406,NM_00101597	homeodomain transcription factor	XI.79878,XI.80826	1.02	0.09%	117	92	193	230
91	<i>mn1</i>	NM_001100202,BC135419	Chitinase	XI.57334,XI.69093,XI.82818	1.01	0.98%	598	499	1198	1017
92	<i>spry2</i>	AY714335,BC064204,NM_00100693	regulation of signal transduction	XI.11964,XI.11965	1.01	0.99%	1781	1675	3743	3226
93	<i>XI.85251</i>			XI.85251	-1.06	0.75%	85	80	43	35
94	<i>XI.13572</i>			XI.13572	-1.06	0.47%	130	112	56	59
95	<i>twist1</i>	NM_204084,BK006266,BC074558,C	transcription factor	XI.879,XI.23366,XI.68451,XI.82751,XI.8	-1.17	1.23%	217	260	101	108
96	<i>pdgfb</i>	XM_002933750	growth factor	XI.14185,XI.13630	-1.59	0.00%	218	252	102	61

Tab. 6.8 RNA-sequencing of explants 1h after RA addition in the presence of CHX. Normalized data (1h + CHX).

Genes with > 60 mapped reads in samples with RA.

no.	symbol	accession	gene function	UnigeneID_XL	log2FC +RA/-RA	FDR	- RA +CHX		+ RA +CHX	
							A	B	A	B
1	<i>hoxa1</i>	BC080895,NM_001008016	homeodomain transcription factor	XI.23512,XI.283	3.58	0.00%	65	17	307	602
2	<i>hoxa2</i>	CU025162	homeodomain transcription factor	XI.12098,XI.751	2.69	0.00%	21	6	70	108
3	<i>XI.9874</i>			XI.9874	2.21	0.00%	24	29	98	159
4	<i>XI.15091</i>			XI.15091	1.99	0.00%	17	12	81	39
5	<i>dup6</i>	NM_001045578,CR848381,BC118778,BC37790	MAP kinase phosphatase	XI.31935,XI.49155,XI.52935,XI.80026	1.94	0.00%	1009	773	3103	3568
6	<i>nkx6-2</i>	CT010540,XM_002937790	homeodomain transcription factor	XI.55860,XI.49827	1.68	0.00%	116	146	282	622
7	<i>dhrs3</i>	NM_001008431,CR848157,BC080136,CR		XI.77868,XI.59231,XI.83090	1.54	0.00%	1238	1702	3530	5058
8	<i>hoxa5</i>	BC088772,NM_001011405	homeodomain transcription factor	XI.58357	1.53	2.29%	32	27	62	117
9	<i>rgs2</i>	BC091089,NM_001030451		XI.49812,XI.76046,XI.85582	1.13	0.01%	89	43	218	79
10	<i>bhlhe40</i>	BC168818,BC169139,XM_002938312,BC1	basic helix-loop-helix (bHLH)	XI.19778,XI.26256	1.04	4.91%	114	47	191	131

Tab. 6.9 RNA-sequencing of explants 2h after RA addition in the presence of CHX. Normalized data (2h + CHX)

genes with > 60 mapped reads in samples with RA

no.	symbol	accession	gene function	UnigeneID_XL	log2FC +RA/-RA	FDR	-RA +CHX		+RA +CHX	
							A	B	A	B
1	<i>hoxa1</i>	BC080895,NM_001008016	homeodomain transcription factor	Xl.23512,Xl.283	4.82	0.00%	53	52	1352	1639
2	<i>hoxa3</i>	NM_001127429,BC166398	homeodomain transcription factor	Xl.9439	4.64	0.00%	9	7	167	286
3	<i>hoxa2</i>	CU025162	homeodomain transcription factor	Xl.12098,Xl.751	3.82	0.00%	21	21	314	304
4	<i>hoxb4</i>	BC090114,BC161550,NM_001123	Transcription factor zerknullt and related	Xl.54392,Xl.49715,Xl.72333	3.68	0.00%	27	14	216	286
5	<i>foxi4.2</i>	BC158378,NM_203934,BC064241	forkhead domain transcription factor	Xl.5369,Xl.34912	3.42	4.51%	140	14	658	512
6	<i>hoxb1</i>	XM_002938017	homeodomain transcription factor	Xl.85422	3.27	0.00%	11	12	130	102
7	<i>Xl.78389</i>			Xl.78389	3.25	4.90%	61	10	271	245
8	<i>Xl.15091</i>			Xl.15091	3.07	0.00%	13	5	84	76
9	<i>hoxa5</i>	BC088772,NM_001011405	homeodomain transcription factor	Xl.58357	3.02	0.00%	29	43	209	403
10	<i>Xl.67202</i>			Xl.67202	2.72	0.01%	26	58	220	338
11	<i>cyp26c1</i>	XM_002939091	electron transport	Xl.82105,Xl.1946,Xl.41946	2.72	0.00%	6	9	51	58
12	<i>znf703</i>	NM_001030507,BC093467	Zn-finger	Xl.1529,Xl.23634,Xl.69973	2.71	0.01%	1404	778	5731	6984
13	<i>cyp26a1</i>	NM_001016147,CR761993,BC171	retinoic acid hydroxylase	Xl.50113,Xl.456	2.50	0.00%	2167	5301	16230	22874
14	<i>s1pr5</i>	BC161459,NM_001127068		Xl.75787,Xl.9971	2.48	0.25%	83	129	532	657
15	<i>Xl.82687</i>			Xl.82687	2.47	0.00%	9	9	28	91
16	<i>sox9</i>	NM_001016853,CR855424	HMG-box transcription factor	Xl.28992,Xl.1690,Xl.82068	2.34	0.00%	39	70	179	382
17	<i>dusp6</i>	NM_001045578,CR848381,BC118	MAP kinase phosphatase	Xl.31935,Xl.49155,Xl.52935,Xl.80	2.30	0.00%	1363	1003	5859	5629
18	<i>Xl.45046</i>			Xl.45046	2.25	0.00%	80	51	279	334
19	<i>dhrs3</i>	NM_001008431,CR848157,BC080		Xl.77868,Xl.59231,Xl.83090	2.24	0.00%	1510	1943	7370	8933
20	<i>trib1</i>	XM_002938661		Xl.75411,Xl.81850	2.23	0.15%	32	14	77	154
21	<i>hoxd1</i>	CR760220,NM_001016678,BC170	homeodomain transcription factor	Xl.53491,Xl.11612,Xl.76294	2.22	0.01%	744	614	3612	2775
22	<i>Xl.9874</i>			Xl.9874	2.20	0.00%	31	55	154	243
23	<i>cebpd</i>	NM_001030414,CR942782,BC091	basic-leucine zipper (bZIP) transcription	Xl.29876,Xl.25857,Xl.81500	2.16	0.63%	122	27	332	252
24	<i>bhlhe40</i>	BC168818,BC169139,XM_002938	basic helix-loop-helix (bHLH) transcription	Xl.19778,Xl.26256	2.08	0.00%	129	71	508	337
25	<i>hnf1b</i>	CR760425,XM_002939634,XM_0	homeodomain transcription factor	Xl.65135,Xl.12667	2.08	0.00%	636	480	2760	1958
26	<i>gbx2.2</i>	BC088605,NM_001011472	homeodomain transcription factor	Xl.973	2.02	0.96%	12	17	60	65
27	<i>hoxc4</i>	XM_002936638	homeodomain transcription factor	Xl.69442	1.97	0.25%	29	21	89	110
28	<i>Xl.51509</i>			Xl.51509	1.97	0.07%	31	13	94	74
29	<i>tmem72</i>	BC158380,XM_002939555		Xl.17444	1.96	0.01%	25	9	102	39
30	<i>gata3</i>	NM_001004967,BC075479	zinc finger transcription factor	Xl.28002	1.95	4.90%	186	73	389	471

Appendix

no.	symbol	accession	gene function	UnigeneID_XL	log2FC +RA/-RA	FDR	-RA +CHX		+RA +CHX	
							A	B	A	B
31	<i>neurog2</i>	XM_002934243	basic helix-loop-helix transcription factor	XI.369,XI.370,XI.79613	1.83	0.18%	60	23	156	119
32	<i>c10orf140</i>	NM_001126649, BC159015, BC159		XI.52870,XI.80054	1.81	0.00%	126	128	355	532
33	<i>gbx2.1</i>	XM_002932000, XM_002932001	homeodomain transcription factor	XI.77345	1.79	0.00%	75	75	253	272
34	<i>nkx6-2</i>	CT010540, XM_002937790	homeodomain transcription factor	XI.55860, XI.49827	1.71	0.00%	249	281	580	1333
35	<i>Xl.29118</i>			XI.29118	1.70	1.64%	11	36	63	83
36	<i>rgs2</i>	BC091089, NM_001030451		XI.49812, XI.76046, XI.85582	1.69	0.00%	88	28	249	119
37	<i>foxb1</i>	CR761447, NM_001017084	winged helix transcription factor	XI.381	1.62	0.17%	85	80	201	316
38	<i>Xl.58101</i>			XI.58101	1.59	0.00%	101	109	283	358
39	<i>Xl.6091</i>			XI.6091	1.55	0.01%	35	26	90	91
40	<i>klb</i>	XM_002933470	beta-glucosidase		1.52	0.00%	31	24	79	81
41	<i>hoxd4</i>	XM_002935672, XM_002935673	homeodomain transcription factor	XI.34346, XI.85858	1.49	0.19%	47	51	128	150
42	<i>olig4</i>	BC161514, NM_001045715, CR848	transcription factor	XI.72230	1.46	0.00%	45	35	113	109
43	<i>hoxb8</i>	XM_002938021	homeodomain transcription factor	XI.79158, XI.9701	1.42	0.13%	39	17	105	49
44	<i>Xl.84363</i>			XI.84363	1.37	0.45%	67	58	146	178
45	<i>hoxb3</i>	CR848404, BC135406, NM_001015	homeodomain transcription factor	XI.79878, XI.80826	1.35	0.00%	69	75	202	171
46	<i>hoxa4</i>		homeodomain transcription factor		1.29	1.70%	156	97	232	360
47	<i>Xl.13431</i>			XI.13431	1.28	4.51%	23	17	61	41
48	<i>rara</i>	NM_001171194, CT025407	transcription factor, steroid receptor class	XI.158, XI.57139	1.21	0.24%	258	174	429	555
49	<i>myc</i>	BC064880, NM_204059, CR761143		XI.826, XI.1155	1.20	0.25%	1560	767	3167	1987
50	<i>igf3</i>	BC161167, CR848377, NM_001126		XI.12078, XI.78527	1.20	0.18%	54	32	108	91
51	<i>nr2f5</i>	XM_002938463	hormone receptor	XI.1157, XI.13423, XI.81917, XI.835	1.19	1.22%	46	43	136	74
52	<i>edn1</i>	XM_002932664, BC161190	secreted peptide precursor	XI.68930, XI.63796	1.16	0.57%	54	52	115	125
53	<i>hunk</i>	NM_001127077, BC161479		XI.24322, XI.12483, XI.83064	1.15	0.03%	649	566	1215	1468
54	<i>Xl.79790</i>			XI.79790	1.14	0.80%	22	49	55	102
55	<i>Xl.41047</i>			XI.41047	1.11	0.56%	68	52	188	86
56	<i>meis3</i>	CR760178, BC075589, NM_001006	homeodomain transcription factor	XI.23066, XI.452, XI.80020, XI.8297	1.09	0.07%	3434	2009	6277	5044
57	<i>kiaa0182</i>	XM_002936097, BC125792		XI.78028, XI.1433, XI.78276	1.08	0.46%	329	297	615	709
58	<i>tril</i>	XM_002933390		XI.73400, XI.78580	1.05	0.16%	895	413	1695	941
59	<i>Xl.74263</i>			XI.74263	1.04	4.90%	136	89	242	216
61	<i>fzd4</i>	XM_002936543	transmembrane receptor in the wnt	XI.460, XI.53888	0.93	0.69%	1032	741	1679	1690
60	<i>twist1</i>	NM_204084, BK006266, BC074558	transcription factor	XI.879, XI.23366, XI.68451, XI.8275	-1.10	4.50%	261	222	82	155

6.7 Nanostring analysis data for the verification of RA-responsiveness of putative RA-target genes

Tab. 6.10 Overview of Nanostring analysis results.

Indicated is the fold induction upon activation of RA-signaling and fold reduction upon inhibition of RA-signaling. Candidates highlighted in grey are confirmed RA-responsive genes.

no.	direct	gene	RA-inducibility fold induction +RA/-RA					RA-dependency fold reduction +RA/-RA			
			pancreatic organoids		whole embryo			dorsal tissue	whole embryo		
			1h	2h	st.12	st.13	st.14	st.11	st.12	st.13	st.14
1	•	<i>bhlhe40</i>	2.05	4.01	4.72	3.24	3.78	/	/	/	/
2	•	<i>c10orf140</i>	/	/	/	/	/	1.00	/	/	/
3		<i>cass4</i>	0.64	1.49	1.17	1.54	1.61	0.91	1.19	1.09	1.09
4		<i>cdx4</i>	1.45	2.09	1.26	1.24	1.00	1.15	1.14	1.25	1.19
5	•	<i>cebpd</i>	1.44	18.71	3.35	7.92	7.14	2.05	0.96	0.82	1.33
6		<i>cxcr7</i>	1.54	1.69	/	/	/	1.23	0.96	1.04	0.95
7	•	<i>cyp26a1</i>	4.39	14.23	6.70	13.96	14.19	2.29	1.81	1.44	1.53
8		<i>dact1-a/b</i>	0.89	1.51	1.82	1.89	1.74	1.07	1.08	1.01	1.28
9	•	<i>dhrs3</i>	5.87	8.86	4.13	7.43	7.80	2.76	1.78	1.56	2.05
10		<i>dusp5</i>	0.91	2.28	1.96	2.42	2.29	1.20	1.49	1.31	1.31
11	•	<i>dusp6</i>	2.86	5.39	3.55	4.47	4.43	1.31	1.05	1.27	0.99
12		<i>erf</i>	0.62	1.50	1.23	1.90	1.71	0.97	1.09	1.06	1.30
13		<i>fgfr4-a/b</i>	1.03	1.40	1.09	1.00	0.89	0.99	0.94	0.99	1.05
14	•	<i>foxh1</i>	0.65	2.49	1.42	1.56	1.49	1.02	1.32	1.72	1.41
15		<i>fst</i>	1.59	1.73	1.75	2.57	2.91	2.44	1.91	1.13	1.52
16	•	<i>fzd4</i>	1.27	2.26	1.92	2.87	2.51	0.90	1.43	1.61	1.90
17	•	<i>gbx2.1</i>	2.21	4.56	2.07	2.92	2.99	1.45	1.76	1.74	1.64
18		<i>hey1</i>	1.06	1.57	0.92	1.30	1.41	1.48	1.11	1.20	1.25
19	•	<i>hnf1b</i>	1.95	3.00	2.47	4.09	3.21	1.08	1.71	2.51	3.11
20	•	<i>hoxa1-b</i>	9.53	44.33	3.27	4.21	4.33	4.24	2.66	3.42	7.32
21	•	<i>hoxa2</i>	/	/	0.98	1.82	1.26	/	/	/	/
22	•	<i>hoxa3</i>	/	/	108.71	9.31	10.49	/	/	/	/
23	•	<i>hoxa5</i>	/	/	/	/	/	/	/	/	/
24	•	<i>hoxb1</i>	9.81	21.42	2.56	2.69	2.31	/	1.81	2.31	1.62
25	•	<i>hoxb3</i>	/	/	25.56	5.85	5.01	/	/	/	/
26	•	<i>hoxb4</i>	0.85	2.23	2.46	2.64	3.43	0.83	0.93	1.37	1.37
27	•	<i>hoxd1</i>	2.54	6.94	1.75	1.97	2.09	1.17	1.39	1.54	1.70
28	•	<i>hoxd4</i>	2.33	41.83	6.07	4.26	4.46	1.43	1.22	1.66	0.81
29	•	<i>hunk</i>	0.77	2.64	2.02	2.25	2.11	1.00	1.26	1.31	1.31
30	•	<i>igf3</i>	3.45	3.38	1.92	2.29	2.61	1.69	1.53	1.41	0.88
31	•	<i>kiaa0182</i>	0.47	2.04	1.07	1.56	1.85	1.01	1.30	1.31	1.12
32		<i>kirrel2</i>	0.66	1.87	1.41	1.22	1.21	1.39	1.09	1.17	1.23
33		<i>lhx1</i>	0.98	2.42	4.00	3.96	4.43	1.34	1.16	1.51	1.53
34	•	<i>meis-a</i>	1.35	2.59	1.96	2.58	2.72	1.39	1.74	1.56	1.41
35		<i>mespa</i>	2.86	7.19	1.73	2.19	1.35	1.39	/	/	/
36		<i>mespb</i>	3.53	2.51	1.02	1.26	1.05	1.04	0.96	0.81	1.09
37		<i>mxi1</i>	0.91	3.05	2.08	2.05	1.97	1.18	1.54	1.19	1.45
38	•	<i>myc-a/b</i>	0.60	1.99	1.19	1.30	1.26	/	1.14	1.56	1.22
39	•	<i>neurog2</i>	/	/	1.02	0.88	0.99	1.65	1.21	0.93	1.11
40	•	<i>nkx6-2</i>	1.52	4.32	2.49	2.38	3.48	2.09	1.84	1.37	1.07
41		<i>nodal1</i>	1.21	1.75	/	/	/	1.39	/	/	/

Appendix

no.	direct	gene	RA-inducibility fold induction +RA/-RA					RA-dependency fold reduction +RA/-RA			
			pancreatic organoids		whole embryo			dorsal tissue	whole embryo		
			1h	2h	st.12	st.13	st.14	st.11	st.12	st.13	st.14
42		<i>nodal2</i>	1.07	1.36	/	/	/	0.86	/	/	/
43	•	<i>nr2f5</i>	/	/	/	4.38	3.97	0.93	/	/	/
44		<i>pdgfb</i>	0.71	1.24	3.87	1.23	1.76	1.22	/	/	/
45		<i>pim1</i>	1.23	1.76	1.33	1.96	1.59	1.33	1.14	1.31	1.20
46		<i>pkdcc.1</i>	1.02	1.05	1.32	1.16	1.23	1.07	0.97	1.05	1.44
47		<i>prph</i>	/	31.75	4.68	5.07	3.60	/	2.85	2.39	1.63
48	•	<i>rara</i>	/	/	1.89	2.05	2.02	1.06	1.60	1.18	1.40
49		<i>rgs14</i>	2.40	4.24	/	/	/	/	/	/	/
50	•	<i>rgs2</i>	1.93	4.71	2.43	1.73	1.68	1.40	1.07	1.11	1.08
51	•	<i>sox9</i>	1.60	6.45	2.96	2.21	2.40	0.84	1.15	1.44	0.87
52		<i>spry2</i>	1.31	1.61	1.34	1.48	1.55	0.90	0.96	0.95	1.03
53		<i>stox1</i>	0.81	1.04	0.92	1.13	0.95	0.87	1.18	0.93	1.15
54		<i>tdgf1p2-a/b</i>	/	/	/	/	/	/	/	/	/
55	•	<i>tmem72</i>	2.74	5.25	1.77	2.50	1.69	1.46	1.15	1.33	1.49
56	•	<i>trib1</i>	0.52	4.58	0.73	1.27	1.00	/	1.10	0.90	1.04
57	•	<i>twist1</i>	0.55	0.71	0.77	0.30	0.34	1.52	0.99	0.91	0.75
58		<i>txnip</i>	2.72	7.40	1.37	2.10	1.36	1.14	0.91	1.06	1.25
59	•	<i>Xl.15091</i>	/	/	/	/	/	/	/	/	/
60		<i>Xl.16263</i>	/	/	/	/	/	/	/	/	/
61		<i>Xl.32109</i>	/	/	/	/	/	/	/	/	/
62	•	<i>Xl.45046</i>	1.27	7.03	1.84	2.27	2.50	1.53	2.02	1.97	1.39
63		<i>Xl.47239</i>	0.91	3.34	1.70	1.71	1.62	1.00	1.41	1.77	0.96
64		<i>Xl.4906</i>	1.11	3.14	1.15	0.99	0.78	0.84	0.97	1.04	1.18
65	•	<i>Xl.51509</i>	1.63	30.14	3.88	4.96	4.33	2.23	1.74	1.78	1.90
66		<i>Xl.57027</i>	0.64	14.12	2.72	1.49	1.44	0.76	/	/	/
67		<i>Xl.57926</i>	0.84	1.99	2.37	2.99	2.91	1.27	1.43	1.53	1.56
68	•	<i>Xl.58101</i>	/	/	/	/	/	/	/	/	/
69		<i>Xl.59256</i>	/	/	/	/	/	/	/	/	/
70	•	<i>Xl.6091</i>	/	/	/	/	/	0.75	/	/	/
71	•	<i>Xl.67202</i>	/	/	/	/	/	/	/	/	/
72		<i>Xl.68408</i>	/	/	/	/	/	/	/	/	/
73		<i>Xl.70850</i>	/	/	/	/	/	/	/	/	/
74		<i>Xl.71159</i>	0.70	0.66	0.68	0.51	0.48	0.95	0.79	0.86	0.88
75	•	<i>Xl.74263</i>	/	/	/	/	/	/	/	/	/
76	•	<i>Xl.79790</i>	0.97	2.24	2.18	2.07	1.40	/	/	/	/
77		<i>Xl.80297</i>	1.64	1.90	2.08	1.94	1.99	1.23	1.19	1.01	1.00
78		<i>Xl.8753</i>	/	/	/	/	/	1.00	/	/	/
79		<i>Xl.85251</i>	/	/	/	/	/	1.00	/	/	/
80		<i>Xl.9822</i>	0.54	2.23	/	/	/	2.29	/	/	/
81	•	<i>Xl.9874</i>	/	/	/	/	/	/	/	/	/
82	•	<i>znf703</i>	1.41	8.98	1.94	2.52	2.54	1.37	1.64	1.76	1.55

Tab. 6.11 Raw data of RA-inducibility in explants

gene	1h				2h			
	/	RA	CHX	RA / CHX	/	RA	CHX	RA / CHX
bhlhe40	23	72	2	81	53	94	48	123
c10orf140	2	7	1	6	6	6	5	9
cass4	251	266	5	345	310	261	386	492
cdx4	429	988	12	1212	780	808	1150	1422
cebpd	40	91	1	51	24	122	28	154
cxcr7	197	487	4	637	339	309	539	677
cyp26a1	460	3225	6	2458	572	4387	599	5018
dact1-a	334	349	5	321	327	247	378	516
dact1-b	1509	2175	41	2537	1822	1511	2206	3092
dhrs3	184	1779	5	1419	317	1496	413	2206
dusp5	796	1165	31	1166	876	1089	1091	1753
dusp6	342	1411	10	1632	463	1342	679	2460
e_Cerberus	8391	14195	241	13089	14634	6226	11690	11101
e_darmin	4	12	1	5	10	10	4	6
e_Sox17alpha	2721	3750	91	4838	3950	2018	5675	5995
e_Sox17beta	1512	2351	72	2890	1840	974	3285	3269
e_TGIF2	1048	1219	8	1276	1388	607	1479	1514
e_vpp1	40	46	1	36	55	32	38	36
ec_Sox2	284	463	3	509	195	538	564	882
ec_tubb2b	18	27	1	33	41	23	28	25
ec_xk81a1	468	308	8	110	105	290	104	351
em_BMP2-a	426	631	6	519	689	337	471	541
em_BMP4-a	1432	2078	37	2404	2363	1291	2235	3053
erf	369	376	14	394	394	319	396	494
fgfr4-a	735	1226	26	1043	917	700	898	1050
fgfr4-b	471	833	18	810	614	487	652	964
foxh1	291	313	5	350	234	308	285	447
fst	240	614	8	958	525	493	482	1494
fzd4	362	741	13	783	444	542	579	1102
gbx2.1	28	91	1	108	39	71	43	190
hey1	92	176	3	146	117	87	122	174
hk_g6pd	261	392	10	385	404	226	337	298
hk_gapdh	177	328	5	243	307	188	263	244
hk_H4	81031	121843	2423	146020	130802	67733	157329	153353
hk_ODC	6783	10937	313	10021	12306	6377	9821	9213
hnf1b	194	603	8	445	413	665	300	905
hoxa1-a	1	25	1	35	1	40	6	66
hoxa1-b	14	127	3	164	14	193	22	407
hoxa2-a	14	33	1	31	22	15	21	29
hoxa3	5	30	1	30	8	52	7	130
hoxa5	2	21	1	20	1	22	3	59
hoxb1	7	32	1	26	12	21	12	44
hoxb3	6	15	1	21	11	26	15	27
hoxb4	35	52	2	65	47	47	49	101
hoxd1	265	1114	12	1386	393	1459	704	2098
hoxd4	2	15	1	18	4	38	7	66
hunk	351	438	6	562	367	520	451	972
igf3	17	75	1	86	42	62	35	119
kiaa0182	311	244	1	212	236	256	247	435
kirrel2	98	119	2	158	109	104	128	221
lhx1	223	356	6	550	241	309	355	879
m_Chordin	14236	20467	597	20254	21964	11183	18640	20494
m_Xbra-a/b	1938	2480	56	3743	3593	1911	4577	3849
m_Xwnt8	1109	1508	33	1488	1577	739	1655	1494
me_ventx2.1	612	1298	40	2482	752	428	3005	4569
meis3-a	333	725	3	729	457	658	489	1127
mespa-a	14	50	1	187	21	38	87	280

gene	1h				2h			
	/	RA	CHX	RA / CHX	/	RA	CHX	RA / CHX
mespb	76	412	11	1044	236	313	475	1368
mxi1	164	244	1	221	174	276	169	373
myc-a	46	51	1	57	54	50	45	105
myc-b	217	458	6	435	315	537	306	587
ndrg1-a	1	2	1	3	1	1	2	4
ndrg1-b	2	3	1	2	1	1	3	1
neurog2	18	29	1	30	18	45	26	50
nkx6-2	251	613	1	522	254	579	224	945
nodal1	89	160	6	311	107	88	219	500
nodal2	454	788	20	887	510	376	944	968
nr2f5	15	28	1	29	18	21	13	32
pdgfb	32	43	1	41	32	18	44	35
pim1	140	277	6	408	237	222	330	614
pkdcc.1	648	1072	42	1181	930	534	1009	1140
prph	12	14	1	9	7	30	7	18
rara	26	23	1	20	31	36	24	39
rgs14	29	102	1	47	41	71	32	45
rgs2	42	125	1	69	37	68	41	135
sox9-a/b	26	64	1	78	30	67	34	118
spry2	769	1627	27	1854	1316	1172	1807	2027
stox2	318	420	6	398	485	274	366	468
tdgf1p2-a	9	33	1	40	10	18	18	63
tdgf1p2-b	6	10	1	6	7	7	12	23
tmem72	29	115	1	58	39	81	26	75
trib1	30	32	1	40	25	36	32	93
twist1-a	185	163	5	199	241	94	211	146
txnip	27	105	2	133	36	92	116	297
Xl.15091	1	1	1	2	1	1	1	2
Xl.16263	3	2	1	1	2	1	2	2
Xl.32109	4	12	1	10	9	3	12	19
Xl.45046	88	180	4	206	77	246	96	460
Xl.47239	52	80	1	67	48	69	50	93
Xl.4906	306	547	9	700	310	544	690	1161
Xl.51509	18	44	1	50	18	94	23	111
Xl.57027	29	36	1	31	16	31	34	61
Xl.57926	331	451	2	428	372	398	426	783
Xl.58101	4	1	1	1	2	1	1	5
Xl.59256	1	2	1	2	3	1	1	2
Xl.6091	14	21	1	31	22	7	29	22
Xl.67202	2	7	1	3	5	5	1	3
Xl.68408	1	1	1	2	1	1	1	3
Xl.70850	3	5	1	2	4	6	5	12
Xl.71159	567	644	20	1114	829	303	1403	1191
Xl.74263	5	6	1	6	3	1	5	6
Xl.79790	20	34	1	30	25	20	23	48
Xl.80297	233	610	11	816	488	501	695	1084
Xl.85251	1	3	1	2	3	1	6	3
Xl.8753	2	8	1	3	5	5	3	5
Xl.9822	36	38	1	24	33	29	27	41
Xl.9874	5	13	1	10	5	13	8	13
znf703	538	1221	8	1628	430	2069	817	3756
NEG_A	3	1	1	4	3	3	1	1
NEG_B	3	1	1	4	5	3	6	3
NEG_C	3	1	1	1	1	1	1	1
NEG_D	4	4	1	2	4	3	1	1
NEG_E	4	4	1	3	3	3	3	3
NEG_F	7	9	1	16	9	6	11	11
NEG_G	2	1	1	1	1	1	1	1
NEG_H	3	2	1	1	3	1	4	3
POS_A	5323	5854	114	5160	6512	4601	5552	6190
POS_B	1789	2124	32	1839	2227	1663	1784	2095
POS_C	519	637	12	580	713	507	577	700
POS_D	127	151	3	106	126	94	134	162
POS_E	18	21	1	24	27	17	31	26
POS_F	10	14	1	13	14	7	14	17

Tab. 6.12 Normalized data of RA-inducibility in explants

Indicated are the Nanostring counts which were normalized to the internal positive controls and Odc and with subtracted mean of the negative controls as described in the “Materials and Methods” section.

gene	1h				2h			
	/	RA	CHX	RA / CHX	/	RA	CHX	RA / CHX
bhlhe40	20	43	65	48	28	112	26	91
c10orf140	1	1	32	1	1	2	1	1
cass4	285	183	165	249	206	322	283	393
cdx4	491	703	397	909	532	1011	865	1153
cebpd	40	57	32	25	8	148	11	116
cxcr7	222	342	132	471	226	383	400	544
cyp26a1	527	2313	198	1857	388	5514	445	4095
dact1-a	381	243	165	230	218	305	277	412
dact1-b	1744	1557	1360	1918	1254	1895	1669	2520
dhrs3	207	1272	165	1066	211	1876	304	1795
dusp5	917	830	1028	874	598	1364	820	1424
dusp6	390	1007	331	1229	312	1683	506	2003
e_Cerberus	9728	10209	7997	9952	10130	7828	8889	9071
e_darmin	1	0	32	1	1	7	1	1
e_Sox17alpha	3150	2691	3019	3669	2728	2533	4310	4894
e_Sox17beta	1748	1684	2389	2186	1266	1220	2490	2664
e_TGIF2	1209	869	265	957	953	758	1115	1229
e_vpp1	40	25	32	13	29	34	18	20
ec_Sox2	323	325	99	374	126	671	419	712
ec_tubb2b	14	11	32	11	20	23	11	11
ec_xk81a1	536	213	265	70	64	359	69	277
em_BMP2-a/b	488	446	198	381	469	418	348	433
em_BMP4-a/b	1655	1487	1227	1816	1628	1618	1691	2488
erf	421	262	464	286	264	395	291	394
fgfr4-a	846	874	862	780	627	875	673	849
fgfr4-b	540	591	596	603	417	607	486	779
foxb1	331	217	165	252	153	382	206	356
fst	272	433	265	715	355	614	356	1212
fzd4	413	525	430	582	299	676	430	892
gbx2.1	26	57	32	68	18	83	22	146
hey1	100	118	99	97	72	103	82	133
hk_g6pd	296	274	331	279	271	278	246	234
hk_gapdh	199	228	165	171	204	231	190	190
hk_H4	94003	87697	80412	111161	90615	85220	119763	125437
hk_ODC	7863	7864	10387	7616	8517	8018	7466	7527
hnf1b	218	426	265	325	277	831	218	731
hoxa1-a	1	10	32	13	1	44	1	44
hoxa1-b	10	83	99	111	1	237	6	323
hoxa2-a	10	15	32	10	6	13	5	14
hoxa3	1	13	32	9	1	59	1	97
hoxa5	1	7	32	1	1	22	1	38
hoxb1	1	15	32	6	1	20	1	26
hoxb3	0	2	32	2	1	27	1	12
hoxb4	34	29	65	35	24	53	27	73
hoxd1	301	793	397	1041	264	1830	525	1706
hoxd4	1	2	32	1	1	42	1	44
hunk	401	307	198	414	246	648	333	785
igf3	13	46	32	51	20	72	16	88
kiaa0182	354	167	32	147	155	316	177	346
kirrel2	107	77	65	106	67	125	87	171
lhx1	252	248	198	405	158	383	260	709

Appendix

gene	1h				2h			
	/	RA	CHX	RA / CHX	/	RA	CHX	RA / CHX
m_Chordin	16509	14724	19812	15407	15209	14065	14180	16755
m_Xbra-a/b	2242	1777	1858	2836	2481	2399	3474	3139
m_Xwnt8	1280	1077	1094	1119	1084	924	1249	1212
me_ventx2.1-b	703	926	1327	1876	512	533	2277	3728
meis3-a	380	513	99	541	308	822	362	912
mespa-a	10	28	32	128	6	42	56	219
mespb	82	288	364	781	155	388	351	1109
mxi1	184	167	32	154	112	341	118	295
myc-a	47	28	32	29	29	57	24	76
myc-b	245	321	198	317	209	670	222	470
ndrg1-a	1	1	32	1	1	1	1	1
ndrg1-b	1	1	32	1	1	1	1	1
neurog2	14	12	32	9	4	51	9	31
nkx6-2	285	433	32	383	167	723	160	763
nodal1	97	107	198	223	65	105	156	399
nodal2	520	559	663	661	345	467	708	782
nr2f5	11	12	32	8	4	20	1	16
pdgfb	30	22	32	17	13	17	23	19
pim1	156	191	198	297	155	273	241	493
pkdcc.1	745	763	1393	885	636	666	758	923
prph	7	2	32	1	1	32	1	5
rara	24	8	32	1	13	39	8	22
rgs14	27	65	32	22	20	83	14	27
rgs2	42	82	32	39	17	80	21	101
sox9-a/b	24	38	32	45	12	78	15	87
spry2	886	1163	895	1398	903	1469	1365	1648
stox2	362	294	198	289	327	339	268	373
tdgf1p2-a	4	15	32	16	1	17	3	42
tdgf1p2-b	0	1	32	1	1	3	1	9
tmem72	27	74	32	30	18	96	9	52
trib1	28	15	32	16	9	39	14	66
twist1-a	208	109	165	137	158	112	150	110
txnip	25	67	65	87	16	110	78	233
XI.15091	1	1	32.19	1	1	1	1	1
XI.16263	1	1	32	1	1	1	1	1
XI.32109	1	0	32	1	1	1	1	6
XI.45046	95	121	132	143	45	304	62	367
XI.47239	54	49	32	37	25	81	27	66
XI.4906	348	385	298	519	206	678	515	940
XI.51509	14	23	32	24	4	112	7	81
XI.57027	27	17	32	10	2	33	15	40
XI.57926	377	316	65	312	249	495	314	631
XI.58101	1	1	32	1	1	1	1	1
XI.59256	1	1	32	1	1	1	1	1
XI.6091	10	7	32	10	6	3	11	8
XI.67202	1	1	32	1	1	0	1	1
XI.68408	1	1	32	1	1	1	1	1
XI.70850	1	1	32	1	1	2	1	0
XI.71159	651	455	663	834	566	375	1058	965
XI.74263	1	1	32	1	1	1	1	1
XI.79790	17	16	32	9	9	19	7	30
XI.80297	264	431	364	607	329	624	519	877
XI.85251	1	1	32	1	1	1	1	1
XI.8753	1	1	32	1	1	0	1	1
XI.9822	35	19	32	4	14	30	10	24
XI.9874	1	1	32	1	1	10	1	1
znf703	618	870	265	1225	289	2597	611	3063

Tab. 6.13 Raw data of RA-inducibility in whole embryos

CE = control embryo; RA = CE + RA

gene	s22 (A)						s23 (B)					
	st.12		st.13		st.14		st.12		st.13		st.14	
	CE	RA	CE	RA	CE	RA	CE	RA	CE	RA	CE	RA
bhlhe40	21	30	29	77	22	119	19	20	32	68	49	84
c10orf140	5	2	4	6	5	8	6	3	3	3	1	3
cass4	189	147	241	303	151	356	207	173	172	328	273	362
cdx4	1484	1521	1873	2325	1313	2015	1863	1425	1615	2082	2163	1852
cebpd	42	74	28	169	63	215	82	192	47	229	38	259
cxcr7	148	111	114	162	96	161	201	166	128	148	131	161
cyp26a1	814	2337	884	11847	612	12983	1491	8338	740	11128	951	11009
dact1-a	99	82	75	104	67	99	121	139	91	129	147	99
dact1-b	655	759	630	1099	493	1217	974	1272	613	1204	794	1227
dhrs3	378	730	432	2631	308	3191	630	2268	359	3272	429	2960
dup5	308	319	308	694	245	841	390	631	339	884	433	839
dup6	349	506	491	1709	322	2063	314	1002	304	1732	481	1842
e_Cerberus	254	457	89	118	80	66	1461	943	491	695	556	313
e_darmin	693	873	480	1189	911	1490	959	519	530	1094	1209	1108
e_Sox17alph	525	531	623	478	516	455	807	420	565	576	725	459
e_Sox17beta	563	509	570	521	426	444	736	409	577	487	684	438
e_TGIF2	192	190	310	234	186	243	460	293	299	281	243	141
e_vpp1	70	78	35	52	71	35	162	81	93	95	123	52
ec_Sox2	890	659	1139	841	812	1039	1430	1068	1001	1412	1067	1340
ec_tubb2b	43	37	70	77	52	119	39	21	43	43	55	60
ec_xk81a1	3456	2400	6564	6466	5765	8264	4112	2638	6402	8453	10511	8033
em_BMP2-a	457	458	324	399	368	494	661	238	443	308	668	416
em_BMP4-a	1624	1501	1377	1240	1026	1058	2915	1512	1660	1298	1863	1000
erf	221	151	193	299	174	422	304	302	219	508	308	454
fgfr4-a	1100	927	1113	971	894	905	1742	972	1357	1228	1511	1133
fgfr4-b	469	429	526	498	396	510	781	521	468	520	608	485
foxb1	236	197	282	445	165	402	290	321	257	406	338	403
fst	169	183	241	373	183	606	407	559	215	814	276	828
fzd4	450	537	311	1006	328	999	641	871	383	938	448	1037
gbx2.1	384	330	351	910	253	1058	379	710	330	1003	466	1220
hey1	118	117	156	213	101	192	165	68	165	190	163	207
hk_g6pd	186	147	192	161	124	147	296	147	137	165	207	152
hk_gapdh	125	101	165	156	125	245	123	102	120	158	120	186
hk_H4	66093	54788	86152	78237	62183	66486	146073	84833	93587	84235	112190	93322
hk_ODC	7511	6970	8871	9650	6875	9427	9779	6085	6549	7328	8264	6815
hnf1b	416	402	398	1562	425	1928	432	983	388	1678	630	1769
hoxa1-a	18	31	27	140	35	149	40	150	36	208	51	225
hoxa1-b	153	247	251	897	196	994	264	711	236	1060	280	1209
hoxa2-a	17	15	31	38	19	32	30	16	17	32	35	34
hoxa3	61	48	79	345	47	498	12	183	33	401	57	491
hoxa5	4	8	11	61	12	70	5	114	12	200	12	143
hoxb1	132	129	199	507	158	519	98	208	151	422	203	390
hoxb3	18	19	24	73	24	99	16	49	20	102	34	123
hoxb4	39	35	60	129	40	160	57	96	52	141	62	169
hoxd1	1309	1648	1378	2785	931	2703	2262	2791	1570	3129	1451	2769
hoxd4	100	106	193	400	106	650	49	230	107	708	228	892
hunk	623	582	684	1197	468	1414	846	1517	531	1550	801	1468
igf3	73	74	116	236	93	291	94	134	127	315	123	327
kiaa0182	274	215	361	519	215	631	578	435	376	645	498	700
kirrel2	180	174	212	287	195	359	361	363	360	388	403	398
lhx1	83	126	120	327	81	347	90	287	87	468	99	447

Appendix

gene	s22 (A)						s23 (B)					
	st.12		st.13		st.14		st.12		st.13		st.14	
	CE	RA	CE	RA	CE	RA	CE	RA	CE	RA	CE	RA
m_Chordin	1302	1330	1451	849	1085	1034	2672	1872	1554	1423	1495	1220
m_Xbra-a/b	955	912	961	439	533	233	2013	1001	829	440	888	310
m_Xwnt8	396	297	491	240	233	191	859	585	383	514	337	366
me_ventx2.	1328	748	992	1118	179	921	2356	1431	1200	2000	1507	848
meis3-a	703	649	706	1715	505	2034	794	1393	633	1803	934	2026
mespa-a	28	45	27	45	32	61	43	30	37	68	46	47
mespb	196	146	180	199	94	151	348	246	164	243	193	164
mxi1	359	397	330	514	278	657	434	735	309	816	384	769
myc-a	88	101	130	156	101	181	103	60	91	130	144	156
myc-b	1067	1042	1490	1579	907	1505	1378	841	1299	1057	1730	1082
ndrg1-a	1	1	2	1	3	1	1	2	1	1	1	2
ndrg1-b	1	2	2	1	2	6	1	2	2	3	6	2
neurog2	93	73	83	68	49	74	174	115	119	110	86	69
nkx6-2	94	126	112	224	73	352	159	305	124	334	138	378
nodal1	12	6	18	11	10	11	10	13	3	8	3	9
nodal2	13	6	13	4	1	4	14	6	6	5	8	7
nr2f5	19	16	90	347	103	590	18	41	72	311	144	437
pdgfb	15	12	21	22	19	28	17	16	16	19	23	29
pim1	174	179	166	354	133	371	328	284	210	357	317	319
pkdcc.1	213	233	265	266	229	343	512	399	338	470	387	484
prph	50	39	82	312	56	237	49	179	89	493	114	368
rara	54	41	88	97	54	146	52	72	58	175	115	190
rgs14	1	1	1	1	1	1	1	3	1	3	1	4
rgs2	66	144	180	273	119	346	112	131	93	202	124	142
sox9-a/b	107	176	222	483	164	474	147	358	184	431	271	667
spry2	290	339	347	465	239	539	509	395	344	579	389	520
stox2	211	147	169	206	153	204	274	169	171	178	254	219
tdgf1p2-a	25	33	42	72	38	92	37	64	28	97	46	110
tdgf1p2-b	9	6	3	9	9	18	3	10	4	11	11	14
tmem72	104	98	142	314	169	342	154	233	202	541	293	499
trib1	52	40	51	75	37	60	53	21	51	45	63	48
twist1-a	215	188	287	92	244	129	261	83	267	96	374	110
txnip	231	280	207	465	233	488	110	83	115	207	209	212
XI.15091	1	2	6	2	2	2	2	1	1	3	4	4
XI.16263	2	2	1	1	1	3	3	1	2	1	5	2
XI.32109	11	5	8	14	3	8	11	7	10	7	5	19
XI.45046	324	316	497	919	311	1116	508	773	478	1342	694	1333
XI.47239	65	54	82	130	72	160	50	58	76	131	101	137
XI.4906	603	455	578	568	489	626	1131	880	744	773	1062	614
XI.51509	66	79	94	339	74	447	58	166	72	420	133	446
XI.57027	35	33	44	60	35	75	42	76	38	52	70	74
XI.57926	232	350	276	693	160	862	430	757	309	1003	511	823
XI.58101	2	1	2	1	1	5	3	3	2	3	2	1
XI.59256	1	1	1	2	1	2	1	1	1	1	2	5
XI.6091	10	9	16	11	7	14	17	8	14	19	17	18
XI.67202	2	2	4	2	3	1	7	4	3	7	5	1
XI.68408	1	2	3	3	1	3	1	1	1	3	1	1
XI.70850	3	6	5	6	4	11	17	8	7	12	10	13
XI.71159	608	431	775	413	494	382	929	306	629	316	652	258
XI.74263	6	1	1	5	2	3	2	3	1	7	2	4
XI.79790	29	23	60	82	50	75	49	77	47	113	86	114
XI.80297	63	77	72	134	61	135	110	161	77	139	69	127
XI.85251	1	1	5	1	2	4	6	3	3	2	4	2
XI.8753	1	1	1	2	1	5	2	3	2	5	5	4
XI.9822	13	12	23	8	11	10	23	18	16	23	32	9
XI.9874	4	4	8	3	5	7	5	3	2	3	2	3
znf703	2494	2707	2278	5979	1642	6561	2789	4455	2505	6285	3439	6863
NEG_A	2	2	6	4	2	4	5	3	2	4	5	7
NEG_B	2	4	3	3	1	2	5	3	3	7	5	9
NEG_C	1	1	1	1	1	1	1	1	1	1	1	1
NEG_D	1	1	2	1	2	1	1	3	2	5	4	3
NEG_E	2	1	6	2	2	7	4	4	3	2	4	5
NEG_F	8	5	12	10	9	8	14	13	9	9	16	8
NEG_G	1	1	1	1	1	2	1	1	1	1	1	1
NEG_H	1	3	1	1	1	5	1	3	1	1	2	2
POS_A	4427	5014	6295	5330	5094	4745	6726	4348	5441	6022	7964	7603
POS_B	1739	1975	2557	2088	2053	1910	2829	1780	2058	2343	2986	2844
POS_C	511	607	814	686	616	580	787	555	592	718	938	788
POS_D	124	135	160	131	144	121	158	105	133	135	176	184
POS_E	15	21	31	30	18	18	22	35	16	23	38	36
POS_F	4	13	13	6	13	7	13	10	17	10	20	21

Tab. 6.14 Normalized data of RA-inducibility in whole embryos

Indicated are the Nanostring counts which were normalized to the internal positive controls and *Odc* and with subtracted mean of the negative controls as described in the "Materials and Methods" section.

CE = control embryo; RA = CE + RA

gene	A						B					
	st. 12		st. 13		st. 14		st. 12		st. 13		st. 14	
	CE	RA	CE	RA	CE	RA	CE	RA	CE	RA	CE	RA
bhlhe40	17	35	15	68	22	114	2	13	29	62	32	74
c11orf140	1	1	1	1	1	1	1	1	1	1	1	1
cass4	216	193	214	293	188	331	147	214	193	331	245	354
cdx4	1666	2143	1743	2316	1693	1912	1429	1764	1876	2151	2138	1858
cebpd	41	94	15	159	74	196	52	228	47	228	22	251
cxcr7	160	144	95	152	117	144	143	195	141	144	120	152
cyp26a1	912	3142	816	11789	785	12369	1142	11377	855	11536	888	11199
dact1-a	115	115	59	95	79	85	82	162	98	124	125	89
dact1-b	731	1117	579	1185	632	1151	742	1573	717	1239	739	1227
dhrs3	419	978	393	2611	391	3133	475	2814	412	3385	393	2976
dusp5	341	424	277	682	320	793	289	775	387	917	396	836
dusp6	386	676	448	1693	419	1958	231	1237	347	1787	442	1848
e_Cerberus	279	611	72	118	96	54	1118	1163	565	711	513	315
e_darmin	774	1171	438	1175	1172	1411	729	635	611	1125	1133	1117
e_Sox17alpha	585	720	572	467	662	425	612	512	652	588	673	452
e_Sox17beta	628	681	522	520	544	414	557	498	665	495	634	431
e_TGIF2	219	251	279	224	233	223	343	354	342	282	216	131
e_vpp1	72	100	21	43	84	24	112	89	111	89	112	42
ec_Sox2	996	882	1155	828	1144	981	1194	1319	1160	1455	998	1341
ec_tubb2b	41	44	54	68	60	114	17	15	42	35	38	50
ec_xk81a1	3890	3227	6138	6431	7459	7870	3169	3275	7459	8762	9957	8196
em_BMP2-a/b	518	611	292	388	469	462	499	285	519	320	619	419
em_BMP4-a/b	1824	2116	1278	1226	1321	1000	2243	1872	1928	1337	1753	998
erf	242	198	169	289	218	393	222	365	247	517	278	447
fgfr4-a	1233	1243	1131	958	1151	854	1335	1200	1575	1264	1419	1133
fgfr4-b	522	572	481	487	515	477	592	638	538	530	562	479
foxh1	259	260	252	434	216	374	212	388	292	411	316	396
fst	184	241	214	362	229	569	312	685	243	835	247	825
fzd4	511	718	280	993	417	943	483	1174	439	963	412	1136
gbx2.1	426	439	317	897	320	1000	281	873	377	1132	428	1221
hey1	126	152	134	213	123	174	115	73	184	187	141	198
hnf1b	462	536	361	1547	543	1829	321	1213	445	1731	583	1774
hoxa1-a	13	36	14	131	38	133	18	175	34	216	34	216
hoxa1-b	166	327	223	884	246	939	191	874	267	1190	251	1219
hoxa2-a	12	15	17	29	17	21	11	8	12	23	19	23
hoxa3	62	59	62	335	53	466	1	216	31	416	40	485
hoxa5	1	5	1	52	8	58	1	131	6	198	1	133
hoxb1	142	168	175	496	197	486	63	248	168	428	178	383
hoxb3	13	21	12	64	23	85	1	50	15	96	18	113
hoxb4	37	42	45	119	44	143	31	118	53	136	44	160
hoxd1	1469	2214	1279	2764	1198	2568	1738	3466	1823	3237	1362	2784
hoxd4	116	137	169	389	129	612	25	275	117	725	212	889
hunk	695	778	629	1183	598	1339	642	1879	611	1598	745	1472
igf3	75	94	97	226	113	268	60	155	141	317	112	319
kiaa1182	312	284	327	518	272	592	434	531	432	659	458	696
kirrel2	196	229	187	277	245	333	266	442	412	393	368	392
lhx1	87	164	112	317	97	322	57	346	93	476	80	441

Appendix

gene	A						B					
	st. 12		st. 13		st. 14		st. 12		st. 13		st. 14	
	CE	RA	CE	RA	CE	RA	CE	RA	CE	RA	CE	RA
m_Chordin	1462	1786	1348	836	1398	977	2155	2322	1815	1467	1414	1221
m_Xbra-a/b	1170	1223	889	428	683	213	1545	1236	959	447	828	312
m_Xwnt8	439	395	448	230	294	173	652	717	439	523	315	358
me_ventx2.1-b	1491	1112	918	1114	224	869	1811	1771	1392	2165	1415	845
meis3-a	786	869	650	1699	646	1931	612	1724	731	1862	872	2134
mespa-a	25	55	14	36	34	49	21	26	35	62	29	37
mespb	214	191	157	189	114	135	256	295	183	242	169	155
mxi1	398	529	297	513	352	617	323	914	352	837	350	765
myc-a	92	132	111	146	123	163	67	63	98	125	122	147
myc-b	1196	1398	1384	1563	1167	1426	1154	1136	1517	1187	1627	1181
ndrg1-a	1	1	1	1	1	1	1	1	1	1	1	1
ndrg1-b	1	1	1	1	1	1	1	1	1	1	1	1
neurog2	98	93	66	59	56	61	122	132	132	114	67	59
nkx6-2	99	164	93	214	87	326	111	368	137	337	116	372
nodal1	7	3	5	2	5	1	1	5	1	1	1	1
nodal2	8	3	1	1	1	1	1	1	1	1	1	1
nr2f5	14	16	73	337	126	553	1	40	76	313	122	431
pdgfb	10	12	8	13	17	18	1	8	12	10	7	18
pim1	189	236	144	343	164	345	242	342	237	362	286	311
pkdcc.1	233	318	237	256	289	318	383	486	386	478	353	478
prph	49	47	65	312	65	217	25	211	96	512	94	361
rara	54	50	72	88	62	131	27	78	60	172	95	182
rgs14	1	1	1	1	1	1	1	1	1	1	1	1
rgs2	67	189	157	263	146	322	74	152	111	200	113	132
sox9-a/b	114	232	196	472	215	443	112	434	217	437	243	662
spry2	320	451	313	454	312	515	381	482	393	592	355	514
stox2	232	193	147	196	191	185	199	199	191	175	227	211
tdgf1p2-a	21	39	28	63	41	79	16	68	25	92	29	111
tdgf1p2-b	3	3	1	1	4	8	1	2	1	2	1	3
tmem72	111	127	121	314	211	317	116	279	228	551	264	493
trib1	52	48	36	66	41	48	28	15	51	37	45	38
twist1-a	235	248	257	83	318	114	189	92	313	90	341	111
txnip	253	372	182	454	294	456	72	92	126	215	184	213
XI.15091	1	1	1	1	1	1	1	1	1	1	1	1
XI.16263	1	1	1	1	1	1	1	1	1	1	1	1
XI.32109	5	1	1	5	1	1	1	1	4	1	1	8
XI.45046	358	421	454	916	395	1155	381	952	549	1383	644	1334
XI.47239	66	67	65	121	85	143	26	62	82	126	81	127
XI.4906	673	617	530	557	626	588	862	1185	860	792	993	619
XI.51509	67	112	76	329	88	417	32	195	76	426	112	439
XI.57027	32	39	30	52	38	62	20	83	36	44	52	64
XI.57926	255	466	247	681	199	813	320	932	352	1132	471	820
XI.58101	1	1	1	1	1	1	1	1	1	1	1	1
XI.59256	1	1	1	1	1	1	1	1	1	1	1	1
XI.6091	4	7	3	2	1	4	1	1	8	10	2	7
XI.67202	1	1	1	1	1	1	1	1	1	1	1	1
XI.68408	1	1	1	1	1	1	1	1	1	1	1	1
XI.71159	679	575	714	412	632	355	716	370	726	318	614	249
XI.70850	1	3	1	1	1	1	1	1	1	3	1	2
XI.74263	1	1	1	1	1	1	1	1	1	1	1	1
XI.79790	26	26	45	73	57	62	25	84	47	117	67	114
XI.81297	64	98	56	124	71	120	72	189	82	134	51	117
XI.85251	1	1	1	1	1	1	1	1	1	1	1	1
XI.8753	1	1	1	1	1	1	1	1	1	1	1	1
XI.9822	8	12	10	1	6	1	5	12	12	14	16	1
XI.9874	1	1	1	1	1	1	1	1	1	1	1	1
znf703	2815	3641	2122	5945	2119	6246	2145	5539	2914	6511	3248	6915

Tab. 6.15 Raw data of RA-dependency in dorsal tissue

gene	A		B	
	D	D + CYP	D	D + CYP
bhlhe40	25	20	40	18
c10orf140	3	2	3	3
cass4	107	154	274	254
cdx4	381	345	517	485
cebpd	66	47	77	34
cxcr7	146	136	206	169
cyp26a1	813	527	1572	546
dact1-a	227	263	420	348
dact1-b	1191	1406	1947	1700
dhrs3	757	449	972	286
dusp5	950	994	1417	1051
dusp6	512	477	644	447
e_Cerberus	1191	2085	2607	2209
e_darmin	179	196	225	120
e_Sox1alpha	601	777	1121	770
e_Sox17beta	503	778	735	702
e_TGIF2	420	486	889	792
e_vpp1	135	198	85	56
ec_Sox2	1054	1003	1252	1169
ec_tubb2b	24	27	20	30
ec_xk81a1	4	12	17	24
em_BMP2-a/b	305	324	410	298
em_BMP4-a/b	683	675	783	752
erf	246	316	416	377
fgfr4-a	421	524	557	507
fgfr4-b	221	345	364	342
foxh1	314	353	613	567
fst	1177	705	1039	373
fzd4	197	233	302	342
gbx2.1	36	26	59	48
hey1	87	66	125	86
hk_g6pd	150	211	286	268
hk_gapdh	128	151	297	280
hk_H4	69695	88424	135977	123588
hk_ODC	5149	5869	7514	7283
hnf1b	174	205	250	193
hoxa1-a	8	6	14	6
hoxa1-b	36	13	58	22
hoxa2-a	12	11	16	10
hoxa3	5	1	2	5
hoxa5	4	1	2	1
hoxb1	14	3	9	6
hoxb3	7	8	21	8
hoxb4	25	43	45	39
hoxd1	356	363	669	526
hoxd4	8	9	11	5
hunk	381	534	1017	889
igf3	51	35	42	26
kiaa0182	283	338	519	469
kirrel2	328	331	325	192
lhx1	469	450	611	404
m_Chordin	10753	11169	11641	8870
m_Xbra-a/b	3423	5124	4320	4792
m_Xwnt8	210	299	395	333
me_ventx2.1-b	535	880	754	863
meis3-a	273	254	568	360
mespa-a	12	15	34	18
mespb	221	253	316	278
mx1	277	296	371	278
myc-a	46	33	64	41
myc-b	454	523	490	415
ndrg1-a	1	1	1	1
ndrg1-b	1	2	2	1
neurog2	33	21	59	47
nkx6-2	539	316	457	203
nodal1	88	76	115	78
nodal2	56	127	110	91
nr2f5	3	7	2	2
pdgfb	15	12	21	24
pim1	164	151	341	234
pkdccc.1	511	626	709	563
prph	15	35	10	15
rara	25	26	34	30
rgs14	1	3	2	3
rgs2	262	233	241	152
sox9-a/b	61	75	61	71
spry2	1018	1418	1544	1522
stox2	171	237	259	262
tdgf1p2-a	18	5	23	7
tdgf1p2-b	7	16	17	11
tmem72	37	34	66	40
trib1	48	36	47	32
twist1-a	195	114	52	47
txnip	97	87	92	79
Xl.15091	1	1	1	1
Xl.16263	1	2	1	3
Xl.32109	11	5	5	10
Xl.45046	175	146	271	157
Xl.47239	35	42	67	59
Xl.4906	316	442	470	520
Xl.51509	40	18	39	34
Xl.57027	36	71	106	109
Xl.57926	598	701	624	379
Xl.58101	1	2	2	4
Xl.59256	1	3	1	2
Xl.6091	13	16	21	22
Xl.67202	2	1	1	1
Xl.68408	2	1	2	1
Xl.70850	9	15	13	9
Xl.71159	365	462	462	440
Xl.74263	4	1	3	3
Xl.79790	12	13	24	12
Xl.80297	210	201	424	171
Xl.85251	1	1	1	1
Xl.8753	3	1	3	5
Xl.9822	27	13	30	33
Xl.9874	1	5	4	1
znf703	1109	921	1600	1143
NEG_A	1	5	2	1
NEG_B	5	2	3	5
NEG_C	1	1	1	1
NEG_D	2	2	1	1
NEG_E	4	3	9	3
NEG_F	12	10	6	7
NEG_G	1	1	2	1
NEG_H	3	1	4	1
POS_A	4833	6975	6828	5936
POS_B	1783	2551	2451	2069
POS_C	567	745	711	596
POS_D	118	150	175	164
POS_E	15	27	21	20
POS_F	7	12	14	8

Tab. 6.16 Normalized data of RA-dependency in dorsal tissue

Indicated are the Nanostring counts which were normalized to the internal positive controls and Odc and with subtracted mean of the negative controls as described in the "Materials and Methods" section.

gene	A		B		gene	A		B	
	D	D + CYP	D	D + CYP		D	D + CYP	D	D + CYP
bhlhe40	27	17	33	12	m_Xwnt8	319	392	414	352
c10orf140	1	1	1	1	me_ventx2.1-b	814	1168	779	923
cass4	152	197	277	267	meis3-a	415	331	584	382
cdx4	570	452	532	516	mespa-a	7	12	26	12
cebpd	90	54	71	29	mespb	326	329	321	292
cxcr7	212	173	216	175	mxi1	411	387	378	292
cyp26a1	1228	695	1633	581	myc-a	59	35	58	37
dact1-a	335	342	430	368	myc-b	681	691	513	441
dact1-b	1814	1872	2125	1825	ndrg1-a	1	1	1	1
dhrs3	1143	591	1116	311	ndrg1-b	1	1	1	1
dusp5	1437	1320	1471	1125	neurog2	39	19	53	43
dusp6	769	629	664	475	nkx6-2	812	413	468	212
e_Cerberus	1814	2779	2714	2373	nodal1	123	92	111	77
e_darmin	262	253	226	122	nodal2	74	162	116	92
e_Sox17alpha	915	1130	1162	823	nr2f5	1	1	1	1
e_Sox17beta	756	1131	759	749	pdgfb	12	7	13	19
e_TGIF2	629	642	920	846	pim1	239	193	347	245
e_vpp1	195	255	80	53	pkdcc.1	768	828	732	600
ec_Sox2	1596	1332	1299	1253	prph	12	38	1	9
ec_tubb2b	26	27	12	25	rara	27	25	26	25
ec_xk81a1	1	7	9	19	rgs14	1	1	1	1
em_BMP2-a/b	454	424	419	314	rgs2	388	312	243	157
em_BMP4-a/b	1131	893	819	813	sox9-a/b	82	92	55	69
erf	364	413	425	399	spry2	1542	1887	1614	1633
fgfr4-a	632	691	573	539	stox2	250	318	261	275
fgfr4-b	326	452	371	361	tdgf1p2-a	16	1	15	1
foxb1	468	463	631	614	tdgf1p2-b	1	12	9	5
fst	1783	934	1176	395	tmem72	45	36	60	36
fzd4	289	312	316	361	trib1	62	39	41	27
gbx2.1	44	25	53	45	twist1-a	286	143	45	43
hey1	122	79	122	86	txnip	137	117	87	78
hk_g6pd	218	273	290	282	XI.15091	1	1	1	1
hk_gapdh	184	193	311	295	XI.16263	1	1	1	1
hk_H4	116227	118242	142126	133181	XI.32109	6	1	1	4
hk_ODC	7838	7839	7840	7842	XI.45046	256	186	274	162
hnf1b	254	265	252	212	XI.47239	42	47	62	56
hoxa1-a	1	1	6	1	XI.4906	472	582	482	553
hoxa1-b	44	8	52	17	XI.51509	50	15	32	29
hoxa2-a	7	5	8	4	XI.57027	44	86	112	111
hoxa3	1	1	1	1	XI.57926	912	928	643	411
hoxa5	1	1	1	1	XI.58101	1	1	1	1
hoxb1	11	1	1	1	XI.59256	1	1	1	1
hoxb3	1	1	13	1	XI.6091	9	12	13	17
hoxb4	27	48	38	35	XI.67202	1	1	1	1
hoxd1	532	476	690	560	XI.68408	1	1	1	1
hoxd4	1	3	2	1	XI.70850	3	12	5	3
hunk	570	715	1153	952	XI.71159	545	619	474	467
igf3	67	38	35	22	XI.74263	1	1	1	1
kiaa0182	421	443	533	498	XI.79790	7	8	16	6
kirrel2	489	433	331	200	XI.80297	319	259	434	177
lhx1	714	592	629	428	XI.85251	1	1	1	1
m_Chordin	16381	14927	12152	9552	XI.8753	1	1	1	1
m_Xbra-a/b	5217	6843	4513	5157	XI.9822	31	8	22	28
					XI.9874	1	1	1	1
					znf703	1679	1222	1662	1225

Tab. 6.17 Raw data of RA-dependency in whole embryos

gene	A						B					
	st.12		st.13		st.14		st.12		st.13		st.14	
	CE	BMS	CE	BMS	CE	BMS	CE	BMS	CE	BMS	CE	BMS
bhlhe40	21	16	29	28	22	34	19	12	32	29	49	42
c10orf140	5	6	4	4	5	6	6	7	3	1	1	9
cass4	189	162	241	164	151	218	207	137	172	161	273	266
cdx4	1484	1467	1873	959	1313	1637	1863	1156	1615	1457	2163	2023
cebpd	42	64	28	40	63	64	82	48	47	46	38	39
cxcr7	148	147	114	77	96	136	201	173	128	126	131	167
cyp26a1	814	407	884	364	612	575	1491	758	740	620	951	730
dact1-a	99	84	75	58	67	94	121	111	91	87	147	96
dact1-b	655	591	630	441	493	688	974	679	613	622	794	771
dhrs3	378	207	432	146	308	239	630	301	359	315	429	231
dusp5	308	171	308	128	245	288	390	270	339	339	433	364
dusp6	349	370	491	294	322	504	314	214	304	243	481	521
e_Cerberus	254	408	89	161	80	105	1461	1437	491	788	556	417
e_darmin	693	807	480	836	911	1262	959	638	530	629	1209	710
e_Sox17alpha	525	642	623	432	516	642	807	623	565	598	725	629
e_Sox17beta	563	626	570	340	426	561	736	644	577	551	684	641
e_TGIF2	192	251	310	240	186	339	460	441	299	252	243	285
e_vpp1	70	95	35	76	71	70	162	100	93	138	123	88
ec_Sox2	890	720	1139	674	812	895	1430	1140	1001	1096	1067	900
ec_tubb2b	43	48	70	59	52	151	39	31	43	32	55	84
ec_xk81a1	3456	2773	6564	2941	5765	7215	4112	2439	6402	4839	10511	7752
em_BMP2-a/b	457	499	324	355	368	591	661	476	443	511	668	598
em_BMP4-a/b	1624	2012	1377	1005	1026	1612	2915	2402	1660	1893	1863	2073
erf	221	196	193	120	174	213	304	233	219	224	308	252
fgfr4-a	1100	1220	1113	825	894	1361	1742	1376	1357	1322	1511	1611
fgfr4-b	469	519	526	350	396	538	781	649	468	546	608	634
foxb1	236	177	282	97	165	206	290	180	257	184	338	238
fst	169	86	241	105	183	149	407	192	215	280	276	267
fzd4	450	267	311	130	328	247	641	453	383	261	448	285
gbx2.1	384	182	351	161	253	259	379	232	330	188	466	294
hey1	118	136	156	79	101	140	165	95	165	160	163	132
hk_g6pd	186	188	192	105	124	186	296	222	137	212	207	209
hk_gapdh	125	126	165	90	125	173	123	100	120	114	120	150
hk_H4	66093	64900	86152	51542	62183	91163	146073	113620	93587	121011	112190	126582
hk_ODC	7511	9063	8871	5742	6875	11303	9779	6880	6549	7906	8264	8734
hnf1b	416	199	398	94	425	263	432	280	388	194	630	198
hoxa1-a	18	5	27	3	35	12	40	13	36	12	51	15
hoxa1-b	153	60	251	38	196	37	264	89	236	107	280	80
hoxa2-a	17	14	31	8	19	18	30	19	17	20	35	27
hoxa3	61	20	79	20	47	64	12	6	33	16	57	36
hoxa5	4	1	11	5	12	7	5	2	12	5	12	6
hoxb1	132	71	199	64	158	138	98	49	151	73	203	156
hoxb3	18	12	24	19	24	25	16	15	20	7	34	27
hoxb4	39	40	60	22	40	55	57	48	52	53	62	48
hoxd1	1309	890	1378	618	931	752	2262	1388	1570	1092	1451	1051
hoxd4	100	70	193	72	106	245	49	37	107	79	228	255
hunk	623	463	684	352	468	523	846	578	531	443	801	698
igf3	73	50	116	57	93	170	94	51	127	97	123	143
kiaa0182	274	203	361	161	215	303	578	378	376	350	498	471
kirrel2	180	141	212	166	195	253	361	332	360	276	403	346
lhx1	83	79	120	51	81	80	90	55	87	68	99	79
m_Chordin	1302	1497	1451	1055	1085	1452	2672	1809	1554	1811	1495	1992
m_Xbra-a/b	955	1354	961	647	533	699	2013	1624	829	1118	888	1049
m_Xwnt8	396	477	491	182	233	358	859	800	383	624	337	428
me_ventx2.1-b	1328	2695	992	610	179	754	2356	1430	1200	889	1507	909
meis3-a	703	344	706	322	505	655	794	463	633	426	934	630

gene	A						B					
	st.12		st.13		st.14		st.12		st.13		st.14	
	CE	BMS	CE	BMS	CE	BMS	CE	BMS	CE	BMS	CE	BMS
mespa-a	28	21	27	18	32	30	43	14	37	28	46	30
mespb	196	231	180	133	94	162	348	256	164	234	193	166
mxi1	359	253	330	185	278	287	434	211	309	284	384	300
myc-a	88	83	130	60	101	144	103	62	91	61	144	104
myc-b	1067	1046	1490	855	907	1730	1378	991	1299	1101	1730	1868
ndrg1-a	1	1	2	3	3	4	1	1	1	3	1	2
ndrg1-b	1	1	2	2	2	1	1	1	2	2	6	5
neurog2	93	72	83	62	49	68	174	129	119	128	86	86
nkx6-2	94	45	112	53	73	108	159	102	124	101	138	137
nodal1	12	13	18	6	10	3	10	9	3	6	3	8
nodal2	13	11	13	4	1	7	14	11	6	7	8	8
nr2f5	19	6	90	35	103	144	18	8	72	27	144	108
pdgfb	15	13	21	9	19	19	17	11	16	12	23	20
pim1	174	174	166	112	133	216	328	204	210	149	317	243
pkdcc.1	213	250	265	187	229	226	512	366	338	322	387	322
prph	50	19	82	27	56	60	49	27	89	43	114	77
rara	54	30	88	40	54	60	52	39	58	64	115	95
rgs14	1	3	1	2	1	1	1	1	1	1	1	3
rgs2	66	72	180	82	119	220	112	65	93	98	124	91
sox9-a/b	107	111	222	122	164	373	147	86	184	128	271	275
spry2	290	337	347	232	239	357	509	374	344	406	389	405
stox2	211	204	169	123	153	223	274	162	171	194	254	224
tdgf1p2-a	25	25	42	17	38	58	37	10	28	33	46	35
tdgf1p2-b	9	6	3	6	9	8	3	5	4	1	11	4
tmem72	104	86	142	84	169	181	154	114	202	149	293	213
trib1	52	60	51	37	37	62	53	30	51	58	63	60
twist1-a	215	238	287	260	244	522	261	190	267	279	374	512
txnip	231	288	207	204	233	406	110	81	115	96	209	147
XI.15091	1	1	6	1	2	1	2	3	1	3	4	1
XI.16263	2	2	1	2	1	2	3	2	2	1	5	1
XI.32109	11	6	8	3	3	4	11	13	10	12	5	10
XI.45046	324	156	497	210	311	385	508	217	478	236	694	495
XI.47239	65	42	82	29	72	101	50	34	76	53	101	127
XI.4906	603	636	578	426	489	724	1131	902	744	704	1062	881
XI.51509	66	54	94	36	74	68	58	23	72	48	133	79
XI.57027	35	26	44	23	35	35	42	26	38	24	70	63
XI.57926	232	148	276	102	160	178	430	277	309	256	511	329
XI.58101	2	4	2	2	1	1	3	1	2	3	2	1
XI.59256	1	1	1	1	1	2	1	1	1	1	2	3
XI.6091	10	6	16	7	7	17	17	15	14	19	17	24
XI.67202	2	3	4	3	3	4	7	4	3	1	5	6
XI.68408	1	1	3	1	1	1	1	1	1	1	1	2
XI.70850	3	4	5	2	4	4	17	11	7	6	10	6
XI.71159	608	916	775	544	494	756	929	796	629	870	652	921
XI.74263	6	2	1	1	2	2	2	2	1	1	2	1
XI.79790	29	15	60	30	50	66	49	54	47	60	86	66
XI.80297	63	54	72	42	61	77	110	75	77	86	69	92
XI.85251	1	2	5	1	2	2	6	5	3	4	4	1
XI.8753	1	2	1	1	1	3	2	1	2	3	5	2
XI.9822	13	11	23	9	11	16	23	21	16	12	32	11
XI.9874	4	6	8	2	5	6	5	4	2	4	2	3
znf703	2494	1393	2278	965	1642	1713	2789	1514	2505	1443	3439	2292
NEG_A	2	1	6	1	2	4	5	6	2	5	5	6
NEG_B	2	1	3	3	1	3	5	1	3	4	5	7
NEG_C	1	1	1	1	1	2	1	1	1	1	1	2
NEG_D	1	2	2	2	2	3	1	1	2	2	4	4
NEG_E	2	5	6	1	2	3	4	2	3	6	4	1
NEG_F	8	10	12	4	9	8	14	8	9	10	16	15
NEG_G	1	1	1	1	1	1	1	1	1	1	1	1
NEG_H	1	1	1	1	1	2	1	2	1	1	2	2
POS_A	4427	4213	6295	4057	5094	5428	6726	5523	5441	7361	7964	6236
POS_B	1739	1768	2557	1674	2053	2292	2829	2204	2058	2961	2986	2478
POS_C	511	536	814	473	616	662	787	629	592	827	938	762
POS_D	124	100	160	92	144	141	158	145	133	192	176	168
POS_E	15	20	31	17	18	17	22	25	16	47	38	33
POS_F	4	8	13	7	13	9	13	6	17	27	20	13

Tab. 6.18 Normalized data of RA-dependency in whole embryos

Indicated are the Nanostring counts which were normalized to the internal positive controls and Odc and with subtracted mean of the negative controls as described in the "Materials and Methods" section

gene	s22						s23					
	st.12		st.13		st.14		st.12		st.13		st.14	
	CE	BMS	CE	BMS	CE	BMS	CE	BMS	CE	BMS	CE	BMS
bhlhe40	17	8	15	41	21	22	2	4	29	17	32	22
c10orf140	1	1	1	2	1	1	1	1	1	1	1	1
cass4	206	165	214	259	188	181	147	131	193	142	245	214
cdx4	1666	1569	1743	1537	1693	1410	1429	1169	1876	1371	2038	1719
cebpd	40	60	15	60	74	48	51	41	47	33	22	19
cxcr7	160	149	95	120	117	110	143	168	141	109	110	129
cyp26a1	911	429	816	581	785	490	1141	764	855	577	888	611
dact1-a	105	81	59	89	79	74	81	105	98	72	125	68
dact1-b	731	626	579	705	631	588	741	683	707	579	739	646
dhrs3	419	213	393	231	391	199	475	298	411	288	393	184
dusp5	340	175	277	202	310	242	289	267	387	311	396	298
dusp6	386	389	448	468	409	429	230	210	347	220	442	432
e_Cerberus	279	430	72	255	96	83	1118	1455	565	737	513	343
e_darmin	774	859	438	1339	1172	1085	729	641	610	586	1133	594
e_Sox17alpha	585	681	572	690	661	549	612	626	651	557	673	525
e_Sox17beta	628	664	522	542	544	478	557	648	665	512	634	535
e_TGIF2	209	261	279	382	233	286	343	441	341	229	216	230
e_vpp1	72	93	21	118	84	53	112	94	100	121	102	61
ec_Sox2	996	765	1055	1079	1044	768	1094	1153	1160	1029	998	757
ec_tubb2b	41	42	54	91	60	123	17	23	42	20	38	58
ec_xk81a1	3890	2974	6138	4722	7459	6241	3169	2475	7459	4576	9957	6625
em_BMP2-a/b	508	528	292	566	469	504	499	476	509	474	619	498
em_BMP4-a/b	1824	2155	1278	1611	1321	1389	2243	2438	1928	1784	1753	1761
erf	242	202	169	189	218	177	222	229	247	202	278	202
fgfr4-a	1233	1303	1031	1322	1150	1171	1335	1393	1575	1243	1419	1366
fgfr4-b	522	549	481	558	505	458	592	653	538	507	562	529
foxh1	259	181	252	152	206	171	212	175	292	164	306	190
fst	184	83	214	165	229	122	302	187	243	255	247	215
fzd4	500	278	280	205	417	206	483	453	439	237	411	230
gbx2.1	426	187	317	255	320	217	280	228	377	168	428	238
hey1	126	137	134	123	123	114	115	89	184	141	140	99
hk_g6pd	203	193	168	165	153	154	216	218	152	191	182	165
hk_gapdh	134	126	143	141	154	142	82	94	132	98	99	114
hk_H4	74512	69800	80701	82824	80536	78943	113028	115679	109154	114673	106415	108403
hk_ODC	8462	9739	8299	9223	8897	9781	7555	6997	7631	7482	7825	7466
hnf1b	462	205	361	147	543	220	321	277	445	174	583	155
hoxa1-a	13	1	14	1	38	3	18	5	34	1	34	1
hoxa1-b	166	55	223	57	246	25	191	82	267	91	251	54
hoxa2-a	12	6	17	9	17	8	10	11	12	9	19	9
hoxa3	62	12	62	28	53	48	-4	-2	30	5	40	17
hoxa5	1	1	1	4	8	1	1	1	6	1	1	1
hoxb1	142	67	175	99	197	112	63	42	168	59	178	119
hoxb3	13	4	11	26	23	14	-1	7	15	-4	18	9
hoxb4	37	34	45	31	44	40	31	41	53	40	44	27
hoxd1	1469	948	1279	989	1198	644	1738	1405	1823	1025	1362	886
hoxd4	106	66	169	112	129	205	25	29	117	65	202	204
hunk	695	489	629	562	598	445	642	580	611	410	745	584
igf3	75	45	97	88	113	140	60	44	140	82	102	108
kiaa0182	302	209	327	255	271	255	434	377	431	322	458	389
kirrel2	196	142	187	263	245	212	266	330	412	251	368	282
lhx1	87	76	101	78	97	62	57	48	93	54	80	53
m_Chordin	1461	1601	1348	1691	1398	1250	2055	1834	1805	1706	1404	1692
m_Xbra-a/b	1070	1447	889	1036	683	598	1545	1645	959	1049	828	884

Appendix

gene	s22						s23					
	st.12		st.13		st.14		st.12		st.13		st.14	
	CE	BMS	CE	BMS	CE	BMS	CE	BMS	CE	BMS	CE	BMS
m_Xwnt8	439	504	448	288	294	303	652	806	439	581	305	352
me_ventx2.1-b	1490	2890	918	976	224	645	1810	1448	1392	832	1415	764
meis3-a	786	361	650	513	646	560	602	463	730	394	872	525
mespa-a	25	13	14	25	34	18	20	6	35	16	29	12
mespb	214	239	157	210	114	133	256	252	183	212	169	128
mxi1	398	263	297	293	352	241	323	207	352	259	350	243
myc-a	92	80	110	92	123	117	67	55	98	48	122	75
myc-b	1196	1116	1384	1370	1167	1491	1054	1001	1507	1033	1627	1586
ndrg1-a	1	1	1	1	1	1	1	1	1	1	1	1
ndrg1-b	1	1	1	1	1	1	1	1	1	1	1	1
neurog2	98	68	66	96	56	51	122	123	131	111	67	59
nkx6-2	99	39	93	81	87	86	110	96	137	86	116	103
nodal1	7	5	5	6	5	1	1	1	1	1	1	1
nodal2	8	3	0	2	1	1	1	3	1	1	1	1
nr2f5	14	1	73	52	126	117	1	1	76	15	122	78
pdgfb	10	5	8	10	17	9	0	3	11	1	7	3
pim1	189	178	144	176	164	180	241	200	237	131	286	194
pkdcc.1	233	260	237	296	289	188	383	364	386	295	353	262
prph	49	11	65	39	65	44	25	19	96	31	94	52
rara	54	23	71	60	62	44	27	32	60	51	95	67
rgs14	1	1	1	1	1	1	1	1	1	1	1	1
rgs2	67	68	157	128	146	183	74	58	100	83	103	64
sox9-a/b	114	110	196	192	205	316	101	79	207	111	243	221
spry2	320	353	313	369	302	302	381	373	393	375	355	333
stox2	231	210	147	194	190	186	199	157	191	174	227	178
tdgf1p2-a	21	18	28	23	41	43	16	2	25	21	29	16
tdgf1p2-b	3	1	1	6	4	1	1	1	1	1	1	1
tmem72	110	83	121	131	211	149	106	108	228	131	264	168
trib1	52	55	36	55	40	46	28	22	51	45	45	37
twist1-a	235	247	257	414	308	445	189	185	303	254	340	424
txnip	253	301	182	324	294	344	72	74	126	81	184	112
Xl.15091	1	1	1	1	1	1	1	1	1	1	1	1
Xl.16263	1	1	1	1	1	1	1	1	1	1	1	1
Xl.32109	5	1	1	1	1	1	1	5	4	1	1	1
Xl.45046	358	159	454	333	395	326	380	213	549	214	644	410
Xl.47239	66	36	65	43	85	80	26	26	81	40	81	95
Xl.4906	673	675	530	681	626	620	862	910	860	657	993	740
Xl.51509	67	49	76	54	88	51	32	15	76	35	112	53
Xl.57027	32	19	30	33	38	23	20	18	36	13	52	40
Xl.57926	255	150	247	160	199	147	320	274	352	232	470	268
Xl.58101	1	1	1	1	1	1	1	1	1	1	1	1
Xl.59256	1	1	1	1	1	1	1	1	1	1	1	1
Xl.6091	4	1	3	7	1	7	0	7	8	8	2	6
Xl.67202	1	1	1	1	1	1	1	1	1	1	1	1
Xl.68408	1	1	1	1	1	1	1	1	1	1	1	1
Xl.70850	1	1	1	1	1	1	0	3	0	1	1	1
Xl.71159	679	976	714	870	632	647	706	802	726	814	604	775
Xl.74263	1	1	1	1	1	1	1	1	1	1	1	1
Xl.79790	26	7	45	44	57	50	25	47	47	47	67	42
Xl.80297	64	49	56	63	71	59	72	68	82	71	51	65
Xl.85251	1	1	1	1	1	1	1	1	1	1	1	1
Xl.8753	1	1	1	1	1	1	1	1	1	1	1	1
Xl.9822	8	3	10	10	6	6	5	13	11	1	16	1
Xl.9874	1	1	1	1	1	1	1	1	1	1	1	1
znf703	2805	1489	2122	1547	2119	1476	2145	1533	2914	1357	3248	1949

6.8 Nanostring analysis data for expression characteristics of confirmed RA-responsive genes

Tab. 6.19 Raw data of expression characteristics

(CE = control-embryo; DE = dorsal endoderm; VE = ventral endoderm; D = dorsal tissue; V = ventral tissue)

gene	A					B				
	CE	DE	VE	D	V	CE	DE	VE	D	V
bhlhe40	6	10	3	47	21	12	8	8	40	25
c10orf140	1	5	3	2	10	4	7	1	3	10
cass4	320	329	482	151	305	188	422	400	274	608
cdx4	480	7	217	522	2156	723	4	384	517	3075
cebpd	20	144	44	31	17	37	297	50	77	34
cxcr7	163	105	80	123	110	119	64	49	206	173
cyp26a1	724	847	466	922	2029	973	1014	379	1572	1948
dact1-a	168	276	95	240	207	165	264	103	420	236
dact1-b	718	941	692	1055	926	640	866	404	1947	1474
dhrs3	269	745	221	599	286	344	777	248	972	402
dusp5	411	326	451	892	903	447	217	280	1417	1083
dusp6	405	353	317	514	531	295	220	233	644	723
e_Cerberus	2006	7729	1565	1119	137	1601	9325	1841	2607	392
e_darmin	160	859	612	102	13	611	3674	2037	225	115
e_Sox17alpha	884	2049	2028	890	872	799	2587	2321	1121	1070
e_Sox17beta	976	1522	1953	590	790	814	2006	2712	735	1055
e_TGIF2	309	322	416	357	635	218	483	312	889	1160
e_vpp1	34	315	2	89	1	65	423	5	85	7
ec_Sox2	463	8	22	501	389	603	23	11	1252	412
ec_tubb2b	9	25	12	19	7	22	30	25	20	17
ec_xk81a1	293	8	8	6	79	1685	3	15	17	386
em_BMP2-a/b	320	1695	551	308	167	265	2393	518	410	278
em_BMP4-a/b	1397	920	2076	878	3364	1452	1031	2125	783	4052
erf	229	170	290	201	248	229	162	240	416	574
fgfr4-a	772	1241	1212	472	269	565	1428	1167	557	625
fgfr4-b	518	676	583	239	118	396	542	505	364	249
foxh1	299	194	264	211	285	304	304	382	613	645
fst	59	453	119	1535	56	91	224	66	1039	50
fzd4	348	418	280	119	35	296	467	173	302	98
gbx2.1	88	23	18	17	46	64	26	50	59	151
hey1	64	33	62	102	73	62	42	54	125	195
hk_g6pd	122	100	97	112	133	160	126	113	286	350
hk_gapdh	152	134	146	123	139	146	108	106	297	224
hk_H4	108920	60805	63372	88804	111328	83610	55389	45520	135977	133543
hk_ODC	4311	3689	3620	4479	4987	3902	3908	3172	7514	9518
hnf1b	185	650	519	230	96	232	774	590	250	138
hoxa1-a	1	5	1	1	11	6	2	1	14	18
hoxa1-b	33	2	7	54	93	63	3	7	58	188
hoxa2-a	12	7	12	14	15	6	6	7	16	29
hoxa3	2	1	4	6	5	6	4	6	2	10
hoxa5	1	1	1	1	1	3	1	1	2	1
hoxb1	2	2	3	2	12	5	1	2	9	28
hoxb3	9	2	3	14	26	8	1	3	21	29
hoxb4	46	20	17	26	50	23	25	12	45	62
hoxd1	746	24	258	464	1581	1015	44	390	669	3080
hoxd4	3	6	3	9	21	4	6	6	11	25
hunk	314	515	562	200	620	707	976	753	1017	1844
igf3	60	53	49	53	43	49	79	32	42	31
kiaa0182	213	150	199	158	223	310	254	223	519	594
kirrel2	140	387	450	306	344	258	653	746	325	552
lhx1	125	307	260	424	92	80	276	151	611	119
Xl.47239	55	28	51	26	55	31	34	40	67	89
m_Chordin	1128	3549	3	10256	2	1432	1895	2	11641	5
m_Xbra-a/b	2321	175	946	4491	6800	2525	133	616	4320	8718
m_Xwnt8	1041	509	2214	386	3180	518	246	1150	395	3426
me_ventx2.1-b	759	366	1149	448	1880	1207	747	1965	754	3757
meis3-a	266	203	257	244	312	377	254	203	568	453
mespa-a	13	10	34	12	18	10	10	17	34	40
mespb	257	61	579	248	841	194	52	386	316	1308

Appendix

gene	A					B				
	CE	DE	VE	D	V	CE	DE	VE	D	V
mxi1	234	98	138	206	178	250	191	179	371	307
myc-a	33	55	58	44	106	38	68	58	64	98
myc-b	454	147	585	583	2514	922	201	792	490	2530
ndrg1-a	1	1	1	1	1	2	2	1	1	2
ndrg1-b	1	2	2	1	1	1	3	1	2	4
neurog2-b	32	19	12	22	19	30	15	21	59	38
nkx6-2	24	19	7	355	17	33	11	6	457	15
nodal1	57	49	61	103	62	24	24	77	115	142
nodal2	117	14	12	108	113	26	15	12	110	131
nr2f5	22	23	27	18	20	6	7	9	2	6
pdgfb	29	16	18	9	16	10	15	9	21	16
pim1	304	199	128	230	229	261	228	97	341	410
pkdcc.1	196	776	182	407	34	253	674	87	709	33
prph	16	3	1	19	13	27	1	2	10	15
rara	13	14	20	26	42	20	11	22	34	54
rgs14	4	1	1	1	1	2	7	3	2	5
rgs2	24	30	24	140	30	26	8	27	241	129
sox9-a/b	84	89	82	47	187	74	77	57	61	275
spry2	551	375	229	933	815	434	368	115	1544	854
stox2	197	193	127	162	156	175	200	98	259	280
tdgf1p2-a	3	10	2	18	1	6	44	7	23	2
tdgf1p2-b	1	1	4	3	1	3	4	7	17	2
tmem72	33	48	52	63	37	41	111	96	66	46
trib1	26	24	18	31	14	25	12	11	47	24
twist1-a	21	99	37	162	17	53	230	14	52	16
txnip	72	150	118	71	34	76	222	188	92	87
XI.15091	1	1	1	1	1	1	2	1	1	1
XI.16263	5	1	1	1	3	1	3	2	1	3
XI.32109	10	3	3	8	5	6	7	2	5	10
XI.45046	122	68	168	155	294	157	60	163	271	556
XI.4906	899	368	626	332	686	629	227	214	470	1003
XI.51509	11	4	5	59	93	24	3	3	39	70
XI.57027	11	57	48	19	56	111	100	62	106	158
XI.57926	290	222	267	641	575	303	137	152	624	918
XI.58101	3	2	2	1	1	1	3	1	2	1
XI.59256	2	3	2	2	1	1	2	1	1	3
XI.6091	19	11	10	26	34	16	6	13	21	32
XI.67202	4	3	1	1	3	1	2	2	1	4
XI.68408	1	1	1	2	1	1	1	1	2	1
XI.70850	6	1	1	3	2	4	1	3	13	17
XI.71159	517	543	361	418	379	409	497	273	462	592
XI.74263	2	1	1	2	4	1	1	1	3	4
XI.79790	16	18	4	7	14	17	31	5	24	11
XI.80297	30	6	5	280	164	63	1	2	424	120
XI.85251	1	2	1	1	3	2	1	2	1	1
XI.8753	1	1	1	2	1	2	1	1	3	2
XI.9822	14	6	9	9	12	19	11	12	30	38
XI.9874	7	1	3	2	1	3	5	1	4	5
znf703-a/b	999	171	492	1017	2099	1334	220	602	1600	4659
NEG_A	1	4	1	2	2	2	2	3	2	3
NEG_B	2	7	5	4	3	4	3	3	3	7
NEG_C	1	1	1	1	1	1	2	1	1	1
NEG_D	2	3	1	1	1	1	1	2	1	3
NEG_E	6	2	1	7	2	2	5	2	9	4
NEG_F	7	8	8	5	4	4	7	11	6	10
NEG_G	1	1	1	1	1	1	1	3	2	1
NEG_H	1	4	1	1	2	3	1	1	4	1
POS_A	4707	5150	4978	4878	5928	5579	5222	5051	6828	7020
POS_B	1824	1857	1811	1786	2104	2115	2239	2065	2451	2944
POS_C	577	652	631	587	742	706	690	647	711	881
POS_D	115	140	125	127	143	134	119	139	175	185
POS_E	24	23	24	29	31	24	24	22	21	27
POS_F	13	10	12	13	19	13	15	5	14	24

Tab. 6.20 Normalized data of expression characteristics

(Indicated are the Nanostring counts which were normalized to the internal positive controls and Odc and with subtracted mean of the negative controls as described in the “Materials and Methods” section). CE = control-embryo; DE = dorsal endoderm; VE = ventral endoderm; D = dorsal tissue; V = ventral tissue

gene	A					B				
	CE	DE	VE	D	V	CE	DE	VE	D	V
bhlhe40	1	5	1	47	18	11	4	3	19	3
c10orf140	1	1	1	1	6	1	2	1	1	1
cass4	378	455	685	168	314	246	554	646	181	322
cdx4	571	1	304	599	2244	959	1	620	349	1670
cebpd	17	194	55	29	14	44	388	72	44	8
cxcr7	189	139	107	135	111	154	78	71	134	84
cyp26a1	866	1185	662	1063	2112	1292	1342	612	1079	1054
dact1-a	195	380	129	271	212	215	344	159	282	119
dact1-b	859	1317	986	1217	961	848	1145	653	1338	795
dhrs3	317	1041	310	688	294	454	1027	397	664	209
dusp5	488	451	640	1028	937	591	282	449	972	581
dusp6	481	489	448	589	550	388	286	372	437	385
e_Cerberus	2412	10886	2240	1292	139	2129	12401	3008	1795	204
e_darmin	185	1202	871	111	9	809	4882	3330	147	53
e_Sox17alpha	1059	2879	2905	1026	905	1060	3435	3795	767	574
e_Sox17beta	1170	2136	2798	678	820	1080	2662	4436	500	566
e_TGIF2	365	445	590	407	658	286	636	502	606	624
e_vpp1	33	435	1	96	1	82	556	1	50	1
ec_Sox2	551	2	24	574	401	799	23	8	857	215
ec_tubb2b	3	26	10	15	3	25	33	31	5	1
ec_xk81a1	346	2	4	1	78	2241	1	15	3	201
em_BMP2-a/b	378	2380	784	350	170	348	3177	839	275	142
em_BMP4-a/b	1678	1288	2974	1012	3504	1930	1365	3474	533	2204
erf	269	231	409	226	254	300	208	384	279	303
fgfr4-a	924	1740	1733	541	276	748	1893	1903	376	331
fgfr4-b	617	944	830	270	119	523	714	818	243	126
foxh1	353	265	372	238	293	400	397	617	415	342
fst	64	630	163	1775	54	116	291	98	710	17
fzd4	412	580	395	131	32	390	614	274	200	43
gbx2.1	99	23	18	12	44	80	27	72	32	72
hey1	70	38	81	111	72	78	49	79	77	96
hk_g6pd	140	132	132	123	135	208	161	176	189	181
hk_gapdh	176	180	202	135	141	190	137	164	196	112
hk_H4	131375	85703	91025	103093	116080	111420	73695	74614	94094	72950
hk_ODC	5193	5191	5192	5193	5196	5195	5193	5190	5191	5190
hnf1b	216	907	738	260	96	304	1023	957	164	65
hoxa1-a	1	1	1	1	7	3	1	1	1	1
hoxa1-b	32	1	2	55	93	79	1	2	31	92
hoxa2-a	7	1	10	9	12	3	1	2	2	6
hoxa3	1	1	1	1	1	3	1	0	1	1
hoxa5	1	1	1	1	1	1	1	1	1	1
hoxb1	1	1	1	1	8	2	1	1	1	5
hoxb3	3	1	1	9	23	6	1	1	5	6
hoxb4	48	19	17	23	48	26	26	10	22	24
hoxd1	892	25	363	531	1644	1348	51	630	454	1672
hoxd4	1	1	1	3	18	1	1	0	1	3
hunk	371	717	800	225	642	937	1292	1225	695	997
igf3	65	66	63	54	41	60	98	43	20	7
kiaa0182	249	202	278	176	228	408	331	356	350	314
kirrel2	161	537	639	348	355	339	862	1213	216	291
lhx1	143	424	366	485	92	102	360	238	414	55
XI.47239	59	31	66	23	53	36	38	56	37	38

Appendix

gene	A					B				
	CE	DE	VE	D	V	CE	DE	VE	D	V
m_Chordin	1353	4994	1	11900	1	1904	2514	1	8047	1
m_Xbra-a/b	2792	238	1351	5207	7086	3360	170	1000	2981	4753
m_Xwnt8	1248	709	3173	441	3312	686	320	1876	264	1862
me_ventx2.1-b	908	507	1643	513	1956	1604	987	3212	513	2042
meis3-a	313	277	361	276	321	498	331	323	384	237
mespa-a	8	5	41	7	15	9	6	18	14	12
mespb	302	77	824	281	873	254	62	623	210	704
mxi1	275	129	191	232	181	328	247	284	248	157
myc-a	32	69	76	44	106	46	83	85	35	43
myc-b	540	198	833	669	2617	1224	260	1289	330	1372
ndrg1-a	1	1	1	1	1	1	1	1	1	1
ndrg1-b	1	1	1	1	1	1	1	1	1	1
neurog2-b	31	18	10	18	16	35	13	25	32	11
nkx6-2	21	18	2	405	14	39	8	0	307	1
nodal1	61	60	80	112	61	27	25	116	71	67
nodal2	134	11	10	118	114	30	13	10	67	61
nr2f5	19	23	31	14	17	3	2	5	1	1
pdgfb	27	14	18	3	13	9	13	5	5	1
pim1	359	272	176	260	235	343	296	149	227	214
pkdcc.1	229	1085	254	465	31	332	890	133	482	8
prph	12	1	1	15	9	31	1	1	1	1
rara	8	11	21	23	40	22	8	26	14	19
rgs14	1	1	1	1	1	1	2	1	1	1
rgs2	21	33	27	155	27	30	4	35	158	60
sox9-a/b	94	117	110	47	191	94	95	84	33	140
spry2	657	520	321	1076	846	574	483	179	1059	456
stox2	230	263	175	181	159	228	259	151	170	143
tdgf1p2-a	1	5	1	14	1	3	51	2	7	1
tdgf1p2-b	1	1	1	1	1	1	1	2	3	1
tmem72	32	59	67	66	34	50	141	148	37	15
trib1	24	25	18	29	10	29	9	8	23	3
twist1-a	18	131	45	181	14	66	299	13	27	1
txnip	79	202	162	75	31	96	288	298	55	37
Xl.15091	1	1	1	1	1	1	1	1	1	1
Xl.16263	1	1	1	1	1	1	1	1	1	1
Xl.32109	5	1	1	2	1	3	2	1	1	1
Xl.45046	140	87	234	173	302	204	73	257	178	294
Xl.4906	1077	510	892	378	711	833	295	341	316	538
Xl.51509	6	1	1	61	93	27	1	1	18	28
Xl.57027	6	71	61	15	54	143	126	92	64	76
Xl.57926	342	304	376	737	595	399	175	239	423	491
Xl.58101	1	1	1	1	1	1	1	1	1	1
Xl.59256	1	1	1	1	1	1	1	1	1	1
Xl.6091	15	7	7	23	31	17	1	12	5	7
Xl.67202	1	1	1	1	1	1	1	1	1	1
Xl.68408	1	1	1	1	1	1	1	1	1	1
Xl.70850	1	1	1	1	1	1	1	1	1	1
Xl.71159	616	756	511	478	391	540	654	438	311	313
Xl.74263	1	1	1	1	0	1	1	1	1	1
Xl.79790	12	16	1	1	10	18	34	1	8	1
Xl.80297	29	1	1	318	167	79	1	1	284	55
Xl.85251	1	1	1	1	1	1	1	1	1	1
Xl.8753	1	1	1	1	1	1	1	1	1	1
Xl.9822	9	1	5	3	8	21	8	10	12	11
Xl.9874	1	1	1	1	1	1	1	1	1	1
znf703-a/b	1198	232	699	1173	2185	1773	286	977	1098	2535

Tab. 6.21 Calculated mean and standard error of mean (SEM)

Mean and SEM were calculated from the normalized Nanostring counts of two independent experiments

CE = control-embryo; DE = dorsal endoderm; VE = ventral endoderm; D = dorsal tissue; V = ventral tissue

gene	mean					SEM				
	CE	DE	VE	D	V	CE	DE	VE	D	V
bhlhe40	6	4	2	33	11	5.09	0.81	1.19	14.28	7.17
c10orf140	1	2	1	1	4	0.24	0.59	0.00	0.00	2.65
cass4	312	505	665	174	318	66.37	49.80	19.33	6.32	4.03
cdx4	765	1	462	474	1957	193.62	0.04	157.89	124.96	287.11
cebpd	31	291	64	36	11	13.95	97.02	8.37	7.81	2.62
cxcr7	171	109	89	134	97	17.66	30.51	18.30	0.96	13.14
cyp26a1	1079	1264	637	1071	1583	213.04	78.57	25.05	7.90	528.76
dact1-a	205	362	144	276	165	9.97	17.97	15.18	5.17	46.50
dact1-b	853	1231	819	1278	878	5.23	86.15	166.88	60.45	83.17
dhrs3	385	1034	353	676	252	68.33	7.22	43.54	12.22	42.34
dusp5	540	366	545	1000	759	51.32	84.47	95.42	28.32	177.99
dusp6	435	387	410	513	467	46.34	101.51	37.71	76.37	82.39
e_Cerberus	2270	11643	2624	1543	171	141.70	757.48	383.98	251.68	32.61
e_darmin	497	3042	2101	129	31	311.98	1839.84	1229.12	17.81	21.59
e_Sox17alpha	1059	3157	3350	896	740	0.60	277.93	444.88	129.58	165.39
e_Sox17beta	1125	2399	3617	589	693	44.89	262.81	819.25	89.00	126.73
e_TGIF2	325	540	546	507	641	39.75	95.31	44.06	99.54	17.23
e_vpp1	58	495	1	73	1	24.16	60.33	0.00	23.09	0.00
ec_Sox2	675	13	16	716	308	123.91	10.58	7.79	141.56	93.31
ec_tubb2b	14	30	20	10	2	10.58	3.26	10.86	4.95	1.08
ec_xk81a1	1293	2	9	2	139	947.41	0.66	5.54	0.85	61.21
em_BMP2-a/b	363	2779	812	312	156	15.06	398.36	27.84	37.76	14.18
em_BMP4-a/b	1804	1326	3224	772	2854	126.31	38.43	249.75	239.57	650.03
erf	285	220	396	252	279	15.83	11.12	12.57	26.43	24.45
fgfr4-a	836	1817	1818	459	304	87.77	76.32	85.05	82.10	27.44
fgfr4-b	570	829	824	256	122	47.19	114.93	5.80	13.62	3.45
foxh1	377	331	494	326	318	23.59	66.44	122.50	88.79	24.56
fst	90	460	131	1242	36	26.40	169.33	32.38	532.38	18.58
fzd4	401	597	334	165	38	11.30	17.01	60.31	34.58	5.47
gbx2.1	90	25	45	22	58	9.08	2.01	27.05	9.71	14.22
hey1	74	43	80	94	84	4.07	5.60	1.27	16.79	12.16
hk_g6pd	174	146	154	156	158	34.39	14.27	21.95	33.11	23.22
hk_gapdh	183	158	183	166	126	6.96	21.67	18.99	30.53	14.33
hk_H4	121398	79699	82820	98594	94515	9977.92	6004.00	8205.45	4499.58	21565.32
hk_ODC	5194	5192	5191	5192	5193	1.35	0.92	1.01	0.84	3.05
hnf1b	260	965	848	212	81	44.37	57.74	109.84	47.85	15.40
hoxa1-a	2	1	1	1	4	1.09	0.00	0.00	0.18	3.17
hoxa1-b	56	1	2	43	93	23.43	0.00	0.30	12.11	0.18
hoxa2-a	5	1	6	5	9	1.88	0.03	3.89	3.43	2.95
hoxa3	2	1	1	1	1	1.09	0.00	0.45	0.00	0.04
hoxa5	1	1	1	1	1	0.00	0.00	0.00	0.00	0.00
hoxb1	1	1	1	1	7	0.42	0.00	0.00	0.00	1.65
hoxb3	5	1	1	7	14	1.25	0.00	0.00	1.70	8.68
hoxb4	37	23	13	22	36	11.07	3.46	3.38	0.36	12.18
hoxd1	1120	38	496	493	1658	227.76	13.28	133.36	38.70	14.04
hoxd4	1	1	1	2	11	0.24	0.07	0.45	1.04	7.17
hunk	654	1004	1012	460	820	283.07	287.29	212.56	234.97	177.43
igf3	63	82	53	37	24	2.18	16.12	9.97	17.07	17.00
kiaa0182	329	267	317	263	271	79.45	64.19	38.85	87.03	42.95
kirrel2	250	699	926	282	323	88.83	162.61	287.27	66.01	31.61
lhx1	123	392	302	449	73	20.73	31.83	63.98	35.55	18.51
XI.47239	48	34	61	30	46	11.16	3.80	4.85	7.25	7.41

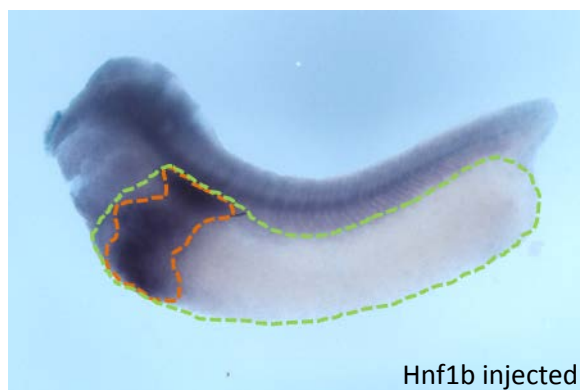
Appendix

gene	mean					SEM				
	CE	DE	VE	D	V	CE	DE	VE	D	V
m_Chordin	1628	3754	1	9973	1	275.23	1239.68	0.00	1926.31	0.00
m_Xbra-a/b	3076	204	1176	4094	5920	284.01	33.94	175.54	1113.01	1166.81
m_Xwnt8	967	514	2524	353	2587	281.33	194.16	648.56	88.23	725.10
me_ventx2.1-b	1256	747	2427	513	1999	347.85	239.94	784.41	0.01	43.09
meis3-a	405	304	342	330	279	92.13	26.83	19.20	54.07	41.97
mespa-a	8	6	30	11	13	0.18	0.52	11.49	3.96	1.51
mespb	278	70	724	245	789	24.38	7.48	100.47	35.46	84.21
mxi1	302	188	237	240	169	26.81	58.92	46.60	7.96	11.99
myc-a	39	76	80	39	75	6.77	7.39	4.87	4.23	31.54
myc-b	882	229	1061	500	1995	341.90	31.04	228.01	169.71	622.63
ndrg1-a	1	1	1	1	1	0.00	0.00	0.00	0.00	0.00
ndrg1-b	1	1	1	1	1	0.00	0.00	0.00	0.00	0.00
neurog2-b	33	15	17	25	13	2.04	2.49	7.59	6.81	2.57
nkx6-2	30	13	1	356	7	8.87	5.15	1.12	48.78	6.30
nodal1	44	42	98	91	64	17.04	17.65	18.29	20.83	3.42
nodal2	82	12	10	93	88	51.89	1.03	0.21	25.47	26.18
nr2f5	11	13	18	7	9	7.92	10.64	13.03	6.26	7.86
pdgfb	18	13	12	4	7	9.47	0.38	6.56	1.20	5.77
pim1	351	284	163	243	224	8.08	12.35	13.43	16.36	10.44
pkdcc.1	281	987	193	473	20	51.73	97.59	60.42	8.23	11.76
prph	21	1	1	8	5	9.69	0.00	0.00	6.84	4.21
rara	15	9	24	19	29	6.84	1.63	2.66	4.17	10.19
rgs14	1	2	1	1	1	0.00	0.59	0.00	0.00	0.00
rgs2	26	18	31	156	44	4.20	14.91	3.88	1.28	16.55
sox9-a/b	94	106	97	40	165	0.00	10.58	13.18	7.01	25.42
spry2	615	501	250	1068	651	41.77	18.55	71.22	8.17	194.67
stox2	229	261	163	175	151	0.85	2.05	11.89	5.26	7.89
tdgf1p2-a	2	28	1	10	1	1.09	23.14	0.37	3.33	0.00
tdgf1p2-b	1	1	1	2	1	0.00	0.00	0.37	0.85	0.00
tmem72	41	100	107	51	25	8.77	40.94	40.33	14.57	9.77
trib1	26	17	13	26	7	2.33	8.01	4.92	2.57	3.79
twist1-a	42	215	29	104	7	24.00	84.16	16.11	76.88	6.30
txnip	88	245	230	65	34	8.57	42.90	68.34	10.22	2.99
Xl.15091	1	1	1	1	1	0.00	0.00	0.00	0.00	0.00
Xl.16263	1	1	1	1	1	0.00	0.00	0.00	0.00	0.00
Xl.32109	4	2	1	1	1	0.68	0.59	0.00	0.46	0.04
Xl.45046	172	80	246	176	298	32.39	7.09	11.94	2.96	4.44
Xl.4906	955	402	616	347	624	121.72	107.43	275.22	30.93	86.71
Xl.51509	16	1	1	40	60	10.71	0.00	0.00	21.59	32.41
Xl.57027	74	99	77	39	65	68.68	27.27	15.34	24.81	10.92
Xl.57926	371	240	308	580	543	28.35	64.40	68.19	157.01	52.06
Xl.58101	1	1	1	1	1	0.00	0.00	0.00	0.00	0.00
Xl.59256	1	1	1	1	1	0.00	0.00	0.00	0.00	0.00
Xl.6091	16	4	9	14	19	0.55	2.85	2.47	8.67	12.03
Xl.67202	1	1	1	1	1	0.00	0.00	0.00	0.00	0.00
Xl.68408	1	1	1	1	1	0.00	0.00	0.00	0.00	0.00
Xl.70850	1	1	1	1	1	0.24	0.00	0.00	0.00	0.00
Xl.71159	578	705	474	394	352	37.93	51.13	36.52	83.62	38.93
Xl.74263	1	1	1	1	1	0.00	0.00	0.00	0.00	0.48
Xl.79790	15	25	1	4	6	3.03	8.86	0.00	3.40	4.73
Xl.80297	54	1	1	301	111	25.24	0.00	0.00	16.66	55.77
Xl.85251	1	1	1	1	1	0.00	0.00	0.00	0.00	0.00
Xl.8753	1	1	1	1	1	0.00	0.00	0.00	0.00	0.00
Xl.9822	15	4	8	7	9	5.57	3.26	2.36	4.32	1.08
Xl.9874	1	1	1	1	1	0.04	0.00	0.00	0.00	0.00
znf703-a/b	1485	259	838	1136	2360	287.73	26.77	139.07	37.56	175.31

6.9 Analysis of the Hnf1b-overexpression phenotype

Tab. 6.22 Quantification of Pdx1 domain in the endoderm

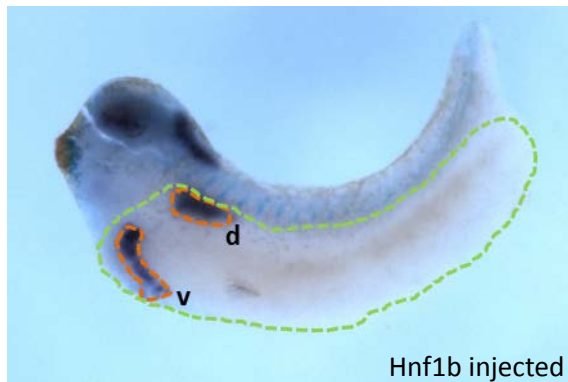
Image J quantification of Pdx1 area size (orange dotted line) within the endoderm (green dotted line).



	% pdx1 domain in the endoderm	
	control	hnf1b
A	12.53	17.16
	16.73	21.40
	14.21	19.05
	17.20	14.84
	11.74	13.68
	10.11	20.14
	10.21	12.70
	10.68	17.27
	8.11	13.95
	12.28	9.31
	9.75	14.98
	10.38	15.40
	9.47	13.82
	11.45	8.39
	4.84	11.78
	8.83	10.69
	4.54	10.90
	5.31	12.81
	6.91	9.79
	6.58	10.71
	5.67	12.66
	7.03	14.98
	7.67	8.71
	7.04	7.69
B	10.15	9.80
	9.55	10.07
	8.88	9.70
	11.11	14.12
	9.46	12.72
	9.80	12.34
	8.54	13.45
	8.70	9.38
	9.76	14.48
	9.93	9.73
	11.92	17.79
	10.07	16.01
	12.41	20.68
	13.41	16.89
	12.70	13.64
	11.41	28.30
	10.11	11.43
	11.88	11.43
	13.21	12.45
	11.70	9.95
	4.50	9.39
	5.94	8.76
	3.30	11.88
	6.18	10.42
	8.53	8.07
	6.25	6.13
	5.40	5.88
	6.70	
	4.20	
	5.88	

Tab. 6.23 Quantification of Ptf1a domain in the endoderm

Image J quantification of Ptf1a area size (orange dotted line) within the endoderm (green dotted line).



	% ptf1a domain in the endoderm					
	control			hnf1b		
	d	v	d+v	d	v	d+v
A	1.69	1.67	3.36	2.33	1.97	4.30
	1.52	1.61	3.13	2.64	1.74	4.39
	2.60	2.00	4.60	4.89	8.30	13.19
	1.43	1.27	2.69	3.50	1.82	5.31
	1.13	2.42	3.55	3.28	3.81	7.09
	0.40	1.29	1.68	1.84	3.67	5.51
	4.25	2.75	7.00	2.65	1.72	4.37
	1.33	1.95	3.29	2.71	0.00	2.71
	1.56	1.28	2.83	1.51	0.00	1.51
	2.63	1.81	4.45	0.97	2.16	3.13
	1.97	0.00	1.97	1.61	0.00	1.61
	1.00	0.00	1.00	3.46	1.62	5.07
	0.77	0.26	1.03	1.85	1.32	3.17
	1.29	0.00	1.29	2.65	1.99	4.64
	0.95	0.25	1.20	3.08	1.49	4.57
	2.93	0.67	3.60	2.68	1.70	4.37
	1.46	0.53	1.99	3.08	1.98	5.06
	0.59	0.00	0.59	2.89	1.67	4.55
	1.60	0.00	1.60	2.62	3.04	5.67
	2.01	0.29	2.30	2.33	1.52	3.85
	0.87	0.00	0.87	2.94	1.91	4.85
B	3.30	0.81	4.11	2.86	1.28	4.14
	3.19	1.65	4.84	3.22	2.71	5.93
	2.09	1.57	3.65	3.73	1.86	5.59
	2.59	0.73	3.31	3.93	1.07	5.00
	3.17	0.84	4.01	3.07	1.18	4.26
	1.38	0.58	1.96	3.01	2.82	5.83
	3.05	1.03	4.08	4.89	2.41	7.30
	2.16	0.82	2.98	3.70	3.75	7.45
	3.85	1.12	4.96	3.33	1.06	4.39
	2.56	1.28	3.83	2.41	1.66	4.07
	3.11	1.20	4.31	2.62	1.13	3.75
	3.72	1.37	5.09	1.54	1.00	2.54
	2.56	2.11	4.67	3.85	2.12	5.97
	3.80	1.35	5.15	0.62	1.31	1.93
	2.56	1.87	4.43	1.34	1.78	3.12
	3.12	1.25	4.37	3.39	3.86	7.25
	3.83	2.20	6.03			
	3.07	1.55	4.62			
	3.42	1.38	4.80			
	1.29	0.94	2.23			
	1.22	1.22	2.44			
	0.90	0.78	1.68			
	0.79	0.25	1.04			
	0.36	0.97	1.33			
	1.33	0.81	2.14			
	1.01	0.76	1.77			
	1.33	0.52	1.85			
	2.59	1.32	3.91			

Tab. 6.24 Predicted Fzd4-gRNA off-target sequences in exonic regions of the *Xenopus laevis* genome

highlighted in green are the tested off-targets; PAM= protospacer adjacent motif

Coordinates	strand	MM	target_seq	PAM	gene name	gene id
Scaffold149 581:4344665- 4344687	+	4	GG AAG ATG[GTGA ACCTGAAG]	AGG	utp14a	XB-GENE- 5954915
Scaffold230 826:3712453- 3712475	-	5	AGAGCAGG [TTGATCCTGATG]	AGG	impad1	XB-GENE- 5751113
Scaffold102 068:223547- 223569	+	5	TGCTCAGT [CTGATCCTGATG]	GGG	kremen2	XB-GENE- 866619
Scaffold139 113:827475- 827497	-	5	GTTTCATG [ATGGTCCTGATG]	CGG	fzd7	XB-GENE- 483735
Scaffold307 11:2325955- 2325977	+	5	GCCTCCTG [ATGAGCCTGATG]	AGG	zmym4	XB-GENE- 1217387
Scaffold719 7:648108- 648130	-	5	GG TACACC [GTTATTCTGATG]	TGG	edc3	XB-GENE- 5890837
Scaffold476 83:3850870- 3850892	-	5	TATACAAG [GTGATCCT GGTG]	AGG	exog	XB-GENE- 981842
Scaffold551 71:287242- 287264	+	5	GG GAA TTG[GTGATCCT GTTA]	GGG	gcdh	XB-GENE- 1016454

6.10 Nanostring code sets

Tab. 6.25 Nanostring Code set used for the confirmation of pancreatic organoid formation

Target	Accession	Target Region	Target sequence
Actb	NM_001088953.1	1179-1279	ATGCTTCTAAAGGACAGACCCTTTCAACATGAACAAA TGTACCTGTGCAGGAAGATCACATTGGCATGGCTTT ACTCTTTTGTGGCGCTTGGCTCAGAA
Amylase alpha2A/ B	NM_001086441.1	555-655	GGATTTGGCAATGGAGAAAGACTATGTTTCGTGGGAA GATTGCCGAATACATGAACAATCTAATTAACATTGGG GTTGCTGGATTGACTGGATGCTGCT
Chordin	NM_001088309.1	1455-1555	GACGTCCGCAAAGCATGTCAGGCATAATCACAGTCA GAAAATCATGTGACACTTTGCAGAGTGTGTTATCGG GTGGTGACGCTTTAAATCCCACCAAAAC
Cyp26a1	NM_001095469.1	984-1084	TCTTGCACTTCACAAAGATGTTCTGGAAAAGGTCCG CAAGGAGCTCGAAAACACAGGGTCTGTTGTCAACGAA ACCCGAGGAGAAAAAGGAAGTAAGCATG
Darmin	BC045077.1	787-887	TATATTTGCTGAACACGCTTGCAGATGGAAAGGGTC GCATCCCTTGTCCAGGGATTTATGAGGCCGTAGCAC CTGTGGGTGAAAATGAAACAGATTTGTA
Dkk1	NM_001085592.1	770-870	GAGATTTTCCAGCGTTGTCAGTGCAGGTCGCGGACTC TCGTGCCGGTTACAGAAAGGAGAATTTACAACGTGC CCTAAAACATCGAGACTTCACACTTGCC
Elastase2 A	NM_001092506.1	512-612	AATGGCCCAGCACCAGATAAACTGCAGCAGGGGCT CTTACTGGTGGTCGATTACCCAACCTGTTCCAGCG GGACTGGTGGTGGAAAAGCGTAAATACCA
FoxE1	NM_001095544.1	1594-1694	CAGTCGGGCATGTGAAATCACGTTGACTATGGTCTG CTGATTGTACCCTTAGATGGGCAGCCATGTAAGGC AAGATACCATTCTCTACAGTCATATTG
FoxE4	NM_001085733.1	16-116	GGATCCCAGATGACTTTTGTCTGTGTTGGGACTGAGA GGGTTTTGTTTATGAATTTGGCAAGTTTCCCTTATTAT TCAGGCATGTGCACCATGACTGCAGA
G6pd	NM_001086550.1	862-962	GTGGAGGATACTTTGACGAATTTGGCATCATCCGGG ATGTCATGCAAAATCACTTGTCTCAAATGATGTGTTT GATGGCTATGGAGAAGCCGGTCTCCAC
Gapdh	NM_001087098.1	773-873	ACCTGCCGCCTGCAGAAGCCGGCCAAGTACGATGA CATCAAGGCCGCCATTAAGACTGCATCAGAGGGCCC AATGAAGGGAATCCTGGGATACACACAAG
GATA-2	NM_001090574.1	192-292	CCAGGACTAACGGGGACAACACTCACTTTCACTTTTAAAC AGCCGAAGCCTTGCTTATAGGAAGGACACATATATC TGGCCGATCTCTGGAGAGAACCTTGCT
GATA- 4a/b	NM_001090629.1	571-671	GCACCCAAACATAGAGTTTTTTGACGATTTTTCCGAG GGCCGAGAATGTGTCAACTGTGGAGCAATGTCAACC CCACTTTGGAGGCGGGATGGAACAGGC
Glucagon	NM_001085673.1	385-485	AGCAATTGGATGAAAAAGCAGCCAAAGAATTTATTGA CTGGCTAATAAATGGAGGACCATCAAAGAAATCATT TCAAGACGCAATGCAGAATTTGAGAG
H4	NM_001094457.1	129-229	GGAGAGGGGGAGTCAAGCGCATCTCTGGCCTCATC TATGAGGAGACTCGTGGGGTCTCAAGGTTTTCTG GAGAATGTCATCCGGGACGCCGTCACCTA
Hes1-a	NM_001087927.1	557-657	GAGGGGTCAACACAGATGTCCGGACCCGACTCCT GGGGCATCTTGCCAACGTGATGAACCAGATCAATGG CATGAACTACCCTACCCAGCCCCAGATGC
HNF6 gene2	DC109227.1	141-241	TGTGTCCAGTTGGCAATGTTATTGGAAGCTTTACTC TTATGAGAGAGGACAGAGTTTTGGGGCCACCAAGTA ACTTTTACAGTCACTATCCCAAAGACA
Hoxa1-b	X62053.1	1149-1249	TGAGATGATGGAATGGTAAAAAGCTCAATGTTTTCT AGCACAGGAGAAACAGCAGTGTTTGTGACCGCATA CCTCAGTAATCTCTCTCATTTACTAGG
Insulin-a	NM_001085882.1	608-708	AGGTGACAGGGCAGGTTACATTTATTAAGTTCAGAT GTAAAAAATAAATACTGGAAGAAAAAGAGCCACC CCAATTGTTAGTCCCCTCTGCTTTTA
Insulin-b	NM_001085881.1	165-265	CTAGTATGTGGGGATAGAGGCTTCTTCTACTACCCTA AGATCAAACGGGACATCGAACAAGCACAGGTCAATG GACCCAGGACAACAGATTAGATGGAA

Target	Accession	Target Region	Target sequence
Isl-1	NM_001110718.1	1102-1202	TACAGAGTGACATTGATCAGCCGGCCTTCAGCAAC TGACCTGTTTCTCACAGGTTAATTTTTTCAGAAGGAGG ACCTGGCTCTAACTCTACAGGGAGTGA
Ngn3	NM_001134785.1	216-316	AAAGAAGCAAAGGGTCAAGCGAATGAGATCAAAAAGT AAAGAGCGACGGCGTCGTCTGTAACAGAGGAGAA ATCGCAGGGTCAAAGCCAATGACAGAGAG
Nkx2.1	NM_001085624.1	1392-1492	TTCAGACTCTCTATGGTGTCAACAACAAGATGCTTGT ACAGTACACAGGGCTTTACTGGAGATCTGGGGATAA GATGCTACTGAAACCTTCAGTCTCAA
Nkx6.1	NM_001099916.1	172-272	AATACATCATTCCCTCTGCAGCTTGAAGTATTAAA CCTCGGCCATCCAACACTACAGCCAGCGTCTGGTAG GATATAGTGATTCACCCTTGGAGTTGT
Nkx2.2	NM_001085622.1	133-233	AGAATTGGGTGCTTTAGCCAGACCTCAGCTAAACC TGACTTTGGCATTTCCTGGAGTTACAACTATAG GAATAGCGCTTGGTGTCCCTCAACTG
Noggin	NM_001085644.1	561-661	ACCCAACCTTATTTTGTGCAGCTGTGTGCAGCATG GATCATTCCCAGTGCCTTGTACTATATATGCTCTGA TGGTCTCTTGGGACTTAGAATAGACC
Odc	NM_001086698.1	855-955	GGATATAATTGGTGTGAGTTCCATGTTGGCAGTGG CTGCACTGATCCACAGACTTATGTACAAGTGTCTCA GATGCACGATGTGTCTTTGACATGGGG
Pax6-b	NM_001172195.1	1339-1439	CTTACAGTGCTTTGCCACCTATGCCTAGTTTTACGAT GGGCAACAATCTACCTATGCAAGTCTCATTTCCCTG GAGTGTGCTCCAGTTCAGTACCC
PDia2	NM_001090179.1	881-981	TGCTGCCAGATCCCAAACCACTTGTGCTGTTTATC AATAAGAGTGACGATTCCCAACTGGTGTCTGGAA CATTTCCGCAAAGCAGCTCCTGACTTT
Pdx1	NM_001172211.1	162-262	CCAGGCAGTCTCCAGACATCTCACCGTATGAAGTG CCTCCATATCTGAAGAGCCATTGTTCTCACCTCC ATCACCATCACTACCATCATCACCACC
Ptf1a-a/b	AY372268.3	149-249	CATTCTCTAGGGACGCCCTGGACGCAGACGACTTT TTGGAAGACGATGTAGACTTCTGGCCGGTCAGATC CAAGACTATTACAGAGACAGCCGAGTGC
RALDH2	NM_001090775.1	966-1066	TGGACTATGCAGTTGAACAAGCACACCAAGGTGTGT TCTTTAACCAAGGACAGTGTGTACTGCTGGCTCGC GGACATTCGTAGAAGATTCCATTTATGA
Somatostatin	NM_001089250.1	178-278	CAGAAATCACTCGCAGCGGCAGGGAAACAGGAGTT GGCCAAGTATTTCTGGCAGAGTTGCTATCAGACCC TTCCACAGACAGAGAATGAAGCATTGGAAT
Sox1	NM_001095674.1	1663-1763	CTGTGCTCATCCTTTTAGAGACAATGCGTCCAGCCT GCTCATCAAGGATCGGGCAGCACACTTGCTCCACT TTGCCACAACCTGCCCTCTCTTTTTCTTT
Sox17a	NM_001088162.1	567-667	TGCTGGGCGCAGATGGAAGGATGTGTCTAGAGAACT TCAGCCTGGGTTATCATGAGCAGACTTACTCCCACG GCCAGGTTCCCTCAGAGCAGCCACTACAG
Sox17b	NM_001088164.1	163-263	ATGGACCGAACCCCTGACCGTGTTCAGGACCTCAA ACCCAAGAGGGATGAAGGATCTGCCGATTCCAGAAG CAAAGCCGAGGGTCCGATCCGCCGACCC
Sox2	NM_001088222.1	901-1001	CCGGGCATGTCTCTGGGATCCATGGGCTCGGTAGT CAAGTCGGAATCCAGCTCCAGTCCACCTGTAGTAC CTCTTCTCCATTGCGGGCTCCGTGCC
Sox3	NM_001090679.1	998-1098	GCTCACTACATATAACACTTTGTGCCCTTTGCTAAA GACGCTTTACTTGCCTGCTGGCAACTATCAGACTGC CGCATAAAACATTTAAAAAAAAAAATC
SP-C	NM_001096721.1	18-118	CCACCTGTCTATTCAGAGTTGCCAATCCCATGTTTCG GTGGGGTTAAGAAGCTTGTCTGTGTGCTCTGGTGG TGGTGGTCTTGTGCTGGTTCTGGTTG
TGIF2	NM_001094168.1	2638-2738	TTTGAGATATTTGTGAAGTGTGCCTTGGGAAGCAGC ACATTTCCCGGTAACACGAGTCTTAGACTGACCTTT TTGAGTACTAGGACAAAAGTAACCTGA
Tm4sf3	NM_001087390.1	133-233	TTTGGGTGTCTCAATTTGGGTCCGAGTCAGCAAAAAT GTGCAAAAAGAACTGAACATTGAAGGAGGAAGCTTG CTTGACAGAGTTGATCTCATGATTGCA
Trypsinogen/trypsin	BC056068.1	390-490	GCCCTCGGCCTGTGCTTCTGCCGGCACCAACTGCCT GATCTGGCTGGGGGAACACCTGAGCAGCGGCA CCAATTACCCAGATCTCCTGCAGTGCCTG

Appendix

Target	Accession	Target Region	Target sequence
Ventx2.1-b	NM_001087981.1	1075-1175	TTCCACAGGACAAAAAATTGCACTGAATGTTGCTATT GGCAAGATGATTACAGAATAGCTGGCTACTATTGGC CTATTTGTTATGTATCTTTACATGATT
Vpp1	NM_001258387.1	177-277	CATCTCTGGTGCAATGTCAGTCATTCCCTCAGCCGGG GGATTTGAGTGGTCTGTGTTCCCGGCACATTCTCCT TCCCAGAACTCCAGATCATCAGCTCCA
Xbra-a/b	NM_001090578.1	534-634	AGCCCACTGGATGAAAGATCCTGTCTCTTTTAGCAAA GTCAAACCTACAAACAAAATGAATGGTGGAGGCCAG ATTATGTTAACTCTTTCACACAAGTAT
xCRABP1	EU816559.1	28-128	TGACGAACTTCTGAAAGCTCTAGGTGTTAATGCTATG CTTAGGAAAAGTGGCTGTAGCAGCAGCTTCTAAGCCT CATGTTGAAATCCGTCAAATGGGGAC
xCRABP2	NM_001085780.1	468-568	CTGACCATGACTGCTGATGATGTTGTCTGCACACGG ATTTACATCAGGGACTAATTTACAGAACTCTATGGGA TAAGAGGCACCATCCTCATCCTTCCCA
Xhex	NM_001085590.1	1387-1487	AACCCTCGCTATGCTTCAATCTCCTCCCAGGGATGG CAGTCCTAAAGTTTGGGAAGGAGTGCAAAGGACATT TTATAGGTGACAAATGTCTGATCATGGTC

Tab. 6.26 Nanostring Code set for the verification of RA-responsive candidates

Target	Accession	Target region	Target sequence
Bhlhe40	BC073563.1	350-450	GAAAGACCTGTTGCCGGAGCACCTCAAACCTGACTACTTTG GGTCACCTTGAGAAAGCCGTGGTCTCGAGCTGACCTTGA AACACGTGCAGTCTTTGTCC
BMP2-a/b	NM_001085 884.1	1290-1390	GTTGCCCCACCTGGGTATCATGCCTTTTACTGCCACGGGG AATGTCTTTTCCACTGGCAGACCATTTAACTCTACAAAC CATGCAATCGTACAAACTT
BMP4-a/b	NM_001088 032.1	1146-1246	GAGATTGTCCATTTCCCTTGGCTGATCACCTAAACTCAACT AACCATGCTATTGTACAAACTCTGGTAAACTCTGTTAACGC AAGCATCCCAAAGCGTG
C10orf140	DR716716.1	783-883	CTGTGCTCTTCACTCCAGTATCATGCGCTGTGACGTATCCT GGGATATCTCACAATCGTGAACGAAAAGCAACTCTCTCCT GATACAGTACCCTCTCA
Cass4	NM_001091 015.1	2773-2873	AGGTTGCCCTGCTAGCTGTTCAAGAGTCTTTGAAGGTGTT TAGGTGGCACACAGGAAGTGTAGCCTGTAGCCATGTAGGT GCCTTTAATCAAGTGCAT
Cdx4	NM_001087 251.1	834-934	TGCAAGCATGTCACTCTGTCCCAATGAACTACTAGCCTTGG CAGTATTAAGTGAACACTGATCACTCAGACATGAGACCTAC AAGTCATCACCATAGTTG
Cebpd	NM_001089 609.1	1695-1795	ACTCAGGATAAGGGTTCATTGATGCCACATTTGTAATCCTA TTAACCTGTTGGATGTATGCCAAGCTGCAGCCATACTCCCT TACTGTTTTCATTCACTC
Cerberus	NM_001088 331.1	754-854	CTGGATCTAAGAATGTAGTAAAGGTTGTATGATGGTAGAG GAATGCACGTGTGAAGCTCATAAGAGCAACTTCCACCAAAC TGCACAGTTAACATGGA
Chordin	NM_001088 309.1	1455-1555	GACGTCCGCAAAGCATGTCAGGCATAATCACAGTCAGAAA ATCATGTGACACTTTGCAGAGTGTGTTATCGGGTGGTGAC GCTTTAAATCCCACCAAAC
Cxcr7	NM_001088 767.1	812-912	GGGGACCAAGAGAGGAGAATCAGTGAAGGCTTATTGTTT CTTATGTAGTTGTGTTTATGGTTTGTGGCTGCCATACCAT GCCATTGTCATACTAGACG
Cyp26a1	NM_001095 469.1	984-1084	TCTTGCACTTCACAAAGATGTTCTGGAAGGTCGCAAGG AGCTCGAAACACAGGGTCTGTTGTCAACGAAACCCGAGGA GAAAAGGAACTAAGCATG
Dact1-a	NM_001088 772.1	41-141	CACGTTGTGCAGAAGTCGGGCTTCGGTCTTGGTTGGGAA TAGCGAGGCGGATTCTCATTGGAGCCCCGTGTACGTGAGT TGCAGCCGCTGCAGATGCTC
Dact1-b	NM_001090 441.1	95-195	GCGCAGGAGACGCTAAGTCGCAGAAGTTGATGCATTGTAT CCGCTGATAAGTACTGGGAGTTTGGTTTCTTGCAGTATAGT GTGAGGATAAAGATCCCCG
Darmin	BC045077.1	787-887	TATATTTGCTGAACACGCTTGCAGATGGAAGGTCGCATC CTTGCCAGGGATTTATGAGGCCGTAGCACCTGTGGGTG AAAATGAAACAGATTTGTA
Dhrs3	NM_001092 373.1	817-917	ATGGCCACATTGTTTGTATAAACTCTGTGCTGGCCTTATCT GCCATCCCTGGTCCATTGACTATTGCACTTCCAAATCGTC CTCCTTTGCCTTCATGGA
Dusp5	NM_001092 854.1	581-681	TGTTGAGATCCTTCCGTTCCATATCTCGGCAGCGCCTATC ACGCTTCCAAATGCGAGTTCCTTGCGAATCTGCACATCACC GCCTTACTCAATGTCTCG
Dusp6	NM_001089 787.1	686-786	TGACAGGGATCCCAGCAGTGCAACAGATTGACACGGTAGT CCTCTATCCAACCCTCAGCCATCATTTCCGTTGAGATCTT ACCCTACCTTACCTCGGT
Erf	NM_001096 253.1	225-325	GCGTCTGTGGGGCGTTCCGAAATGCAAACCGCAGATGAAT TATGATAAACTGAGCCGGCACTCAGGTATTATTATACAA GAGGATTCTCCATAAAACC
Fgfr4-a	NM_001087 718.1	230-330	TTGCTTTCGGTTCGGGGATTATTTTGTGCCGCTGAGGAAC GGAGACTAGTTCCTATGAATGGGATCACGAGTAACCTTCTA ACGGCACCAGGAGATCCG
Fgfr4-b	NM_001088 550.1	2808-2908	TTTATTTCCCGGCCCAAGAGATGGGCAAAAGTAGCACT GTGATCCCACTTGCAGGGCACATGAACTTCTTAGCAACG GAGATAAGTTCACAGCTAAG
Foxh1	NM_001088 351.1	563-663	GGGTAACCTCTGGACGGTGGATGTTAGCCGGATTCTCTG GATGCGATGAAGCTGCAGAACACTGCGTTGACCCGAGGTG GATCAGACTACTTTGTCCAG
Fst	NM_001090 590.1	355-455	ATGTAATAAGTGAACAAGAAGAACAAGCCGAGGTGTGTCTGC GCTCCGGATTGTTCCAACATTAAGTGGAAAGGTTCAAGTGTG CGGAATTGATGGCAAAC
Fzd4	NM_001090 453.1	1046-1146	CATCATGAGATTGGTGGATGCCGATGAATTGACTGGCCTTT GCTACGTGGGCAACCAAACATAGACGCGCTCACGGGCTT TGTGGTCCGCTCTTTTT

Appendix

Target	Accession	Target region	Target sequence
G6pd	NM_001086550.1	862-962	GTGGAGGATACTTTGACGAATTTGGCATCATCCGGGATGT CATGCAAAATCACTTGCTCCAAATGATGTGTTTATGGGCTA TGGAGAAGCCGGTCTCCAC
Gapdh	NM_001087098.1	773-873	ACCTGCCGCCTGCAGAAGCCGGCCAAGTACGATGACATCA AGGCCGCCATTAAGACTGCATCAGAGGGCCCAATGAAGGG AATCCTGGGATACACACAAG
Gbx2.1	NM_001090431.1	1593-1693	GTAGTTTTACGACAGTAATAGGGCCATAATATGGTCATCCC TGGACAATGAACAAAATTAGCCACGGGGTACAGACAATGCAG GTTGTTGGTTGCCAATAAC
H4	NM_001094457.1	129-229	GGAGAGGGGGAGTCAAGCGCATCTCTGGCCTCATCTATGA GGAGACTCGTGGGGTCTCAAGTTTTCTGGAGAATGTC ATCCGGGACGCCGTCACCTA
Hey1	NM_001090457.1	1605-1705	ATCAACAGCAATGCCTTTCAGTAAAGCTGTGCATGGAAGGG GTGTGTGCTGAAAAGTGGGGCCACAAGCATTAGAGGGTT AAACATAACACTGAGTGCAC
Hnf1b	NM_001089811.1	1626-1726	CACAGCAGCCATTTATGGCGACTGTGACTCAGCTACAGAAT TCACACATGTATGCGCACAAGCAAGAGCCTCCCCAGTATTC CCACACATCTCGTTTTCC
Hoxa1-a	NM_001085719.1	168-268	CAACTTTCAGTCGTGCGCAGTCAGTGCTAATAACTGCAAC GGCGACGATCGTTTTGTGGTCCGACGAGGGGTGCAGATAA GTTCTCACACCCATCACCA
Hoxa1-b	X62053.1	1149-1249	TGAGATGATGGAATGGTAAAAAGCTCAATGTTTTCTAGCA CAGGAGAAAACAGCAGTGTGGTCTGACCGCATACTCAGTA ATCTCTCTCATTACTAGG
Hoxa2-a	NM_001085750.1	130-230	GGCTGAGTTGTTAAAGGGCTTGGAGGAGAGGGCCATGAA TTACGAATTTGAGCGAGAGATTGGTTTTATCAATAGTCAGC CGTCGCTTGCTGAGTGCCT
Hoxa3	NM_001086824.1	277-377	CATTGGAGGAGGAACGCCACGTGACAGAGGGGTGCCAAT GTTATTCCTTACGGGTGTCAAGACCCTGTCAGTTTGTGAAA TAAATATTGGGAAACAACGA
Hoxa5	AC236444_r a.1	298-398	ACTTCTCTGTGACTTCTGTGAAGTACCCTCCTCCCCAA TCTCTTGTCCACCCTTTATCCTAGCAATGAGCCTTTAAACT GGGTGAAATAGCTTCAA
Hoxb1	FJ422584.1	486-586	CTCCTGCCCTCCAGATCAAGCTCTACCCAACCACACCTTTG ACTGGATGAAAGTAAAGAGAAATCCTCCAAGACAACCAAAA CCAATGGACTATGGACCC
Hoxb3	M91588.1	8-108	AGCGCGCACCCGTTACACGAGCGCACAACTGGTGGAACTG GAGAAGGAGTTTCACTTTAATCGCTACCTGTGCCGCCCA GGAGGGTGGAGATGGCCAAC
Hoxb4	NM_001096264.1	217-317	GCAATAGCAGCAGCAGCGCTCCTACTCCTCCTGCCAAGG ATCTGTGCGTCAAAGCGCAAGGCTGCCTCACTCATCTGGA CTTGTCACAGCGAGAAAAGC
Hoxd1	NM_001090566.1	58-158	CGGCCAGAGAAGTCTCCCTAGAGATGAATTCCTACCTAGA ATACACTTCTTCCGGGATGTTTTAGCTTTTTACCCAAGTT CTGCCGACGCGACCACAG
Hoxd4	NM_001173995.1	1013-1113	CAGGAAATAATGACTCCAGGGCAGTCAATTTATAGGTGAT GCTGTGTAAAGGATTTCTATGGCAATAAGGGACTATTAGT TCAGAGGCACAACCAACA
Hunk	NM_001091243.1	1214-1314	CCACATGTCTGAGAAACTTGGCTACAAAACACAGCGATGTGA TCAACGTCATTCTCTCCAATCGAGCTTGCCATACCCTGGCC GTCTACTTCTCCTAAAC
Igf3	NM_001088668.1	389-489	CTATCCTCGAGTCTTACTGTGCGGCTCCAGTCACTAACTTC ACTGGCAGAGAAGAGCAAAAAGTCCCTAAGATCATTCTCCAAG ACCTATGCCACCAGTTTA
Kiaa0182	NM_001097124.1	2037-2137	GAGTTGGCAGAGAAGTATCAATCACAAAGAGAGTCTTCAG CCATGGAACATGCAGGTTACACGCATACTCCATTCTTAGCT GAGCTAGAAAAGTCAACTC
Kirrel2	NM_001086488.1	690-790	CCCAGTCGCCAATGTCCTGCTTGATGTACCCTACAATCTCA CCTGTCTTGCTTCCGTCGCTAAGCCTGCTGCAGAGATTACC TGGTTCCGTGATGGAAG
Lhx1	NM_001090659.1	21-121	TCTATTCTCCTAATCCGCCATTCCTCTAAAATCCCAAATAA CCAAAGGCAATGGTTCACTGTGCTGGATGCGAAAAGGCCCA TTCTGGACCGTTTTCTTGT
LOC100158377	NM_001127821.1	392-492	GTCTATAAGGTGACACAGGGTATTGGATCTAAGTCGATGGT GGTGAAAATTTACAAAACGATGTGATGAGGAGGGAATTG TCCGAGAGATCACTTTGC
Meis3-a	NM_001088397.1	1517-1617	CTATGATTGACCAATCTAATCGCACAGGGCAAGGAGGTGC TCCCTACAGTCCAGATGGTCAGAACATGGGAGGATATGTC ATGGATGGACAACAACACAT
Mespa-a	NM_001085581.1	1570-1670	TGTGAAAGGCTATGGCATTAAATATACTGTCTTCTGAAAGA ATCTTGGCTTCCCTAGTGTCTTCTGTGAAACAATAGGTAATG GCTGCAATAAAAAGGTCC
Mespb	NM_001135226.1	725-825	TATTAAGCAGGACATGACCTCCCCACAGTACAATAGCACA GTAGCTACGCCTGTCAGTCAACAGTATGTGACAGGGCTCC

Target	Accession	Target region	Target sequence
			AACACACGATTCACCTGTAA
Mxi1	NM_001095701.1	2418-2518	GCTGCTGCAGGTCATTATCATTCTGCAATCTGTGTTTGGGTGGACTTCCCCTTTAACTCTGTTACAAACCAGAAATGACACATCCCAGAATCCTCAGCTCC
Myc-a	NM_001085896.1	523-623	TCTGCTTCTTCTTCTCCGTGCCGAGTCAACCACCACCGAGCCCGCTTAAGTCTCCCTCGTGTGCATGGGAGCCTGAGTCTGGGAGGGACCCACAGGAGC
Myc-b	NM_001090653.1	76-176	AGCTTGTGATACAACGAGAGGAGAGGGAGGGAGTCAAAGCGTCGGCTCAGCCTGTGGATTTACAAGCGGACAGCTCTCATAGGAAACCTTGGACTTGT
Ndr1-a	NM_001094390.1	1428-1528	AAAGACCTGCTTGCCAATTGAAACATCCTACCCTTCCCCTATCTGGGTTACTCCACCAGCAAATGGGGGGTTATGTTTTGATATAACTGTGAACT
Ndr1-b	NM_001087158.1	1429-1529	GAAGACCTGCTTGTCTAATTGAAACATCTTAACTCTTCGCTGTCTGGGTTACTCCACCAGCAAACGAAAGGGGGAGGCTACGTTTTGATATAACTGTGAA
Neurog2-b	NM_001088335.1	1172-1272	CATCGTTAGCTATGTGATTAGGAAACTGTCTATCCCTCATCTGCACCTGTAGACTACAGCTACCAACTTCTGTTACCAGGGGCTACTGGGTAATGT
Nkx6-2	NM_001096886.1	28-128	TGTTTGTGCGCCGCTGCATGTGTGGGATCATTACTGCCCTGAACCTTGCCTGATCGCCGGGAAGTTGCGACAGAAGCCGTTGGCTCGGGGACTTCTCTC
Nodal1	NM_001085796.1	781-881	CTCTGCCAACCATATTGGCTTTCCAGCCTCATCAAGACAGCAGAGTCATCCAAATACGTTGACATAGAGAAAGCTAGTAGAGTGCCCTGGTATTAGGAGA
Nodal2	NM_001087967.1	776-876	GACAAGCCCACTGCTAGTCATTTTGGATCTCCTAGTCTCATCCACTGTGGAGTCTTCCAAGTATGTCATGAGTGAAAACA CAGTCAGGGTGACAGATA
Nr2f5	NM_001101759.1	301-401	AGTTCACCTGTGAAGGGTGCAAGAGTTTCTTTAAGAGGTCGTGAGGAGGAACCTAACCTACACATGTAGGAGCAACAGAGACTGTCTATAGATCAACA
Odc	NM_001086698.1	855-955	GGATATAATTGGTGTGAGTTTCCATGTTGGCAGTGGCTGCACTGATCCACAGACTTATGTACAAGCTGTCTCAGATGCACGATGTGCTTTGACATGGGG
Pdgfb	NM_001094466.1	345-445	CGGGTCATTTCGAGCTTAGATGCAGAAACAAGCCGTCCTTG CAGAGTGCAAACCCCGCTCGAAGTGTGTTGAGATTTCTCG CAAGTTAGTGGACCCCACTA
Pim1	NM_001095150.1	1270-1370	AGACATGTGGTGACCTCAGACTGTGATACTTACCTTGGTGGTTCCCTCCTCTTCTAAAAGATGGACTTTGAAGGTGTGAGGAGAGATGAGAAGGGTTTTG
Pkdcc.1	NM_001097762.1	1330-1430	TCCCGTGTTTACATGAAAAAACAAGCAACCTCAAAAAGTGATGCGGATGGGAAGAGTCACGCTCGCTTATATGATGCACTGAAGTACTAATTGGCTTTA
Prph	NM_001087060.1	1440-1540	GACCCAGTTCATTGCAATACCTCTCCATGGACGGAACCTCCTGTGCTTTTCTAATTGATGGATACTGAGGGTCATCTCCACTAACACACTCCTTTATCT
Rara	NM_001090254.1	2435-2535	ACCTGAACAGTCTAAAGGGTTTGGGGAGCAGTTAAAGGGGAAATAAAGAGAGGAGATGTGAGTGCTTTGTGCTTGGGTGTGTGATGGAAGTGAAGAGGAA
Rgs14	NM_001092238.1	752-852	AAGGACATTGCAAAGAACTTTAGACAGCCGCGAACTCTCACTCGCCGGGAATCATGGGTACTTAACTCCAATAACAGTCTGGAGCTGAGTCTCAA
Rgs2	NM_001095045.1	24-124	CTCTTACTAGCATCACTGACTAATCCAGAACAAGCAGAA TCGAGCACAGGGACTTATACAAATCCTTGGAGGGAAATTATGCAGAGCGCAATGTTTCT
Sox17alpha	NM_001088162.1	567-667	TGCTGGGCGCAGATGGAAGGATGTGTCTAGAGAACTTCAGCCTGGGTTATCATGAGCAGACTTACTCCCACGGCCAGGTT CCTCAGAGCAGCCACTACAG
Sox17beta	NM_001088164.1	163-263	ATGGACCGAACCCCTGACCGTGTTCAGGACCTCAAACCC AAGAGGGATGAAGGATCTGCCGATTCCAGAAGCAAAGCCGAGGGTCCGATCCGCCGACCC
Sox2	NM_001088222.1	901-1001	CCGGGCATGTCTCTGGGATCCATGGGCTCGGTAGTCAAGT CGGAATCCAGCTCCAGTCCACCTGTAGTCACCTCTTCTTCC CATTCCGGGGCTCCGTGCC
Sox9-a/b	NM_001090807.1	441-541	GAAGTCCCCGTGTGCATCAGAGAAGCGGTGAGCCAGGTGTTGAAGGATATGATTGGACCTGGTACCGATGCCAGTCA GAGTTAATGGATCCAGCAAG
Spry2	NM_001088769.1	157-257	TTCCCTCACACTTCATTTAGTGGATAACAAGGATCGCGCTG GATTGGGGGAGCCCTGGAACCTGACACATGTTTTCTGTGTCCCTCTATCGGGCTTGG
Stox2	NM_001093369.1	162-262	TTTTTCCAGGTGTACCCACTCCAAGTCCAGAGGTACTTCG GCATACACTTAACATGCTTGTGCGAGAGAGAAAGATCTACCCTACTCCCGACGGATATT

Target	Accession	Target region	Target sequence
Tdgf1p2-a	NM_001095665.1	843-943	CACCAGAGAAAACAAGGCTGCATTATCGTAGAAGATCCTGCATAGAAAAAATCTCACTGCTCTATAAGCATAAAATATCTACATTAACCTCTCCCATGGA
Tdgf1p2-b	NM_001127822.1	1958-2058	GGAAGGCCAAATTGGACAGTAATGCTCATATACAAATGCAAGCGCAAATCGCTATAATGGATTAATAAATCAGCACCCATTGACACTGTTTCAGAAAGCT
TGIF2	NM_001094168.1	2638-2738	TTTGAGATATTTGGAAGTGTGCCTTGGGAAGCAGCACATTTCCCGGTAACACGAGTCCCTAGACTGACCTTTTTGAGTACTAGGACAAAAGTAACCTGA
Tmem72	BC133254.1	204-304	TGTGCTTAGGCCAAAACAGGACGCATGGGAGGATTTCAAAAATTTGTGGGATATGGCCTGCTATCAGTGGCTTGTCTTTTGCACCCAGTTTTGGTCTGGCA
Trib1	NM_001095725.1	3019-3119	GCACTAAACCTCCTTGCGGTTTCGGTGATTACTGTATCTGTGATACAATGGAGCGACTCTGTAATAGTGACGCGCATTTCGTCAGAAAGAACTGATTGCA
Tubb2b	NM_001086064.1	900-1000	TGCACTTTTTATGCCAGGCTTTGCCCATTAACAAGTCGTGGCAGCCAACAATACCGAGCCCTGACAGTGCCAGAATAACACAGCAAATGTTTGATTC
Twist1-a	NM_001085883.1	619-719	AGGGAGCCTGGTCCATGTCTGCATCTCACTAACAGCAATGCCACTACAGCTCAGGCCACACACAAAGATTATACTTATACC AATGAATGGGAAAAAACA
Txnip	NM_001093153.1	1515-1615	TTTGACACTTGCCTTAAACCTACATCACCTGATGATGTGCCATGAAGAGAAAGAGTTGTCTGTTTCCACCACATACAGTATGTGGACAGGAATCTGTGGCC
Ventx2.1-b	NM_001087981.1	1075-1175	TTCCACAGGACAAAAAATTGCACTGAATGTTGCTATTGGCAAGATGATTACAGAATAGCTGGCTACTATTGGCCTATTTGTTATGTATCTTTACATGATT
Vpp1	NM_001258387.1	177-277	CATCTCTGGTGCAATGTCAGTCATTCCTCAGCCGGGGGATTTGAGTGGTCTGTGTTCCCGGCACATTCTCCTCCAGAAA CTCCAGATCATCAGCTCCA
Xbra-a/b	NM_001090578.1	1529-1629	TGTAGGCCTCCAAAACAACCTTAAAGATGTGCTTAGGCAAGTATATCAGTGTTACCTGCTTCAAAGACTTCATGGGCCCA ACCAGGTGTGGGTGGTCT
Xk81a1	NM_001086376.1	323-423	AAGTGAGAGCCTTGAAGCCGCCAATAACGACCTGGAAGGGAAGATCCGTAACCTGGTACGATAAGCAATCAGATGCAGGCATTGGTGTGGGTCTAAAGA
Xl.15091	BI443651.1	131-231	TACAAATGATTTGGAGAGAAACATTCCTTTCCAAAAATAGGTTCAATCTTTGGCAGTGGGGAAATCGAAGTGAGATTTGTGAAATGGCTAGGATGAAA
Xl.16263	DC025247.1	247-347	ACGTTAGGACATTACAGGAAGGGGCATTGTTAATCTCATAAACCACTGATTGTTGAAGACACAAAGGCATTGAAGGCATAAAGACCTGCGTATTTCTACA
Xl.32109	BP735133.1	170-270	GGGTTGAAATTGCCCTTTAGTAGGCCAATCCAGTCCTGTA AACACAGGTAGCACAGCAAGGTGTCTGCCATCAACCTTAGAGTCTCTCCAGCTTTCTT
Xl.45046	CF286593.1	284-384	ACTGAAAAAGGGGAGTTTTAGTTCTGCAACATTGGCTGTACCATGTCTGCTGTACCTGTATATTTCAAGCTGGCCATACACAGCAAGCAATACAAT
Xl.4906	DC050951.1	373-473	TCCAGAGAAGCCTGGCCACAAGTGCCAGTGGTTCTCGTCCAACCCCAACATCCAGTCCAGCAGCAACATCTCCGTCGAGGACCATTTCTCCAAAGC
Xl.51509	DY570900.1	86-186	CTTACAAGGGAATGGGGGCGCCTATGTGTCACCCAATATGCAAGCAAGTCCGGTGTACGTAGGGGTAACATATGTGGATTCTGTGCCAGCACAAAGGCCCT
Xl.57926	DQ096998.1	670-770	ACCGCACAAAACATTTAACCTCTTCCATGCCAGTCCAATACCCCCAAAGCAGCCCGTTACAGCTGCACATGTAATCTCCAGTTACCCTCATGCTTGTA
Xl.58101	BJ089218.1	113-213	TCCAAAAAGAGGTTACAACCTTTGGCAGTGGGGAATTTGAAAGAGAGATTTGTGAAATGGCTTTGGCTGAAAACCTGTCATTGGAAGCAGTTGTGCGGTC
Xl.59256	DR729445.1	601-701	TTTAACCGGAAGTTCCCTTAATACCCAAGGTGTCTTGCCTATGGACACAATGGCATAAAGCAAGGGATGCAAACTAGGGCCAATCTTTCCAAGTTACAGTT
Xl.6091	DC024574.1	286-386	AACTGAATCTGGCCAGTATATCTCATTGCTTATGGTGTGCATCAATTTTTTGCAGTACAGTAGCACATACATGGGGTACCTGAGAAATATGGCGC
Xl.67202	DC016425.1	34-134	ACAAATGTTATGTTTGTGAGTCATTAATAACTGAGGAATGAGAGCTGATTGCACATGGATACAGGGCAGTGATTGGCTGTTCC TTTTAGGGTTGCACCGAAT
Xl.68408	DC067179.1	265-365	GGATCAGACAGTGTCTTTGCATGTTGATACCTGAGGAATGTGGTAAAGATATGAATCTTAGTTGGGCAGCCCAAGGATGAGCCCCAATTTACATCA
Xl.70850	BJ622644.1	207-307	CCCATAGAGAGTCGCCGACCCCTGGGAGCCGCATACAGA GAAGATATTTATACTGCTCATTGTGGCTCTAACTTAGGG

Target	Accession	Target region	Target sequence
			CCACACATAGTGCTACACAG
XI.71159	NM_001086068.1	26-126	GTGCTGAGCTATTGTGTATCGGCAATTCGGAGAACTGAGG TGAAACTTTCCAGAGCCCAGAAAGAGCCTCGTTACTAGTGT CAGCGTCCAGTTGATCTGT
XI.74263	BJ631099.1	266-366	CTAAGGATCTCTGCAAAGTCTATTGTCCAATTGGGGAA CATGTCAGGCAGCAGGACAAAAAATTGTGGGATATTCCG AAAATGCTTGAAGGACACC
XI.79790	DR715148.1	408-508	GGCAATGAGCCCCGATTTCTGGCCGCCTGGTTCGGATTGG CCCAACTGGGGTGGTGTCCGCCTTCTCAACACCAACGT GCGGAAAGGGGCCCTAATGC
XI.80297	BI449170.1	41-141	GTGTCCATCTGCCCATCAATGAGCATTGTCTTCTAAGAGGA TCCAAAACCATAAAGAATTGGATACAGCTGTTTCGGAACCTG GATTTTCCAGCATTCCC
XI.85251	EE318610.1	705-805	TCGAACTTGATGGTTTGACTACACGTTGATCTAGTCAGCCT AATCTACCTCTACAATCAGAGGTGTGGCAATGCACTGACCC GTTATCTTTTCTCGCTCC
XI.8753	BC057717.1	143-243	GCACGTTTAAACCACCAACTCACCCCTCTGATGCCCGTTCCG GTGTTGTTTACAGAAGATCACAGGCTGGTGACATCATGCT GGTATCGGCATTACCGTC
XI.9822	NM_001096102.1	3424-3524	GGACGGTAGCGTATCAGTGTGAAGGCTCTGTGACTCTTCT GATTTTACTGAACTACTAATCCCAGCAGTCCCACAGATCCT GCTGTTGGTACAGTATGAA
XI.9874	DC012344.1	489-589	AGCAGCATATGATGATAACTCAAGGTCACAAATCAGGCTTC ATGTGACAGATAGCCTCCCCTGAAAAGTTCAATCTTGTTCA ATGCACAACCACCGGCTT
Xwnt8	NM_001088168.1	125-225	GTCAGTCAATAACTTTCTGATGACAGGACCCAAGGCATATC TGACATACTCAGCGAGTGTGCCGTGGGTGCGCAGAATGG AATTGAGGAGTGTAATAT
Znf703-a/b	BC046863.1	1582-1682	ATCCTACTACTCCCCATACGCATTATATGGACAGAGGCTAA CATCAGCTTCAGCGCTAGGATACCAGTAAATACGACTCCCA AACTCATAGACTGTATAT

Abbreviations

°C	degrees celsius
µg	microgram
µg	microgram
µl	microliter
µM	micromolar
A	Adenine
AP	Alkaline phosphatase
BCIP	5-Bromo-4-Chloro-3-Indolyl-Phosphate
BMB	Bohringer Mannheim blocking reagent
bp	Base pairs
C	Cytosine
cDNA	complementary DNA
dH ₂ O	distilled water
DIG	Digoxigenin
DNA	deoxyribonucleic acid
dNTP	deoxynucleoside triphosphate
DTT	Dithiothreitol
E. coli	Escherichia coli
EDTA	ethylene diamine tetraacetic acid
et al.	et alii
G	Guanine
GFP	green fluorescent protein
h	hour(s)
hCG	human chorionic gonadotropin
LB	Luria-Bertani
M	molar
mg	milligram
min	minute(s)
ml	milliliter
mM	millimolar

Abbreviations

mRNA	messenger RNA
NBT	Nitro-Blue Tetrazolium
ng	nanogram
nl	nanoliter
PBS	phosphate buffered saline
PCR	polymerase chain reaction
pH	negative decade logarithm of hydrogen ion concentration
RNA	ribonucleic acid
rpm	revolutions per minute
RT	reverse transcriptase
sec	second(s)
T	Thymine
T7E1	T7 endonuclease I
Taq	<i>Thermus aquaticus</i>
T _m	melting temperature
Tris	Tris(Hydroxymethyl)Aminomethane
U	uracil / unit(s)
UTR	untranslated region
w/v	weight per volume
WMISH	whole mount in situ hybridization
X-Gal	5-Bromo-4-Chloro-3-Indolyl- β -d-Galactoside

List of figures

Fig. 1.1	Pancreas organogenesis in <i>Xenopus laevis</i>	15
Fig. 1.2	Model for dorsal endoderm patterning, mesoderm induction and organizer formation in <i>Xenopus</i>	17
Fig. 1.3	Fate maps of <i>Xenopus</i> endoderm from gastrula to early somite stage and overview of signals involved in pancreas specification.	20
Fig. 1.4	Overview of pancreas organogenesis and lineage decisions	23
Fig. 1.5	Paracrine RA-signaling and expression of RA-metabolizing enzymes during <i>Xenopus</i> gastrulation	26
Fig. 1.6	Therapeutic potential of <i>in vitro</i> generated organoids.....	30
Fig. 3.1	RA-dependent induction of pancreatic marker genes in Vegf/Noggin-programed explants	62
Fig. 3.2	Formation of pancreatic organoids that recapitulate the process of pancreas development.....	64/65
Fig. 3.3	Formation of pancreatic organoids from RA-programed explants (WMISH)	67
Fig. 3.4	Direct RA-target gene Cyp26a1 is induced within one hour	69
Fig. 3.5	Identification, verification and expression characteristics of early RA-responsive genes in the context of pancreas specification.....	71
Fig. 3.6	Hnf1b is directly induced by RA and required for pancreas specification in pancreatic organoids.....	77
Fig. 3.7	Hnf1b is required for pancreas specification <i>in vivo</i>	82
Fig. 3.8	Hnf1b is not sufficient to substitute for RA in pancreas specification in ectodermal explants.....	84
Fig. 3.9	Fzd4 and Fzd4s are directly induced by RA and required for pancreas specification in pancreatic organoids	90
Fig. 3.10	Wnt-signaling in programed explants	93
Fig. 4.1	Model of pancreas specification involving direct RA-targets, Fzd4 and Hnf1b, in <i>Xenopus</i> embryos.....	109

Fig. 6.1	Detection of endodermal, mesodermal and neuro-ectodermal marker genes	129
Fig. 6.2	Detection of marker genes for pancreatic structures.....	130
Fig. 6.3	Detection of early direct and indirect RA-target genes by RNA-sequencing	131
Fig. 6.4	Confirmation of RA-responsiveness	132
Fig. 6.5	Expression of RA-responsive genes at gastrula stage by WMISH.....	133
Fig. 6.6	Expression characteristics of endodermal, mesodermal and ectodermal markers at gastrula stage by Nanostring analysis.....	134
Fig. 6.7	Expression characteristics of RA-responsive genes at gastrula stage by Nanostring analysis	135
Fig. 6.8	RA-responsive expression of Hnf1b in the dorsal endoderm	136
Fig. 6.9	Knockdown of Hnf1b through loss of exon 2.....	137
Fig. 6.10	Fzd4 has an alternative splice variant Fzd4s	138
Fig. 6.11	Fzd4/Fzd4s expression analysis.....	139
Fig. 6.12	RA-responsive expression of Fzd4/Fzd4s	140
Fig. 6.13	Mutation analysis of CRISPR/Cas treated pancreatic organoids by DNA sequencing.....	141

List of tables

Tab. 2.1	Provided constructs for sense RNA	34
Tab. 2.2	Provided constructs for anti-sense RNA	35
Tab. 2.3	Luciferase assay constructs.....	36
Tab. 2.4	CRISPR/Cas system constructs	36
Tab. 2.5	Real-time PCR constructs	36
Tab. 2.6	Cloning oligonucleotides.....	37
Tab. 2.7	Sequencing oligonucleotides	38
Tab. 2.8	RT-oligonucleotides and working conditions	38
Tab. 2.9	Real-time PCR oligonucleotides	40
Tab. 2.10	Morpholino oligonucleotides	40
Tab. 6.1	Normalized data of two independent experiments	143
Tab. 6.2	Calculated mean and standard error of mean (SEM)	144
Tab. 6.3	Summary of 102 differentially expressed genes in the absence of CHX.	145
Tab. 6.4	Summary of differentially expressed genes in the presence of CHX ...	146
Tab. 6.5	Comparison of differentially expressed genes absence versus presence of CHX (putative direct RA-targets).....	147
Tab. 6.6	RNA-sequencing of explants 1h after RA addition in the absence of CHX. Normalized data (1h Ø CHX).....	148
Tab. 6.7	RNA-sequencing of explants 2h after RA addition in the absence of CHX. Normalized data (2h Ø CHX).....	149
Tab. 6.8	RNA-sequencing of explants 1h after RA addition in the presence of CHX. Normalized data (1h + CHX).	152
Tab. 6.9	RNA-sequencing of explants 2h after RA addition in the presence of CHX. Normalized data (2h + CHX)	153
Tab. 6.10	Overview of Nanostring analysis results.	155
Tab. 6.11	Raw data of RA-inducibility in explants	157
Tab. 6.12	Normalized data of RA-inducibility in explants	159

Tab. 6.13	Raw data of RA-inducibility in whole embryos	161
Tab. 6.14	Normalized data of RA-inducibility in whole embryos	163
Tab. 6.15	Raw data of RA-dependency in dorsal tissue	165
Tab. 6.16	Normalized data of RA-dependency in dorsal tissue	166
Tab. 6.17	Raw data of RA-dependency in whole embryos	167
Tab. 6.18	Normalized data of RA-dependency in whole embryos	169
Tab. 6.19	Raw data of expression characteristics	171
Tab. 6.20	Normalized data of expression characteristics.....	173
Tab. 6.21	Calculated mean and standard error of mean (SEM).....	175
Tab. 6.22	Quantification of Pdx1 domain in the endoderm	177
Tab. 6.23	Quantification of Ptf1a domain in the endoderm	178
Tab. 6.24	Predicted Fzd4-gRNA off-target sequences in exonic regions of the <i>Xenopus laevis</i> genome	179
Tab. 6.25	Nanostring Code set used for the confirmation of pancreatic organoid formation	180
Tab. 6.26	Nanostring Code set for the verification of RA-responsive candidates.....	183

Acknowledgements

I would like to express my appreciation to Prof. Tomas Pieler for providing me such an interesting research project. I am grateful for his guidance and constructive feedback throughout my studies.

I thank my thesis committee members Prof. Herbert Jäckle and Prof. Andreas Wodarz for their continuous interest in my work and for the helpful discussions.

Furthermore, I would like to thank Dr. Kristine Henningfeld for her support and reasonable suggestions.

I also want to thank Prof. Ahmed Mansouri, Prof. Ernst Wimmer and Prof. Matthias Dobbstein for their participation as extended thesis committee members.

Moreover, I have to thank all my colleagues in the department of Developmental Biochemistry, especially Dr. Juliane Melchert, Dr. Patrick Berndt, Sven Richts, Dr. Juliane Pfennig, Dr. Diana, Bauermeister, Katja Ditter and Ilona Wunderlich for the nice working atmosphere and support.

My special thanks to Patrick Becker for his patience, interest in my work and continuous support.

Curriculum Vitae

Name: Maja B. Gere
Date of Birth: 27.02.1980
Place of Birth: Hoyerswerda, Germany
Address: Pfalz-Grona-Breite 45, 37081 Göttingen, Germany
e-Mail: maja.gere@med.uni-goettingen.de, mgere@web.de

02/2012 – 03/2016 **Doctoral studies:** “Characterization of the retinoic acid-induced gene network responsible for pancreas specification in *Xenopus laevis*”

Dept. of Developmental Biochemistry, Georg August University of Göttingen, Supervisor: Prof. T. Pieler

01/2011 – 01/2012 **Research assistant**

Dept. of Chromatin Biochemistry, MPI for Biophysical Chemistry, Göttingen, Dr. W. Fischle

08/2010 – 12/2010 **Research assistant**

Dept. of Developmental Biology, Georg August University of Göttingen, Dr. N. Prpic-Schäper

09/2005 – 08/2010 **Diploma studies:** “RNA-binding proteins as interaction partner of HP1”

Dept. of Developmental Biology, Georg August University of Göttingen, Supervisor: Prof. S. Hoyer-Fender

09/2000 – 09/2005 **Biological technical assistant**

Dept. of Virology, Charité Campus Benjamin Franklin, Berlin, Prof. R. Heilbronn, Prof. T. Cathomen

08/1998 – 07/2000 **Apprenticeship** as Biological technical assistant

OSZ Werder (an der Havel)

08/1992 – 07/1998 **Abitur**

Konrad-Zuse Gymnasium, Hoyerswerda